Modeling traffic on urban road networks with hyperbolic conservation laws

Nicolas Laurent-Brouty

UNIVERSITÉ CÔTE D'AZUR

ÉCOLE DOCTORALE
SCIENCES FONDAMENTALES ET APPLIQUÉES

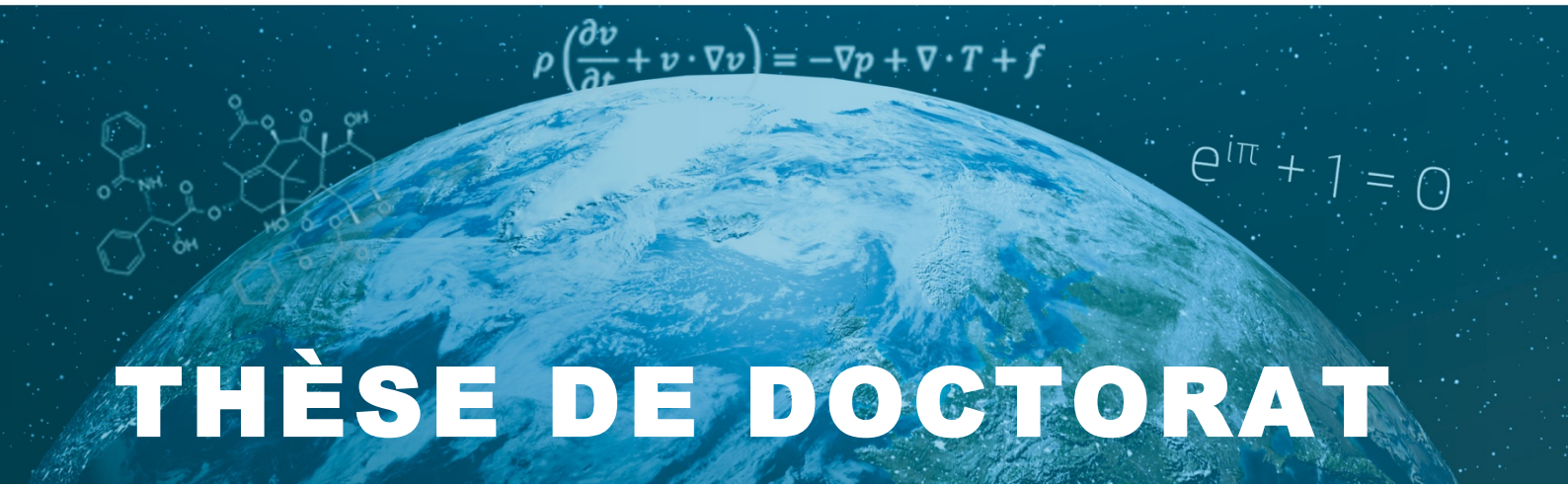

THÈSE DE DOCTORAT

Modeling traffic on urban road networks with hyperbolic conservation laws

Modélisation du trafic sur des réseaux routiers urbains à l'aide des lois de conservation hyperboliques

Nicolas LAURENT-BROUTY

Inria Sophia Antipolis Méditerranée – équipe projet Acumes

Présentée en vue de l'obtention du grade de docteur en Mathématiques **d'**Université Côte d'Azur
Dirigée par : Paola Goatin
Soutenue le : 20 septembre 2019

Devant le jury, composé de :
Debora Amadori, Professeur, Università de L'Aquila
Nicolas Forcadel, Professeur, INSA Rouen
Mauro Garavello, Professeur, Università di Milano Bicocca
Paola Goatin, Directeur de Recherche, Inria
Ludovic Leclercq, Directeur de Recherche, IFSTTAR
Benedetto Piccoli, Professeur, Rutgers University Camden

Inria

« Maintenant je sais mieux qui je suis
et ce que j'ai fait. »
Walter Bonatti

À mes parents, Myriam et Didier,
qui m'ont tant donné.

Remerciements

Je tiens tout d'abord à remercier chaleureusement ma directrice de thèse, Paola Goatin, pour m'avoir accompagné sur cette longue randonnée doctorale. Merci de m'avoir permis d'explorer le monde des lois de conservation hyperboliques, et de m'avoir proposé de nombreuses opportunités de recherche. Je suis fier du travail accompli durant trois ans sous ta direction.

Je me tourne ensuite vers Alexandre M. Bayen, qui m'a le premier fait confiance et m'a permis de découvrir le monde de la recherche à Berkeley. Merci de m'avoir mis le pied à l'étrier et de m'avoir inclus d'emblée dans ton groupe de recherche, qui a constitué durant mon expérience californienne une seconde famille. C'est pourquoi je remercie également à cette occasion l'ensemble des membres du groupe, qui ont chacun contribué à créer une atmosphère de travail chaleureuse et amicale. Naturellement, j'en viens au "second" Alex qui a rythmé ma thèse, Alexander Keimer. Merci pour notre collaboration trois années durant. J'ai particulièrement apprécié ta façon de voir le monde et la science, et je te remercie de m'avoir fait partager ta maîtrise de l'analyse fonctionnelle. Je salue enfin Jeff Calder et James A. Sethian, dont les cours m'ont passionné et m'ont persuadé de me consacrer à l'étude des équations aux dérivées partielles.

Je tiens désormais à remercier l'ensemble des membres de l'équipe Acumes que j'ai pu côtoyer durant ces trois ans : Abdou, Guillaume, Régis, Mickaël, Maxime, Stefano, Montserrat, Jean-Antoine, Elena, Nikodem, Felisia. Merci pour nos nombreuses discussions, toujours animées, et merci également pour vos précieux conseils. Je souhaite adresser mes plus sincères amitiés à Guillaume Costeseque, avec qui j'ai eu la chance et le plaisir de collaborer. Merci à toi pour tes conseils et ton soutien, ce fût un plaisir de travailler ensemble au quotidien. Je tiens également à saluer mes voisins des équipes Nachos, Tosca et Coffee. Un merci particulier à Théophile pour nos séances de grimpe qui permettaient de toujours réattaquer du bon pied !

Je remercie Nicolas Forcadel et Benedetto Piccoli d'avoir accepté de rapporter mon manuscrit durant l'été. Je remercie en outre Debora Amadori, Mauro Garavello et Ludovic Leclercq de prendre part à mon jury de thèse.

Je tiens à présent à saluer mes amis, en commençant par celui qui me connaît depuis toujours, Loïc. Merci de me rattacher encore et toujours à mes chères racines ardéchoises ! Merci également à Edoardo et Henri pour nos escapades sportives le temps d'un week-end. Enfin, je veux saluer mes amis américains Rocky et Max. Merci de m'avoir fait découvrir une nouvelle culture, et merci pour tous nos moments de rire !

Je souhaite maintenant conclure en remerciant infiniment mes proches qui m'ont épaulé chaque jour. J'embrasse tout d'abord mes grands parents, qui ont toujours eu une pensée pour moi. Je tiens ensuite à m'adresser à mes parents, sans qui je ne serais assurément pas là aujourd'hui. Vous m'avez toujours poussé à croire en moi et à viser plus haut. Papa, merci pour tes petites attentions au quotidien. Maman, merci d'avoir cru en moi

lorsque beaucoup doutaient. Enfin, je termine par la personne qui me soutient et partage mon quotidien depuis plus de sept ans désormais. Merci Maëlle pour tout ce que tu m'as apporté. Merci d'avoir été ma boussole et mon guide, dans les hauts mais aussi dans les périodes de creux. Ce chapitre de ma vie se termine mais j'ai hâte de connaître la suite à tes côtés.

Abstract

This thesis is devoted to the modeling of traffic flow using hyperbolic conservation laws, with a specific focus on urban applications. Urban areas are today facing severe episodes of air pollution and increasing congestion due to traffic. The objective is to overcome some of the current limitations of macroscopic traffic flow models in urban situations.

We first study the seminal Aw-Rascle-Zhang model with relaxation. We prove well-posedness of the model using wave-front tracking approximations and splitting technique in a Lagrangian setting. Besides, we provide an estimate on the decay of positive waves. We then show that the solutions of the Aw-Rascle-Zhang system with relaxation converge to a weak solution of the LWR model when the relaxation parameter goes to zero. Finally, we propose a discussion on the entropy aspect of this weak solution of the LWR model.

We then propose a new macroscopic traffic flow model accounting for the boundedness of traffic acceleration, which is required for physical realism. Our model is built on the coupling between the scalar conservation law accounting for the conservation of vehicles and a number of Ordinary Differential Equations (ODE) describing the trajectories of accelerating vehicles, which we treat as moving constraints. We detail a wave-front tracking algorithm to construct approximate solutions of the model, with general flux functions and show existence of solutions to the Cauchy problem for a piecewise constant initial datum. Finally, we provide numerical simulations of the model in different urban situations, from a single Riemann problem to sequences of traffic lights, and confront the results to numerical simulations of the LWR model.

Finally, we introduce a new macroscopic traffic flow model with buffers on road networks. This model features buffers of finite size, enabling backward propagation of congestion on the network, and time-dependent routing functions at the junctions. The dynamics are first defined on the level of conservation laws, and then transformed in an Hamilton-Jacobi formulation. We prove existence, uniqueness and stability of the solutions with respect to the routing ratios and initial datum using a fixed-point problem in a proper Banach space. Thanks to stability, the model provides a controllable framework, using routing ratios as control parameters. This represents an advance towards solving the Dynamic Traffic Assignment (DTA) problem. In the end we detail how this framework applies to a classical road network with several intersections and finite-length links.

Keywords: *Hyperbolic conservation laws, Hyperbolic systems of conservation laws with relaxation, Macroscopic traffic flow models, Wave-front tracking, Temple class systems, PDE-ODE coupling, Flux constraints, Traffic flow on networks, Hamilton-Jacobi equations, Fixed-point problems.*

Résumé

Cette thèse se consacre à la modélisation mathématique du trafic routier à l'aide des lois de conservation hyperboliques. Nous nous intéressons plus particulièrement à l'application des modèles macroscopiques en milieu urbain. L'étude des phénomènes routiers et la modélisation des trajectoires de véhicules est devenue nécessaire au vingtième siècle avec l'avènement du transport automobile. Malgré cela, le trafic routier demeure aujourd'hui un phénomène complexe à comprendre et à représenter. En effet, la complexité des réseaux routiers, la dynamique d'apparition de la congestion routière, l'hétérogénéité du trafic routier et le grand nombre de véhicules évoluant sur les réseaux routiers urbains constituent autant de difficultés à modéliser. En outre, les métropoles sont désormais régulièrement confrontées à des niveaux de congestion record et à des épisodes de pollution atmosphérique marqués. Le trafic routier est responsable d'une dégradation de la qualité de l'air et contribue au dérèglement climatique à moyen-terme [60, 61]. Par ailleurs, le développement des véhicules autonomes risque de bouleverser prochainement nos modes de transport urbain. Contrairement à un conducteur traditionnel, la trajectoire des véhicules autonomes est dictée par des algorithmes mathématiques. Elle peut dès lors être contrôlée et optimisée en fonction de contraintes données [95]. Afin d'établir le problème d'optimisation correspondant, dénommé dans la littérature problème « d'assignation dynamique du trafic » [127], il est nécessaire de pouvoir formuler un problème de contrôle optimal à l'aide du modèle de trafic. Dans ce cadre, nous pouvons imaginer que les véhicules se déplacent dans le futur de manière à minimiser les externalités négatives du trafic que constituent les embouteillages ainsi que les émissions polluantes. C'est pourquoi il est nécessaire de développer des modèles de trafic qui représentent de manière réaliste l'évolution des véhicules en milieu urbain.

Nous pouvons distinguer dans la littérature trois familles de modèles de trafic routier. La première catégorie est constituée par les modèles microscopiques qui consistent à modéliser la trajectoire de chaque véhicule de manière individuelle à l'aide d'une équation différentielle ordinaire, prenant en compte la position et la vitesse des véhicules le précédant [12, 17, 37, 73, 128, 133]. Ces modèles sont précis et permettent le développement de logiciels de microsimulation, comme *Aimsun* ou *PTV Vissim* [33]. Cependant, ils ne sont pas les plus adaptés pour simuler un grand nombre de véhicules sur un réseau routier, puisque le nombre d'équations différentielles à résoudre est au moins égale au nombre de véhicules considérés. La seconde catégorie est la famille des modèles cinétiques, qui reposent sur une analogie avec la physique statistique. Ils utilisent principalement l'équation de Boltzmann, afin de représenter l'évolution d'une fonction de distribution de véhicules sur la route [97, 129, 130, 131]. Ces modèles peuvent être interprétés comme une généralisation des modèles microscopiques, dans lesquels chaque véhicule est considéré comme une particule évoluant selon des lois de mouvement. Dans cette thèse, nous nous concentrons sur la troisième catégorie de modèles : les modèles macroscopiques. Ils appliquent les prin-

cipes de la mécanique des fluides au trafic routier et reposent sur les lois de conservation hyperboliques. L'idée d'assimiler le trafic à un fluide et d'y appliquer les principes de la mécanique des fluides est due à Lighthill et Whitham en 1955 [120] et en 1956 à Richards [134]. Ils établissent que le nombre de véhicules évoluant sur un réseau routier, en prenant en compte les entrées et les sorties, doit être conservé au cours du temps. La variable principale utilisée dans les modèles macroscopiques de trafic routier est la densité de véhicules notée ρ, qui décrit le nombre de véhicules par unité de longueur. La seconde variable considérée est la vitesse moyenne du flux de véhicules v ainsi que la fonction de flux associée f. Cette fonction décrit le nombre de véhicules franchissant une position donnée au cours d'un intervalle de temps, telle que $f = \rho v$. Appliquant le principe de conservation du nombre de véhicules, ce dernier étant décrit par l'intégrale spatiale de la densité, nous retrouvons la loi de conservation scalaire $\partial_t \rho + \partial_x f = 0$. En supposant que la variable v est décrite par une fonction d'équilibre décroissante de la densité, $v = V_e(\rho)$, les auteurs ont ainsi proposé le premier modèle macroscopique de trafic routier dénommé Lighthill-Whitham-Richards (LWR). Ce modèle ne reproduit cependant pas toutes les observations expérimentales, notamment lorsque le trafic est en phase congestionnée. Par la suite, des modèles plus complexes impliquant deux équations aux dérivées partielles ont été proposés, permettant ainsi au trafic d'évoluer à une vitesse hors équilibre. Il s'agit des modèles de second ordre. Le plus commun dans la littérature aujourd'hui est le modèle Aw-Rascle-Zhang (ARZ) [9, 146], qui consiste en un système de deux équations aux dérivées partielles. L'ensemble de ces modèles macroscopiques ont cependant été initialement développés dans le cadre de tronçons routiers sans entrée ni sortie. Nous nous intéressons alors à leur application sur des réseaux routiers plus complexes.

Dans un premier temps, nous considérons le modèle Aw-Rascle-Zhang avec relaxation. Ce modèle se présente sous la forme

$$\begin{cases} \partial_t \rho + \partial_x(\rho v) = 0, \\ \partial_t(v + p(\rho)) + v\partial_x(v + p(\rho)) = \frac{V_e(\rho) - v}{\delta}, \end{cases} \qquad x \in \mathbb{R},\ t > 0,$$

où $p(\rho)$ est une fonction de pression, $V_e(\rho)$ représente une vitesse d'équilibre et $\delta > 0$ est un paramètre de relaxation représentant le temps de réaction des conducteurs. Nous construisons une suite de solutions approchées à l'aide de la méthode de suivi des fronts (*wave-front tracking* en anglais) couplée à une méthode de décomposition temporelle (*splitting* en anglais) en référentiel Lagrangien. Pour chaque valeur $\delta > 0$, nous montrons que cette suite converge vers une solution faible et entropique du système pour une donnée initiale à variation bornée. Par la suite, nous calculons une borne supérieure sur la décroissance des ondes positives. Nous démontrons que les solutions du système convergent vers une solution faible du modèle LWR, c'est à dire vers la solution de la loi de conservation scalaire, lorsque le paramètre de relaxation δ tend vers zéro. Nous concluons par une discussion sur le caractère entropique de cette solution faible du modèle LWR.

Dans un second temps, nous proposons un nouveau modèle macroscopique de trafic routier qui préserve le caractère borné de l'accélération des véhicules. Notre modèle couple une Équation aux Dérivées Partielles (EDP), la loi de conservation scalaire, à plusieurs

Équations aux Dérivées Ordinaires (EDO), décrivant la trajectoire de véhicules accélérant à taux constant. Ces véhicules sont traités dans le modèle comme des goulots d'étranglement mobiles. Nous proposons la construction de solutions approchées avec un algorithme de suivi des fronts d'ondes et prouvons l'existence et l'unicité de la solution pour le problème de Cauchy associé à une donnée initiale constante par morceaux. Nous produisons ensuite des simulations numériques de notre modèle dans différentes situations urbaines, allant de la résolution du problème de Riemann à la simulation d'un axe urbain comportant plusieurs feux de signalisation. Enfin nous comparons ces simulations aux solutions du modèle LWR appliqué aux mêmes situations.

Pour terminer, nous proposons un nouveau modèle macroscopique de trafic routier avec des stockages tampon (*buffers* en anglais) aux intersections afin de résoudre le modèle LWR sur des réseaux routiers. Ce modèle utilise des *buffers* de dimension finie, qui garantissent la propagation de la congestion au sein du réseau. Il comporte également des fonctions de répartition de véhicules aux jonctions qui sont dépendantes du temps, et peuvent dès lors être contrôlées au cours du temps. La dynamique du trafic est d'abord établie à l'aide des lois de conservation hyperboliques, conformément au modèle LWR, puis retranscrite dans une formulation de Hamilton-Jacobi. Nous prouvons alors l'existence, l'unicité et la stabilité des solutions vis à vis des données initiales en résolvant un problème de point fixe dans un espace de Banach approprié. La propriété de stabilité garantit que la solution du problème peut être contrôlée et optimisée en modifiant les fonctions de répartition des véhicules aux jonctions. Cela représente une avancée dans la résolution du problème d'assignation dynamique du trafic routier. Pour finir, nous détaillons l'application du modèle à un réseau routier réaliste comportant plusieurs intersections et des routes de longueur finie.

Mots clés : *Lois de conservation hyperboliques, Systèmes de conservation hyperboliques avec relaxation, Modèles macroscopiques de trafic routier, Suivi de fronts d'onde, Systèmes de Temple, Couplage EDP-EDO, Contraintes de flux, Trafic routier sur les réseaux, Équations d'Hamilton-Jacobi, Méthodes de point fixe.*

Contents

1 Introduction to hyperbolic conservation laws and traffic flow modeling 1
1.1 Hyperbolic conservation laws . . . 2
1.1.1 The scalar conservation law . . . 3
1.1.2 Systems of conservation laws . . . 10
1.1.3 Wave-Front Tracking approximations . . . 13
1.2 Macroscopic traffic flow models . . . 15
1.2.1 The Lighthill-Whitham-Richards Model . . . 15
1.2.2 Second order traffic flow models . . . 17
1.2.3 Traffic flow models in urban applications . . . 19
1.3 Contributions and outline of the thesis . . . 24

2 The zero relaxation limit for the Aw-Rascle-Zhang traffic flow model 27
2.1 Introduction . . . 28
2.2 Wave-Front Tracking approximations . . . 30
2.2.1 Construction of approximate solutions via wave-front tracking . . . 31
2.2.2 Estimates on WFT approximate solutions . . . 32
2.3 Convergence of the WFT approximations to a solution of the relaxed ARZ system . . . 38
2.4 Estimates of positive waves . . . 42
2.5 Convergence of the relaxed ARZ system towards the LWR model . . . 48
Appendix . . . 52

3 Well-posedness of a macroscopic traffic flow model with bounded acceleration 55
3.1 Introduction . . . 56
3.2 A coupled PDE-ODE model accounting for bounded acceleration . . . 57
3.2.1 Mathematical formulation and definition of solutions . . . 57
3.2.2 The Riemann problem . . . 59
3.2.3 Construction of approximate solutions with Wave-Front Tracking . . . 60
3.3 Existence of weak solutions . . . 64
3.3.1 Convergence of approximate solutions . . . 64
3.3.2 Existence of weak solutions . . . 66
3.3.3 The trajectory is a Caratheodory solution . . . 67
3.3.4 Proof of the flux constraint . . . 68
3.4 Numerical simulations of the PDE-ODE model . . . 70
3.4.1 The Riemann problem . . . 70
3.4.2 A Cauchy problem with several moving bottlenecks . . . 72

3.4.3 A dynamic sequence of traffic lights 74
3.5 Conclusion 75
Appendix 76

4 A macroscopic traffic flow model with finite buffers on networks: Well-posedness by means of Hamilton-Jacobi equations 81
4.1 Introduction 82
4.2 The model 83
4.2.1 Network representation 83
4.2.2 Link dynamics 84
4.2.3 Node dynamics 85
4.2.4 Derivation of the corresponding Hamilton-Jacobi framework 87
4.3 Definition of solutions 90
4.4 Existence and uniqueness of solutions to the Hamilton-Jacobi formulation . 91
4.4.1 Basic results and properties of Hamilton-Jacobi equations 91
4.4.2 The fixed-point problem 96
4.4.3 Estimates for the involved mappings 98
4.4.4 Existence and uniqueness of solutions 104
4.5 Stability of the solution 109
4.6 Optimal routing 113
4.7 Practical implementation of the model on road networks 115
4.8 Further work and conclusion 119

Conclusion and perspectives 121

List of Figures

1.1 Conservation of the number of vehicles on an unidirectional stretch of road. 3
1.2 A situation in which characteristics cross. 4
1.3 Notations to introduce Rankine-Hugoniot conditions. 5
1.4 Shock wave solving a Riemann problem. 8
1.5 Rarefaction wave solving a Riemann problem. 9
1.6 Illustration of the Wave-Front Tracking algorithm. 15
1.7 Experimental fundamental diagram on highway A50 in France. 16
1.8 The linear velocity and the associated fundamental diagram. 17

2.1 Notations used in step 3 of the algorithm. 32
2.2 Notations used for Godunov scheme. 52

3.1 Example of the WFT approximate solution and notation used in the algorithm. 61
3.2 Comparison of solutions for a Riemann initial datum. 70
3.3 Density difference between the solutions to the LWR model and to the PDE-ODE model for a Riemann initial datum. 71
3.4 Queue lengths obtained for the LWR model and the PDE-ODE model for a Riemann initial datum. 72
3.5 Comparison of solutions for a series of traffic lights. 72
3.6 Density difference between the solution to the LWR model and the solution to the PDE-ODE model for the series of traffic lights. 73
3.7 Queue lengths obtained for the LWR model and the PDE-ODE model. . . 73
3.8 Comparison of solutions for the same sequence of traffic lights. 74
3.9 Cumulated number of vehicles passing through the traffic lights. 75

4.1 Illustration of the archetype network. 84
4.2 Illustration of the finite speed propagation argument on one link. 119

Chapter 1

Introduction to hyperbolic conservation laws and traffic flow modeling

In this thesis we investigate the mathematical modeling of traffic flow, with a specific focus on urban applications. Modeling traffic flow and vehicle trajectories became a necessity in the twentieth century with the rise of car mobility in modern societies. Yet, it remains a complex physical phenomenon to understand and model accurately. The complexity of road networks, the dynamics of traffic congestion, the heterogenity of vehicle sizes and performances, drivers' behavior and the large number of vehicles involved in the modeling process represent many challenges to overcome. Furthermore, urban areas are faced today with increasing levels of congestion and pollution due to transportation. The quality of air is declining in major cities, and vehicle emissions are significantly contributing to climate change on the long-term [60, 61]. In addition, autonomous vehicles are expected to be the next revolution of urban transportation. Contrary to classical drivers, these vehicles will be routed following mathematical algorithms, which will provide full optimal control of the trajectories with respect to given constraints [95]. This optimization problem is known in transportation as the *Dynamic Traffic Assignment* problem [127], and requires a controllable modeling framework. In this context, traffic could in the future be routed in order to minimize its negative externalities like emissions and congestion. For all these reasons, it is urgent to develop traffic models which represent accurately the behavior of vehicles on urban road networks, and this will be the motivation of the present work.

Today, we distinguish three different, yet complementary, categories of traffic models. The first category is microscopic modeling, in which each vehicle is considered individually, and each trajectory is described by an Ordinary Differential Equation (ODE) depending on the position and velocity of preceding vehicles [12, 17, 37, 73, 128, 133]. These models, often referred to as the *car-following models*, are precise, and enable the development of microsimulation software tools, like *Aimsun* or *PTV Vissim* [33]. Nonetheless, they are not easily scalable and robust, especially on large networks, since the number of ODEs is at least equal to the number of vehicles considered. The second category is kinetic modeling, which lies on an analogy with statistical physics and Boltzmann equations to model distribution functions of cars [97, 129, 130, 131]. These models can be seen as a generalization of microscopic models, in which each vehicle is not considered individually

but as a particle following physical laws of motion. In this thesis, we focus on the third category, macroscopic traffic flow models, which relies on hyperbolic Partial Differential Equations (PDE) and applies fluid dynamics principles to traffic averaged quantities such as vehicle density and mean traffic velocity.

In Section 1.1 we recall the principal mathematical properties of conservation laws, in order to ease the reading of the following chapters. In Section 1.2 we present the main macroscopic traffic flow models while discussing their strengths and their limits for urban applications. Finally, we present in Section 1.3 the outline of this thesis and summarize our contributions.

1.1 Hyperbolic conservation laws

Conservation laws are a category of partial differential equations which describes the conservation of given physical quantities. The general form of a conservation law is the following

$$\partial_t u + \operatorname{div} f(u) = 0, \tag{1.1.1}$$

where $u : [0, \infty[\times\mathbb{R}^d \mapsto \mathbb{R}^n$ denotes the vector of conserved quantities and $f : \mathbb{R}^n \mapsto \mathbb{R}^{n\times d}$ is a flux function, possibly non-linear, describing the physical flow of u at a given position.

In this thesis, we will focus on the one dimensional Cauchy problem ($d = 1$), *i.e.* $u : [0, \infty[\times\mathbb{R} \mapsto \mathbb{R}^n$:

$$\begin{cases} \partial_t u(t,x) + \partial_x\big[f(u(t,x))\big] = 0, & (t,x) \in \mathbb{R}_+ \times \mathbb{R}, \\ u(0,x) = u_0(x), & x \in \mathbb{R}, \end{cases} \tag{1.1.2}$$

where $u_0 : \mathbb{R} \to \mathbb{R}^n$. These equations were extensively studied since the fifties, for instance by Lax [104, 105]. For systems ($n > 1$) the existence of weak entropy solutions to (1.1.2) has been proved by Glimm in [75], when the initial datum u_0 has small total variation and under suitable regularity assumptions on f. He used a probabilistic algorithm, which is referred to as the *Glimm scheme*. A complementary approach to construct solutions and prove well-posedness, referred to as *Wave-Front Tracking* (WFT), was introduced by Dafermos for scalar equations in [54] and then extended to systems in [18, 59, 135]. Existence and uniqueness of entropy solutions was discussed by Oleinik in [122, 123, 124]. Kruzkov proved existence and uniqueness of general $\mathbf{L}^\infty$ solutions in [98] for the scalar conservation law ($n = 1$).

To illustrate the mathematical conservation of u in the one-dimensional case, Equation (1.1.1) can be formally integrated over any interval $[a, b]$ for a given time t:

$$\begin{aligned} \frac{d}{dt}\int_a^b u(t,x)dx &= \int_a^b \partial_t u(t,x)dx \\ &= -\int_a^b \partial_x f(u(t,x))dx \\ &= f(u(t,a)) - f(u(t,b)). \end{aligned} \tag{1.1.3}$$

The quantity u contained between a and b, when adding the inflow in a and subtracting the outflow in b, is conserved over time. We provide an illustration in Figure 1.1, where u represents the density of vehicles, *i.e.* the number of vehicles per unit length.

Figure 1.1 – Conservation of the number of vehicles on an unidirectional stretch of road.

When $n > 1$, (1.1.2) is a system of conservation laws. A classical example of such a system is Euler's equations for compressible gas flow in one space dimension, which reads as

$$\begin{cases} \partial_t \rho + \partial_x(\rho v) = 0 \text{ (conservation of mass)}, \\ \partial_t(\rho v) + \partial_x(\rho v^2 + p) = 0 \text{ (conservation of momentum)}, \\ \partial_t(\rho E) + \partial_x(\rho E v + p v) = 0 \text{ (conservation of energy)}, \end{cases} \quad (t,x) \in \mathbb{R}_+ \times \mathbb{R}, \quad (1.1.4)$$

where ρ represents the density of the fluid, v the velocity, E is the energy density and p is a pressure function.

Remark 1.1. We only consider here functions u defined on a one dimensional space $\mathbb{R}$. In physics, systems of conservation laws defined on $\mathbb{R}^d$ with $d > 1$, like Euler's equation in $\mathbb{R}^3$, are common and widely used. Nonetheless, the mathematical understanding of systems of hyperbolic conservation laws in multi-space dimension is still a wide area of research, and existence and uniqueness properties are not fully established in the general case.

1.1.1 The scalar conservation law

In this section, we analyse mathematically the scalar conservation law, *i.e.* where $u : \mathbb{R}_+ \times \mathbb{R} \to \mathbb{R}$ is a scalar quantity. More precisely, we investigate the Cauchy problem (1.1.2), with $n = 1$. Assuming first that the solution to (1.1.2) is smooth, one can use the chain rule to rewrite the equation in its quasi-linear form:

$$\partial_t u + f'(u)\partial_x u = 0. \quad (1.1.5)$$

Equation (1.1.5) corresponds to a non-linear transport equation, in which the information is propagated at speed $\lambda(u) = f'(u)$. For a constant speed $\lambda \in \mathbb{R}$, the solution to the linear transport equation

$$\begin{cases} \partial_t u(t,x) + \lambda \partial_x u(t,x) = 0, & (t,x) \in \mathbb{R}_+ \times \mathbb{R}, \\ u(0,x) = u_0(x), & x \in \mathbb{R}, \end{cases} \quad (1.1.6)$$

is classically defined by $u(t,x) = u_0(x - \lambda t)$. In (1.1.5), $\lambda(u) = f'(u)$ is non constant if f is non-linear. The information is thus propagated at different speeds, depending on the initial

value u_0, and thus the solution may develop discontinuities. In this case, the derivative $\partial_x u$ is not properly defined, and then (1.1.5) has no mathematical sense. In (1.1.2), the information is transported along *characteristics*. A *characteristic* is a curve $t \mapsto x(t; x_0)$, which propagates the value $u_0(x_0)$ from $(0, x_0)$ along $(t, x(t))$, according to (1.1.5). Along the curve, the solution is constant and equal to $u_0(x_0)$. Therefore, the characteristic is solution of the following Cauchy problem:

$$\dot{x}(t) = f'(u(t, x)), \quad x(0) = x_0. \tag{1.1.7}$$

By the implicit function theorem, for smooth initial datum, the map $t \mapsto x(t)$ is locally invertible on an open neighborhood of $(0, x_0)$, and thus the map $u(t, x(t))$ is solution to Equation (1.1.5). Nonetheless, for larger times t, characteristics may cross (Figure 1.2), and the solution is thus not uniquely defined globally in time.

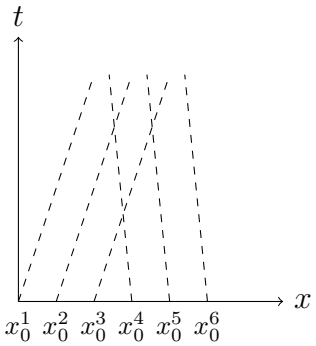

Figure 1.2 – A situation in which characteristics cross.

Since classical (smooth) solutions to the Cauchy problem (1.1.2) do not exist in general, we need to propose a weaker notion of solutions. We thus define them in the distributional sense. We present formally the idea in Equation (1.1.8), still assuming that the solutions u are smooth. The principle is to multiply the PDE by a smooth *test function* $\phi \in C_c^1([0, \infty) \times \mathbb{R})$, and then integrate by parts to transfer the derivatives on ϕ.

$$\begin{aligned} 0 &= \int_{\mathbb{R}_+} \int_{\mathbb{R}} (\partial_t u + \partial_x f(u)) \cdot \phi \; dxdt \\ &= -\int_{\mathbb{R}_+} \int_{\mathbb{R}} u \partial_t \phi dxdt - \int_{\mathbb{R}} u_0 \phi dx - \int_{\mathbb{R}_+} \int_{\mathbb{R}} f(u) \partial_x \phi dxdt. \end{aligned} \tag{1.1.8}$$

We now formulate the definition of weak solutions. While we use in this section the scalar case $n = 1$ to introduce mathematical definitions and properties, most of these will also apply to systems $n > 1$, and we then provide the general definitions for $n \in \mathbb{N}$ when possible.

Definition 1.1.1 (Definition of weak solutions)**.** Assume $u_0 \in \mathbf{L}^1_{\text{loc}}(\mathbb{R};\mathbb{R}^n)$. We say that a function $u : [0,\infty) \times \mathbb{R} \mapsto \mathbb{R}^n$ is a weak solution to the Cauchy problem (1.1.2) if $u \in C([0,\infty);\mathbf{L}^1_{\text{loc}}(\mathbb{R};\mathbb{R}^n))$ and it satisfies

$$\int_0^\infty \int_{\mathbb{R}} \big(u(t,x)\partial_t\phi(t,x) + f(u(t,x))\partial_x\phi(t,x)\big)dxdt + \int_{\mathbb{R}} u_0(x)\phi(0,x)dx = 0 \tag{1.1.9}$$

for any test function $\phi \in C^1_c([0,\infty)\times\mathbb{R};\mathbb{R}^n)$.

Since we expect the solution to develop discontinuities, let us investigate its behavior along discontinuity curves. Let us consider an open set $\Omega \subset \mathbb{R}_+ \times \mathbb{R}$ containing a smooth curve $\mathcal{C}$. We denote respectively by Ω_l and Ω_r the left and right side of Ω with respect to $\mathcal{C}$. Assume that u is smooth on each side of the curve, denoted by u_l on Ω_l and u_r on Ω_r. Finally suppose that $\mathcal{C}$ is a parametric curve $x = s(t)$, with speed $\dfrac{dx}{dt} = \dot{s}(t) = \sigma(t)$.

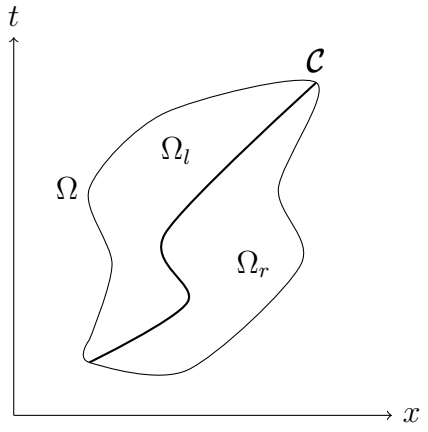

Figure 1.3 – Notations to introduce Rankine-Hugoniot conditions.

We select ϕ a test function with compact support in Ω, and assume that u is a weak solution of the scalar conservation law. Applying (1.1.9), we deduce

$$0 = \int_{\Omega_l} \big(u\partial_t\phi + f(u)\partial_x\phi\big)dxdt + \int_{\Omega_r} \big(u\partial_t\phi + f(u)\partial_x\phi\big)dxdt. \tag{1.1.10}$$

Since ϕ has compact support included in Ω and u is smooth on Ω_l, the Green-Gauss theorem yields

$$\int_{\Omega_l} \big(u\partial_t\phi + f(u)\partial_x\phi\big)dxdt = \int_{\mathcal{C}} (u_l n_1 + f(u_l)n_2)\phi dxdt \tag{1.1.11}$$

where $\underline{n} = (n_1, n_2)$ denotes the unit normal vector to $\mathcal{C}$ pointing outside Ω_l. Applying the same reasoning on Ω_r, and using (1.1.10) yields

$$\int_{\mathcal{C}} \big((u_r - u_l)n_1 + (f(u_r) - f(u_l))n_2\big)\phi dxdt = 0. \tag{1.1.12}$$

This remains valid for any test function ϕ, thus

$$(u_r - u_l)n_1 + (f(u_r) - f(u_l))n_2 = 0,\ (t,x) \in \mathcal{C}. \tag{1.1.13}$$

Since the curve is parametrized by $x = s(t)$ then $\underline{n} = \frac{(1,-\dot{s}(t))}{(1+\dot{s}(t)^2)^{1/2}}$. This with (1.1.13) implies

$$\sigma(t)(u_r - u_l) = f(u_r) - f(u_l). \tag{1.1.14}$$

Equation (1.1.14) is called the *Rankine-Hugoniot* condition and must be satisfied by weak solutions. As pointed out in [63, Section 3.4], weak solutions are in general not unique, and additional conditions must be enforced to derive uniqueness of the solution. [20, Section 4] proposes admissibility conditions to provide physical uniqueness of the solution.

Definition 1.1.2 (Entropy/entropy-flux pair)**.** We denote by (η, q) an entropy/entropy-flux pair for the conservation law $\partial_t u + \partial_x[f(u)] = 0$ if $\eta : \mathbb{R}^n \to \mathbb{R}$ is a continuously differentiable convex function, if $q : \mathbb{R}^n \to \mathbb{R}$ is continuously differentiable and if the following equality is satisfied:

$$\nabla\eta(z) \cdot Df(z) = \nabla q(z), z \in \mathbb{R}^n, \tag{1.1.15}$$

where Df corresponds to the Jacobian of f.

Remark 1.2. We note that (1.1.15) yields $\partial_t\eta(u) + \partial_x\big[q(u)\big] = 0$ if u is a classical solution to the conservation law. In addition, in the scalar case, any convex fonction η provides an entropy, associated to the flux $q(z) = \int_0^z \eta'(y)f'(y)dy$.

Definition 1.1.3 (Entropy inequality)**.** A weak solution u of (1.1.2) is *entropy admissible* if

$$\eta(u)_t + q(u)_x \leq 0 \tag{1.1.16}$$

in the distributional sense, for every pair (η, q) satisfying Definition 1.1.2. This corresponds to satisfying the following inequality:

$$\int_0^\infty \int_{-\infty}^\infty \big\{\eta(u(t,x))\phi_t(t,x) + q(u(t,x))\phi_x(t,x)\big\}dxdt \geq 0, \tag{1.1.17}$$

for any positive test function $\phi \in C_c^1([0,\infty) \times \mathbb{R}; \mathbb{R}_+)$.

An additional condition is derived in [105]. This physical criterion ensures that characteristic curves, and thus the propagation of solutions, all originate from the initial datum and not from shock curves.

Definition 1.1.4 (Lax condition)**.** A weak solution u of Equation (1.1.1) is admissible if at every point of discontinuity traveling with speed σ, separating two states u_l on the left and u_r on the right, the following inequality is satisfied:

$$f'(u_l) \geq \sigma \geq f'(u_r). \tag{1.1.18}$$

Remark 1.3. Definition 1.1.3 and Definition 1.1.4 are equivalent when the flux function f is strictly concave or convex in the scalar case.

Finally, we provide the general definition of the unique weak entropy solution of the Cauchy problem (1.1.2) with $n = 1$, as proposed by Kruzkov in [98].

Definition 1.1.5. A continuous map $u(t,\cdot) : [0,\infty) \mapsto \mathbf{L}^1_{\text{loc}}(\mathbb{R};\mathbb{R})$ is an entropy solution of (1.1.2) if it satisfies, for every constant $k \in \mathbb{R}$ and every $\phi \in C^1_{\text{c}}([0,\infty)\times\mathbb{R};\mathbb{R}_+)$

$$\int_0^\infty \int_{-\infty}^\infty \big\{|u-k|\partial_t\phi + sgn(u-k)(f(u)-f(k))\partial_x\phi\big\}dxdt + \int_{-\infty}^\infty |u_0-k|\phi(0,x)dx \geq 0. \tag{1.1.19}$$

Remark 1.4. For any $k \in \mathbb{R}$ one can define the entropy/entropy pair

$$\eta_k(u) = |u-k|, \quad q_k(u) = sgn(u-k)(f(u)-f(k)),\ u \in \mathbb{R} \tag{1.1.20}$$

which are called Kruzkov's entropies. This is an explicit formulation of entropy/entropy-flux pairs to consider in Definition 1.1.3 for scalar conservation laws.

Now that we have detailed admissibility conditions in order to obtain uniqueness of the solution, let us study a specific scalar Cauchy problem (1.1.2), *the Riemann problem*, in which the initial datum u_0 is a piecewise constant function, with a unique discontinuity:

$$u_0(x) = \begin{cases} u_l \text{ if } x < 0, \\ u_r \text{ if } x \geq 0. \end{cases} \tag{1.1.21}$$

The Riemann problem is used as a foundation to build solutions to more complex Cauchy problems. The mappings developed to solve Riemann problems are referred to as Riemann solvers. For simplicity, we assume here that f is a smooth strictly concave function, by coherence with the macroscopic traffic flow models detailed later. Since u is a solution in the distributional sense, and by linearity of both derivation and integration, we note that any function $u^\alpha = u(\alpha t, \alpha x), \alpha \in \mathbb{R}$, is also a solution. By uniqueness of the solution, we then look for self-similar solution $u(t,x) = u^\alpha(t,x),\ \forall\ \alpha \in \mathbb{R}$. Following the admissibilty conditions detailed above, we need to distinguish two cases.
Since f is stricly concave, condition (1.1.18) implies that a discontinuity line can only appear if $u_l < u_r$. Assume then that $u_l < u_r$. Based on the Rankine-Hugoniot condition, the unique entropy solution is a *shock wave* (see Figure 1.4), traveling with speed

$$u(t,x) = \begin{cases} u_l \text{ if } x < \sigma t, \\ u_r \text{ if } x \geq \sigma t, \end{cases} \tag{1.1.22}$$

where

$$\sigma = \frac{f(u_r)-f(u_l)}{u_r-u_l}. \tag{1.1.23}$$

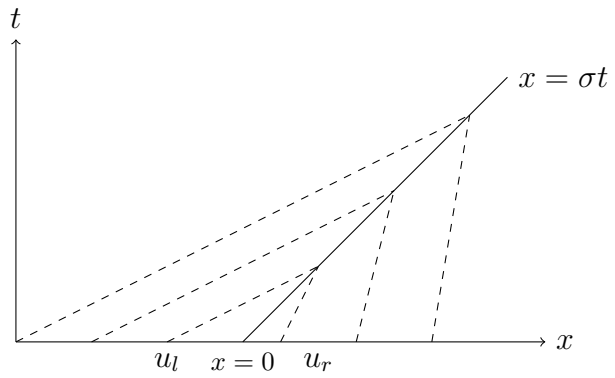

Figure 1.4 – Shock wave solving a Riemann problem with $u_l < u_r$.

Now assume that $u_l > u_r$, and suppose existence of a unique weak solution u of (1.1.2), (1.1.21). We then look for a stationary solution of the form $u(x,t) = v(\frac{x}{t})$. Let $\xi = \frac{x}{t}$. Assuming first that v is smooth, we can compute:

$$u_t + \big[f(u)\big]_x = -\frac{x}{t^2}v'(\xi) + f'(v(\xi))v'(\xi)\frac{1}{t} \tag{1.1.24}$$

$$= v'(\xi)\frac{1}{t}\big[f'(v(\xi)) - \xi\big]. \tag{1.1.25}$$

If the solution is non-constant, we necessarily have

$$f'\big(v(\xi)\big) = \xi. \tag{1.1.26}$$

In addition, we note that, if $\xi = f'(u_l)$ then $v(\xi) = u_l$ and the same way if $\xi = f'(u_r)$ then $v(\xi) = u_r$. Since we have assumed f to be strictly concave, then f' is locally invertible on $[f'(u_l), f'(u_r)]$. This, combined with the admissibility conditions, enables us to state that the unique weak solution to (1.1.2), (1.1.21) is given by

$$u(t,x) = \begin{cases} u_l & \text{if } x < f'(u_l)t, \\ f'^{-1}(\frac{x}{t}) & \text{if } f'(u_l)t \le x \le f'(u_r)t, \\ u_r & \text{if } x > f'(u_r)t. \end{cases} \tag{1.1.27}$$

This solution is called a *rarefaction wave* (see Figure 1.5). It satisfies both Equation (1.1.9) and admissibility conditions from Definition 1.1.4.

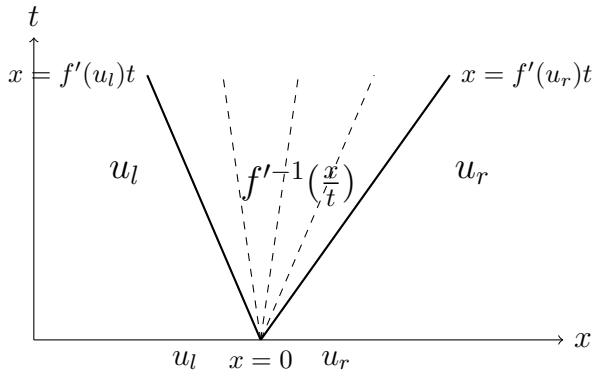

Figure 1.5 – Rarefaction wave solving a Riemann problem with $u_l > u_r$.

We can then summarize by providing the definition of the Riemann solver $\mathcal{R}$ for scalar conservation laws [69].

Definition 1.1.6. Consider the scalar conservation law (1.1.2) with the following Riemann datum, for $y_0 \in \mathbb{R}$:

$$u_0(x) = \begin{cases} u_l & \text{if} \quad x < y_0, \\ u_r & \text{if} \quad x \geq y_0. \end{cases}$$

The unique weak entropy solution to (1.1.2) is given by

$$u(t,x) = \mathcal{R}(u_l,u_r)(\xi) = \begin{cases} u_l & \text{if } u_l < u_r,\ \xi < \dfrac{f(u_l)-f(u_r)}{u_l-u_r} \\ & \text{or } u_l \geq u_r,\ \xi < f'(u_l), \\ u_r & \text{if } u_l < u_r,\ \xi \geq \dfrac{f(u_l)-f(u_r)}{u_l-u_r} \\ & \text{or } u_l \geq u_r,\ \xi > f'(u_r), \\ (f')^{-1}(\xi) & \text{if } u_l \geq u_r,\ f'(u_l) \leq \xi \leq f'(u_r), \end{cases} \tag{1.1.28}$$

with $\xi := \frac{x-y_0}{t}$, for $(t,x) \in (0,\infty) \times \mathbb{R}$.

Before providing an existence and uniqueness theorem, we need to recall the definition of functions with bounded variation.

Definition 1.1.7. Let a function $u \in \mathbf{L}^1_{\text{loc}}(\mathbb{R};\mathbb{R}^n)$. We define the *total variation* of u by

$$TV(u) = \sup \left\{ \sum_{i=1}^{N} |u(x_i) - u(x_{i-1})| \right\} \tag{1.1.29}$$

where the supremum is taken over all N-tuples $\{x_1, ..., x_N\} \in \mathbb{R}^N, N \in \mathbb{N}$. In addition we say that u is of *bounded variation*, and write $u \in BV(\mathbb{R})$, if $TV(u) < \infty$.

We can now provide the main result, and refer the reader to the pioneering work [98] and to [20, Section 6] for the details.

Theorem 1.1.1. *Let f be locally Lipschitz continuous, and let $u_0 \in \mathbf{L}^\infty(\mathbb{R})$. Then the Cauchy problem* (1.1.2) *admits a unique weak entropy solution u.*
In addition, if $u_0 \in BV(\mathbb{R})$, then u satisfies

$$\begin{aligned} &TV(u(t,\cdot)) \leq TV(u_0), \quad ||u(t,\cdot)||_{\mathbf{L}^\infty(\mathbb{R})} \leq ||u_0||_{\mathbf{L}^\infty(\mathbb{R})}, \quad \forall t \geq 0. \\ &||u(t,\cdot) - u(s,\cdot)||_{\mathbf{L}^1(\mathbb{R})} \leq ||f'||_\infty |t-s|\ TV(u_0), \qquad \forall t,s \geq 0. \end{aligned}$$

Now that we have exposed the main concepts on the scalar conservation law, we will investigate the case of systems of conservation laws, *i.e.* the case where $u \in \mathbb{R}^n, n > 1$ is actually a vector.

1.1.2 Systems of conservation laws

We now assume that $u : \mathbb{R}_+ \times \mathbb{R} \to \mathbb{R}^n, n > 1$, and consider the Cauchy problem (1.1.2), where $f : \mathbb{R}^n \to \mathbb{R}^n$ is a smooth flux function, and $u_0 : \mathbb{R} \to \mathbb{R}^n$.

The definition of weak entropy solutions to systems of conservation laws are given by Definitions 1.1.2 to 1.1.4. Nonetheless, there is no equivalent formulation of Krukzkov's entropies (Definition 1.1.5) to systems, *i.e.* there is no explicit formula of admissible entropy/entropy-flux pairs for systems of conservation laws.

Let us now formally explain the construction of solutions to systems of conservation laws. Assume first that u is a classical solution of (1.1.2). We can then rewrite the system in its quasilinear form, where $Df(u)$ denotes the jacobian matrix of the flux f

$$u_t + Df(u)u_x = 0. \tag{1.1.30}$$

Definition 1.1.8 (Hyperbolic system)**.** We say that the system (1.1.30) is *strictly hyperbolic* if for every $u \in \mathbb{R}^n$, $Df(u)$ has n distinct real eigenvalues $\lambda_1(u) < \cdots < \lambda_n(u)$.

For strictly hyperbolic systems and for each $u \in \mathbb{R}^n$, we can derive a normalized base of right eigenvectors of $\mathbb{R}^n$, denoted $\{r_1(u), .., r_n(u)\}$. This leads us to the next definition:

Definition 1.1.9. For $i \in \{1, .., n\}$, we say that the i-th characteristic field is *genuinely non-linear* if

$$\nabla\lambda_i(u) \cdot r_i(u) \neq 0, \quad \forall\ u \in \mathbb{R}^n.$$

Else, we say that the i-th characteristic field is *linearly degenerate* if

$$\nabla\lambda_i(u) \cdot r_i(u) = 0, \quad \forall\ u \in \mathbb{R}^n.$$

Remark 1.5. For any genuinely non-linear field, we can choose the orientation of the eigenvector r_i such that $\nabla\lambda_i(u) \cdot r_i(u) > 0,\ \forall\ u \in \mathbb{R}^n$.

Let us now detail the construction of the solutions to the Riemann problem for systems, *i.e.* consider (1.1.2), (1.1.21). Since u is a vector, the two states u_l and u_r are no longer necessarily connected by a single rarefaction wave or a a shock wave. We first define rarefaction curves and shock curves.

Definition 1.1.10. Let $u_0 \in \mathbb{R}^n$ be given and $i = \{1, .., n\}$. We denote by $s \mapsto R_i(s)(u_0)$ the parametrized integral curve of the eigenvector r_i passing through u_0 and call it i-th rarefaction curve through u_0. It satisfies the following Cauchy problem:

$$\begin{cases} \dfrac{d}{ds} R_i(s)(u_0) &= r_i(R_i(s)(u_0)), \quad s \in \mathbb{R}, \\ R_i(0)(u_0) &= u_0. \end{cases}$$

Assume now that there exists $i \in \{1, .., n\}$ and some parameter $\bar{s} > 0$ such that u_l and u_r are connected through the i-rarefaction curve, *i.e.* $u_r = R_i(\bar{s})(u_l)$. By genuine non-linearity, the function $s \mapsto \lambda_i(R_i(s)(u_l))$ is strictly increasing and maps $[0, \bar{s}]$ onto $[\lambda_i(u_l), \lambda_i(u_r)]$. Then the following function $u(t, x)$ is a weak entropy solution of (1.1.2), (1.1.21) for $(t, x) \in [0, \infty) \times \mathbb{R}$ [20]:

$$u(t,x) = \begin{cases} u_l & \text{if } x/t < \lambda_i(u_l), \\ R_i(s)(u_l) & \text{if } x/t \in [\lambda_i(u_l), \lambda_i(u_r)],\ x/t = \lambda_i(R_i(s)(u_l)), \\ u_r & \text{if } x/t > \lambda_i(u_r). \end{cases} \tag{1.1.31}$$

We now detail the construction of shocks. We aim at generalizing the Rankine-Hugoniot conditions introduced in Section 1.1.1. Given a left state u_l, we need to determine the set of right states u_r such that u_l and u_r can be connected through a shock wave moving with speed λ, *i.e.* such that $f(u_r) - f(u_l) = \lambda(u_r - u_l)$. We can thus define shock curves with the following theorem:

Definition 1.1.11. Given an initial state $u_l \in \mathbb{R}^n$, for any $i = \{1, .., n\}$, we define the i-th shock curve S_i passing through u_l by

$$S_i(u_l) = \big\{ u_r \in \mathbb{R}^n | f(u_r) - f(u_l) = \lambda(u_r - u_l), \exists\ \lambda = \lambda(u_l, u_r) \in \mathbb{R} \big\}. \tag{1.1.32}$$

The velocity λ satisfies

$$\lim_{u_r \to u_l} \lambda(u_l, u_r) = \lambda_i(u_l). \tag{1.1.33}$$

In addition, if the i-th characteristic field is genuinely non-linear, and if $u_r \in S_i(u_l)$, we say that the shock connecting u_l to u_r with speed $\lambda(u_l, u_r)$ is *Lax-admissible* if it verifies

$$\lambda_i(u_l) > \lambda(u_l, u_r) > \lambda_i(u_r). \tag{1.1.34}$$

Remark 1.6. The velocity λ of the wave is then decreasing between $\lambda_i(u_l)$ and $\lambda_i(u_r)$. The shock curve S_i can be rewritten as a parametric curve $S_i(s)(u_l), s \in \mathbb{R}$, for s sufficiently

small. If the i-th characteristic field is genuinely non-linear, the inequality $\nabla\lambda_i(u_0)\cdot r_i(u_0) > 0$ uniquely determines the orientation of the eigenvector $r_i(u_0)$ and then the parametrization choice of S_i. On the other hand, if the field is linearly degenerate, the orientation can be chosen arbitrarily following Theorem 1.1.2. We refer the reader to [20, Section 6] for the details.

If the i-th charateristic field is linearly degenerate, it satisfies the following theorem:

Theorem 1.1.2. *Assume that the i-th characteristic field is linearly degenerate. Then for each $u_l \in \mathbb{R}^n$, the shock curve $S_i(u_l)$ and the rarefaction curve $R_i(u_l)$ coincide. In addition, the velocity of the wave, called contact discontinuity, is equal to $\lambda_i(u_l)$.*

The states u_l and u_r can in general be connected by a set of n rarefactions or shock curves if they are sufficiently close. Define the parametric function

$$\psi_i(s)(u_l) = \begin{cases} R_i(s)(u_l) & \text{if } s \geq 0, \\ S_i(s)(u_l) & \text{if } s < 0. \end{cases} \tag{1.1.35}$$

We can then identify a set of n parameters s_i such that $u_r = \psi_n(s_n) \circ ... \circ \psi_1(s_1)(u_l)$. This set of parameters enable to derive a set of intermediate states $w_0, .., w_n$ iteratively defined such that

$$w_0 = u_l, \quad w_i = \begin{cases} R_i(s_i)(w_{i-1}) & \text{if } s_i \geq 0, \\ S_i(s_i)(w_{i-1}) & \text{if } s_i < 0. \end{cases}, \quad w_n = u_r. \tag{1.1.36}$$

Therefore, we can provide the following formulation for the solution of the Riemann problem (1.1.2), (1.1.21) for $(t, x) \in [0, \infty) \times \mathbb{R}$:

$$u(t,x) = \begin{cases} u_l & \text{if } x/t < \lambda_1(u_l), \\ w_i & \text{if } \lambda_i(w_i) < x/t < \lambda_{i+1}(w_i), i = \{1, .., n-1\}, \\ R_i(s)(w_{i-1}) & \text{if } \lambda_i(w_{i-1}) \leq x/t \leq \lambda_i(w_i) \text{ and } x/t = \lambda_i(R_i(s)(w_{i-1})), i = \{1, .., n\}, \\ u_r & \text{if } x/t > \lambda_n(u_r). \end{cases} \tag{1.1.37}$$

From all this elements, we can provide the following theorem (see [20] for details):

Theorem 1.1.3. *Let $u_l \in \mathbb{R}^n$. Then there exists a compact neigborhood K of $\mathbb{R}^n$ centered around u_l, such that for any $u_r \in K$, the Riemann problem* (1.1.2), (1.1.21) *admits a weak solution $u(t, x)$ of the form* (1.1.37).

The Riemann problem is then again used as a building block to construct global weak entropy solutions of system (1.1.2). The proof of uniqueness of these weak entropy solutions to hyperbolic systems relies on the construction of Lipschitz continuous semigroups. We refer the reader to the pioneering work [19] and to [21, 23, 24, 26].

In Chapter 2, we will use the notion of Temple class systems [138], which is a notion particularly fitted for explicit computation of both solutions and entropies. We refer the reader to [137] for the mathematical details.

Definition 1.1.12. We say a differentiable function $w^i : \mathbb{R}^n \mapsto \mathbb{R}$ is an i-th Riemann invariant for the system (1.1.2) if it satisfies

$$\nabla w^i(u) \cdot r_i(u) = 0, \ i = \{1, .., n\}, \ u \in \mathbb{R}^n. \tag{1.1.38}$$

This is equivalent to state that w^i is constant along the rarefaction curve R_i.

Remark 1.7. If $n \geq 3$, Riemann invariants do not exist in general.

Definition 1.1.13. We say that a $n \times n$ system of conservation laws (1.1.2) is a *Temple class system* if it is strictly hyperbolic and if for each $i = \{1, .., n\}$, there exists n i-th Riemann invariant w_i, and the i-th shock curve and the i-rarefaction curve coincide.

Remark 1.8. This definition follows the work of [138], and is actually weaker than the notion presented in [137], in which the author imposes that the level sets $\{u \in \mathbb{R}^n, w_i(u) = \text{constant}\}$ are hyperplanes.

For Temple class systems, we can define positively invariant domains $\mathcal{D}$, which are compact subsets of $\mathbb{R}^n$ of the shape $[a_1, b_1] \times \ldots \times [a_n, b_n]$ in Riemann coordinates such that, if $u_0 : \mathbb{R} \mapsto \mathcal{D}$ with bounded variation then the solution to (1.1.2) is included in $\mathcal{D}$. We can then precise the following theorem, which will be used in Chapter 2.

Theorem 1.1.4 ([117])**.** *Assume that* (1.1.2) *is a Temple class system, and $\mathcal{D}$ is a positively invariant domain compact in $\mathbb{R}^n$. For any initial datum $u_0 : \mathbb{R} \mapsto \mathcal{D}$ with bounded variation, there exists a constant $C_{\mathcal{D}}$ such that the Cauchy problem* (1.1.2) *admits a weak entropy solution $u : \mathbb{R} \mapsto \mathcal{D}$ which satisfies*

$$TV(u(t, \cdot)) \leq C_{\mathcal{D}} \ TV(u_0), \quad ||u(t, \cdot) - u(s, \cdot)||_{\mathbf{L}^1(\mathbb{R})} \leq C_{\mathcal{D}} \ |t - s| \ TV(u_0), \quad \forall s, t > 0.$$

1.1.3 Wave-Front Tracking approximations

We have detailed in the previous section how to solve a Riemann problem for conservation laws. In this section, we detail the Wave-Front Tracking method, which consists in an algorithm to construct piecewise constant approximate solutions to a Cauchy problem with more general initial datum. It relies on the fact that for any Riemann problem we can explicitly build a solution, and that the obtained solution propagates with finite speed. As we will see later, this method can be used to prove existence of solutions (Chapter 2), and to generate numerical simulations (Chapter 3). In this last sense, Wave-Front Tracking represents an alternative to the classical Finite Volume methods popular in numerical approximations of conservation laws [79, 116].

Let us precise the mathematical approach, and detail each step of the method, for Cauchy problem (1.1.2). Let $\epsilon > 0$ and a given time horizon $T > 0$.

Step 1. Approximate the initial datum $u_0 \in BV(\mathbb{R})$ by a piecewise constant function u_0^ϵ which satisfies $TV(u_0^\epsilon) \leq TV(u_0)$ and $||u_0^\epsilon - u_0||_{\mathbf{L}^\infty} \leq \epsilon$. Existence of such a function is guaranteed by [20, Lemma 2.2].

Step 2. At time $t = 0$, solve the Riemann problem at each discontinuity of u_0^ϵ. To do so, we consider an approximate Riemann solver in order to generate piecewise constant approximate solutions. This solver does not modify shock waves and contact discontinuities, which are by nature piecewise constant. If the Riemann problem includes a centred rarefaction wave (1.1.31), which is a continuous function, we need to provide a method to approximate up to ϵ the rarefaction fan by piecewise constant functions. Following [20, Section 7], any i-centred rarefaction wave is approximated by a fan of waves $(t, x_\alpha(t))$ of size ϵ. One can define $n+1$ intermediate states $w_0, .., w_n$ such that $w_0 = u_l, w_n = u_r$ and two consecutives fronts w_{j-1}, w_j are separated by a jump with speed λ_j, and such that $|\lambda_j - \lambda_i(w_{j-1}, w_j)| \leq \epsilon$. The fronts violate the Rankine-Hugoniot and the entropy conditions with a global error of order $\mathcal{O}(\epsilon)$, which will enable us to retrieve the weak entropy inequalities when sending ϵ to zero. We then define the approximate function

$$u^\epsilon(t,x) = \begin{cases} u_l & \text{if } x/t < \lambda_i(u_l), \\ w_1 & \text{if } x/t \in [\lambda_i(u_l), \lambda_1], \\ w_2 & \text{if } x/t \in [\lambda_1, \lambda_2], \\ \dots, & \\ w_{n-1} & \text{if } x/t \in [\lambda_{n-1}, \lambda_i(u_r)], \\ u_r & \text{if } x/t > \lambda_i(u_r). \end{cases}$$

Step 3. The approximate solution can be prolonged until the first time $t_1 > 0$ at which two fronts interact. We can assume without loss of generality that only two waves interact at a given time, by possibly altering slightly their speed. At time t_1, treat $u^\epsilon(t_1, x)$ as a new piecewise initial datum, and restart the process at Step 1, up to $T > 0$.

For every $\epsilon > 0$, we then build a sequence of approximations $u^\epsilon(t,x), (t,x) \in [0,T] \times \mathbb{R}$. For general $n \times n$ systems, the main difficulty lies in the fact that the number of waves may become infinite in finite time, thus preventing from reaching any horizon $T > 0$. In [20, Section 7], the author proposes two modified algorithms, one using an accurate Riemann solver, and the second using a simplified Riemann solver introducing non-physical fronts, to ensure that the number of waves remains finite. We then use these approximations to prove existence of a limit u when $\epsilon \to 0+$, usually using Helly's Theorem [20, Theorem 2.4], and then prove that this limit satisfies the integral conditions of a weak entropy solution.

Theorem 1.1.5 (Helly's Theorem)**.** *Consider a sequence of functions $\{u_N\}_{N\in\mathbb{N}} : [0,\infty) \times \mathbb{R} \mapsto \mathbb{R}^n$ with the following properties:*

$$TV(u_N(t,\cdot)) \leq C, \quad |u_N(t,x)| \leq M, \ \forall (t,x) \in [0,\infty) \times \mathbb{R},$$
$$\int_{-\infty}^{\infty} |u_N(t,x) - u_N(s,x)| dx \leq L|t-s|, \quad \forall t, s \geq 0,$$

for some constants C, M, L. Then there exists a subsequence u_μ which converges to some

function $u \in \mathbf{L}^1_{loc}([0,\infty) \times \mathbb{R}; \mathbb{R}^n)$*, which satisfies:*

$$\int_{-\infty}^{\infty} |u(t,x) - u(s,x)| dx \leq L|t-s|, \quad \forall t, s \geq 0.$$

We illustrate the Wave-Front Tracking algorithm in Figure 1.6 for the scalar conservation law.

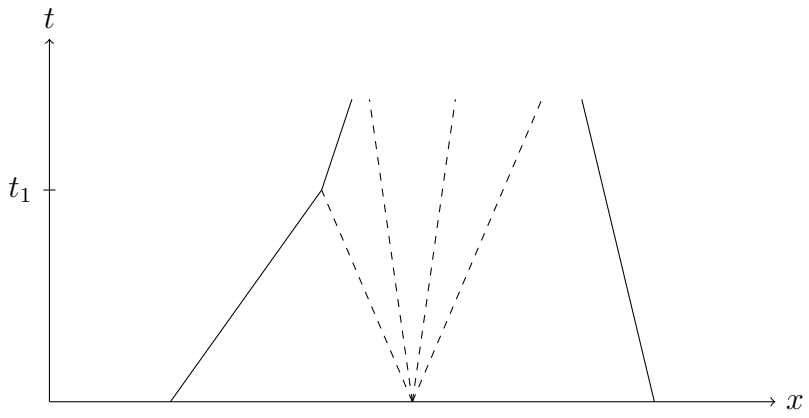

Figure 1.6 – Illustration of the Wave-Front Tracking algorithm. Shock waves are represented in full line, while approximate rarefaction fans are represented in dashed lines.

1.2 Macroscopic traffic flow models

In this section, we detail the application of hyperbolic partial differential equations to traffic flow modeling.

1.2.1 The Lighthill-Whitham-Richards Model

The idea of modeling traffic as a fluid was described in 1955 with Lighthill and Whitham [120] and separately in 1956 with Richards [134]. In these articles, the authors introduce the notion of conservation of vehicles on a given road, and use a scalar conservation law to describe the dynamics in both space and time. The main variable they propose to describe traffic is the density of vehicles, denoted by ρ, which represents the number of vehicles per unit length of road. In addition, they introduce the mean velocity of vehicles, denoted by v. Finally, they define the flow of vehicles f, *i.e.* the number of vehicles crossing a given position during a given time period, such that $f = \rho v$.
Consider now a unidirectional stretch of road, spatially described by the space variable $x \in \mathbb{R}$. In addition, the time is indexed by $t \geq 0$. The model is based on the physical assumption that the number of vehicles, *i.e.* the integral of the density, must be conserved

through time on any segment $[a, b]$ of the road (see Figure 1.1). This mathematically corresponds to

$$\int_a^b \partial_t \rho(t,x)dx = \frac{d}{dt}\int_a^b \rho(t,x)dx = f(\rho(t,a)) - f(\rho(t,b)) = -\int_a^b \partial_x\big[f(t,x)\big]dx.$$

We thus retrieve the scalar conservation law

$$\partial_t \rho + \partial_x\big[\rho v\big] = 0. \tag{1.2.1}$$

The density is such that $\rho \in [0, \rho_{\max}]$, where $\rho_{\max} > 0$ is the maximum density and describes a bumper-to-bumper situation. In order to close the model, they assume that the velocity of vehicles only depends on the density, $v = V_e(\rho)$, and it is a non-increasing function, from a given maximum speed $V_e(0) = v_{\max} > 0$ to $V_e(\rho_{\max}) = 0$. The Lighthill-Whitham-Richards model is then the following:

$$\begin{cases} \partial_t \rho + \partial_x\big[f(\rho)\big] = 0, & x \in \mathbb{R},\ t > 0, \\ \rho(0,x) = \rho_0(x), & x \in \mathbb{R}, \end{cases} \tag{1.2.2}$$

where we assume that $f : [0, \rho_{\max}] \mapsto [0, f_{\max}]$ is a smooth function which verifies $f(0) = f(\rho_{\max}) = 0$, $f(\rho) = \rho V_e(\rho)$ and $\rho_0(\cdot) \in [0, \rho_{\max}]$ is an appropriate initial datum. In order to calibrate the model(*i.e.* the flux function f), experimental campains were realized on public roads, by observing the fluxes of vehicles as a function of the density (see [96]). An example is illustrated in Figure 1.7.

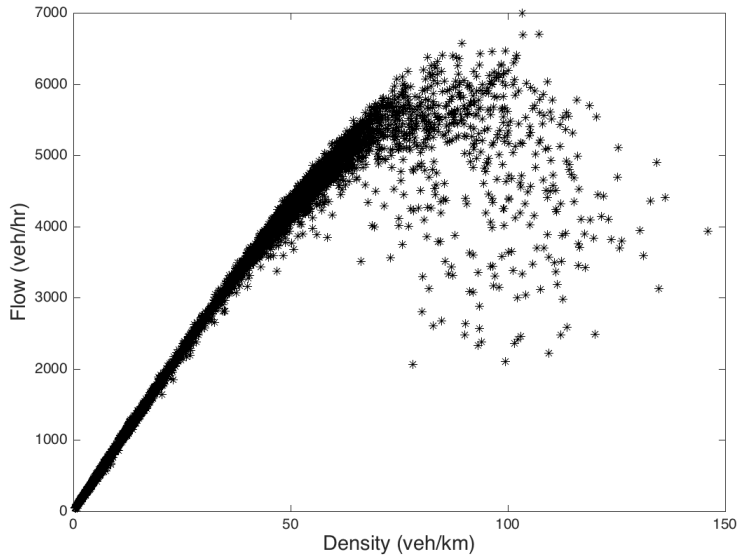

Figure 1.7 – Experimental fundamental diagram on highway A50 in France, 2015.

Following these observations, many models were proposed for the function $f(\rho)$, which is also frequently referred to as *fundamental diagram*. The easiest assumption is to suppose that the velocity $V_e(\rho)$ is linear (see Figure 1.8):

$$V_e(\rho) = v_{\max}(1 - \frac{\rho}{\rho_{\max}}), \tag{1.2.3}$$

$$f(\rho) = \rho v_{\max}(1 - \frac{\rho}{\rho_{\max}}). \tag{1.2.4}$$

This model is referred to as the *Greenshields* fundamental diagram [83]. Other modeling assumptions were proposed in the literature, we refer the reader to [72, 121] for additional examples and comparisons. In the following, we will assume that the flux function f is a strictly concave smooth function. Thus it admits a unique maximum point attained for $\rho_{\text{crit}} \in [0, \rho_{\max}]$, such that $f(\rho_{\text{crit}}) = f_{\max}$. For $\rho \leq \rho_{\text{crit}}$ the traffic is said to be in free flow and for $\rho > \rho_{\text{crit}}$ the traffic is congested.

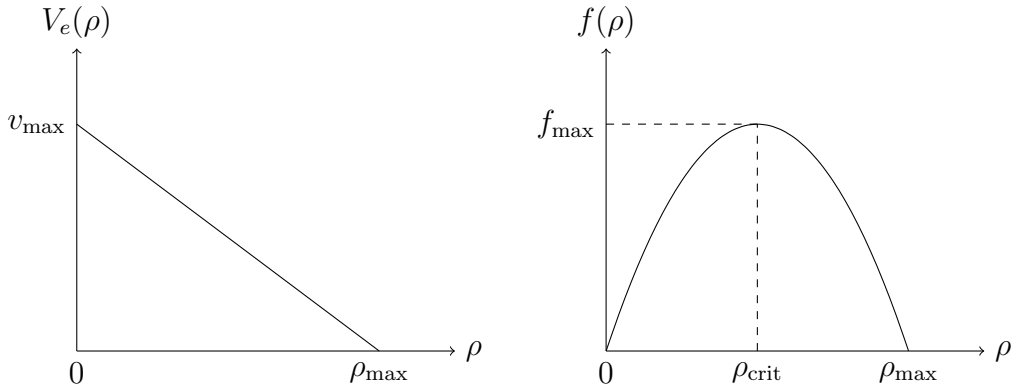

Figure 1.8 – The linear velocity and the associated fundamental diagram.

The solutions of the Riemann problem and the Cauchy problem (1.2.2) can then be solved according to the description detailed in Section 1.1.1.

1.2.2 Second order traffic flow models

In the LWR model, the assumption that the velocity v only depends on the density of vehicles seems rather restrictive, and does not enable to include other parameters to model more accurately physical observations, especially in the congested phase, see Figure 1.7. The function $V_e(\rho)$ describes an equilibrium state, which is not always observed in reality. In order to capture particular characteristics of traffic flow, like stop-and-go waves, second-order models were developed afterwards. The first one was the Payne-Whitham model (PW) [126, 143]. It consists of a 2×2 system, coupling the mass conservation law to a second partial differential equation modeling the evolution of convective acceleration of

traffic. In the following, the velocity of traffic v is an independent variable, contrary to the LWR model. The PW model reads as

$$\begin{cases} \partial_t \rho + \partial_x(\rho v) = 0, \\ \partial_t v + v\partial_x v + \frac{1}{\rho}\partial_x(A_e(\rho)) = \frac{V_e(\rho)-v}{\delta}, \end{cases} \qquad x \in \mathbb{R},\ t > 0, \tag{1.2.5}$$

where $\frac{1}{\rho}\partial_x A_e(\rho)$ represents an ancitipation term, and models the reaction of drivers for a given density situation. Several models were proposed in the literature, for instance $A_e(\rho) = D\rho, D > 0$, by Whitham [143]. $V_e(\rho)$ represents the equilibrium speed of traffic. The right hand side of the second equation $\frac{V_e(\rho)-v}{\delta}$ represents a relaxation term of the velocity towards the equilibrium speed, in which $\delta > 0$ models the reaction time of drivers.

Unfortunately, as mentioned in [56], model (1.2.5) presents some drawbacks, like the unrealistic fact that information may propagate faster than the actual velocity of cars, and also that in specific cases vehicles may travel backwards. These drawbacks are the consequence of the differences of physical behavior between a classical fluid and traffic flow. For instance, traffic is anisotropic, meaning that vehicles adapt mostly to the others in front of them, while a fluid is isotropic. In addition, contrary to fluid particles, drivers may have an instrinsic behavior, like a tendency to aggressive driving, independ from the traffic density.

Taking these limitations into account, Aw, Rascle [9] and Zhang [146], proposed a new second-order model, which is referred to as the Aw-Rascle-Zhang (ARZ) model:

$$\begin{cases} \partial_t \rho + \partial_x(\rho v) = 0, \\ \partial_t(v + p(\rho)) + v\partial_x(v + p(\rho)) = 0, \end{cases} \qquad x \in \mathbb{R},\ t > 0, \tag{1.2.6}$$

where $p(\rho)$ is a pseudo-pressure function accounting for drivers' anticipation of downstream density changes. A possible choice of pressure is $p(\rho) = \rho^\gamma, \gamma > 0$. The system can be written under conservative form:

$$\begin{cases} \partial_t \rho + \partial_x(\rho v) = 0, \\ \partial_t(\rho(v + p(\rho))) + \partial_x(\rho v(v + p(\rho))) = 0, \end{cases} \qquad x \in \mathbb{R},\ t > 0. \tag{1.2.7}$$

Finally, in [81, 132], the authors introduce the notion of relaxation which appeared in the Payne-Whitham model to force the velocity of the flow to relax towards the equilibrium speed:

$$\begin{cases} \partial_t \rho + \partial_x(\rho v) = 0, \\ \partial_t(\rho(v + p(\rho))) + \partial_x(\rho v(v + p(\rho))) = \rho\frac{V_e(\rho)-v}{\delta}, \end{cases} \qquad x \in \mathbb{R},\ t > 0, \tag{1.2.8}$$

where $V_e(\rho) \geq 0$ is a non-increasing function which still represents the equilibrium speed, and $\delta > 0$ is a relaxation parameter. The ARZ model with relaxation is today the most classical second order model, and we will prove its well-posedness in Chapter 2. In [8], the authors describe the connection between the ARZ model and microscopic follow-the-leader

model, and show that the homogeneous ARZ model (1.2.6) can be interpreted as the limit of a discrete microscopic model. In [64], the authors discuss the calibration of the model with experimental data, and more particularly the choice of the equilibrium speed $V_e(\rho)$ in the ARZ model with relaxation (1.2.8). In the engineering literature, second order models are usually referred to as *Generic Second Order Models (GSOM)*, a notion which embeds the models cited above [109, 111].

We can cite many more macroscopic traffic flow models, which we summarize in the listing below (for a complete review, see [67]):

- Following [96], who observed that a fundamental diagram is not necessarily well defined experimentally, phase transition models were introduced in [45]. They distinguish a free flow phase, in which they only consider the LWR model, from a congested phase, in which they impose a second order model, thus allowing for non-continuous fundamental diagrams. Well-posedness of the model was proved in [47]. Phase transitions in the Aw-Rascle-Zhang model are introduced in [76].

- In order to differentiate categories of vehicles, driving habits or destination constraints for instance, multipopulation models were introduced separately by [144] and [14]. They consists in an extension of the LWR model, since each population indexed by i is assumed to satisfy the LWR model with density ρ_i and velocity v_i. The interaction between categories of vehicles is then embedded in the speed function.

- An extension to the LWR model for multilane roads was proposed in [82]. In this model, the authors introduce two different equilibrium velocity curves. When the traffic density is low, overtaking and switching lane is easy, and thus the corresponding equilibrium velocity is high. When the traffic is dense, overtaking and changing lane may not be possible, and then the equilibrium velocity is lower. We also refer the reader to [46, 92].

- [86] introduced a third order model, in which a third equation is added to describe evolution of a variance θ of velocity, describing the probability of apparition of traffic jams.

1.2.3 Traffic flow models in urban applications

In the following section, we focus on the application of macroscopic traffic flow models to urban situations.

1.2.3.a Connecting traffic flow models at intersections

All the models detailed in the previous section were initially designed for highway applications, which represent the simplest case study, since it can be modeled by long stretches of road with few entries or exits. Nonetheless, these models do not necessarily adapt realistically to urban applications, in which the road environment is significantly

different. On a urban road network, one can find multiple intersections, stop signs, traffic lights, pedestrian crossings, and traffic with various origins and destinations, which are absent from highways.

In [67, Section 2.14], the authors identify three required features of traffic flow models for urban applications and confront the macroscopic traffic flow models to these criteria:

- vehicles must travel with postive speed,
- vehicles can only have a zero velocity when they encounter maximum density $\rho_{\max}$,
- right before a red light, the density must be equal to the maximum density.

Solving conservation laws on networks is not trivial, because of the difficulty of modeling the dynamics at the junctions, and more precisely the fact that the boundary conditions on incoming and outgoing links at a given junction are coupled and may depend on the solutions on adjactent links. In order to allocate flow at junctions one has to define additional constraints. The LWR model was first applied to unidirectional networks in [91]. The authors note that drivers will generally try to avoid congestion by possibly changing paths. That is why they propose an "entropy condition" which maximizes the flux of vehicles at the level of the junction. Their work was extended to general networks in [44]. We also refer the reader to [32, 57, 67, 68, 69, 70, 87, 89]. A road network can be represented by a directed graph $\mathcal{G} = \{\mathcal{L}, \mathcal{J}\}$ (Figure 1.9a), where $\mathcal{L}$ is a set of oriented links representing the roads and $\mathcal{J}$ is a set of nodes representing the intersections. Each link $l \in \mathcal{L}$ can be spatially represented by an open set I_l. We can then define the density of vehicles $\rho_l = \rho_l(t, x)$ for $(t, x) \in \mathbb{R}_+ \times I_l$ and use the LWR model to describe the dynamics of vehicles on each road. In addition, one needs to define coupling conditions to allocate traffic at junctions. Since we consider here the LWR model, with strictly concave flux function f and densities contained in the compact set $[0, \rho_{\max}]$, the information propagates at finite speed, and any road network can be mathematically reduced to one junction (Figure 1.9b), with a set $\mathcal{I}$ of incoming links and a set $\mathcal{O}$ of outgoing links. Each incoming link $i \in \mathcal{O}$ is modeled by the half line $]-\infty, 0[$, and each outgoing link $j \in \mathcal{O}$ is modeled by the half line $]0, \infty[$.

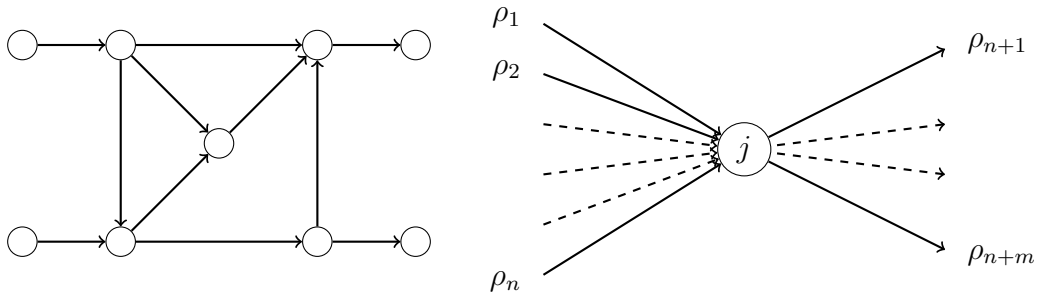

(a) A road network modeled as a directed graph.

(b) Illustration of junction $j \in \mathcal{J}$, with a set $\mathcal{I}$ of n incoming links and a set $\mathcal{O}$ of m outgoing links.

In order to construct solutions at a given junction, the authors define Riemann problems and Riemann solvers.

Definition 1.2.1. At a given intersection with n incoming links and m outgoing links, a Riemann problem is a Cauchy problem with initial data constant on every adjacent link. A Riemann solver is a map that associates to the initial datum on each link $(\rho_{1,0}, .., \rho_{n,0}, \rho_{n+1,0}, ..\rho_{n+m,0})$ the corresponding traces values at the junction $(\bar{\rho}_1, .., \bar{\rho}_n, \bar{\rho}_{n+1}, ..\bar{\rho}_{n+m})$. The solution on a given incoming link i is given by waves solutions to the Riemann problem $(\rho_{i,0}, \bar{\rho}_i)$ traveling with negative speed, and the solution on a given outgoing link j is given by waves solutions to the Riemann problem $(\rho_{j,0}, \bar{\rho}_j)$ traveling with positive speed.

We note that solutions to general initial boundary value problems may not necessary attain boundary conditions [13, 69]. That is why Definition 1.2.1 enforces a condition on the sign of waves, in order to define Riemann solvers in terms of fluxes and then ensure that the boundary conditions are compatible with the solutions to the Cauchy problem. To conserve the number of vehicles at the junction, we assume that the sum of flows is conserved at the junction, *i.e.*

$$\sum_{i\in\mathcal{I}} f(\rho_i(t,0-)) = \sum_{j\in\mathcal{O}} f(\rho_i(t,0+)),\ \forall t > 0.$$

Depending on the choice of the Riemann solver, additional rules may be required to properly define the model. We state the two most usual:

(i) For any intersection with $\mathcal{I}$ incoming links and $\mathcal{O}$ outcoming links, there exists a distribution matrix $\boldsymbol{\theta} \in [0,1]^{n\times m}$ such that $\left\{\boldsymbol{\theta}_{i,j}\right\}_{i\in\mathcal{I},j\in\mathcal{O}}$ represents the ratio of vehicles traveling from road i to j and $\sum_{j\in\mathcal{O}} \boldsymbol{\theta}_{i,j} = 1, \forall\ i \in \mathcal{I}$. In addition, the sum of the incoming fluxes at the junction is maximized.

(ii) In order to allocate incoming flows on the outgoing roads, for each incoming link $i \in \mathcal{I}$, we define a time-dependent priority coefficient $\mathbf{c}_i(t) \in [0,1],\ t \geq 0$, which denotes the order of priority given to the entry i in the junction at time t. We will precise the use of such coefficients in Chapter 4.

Once these Riemann solvers and modeling assumptions are established, wave-front tracking or finite volume methods enable us to build approximate solutions to more general Cauchy problems. The construction of Riemann solvers to solve $1\times 1, 2\times 1, 1\times 2$ and 2×2 junctions are fully detailed in [67]. Unfortunately the general formulation of the Riemann solver for a general $n\times m$ junction is not explicit. In addition, these methods may involve a loss of information at junctions, because they maximize the sum of incoming and outgoing fluxes, without keeping track of every commodity. Finally, the solution does not necessarily depend in a Lipschitz continuous way on the initial datum, as pointed out in [69, Section 5] and [31]. Continuity with respect to the initial datum is required to rigorously solve global optimization problems, for instance to address the *Dynamic Traffic*

Assignment (DTA) problem, which consists in optimizing trajectories of vehicles on networks in order to reduce travel times and congestion.

1.2.3.b Traffic flow models on networks with buffers

To overcome these limitations, traffic flow models with buffers at junctions have been introduced. The dynamics of each buffer, formally representing a queue of cars stored at the level of the junction, is then described by an ordinary differential equation coupling the incoming and outcoming fluxes. This method was first proposed for supply-chain networks in [80, 84, 88] and then adapted to traffic flow on networks in [66, 71, 89].

Let us now explain the single buffer model with limited capacity, as described in [66] and consider a prototype network of a single junction with $\mathcal{I}$ incoming roads and $\mathcal{O}$ outgoing roads. On each link indexed by $l \in \{1, \dots, n+m\}$, the density $\rho_l(t,x) \in [0, \rho_{l\max}], (t,x) \in [0,\infty[\times I_l$ satisfies the LWR model

$$\begin{cases} \partial_t \rho_l(t,x) + \partial_x \big[f_l(\rho_l(t,x)) \big] = 0, & (t,x) \in \mathbb{R}_+ \times I_l, \\ \rho_l(0,x) = \rho_{l,0}(x), & x \in I_l. \end{cases} \tag{1.2.9}$$

The flux f_l is a strictly concave smooth function satisfying $f_l(0) = f_l(\rho_{l\max}) = 0$. The junction is associated to a buffer, characterized by a time-dependent state variable $q(t) \in [0, M], t \geq 0$, where $M > 0$ represents the capacity of the buffer, *i.e.* formally the maximum number of vehicles that can be stored at the level of the junction. We note here that the finite capacity of the buffer is essential from a traffic point of view. It will enable the model to transmit information backwards, and propagate congestion from outgoing links to incoming links, and then to surrounding junctions. The buffer state represents the number of vehicles stored in the buffer at a given instant. That is why it must be an increasing function of the incoming flux and a decreasing function of the outgoing flux. Given an initial buffer state $q_0 \in [0, M]$, the buffer dynamics is modeled with the following Cauchy problem:

$$\begin{cases} q'(t) = \sum\limits_{i \in \mathcal{I}} f_i(\rho_i(t,0-)) - \sum\limits_{j \in \mathcal{O}} f_j(\rho_j(t,0+)), & t > 0, \\ q(0) = q_0. \end{cases} \tag{1.2.10}$$

The number of vehicles stored in the buffer evolves with the difference between the number of vehicles entering the intersection and the number of vehicles leaving it. The authors prove that the Cauchy problem (1.2.9),(1.2.10) is well-posed. In [27, 28, 29], the authors extend this model to a multi-buffer scenario. They define one buffer state $q_j(t) \in [0, M_j], t \geq 0$ per outgoing link $j \in \mathcal{O}$, which satisfy the following ODE:

$$q_j'(t) = \sum_{i \in \mathcal{I}} \boldsymbol{\theta}_{i,j} \bar{f}_i - \bar{f}_j, \quad t > 0, j \in \mathcal{O},$$

where $\bar{f}_i, \bar{f}_j$ denote respectively the incoming flux from i and the outgoing flux to j at the level of the intersection. Two options to construct $\bar{f}_i, \bar{f}_j$ are proposed and called respectively the *single buffer junction* and the *multiple buffer junction*. The multi-buffer model enables to distinguish the behavior of vehicles depending on their routing choice of exit j. Additional scenarios and description of the model will be detailed in Section 4.2.

1.2.3.c Macroscopic traffic flow models accounting for bounded acceleration

The solutions to macroscopic traffic flow models can display discontinuous densities in space and time. These discontinuities correspond to instantaneous increase or decrease of the velocity of traffic, thus corresponding to unbouded acceleration or deceleration rates. Modeling acceleration of traffic accurately is a key element of traffic flow models in urban applications, since it is the most influential factor on energy consumption and polluting emissions at low average speeds [140]. In addition, in urban road networks, one can find infrastructure constraints like stop signs, traffic lights, pedestrian crossing and interesections, which force vehicles to accelerate and decelerate regularly, thus amplifying the need to accurately describe these transitory phases. In this context, the first macroscopic traffic flow models accounting for bounded acceleration were introduced in [74, 106, 112, 113]. The numerics are discussed in [114]. The principle of these models is to insert additional constraints on the convective acceleration when discretizing and solving the LWR model using Godunov's scheme.

In [108], Lebacque summarizes the previous approaches and proposes a two-phase bounded acceleration model. He aims at conserving the modeling features of the LWR model, while imposing an upper bound $A > 0$ on the acceleration of traffic, mathematically described by the convective acceleration $\partial_t v + v\partial_x v$. He proposes the following set of equations:

$$\begin{cases} \partial_t \rho + \partial_x \big[f(\rho, v) \big] = 0, \\ f(\rho, v) = \rho v, \\ \begin{cases} v = V_e(\rho) \text{ and } \partial_t v + v\partial_x v \leq A, & \text{(equilibrium phase)} \\ v \leq V_e(\rho) \text{ and } \partial_t v + v\partial_x v = A. & \text{(bounded acceleration phase)} \end{cases} \end{cases} \tag{1.2.11}$$

System (1.2.11) leads to the distinction between two phases: the equilibrium phase, in which the LWR model is satisfied, and the bounded acceleration (BA) phase, in which vehicles accelerate at constant rate. In this second phase, the author returns to a microscopic formulation, in which the trajectory of vehicles are described by parabolas, corresponding to an acceleration at constant rate A from an initial velocity to a target velocity. Nonetheless, the characteristics of the transition between both phases cannot be determined a priori, and the authors provides calculation rules which cannot be extended to general cases. That is why we will propose a new approach to model bounded acceleration of traffic in Chapter 3.

1.3 Contributions and outline of the thesis

The work presented in this thesis is motivated by the current situation of traffic in urban areas. Vehicles generate significant negative externalities, such as congestion and pollution, which impact dangerously the health of citizens and contribute to global warming. The objective is then to overcome some of the current limitations of macroscopic traffic flow models detailed in Section 1.2, and more particularly when applied in urban situations. Developing a framework capable of evaluating and controlling vehicle emissions on road networks raises several scientific challenges. First, how can we derive traffic flow models which are realistic, robust and scalable on large networks? Macroscopic traffic flow models, using averaged traffic variables, are convenient when simulating large number of vehicles. Second order models seem realistic, but their mathematical properties are not exhaustively detailed in the existing literature (Section 1.2.2). In addition, can we propose macroscopic traffic flow models which account for bounded acceleration of traffic? Traffic acceleration is indeed the most influential factor on vehicle emissions. We have exposed in Section 1.2.3.c the current state of the art, and noticed that these models cannot be extended to general frameworks. The solutions to general Cauchy problems are not necessarily well-defined and general fundamental diagrams cannot be used. Finally, how to connect traffic flow models at each junction of a given network? In Section 1.2.3.a, we have noted that the solutions to traffic flow models connected with Riemann solvers at junctions may not depend continuously on the initial datum of the problem. This limitation prevents implementation of a control framework, and to approach the Dynamic Traffic Assignment problem.

Based on these observations, we first focus on the ARZ model, which is the classical second order model in the literature. We prove well-posedness of the model using wave-front tracking approximations. In addition, we show that the solutions of the Aw–Rascle–Zhang system with relaxation converge to a weak solution of the LWR model when the relaxation parameter goes to zero. Finally, we propose a discussion on the entropy aspect of this weak solution of the LWR model. These results are detailed in Chapter 2.

We then focus on macroscopic models accounting for bounded acceleration. We propose a new mathematical model accounting for the boundedness of traffic acceleration at a macroscopic scale. Our model is built on the coupling between the scalar conservation law accounting for the conservation of vehicles and a number of ordinary differential equations describing the trajectories of accelerating vehicles, which we treat as moving constraints. Using wave-front tracking, we show existence of solutions to the Cauchy problem, and provide numerical simulations of the model in urban situations, including roads with sequences of traffic lights. This model is presented in Chapter 3.

Finally, we introduce a new macroscopic traffic flow model with buffers on networks. This model features buffers of finite size, enabling propagation of congestion on the network, and time-dependent routing functions at the junctions. We prove existence, uniqueness and stability of the solutions with respect to the routing ratios and initial datum. Thanks to the stability, the model provides a controllable framework, using routing ratios as control

parameters. This represents an advance towards solving the DTA problem. Finally, we detail how this framework applies to a classical road network with several intersections and finite-length links. This approach is precised in Chapter 4.

In Conclusion of the thesis, we sum up our contributions and propose a discussion about future research opportunities.

List of papers

During this PhD, the following papers were published or submitted:

- N. Laurent-Brouty, G. Costeseque, and P. Goatin. A macroscopic traffic flow model accounting for bounded acceleration. preprint, June 2019;

- N. Laurent-Brouty, A. Keimer, P. Goatin, and A. M. Bayen. A macroscopic traffic flow model with finite buffers on networks: Well-posedness by means of Hamilton-Jacobi equations. preprint, May 2019;

- P. Goatin and N. Laurent-Brouty. The zero relaxation limit for the Aw-Rascle-Zhang traffic flow model. *Z. Angew. Math. Phys.*, 70(1):Art. 31, 24, 2019;

- A. Keimer, N. Laurent-Brouty, F. Farokhi, H. Signargout, V. Cvetkovic, A. M. Bayen, and K. H. Johansson. Information patterns in the modeling and design of mobility management services. *Proceedings of the IEEE*, 106(4):554–576, 2018;

- N. Laurent-Brouty, G. Costeseque, and P. Goatin. A coupled PDE-ODE model for bounded acceleration in macroscopic traffic flow models. *IFAC-PapersOnLine*, 51(9):37 – 42, 2018. 15th IFAC Symposium on Control in Transportation Systems CTS 2018;

- J. Thai, N. Laurent-Brouty, and A. M. Bayen. Negative externalities of gps-enabled routing applications: A game theoretical approach. In *2016 IEEE 19th International Conference on Intelligent Transportation Systems (ITSC)*, pages 595–601, Nov 2016.

Chapter 2

The zero relaxation limit for the Aw-Rascle-Zhang traffic flow model

Abstract

In this chapter we study the behavior of the Aw-Rascle-Zhang model when the relaxation parameter converges to zero. In a Lagrangian setting, we use the Wave-Front Tracking method with splitting technique to construct a sequence of approximate solutions. We prove that this sequence converges to a weak entropy solution of the relaxed system associated to a given initial datum with bounded variation. Besides, we also provide an estimate on the decay of positive waves. We finally prove that the solutions of the Aw-Rascle-Zhang system with relaxation converge to a weak solution of the corresponding scalar conservation law when the relaxation parameter goes to zero.

The content of this chapter was published under the following references:
P. Goatin and N. Laurent-Brouty. The zero relaxation limit for the Aw-Rascle-Zhang traffic flow model. *Z. Angew. Math. Phys.*, 70(1):Art. 31, 24, 2019

2.1 Introduction

In this chapter, we consider the Aw-Rascle-Zhang model with relaxation (see Section 1.2.2). This model relies on the homogeneous Aw-Rascle-Zhang model [9, 146]

$$\begin{cases} \partial_t \rho + \partial_x(\rho v) = 0, \\ \partial_t(v + p(\rho)) + v\partial_x(v + p(\rho)) = 0, \end{cases} \qquad x \in \mathbb{R},\ t > 0, \tag{2.1.1}$$

where $p(\rho)$ is a pseudo-pressure function accounting for drivers' anticipation of downstream density changes. To ensure that system (2.1.1) is strictly hyperbolic, with a genuinely nonlinear and a linearly degenerate characteristic fields, we impose the following constraints:

$$\rho > 0, \qquad p(\rho) > 0, \qquad p'(\rho) > 0, \qquad 2p'(\rho) + \rho p''(\rho) > 0. \tag{2.1.2}$$

A relaxation term is then added [81, 132], to force the velocity of the flow to relax towards the equilibrium speed:

$$\begin{cases} \partial_t \rho + \partial_x(\rho v) = 0, \\ \partial_t(v + p(\rho)) + v\partial_x(v + p(\rho)) = \frac{V_e(\rho) - v}{\delta}, \end{cases} \tag{2.1.3}$$

where $V_e(\rho) \geq 0$ is a non-increasing function which represents the equilibrium speed, and $\delta > 0$ is a relaxation parameter. To ensure a well-defined problem, the system must satisfy the so-called *subcharacteristic condition* [38, 39]:

$$-p'(\rho) \leq V_e'(\rho) \leq 0 \quad \text{for } \rho > 0. \tag{2.1.4}$$

Note that if $p'(\rho) = -V_e'(\rho)$, the system can be decoupled and reduced to the scalar case [118]. The case $V_e'(\rho) = 0$ does not make sense for traffic modeling, since it would imply that the equilibrium velocity is independent of the density. For these reasons, we will consider strict inequalities in the rest of the chapter:

$$-p'(\rho) < V_e'(\rho) < 0 \quad \text{for } \rho > 0. \tag{2.1.5}$$

Multiplying the first equation of (2.1.3) by $p'(\rho)$ and subtracting its terms to the second equation, we obtain

$$\begin{cases} \partial_t \rho + \partial_x(\rho v) = 0, \\ \partial_t v + (v - \rho p'(\rho))\partial_x v = \frac{V_e(\rho) - v}{\delta}. \end{cases} \tag{2.1.6}$$

Under hypotheses (2.1.2), the associated homogeneous system is strictly hyperbolic (away from vacuum) with eigenvalues $\lambda_1 = v - \rho p'(\rho)$ and $\lambda_2 = v$.
The conservative form of (2.1.3), (2.1.6) is given by (see [9]):

$$\begin{cases} \partial_t \rho + \partial_x(\rho v) = 0, \\ \partial_t(\rho(v + p(\rho))) + \partial_x(\rho v(v + p(\rho))) = \rho\frac{V_e(\rho) - v}{\delta}. \end{cases}$$

Defining $w := v + p(\rho)$, we obtain:

$$\begin{cases} \partial_t \rho + \partial_x(\rho v) = 0, \\ \partial_t(\rho w) + \partial_x(\rho v w) = \rho \frac{V_e(\rho) - v}{\delta}, \end{cases} \tag{2.1.7}$$

which can be rewritten into Lagrangian coordinates (t, X) [50] as follows. We denote by τ the specific volume, such that $\tau = \frac{1}{\rho}$. Using the notations

$$\tilde{p}(\tau) = p\left(\frac{1}{\tau}\right), \qquad \tilde{V}(\tau) = V_e\left(\frac{1}{\tau}\right), \qquad \tilde{p}'(\tau) = -\frac{1}{\tau^2} p'\left(\frac{1}{\tau}\right) < 0,$$

we obtain the following equivalent hyperbolic system

$$\begin{cases} \partial_t \tau - \partial_X v = 0, \\ \partial_t w = \frac{\tilde{V}(\tau) - v}{\delta}, \end{cases} \tag{2.1.8}$$

where

$$\partial_x X = \rho, \qquad \partial_t X = -\rho v,$$

with initial data

$$\begin{cases} \tau(0, \cdot) = \tau_0, \\ w(0, \cdot) = w_0. \end{cases} \tag{2.1.9}$$

Remark 2.1. The question of the equivalence of solutions to (2.1.1) and the homogeneous part of (2.1.8) is discussed in [142]. Using the chain rule, one can show that the two systems are equivalent for classical solutions, and that there is a one-to-one correspondance. Nonetheless, these equations may develop discontinuities, so weak solutions must be considered and the chain rule does not hold to conclude on the one-to-one correspondance. As explained by Wagner, the Rankine-Hugoniot conditions of both systems are equivalent, but this does not guarantee that the Cauchy problems are equivalent. In [142, Theorem 1], the author proves that there exists a one-to-one correspondance between weak entropy solutions of the eulerian and the lagrangian formulation of the system, as long as the density ρ and the specific volume τ lies in a striclty positive compact set. Since we assume that the density is strictly positive in (2.1.2), and in addition the usual setting of traffic assumes existence of a maximum density $\rho_{\max} > 0$, the results will apply to our framework and we will have one-to-one correspondance between solutions to both systems.

In Lagrangian notations, the subcharacteristic condition (2.1.5) becomes

$$\tilde{p}'(\tau) < -\tilde{V}'(\tau) < 0. \tag{2.1.10}$$

The homogeneous system in (2.1.8) admits as eigenvalues $\lambda_1 = \tilde{p}'(\tau) = -\rho^2 p'(\rho) < 0$ and $\lambda_2 = 0$, and the associated Riemann invariants are w and v. The first characteristic field

is genuinely non-linear, while the second is linearly degenerate. The system is a Temple class system, since shock and rarefaction curves coincide [138].

In this chapter, we provide a rigorous proof of existence of solutions for the relaxed ARZ system (2.1.8), as well as the convergence of these solutions to the equilibrium LWR equation

$$\partial_t \tau - \partial_X \tilde{V}(\tau) = 0,$$

as $\delta \to 0$. The proofs are based on the construction of approximate solutions by means of the wave-front tracking technique. This choice is motivated by the lack of Total Variation (TV) bounds on classical finite volume (Godunov) approximations, which were used in [8, 10, 81]. Indeed, it is well-known that, since these schemes are constructed taking means of the conservative variables, they are not able to preserve the total variation of Riemann invariants. In particular, in the case of the ARZ system, they may not capture correctly contact discontinuities, and adapted schemes must be used [36]. This point will be discussed in Appendix.

The chapter is organized as follows. In Section 2.2, we detail the construction of WFT approximations and we derive the necessary L^∞ and TV uniform bounds to guarantee their convergence towards a solution of (2.1.8), which is detailed in Section 2.3. In Section 2.4 we prove some estimates for positive genuinely non-linear waves occurring in solutions of system (2.1.8). Finally, Section 2.5 is devoted to the proof of the relaxation limit.

2.2 Wave-Front Tracking approximations

In this section, we construct wave-front tracking approximations of the solution following the approach developed for similar cases in [2, 11]. The approximate solution is constructed in a two-step process, which successively solves the homogeneous system for a given piecewise constant initial datum, and then integrate the source term contained in the following ODE:

$$w_t = \frac{\tilde{V}(\tau) - v}{\delta}.$$

Given two constants $0 < \check{\tau} < \hat{\tau} < +\infty$, let us define the domain $\mathbf{E}$ as

$$\mathbf{E} = \mathbf{E}(\check{\tau}, \hat{\tau}) := \Big\{ u = (\tau, w) \in [\check{\tau}, \hat{\tau}] \times [0, +\infty[\colon \tilde{V}(\check{\tau}) \leq w - \tilde{p}(\tau) \leq \tilde{V}(\hat{\tau}), \\ \tilde{V}(\hat{\tau}) + \tilde{p}(\hat{\tau}) \leq w \leq \tilde{V}(\check{\tau}) + \tilde{p}(\check{\tau}) \Big\}.$$

In particular, note that vacuum states are excluded by the above domain. For any $M > 0$, we define the family of functions:

$$\mathcal{D}(M) := \{ u : \mathbb{R} \to \mathbf{E} \colon TV(w(u)) + TV(v(u)) \leq M \},$$

where $v(u) = w - \tilde{p}(\tau)$ is the second Riemann invariant.

2.2.1 Construction of approximate solutions via wave-front tracking

Given a fixed time horizon $T > 0$, consider a sequence of time-steps $\Delta t^\nu > 0$, $\nu \in \mathbb{N}$, such that $\Delta t^\nu \xrightarrow[\nu\to\infty]{} 0$. Let $U_0 = (\tau_0, w_0) \in \mathcal{D}(M)$. For each $\nu \in \mathbb{N}$, the interval $(0, T)$ can be partitioned in segments of the form $[n\Delta t^\nu, (n+1)\Delta t^\nu]$, $n \in \mathbb{N}$. We denote $U^\nu(t,x) = (\tau^\nu, w^\nu)(t,x)$, $t \in [0,T]$, $x \in \mathbb{R}$, the sequence of WFT approximations of the solution of system (2.1.8). We construct it iteratively, for each $\nu \in \mathbb{N}$, with the following process:

1. Define a sequence of piecewise constant functions $U_0^\nu = (\tau_0^\nu, w_0^\nu) \in \mathcal{D}(M)$ satisfying:

$$TV(w_0^\nu) \leq TV(w_0), \qquad \|w_0^\nu - w_0\|_{\mathbf{L}^\infty} \leq \frac{1}{\nu}, \qquad \|\tau_0^\nu - \tau_0\|_{\mathbf{L}^1} \leq \frac{1}{\nu}, \tag{2.2.1}$$

$$TV(v(U_0^\nu)) \leq TV(v(U_0)), \quad \|v(U_0^\nu) - v(U_0)\|_{\mathbf{L}^\infty} \leq \frac{1}{\nu}, \quad \|v(U_0^\nu) - v(U_0)\|_{\mathbf{L}^1} \leq \frac{1}{\nu}. \tag{2.2.2}$$

   The existence of such U_0^ν is provided by [20, Lemma 2.2].

2. For each $\nu \in \mathbb{N}$, the piecewise constant function U_0^ν has a finite number of discontinuities. Solve the homogeneous system

$$\begin{cases} \partial_t \tau - \partial_X v = 0, \\ \partial_t w = 0, \end{cases} \tag{2.2.3}$$

   for each Riemann problem arising at all discontinuities for $t \in [0, \Delta t^\nu)$ using wave-front tracking method [11], and name $U^\nu(t,\cdot)$, $t \in [0, \Delta t^\nu)$, the corresponding piecewise constant function.

   We recall that the system (2.2.3) admits as eigenvalues $\lambda_1 = \tilde{p}'(\tau) = -\rho^2 p'(\rho) < 0$ and $\lambda_2 = 0$, and the associated Riemann invariants are w and v. Each Riemann problem can thus be solved by a shock or rarefaction with negative speed and/or a stationary contact discontinuity. More precisely, we fix the parameter $\epsilon_\nu = 2^{\frac{-1}{\Delta t^\nu}}$, and we consider an approximate Riemann solver in order to generate piecewise constant approximate solutions. In particular, the solver does not modify shock waves and contact discontinuities. Any rarefaction is approximated by a fan of waves of size ϵ_ν moving with speed $\dot{x_\alpha}(t) = \lambda_1(\tau, w)(t, x_\alpha+)$ and thus violating the Rankine-Hugoniot and the entropy conditions with a global error of order $\mathcal{O}(\epsilon_\nu)$ (see [20, Section 7.1]). The approximate Riemann solver can then be applied at each discontinuity, and the corresponding solutions be propagated until a wave interaction occurs for $t < \Delta t^\nu$. We can assume without loss of generality that only two waves interact at a given time, by possibly altering slightly their speed. When two waves interact, a new Riemann problem can be solved approximately and the solution prolonged until the next interaction.

3. At $t = \Delta t^\nu$, we define

$$\tau^\nu(\Delta t^\nu, \cdot) = \tau^\nu(\Delta t^\nu -, \cdot), \tag{2.2.4}$$

$$w^\nu(\Delta t^\nu, \cdot) = w^\nu(\Delta t^\nu -, \cdot) + \Delta t \frac{\tilde{V}(\tau^\nu(\Delta t^\nu, \cdot)) - v(U^\nu(\Delta t^\nu -, \cdot))}{\delta}. \tag{2.2.5}$$

Note that τ is conserved during the splitting scheme, while w is updated according to the relaxation term:

$$w^+ = w^- + \Delta t \frac{\tilde{V}(\tau) - v^-}{\delta},$$

see Figure 2.1 for the detail of notations.

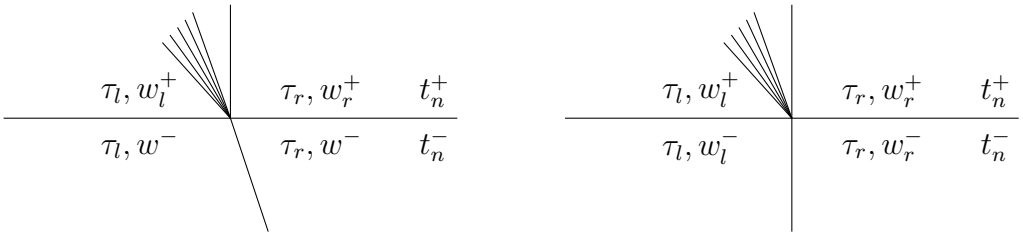

Figure 2.1 – Notations used in step 3.

4. Treat $U^\nu(\Delta t^\nu, \cdot)$ as a new piecewise constant initial condition and repeat the previous steps 2-3 to define the solution $U^\nu(t, \cdot)$ for each $t \in [0, T]$, for any $T > 0$ fixed.

We observe that for each ν the total number of waves generated is finite. It does not increase when solving the homogeneous system (2.2.3) between two consecutive time-steps, and can only increase by a finite rate at each time-step $t = t_n = n\Delta t^\nu$, $n \in \mathbb{N}$, when generating approximate rarefaction fans.

2.2.2 Estimates on WFT approximate solutions

In order to achieve the necessary L^∞ uniform bounds, we identify the invariant domains [90] of system (2.1.8). For simplicity of notations we fix $\nu > 0$, $\Delta t = \Delta t^\nu$ and work on $U = U^\nu$.

Lemma 2.2.1. *For $\Delta t \leq \delta$, the set $\mathbf{E}$ is an invariant domain for the proposed WFT scheme.*

Proof. Since w and $v = w - \tilde{p}(\tau)$ are the two Riemann invariants of (2.2.3), which is a Temple class system, this ensures that the inequalities $\tilde{V}(\check{\tau}) \leq v \leq \tilde{V}(\hat{\tau}), \tilde{V}(\hat{\tau}) + \tilde{p}(\hat{\tau}) \leq w \leq \tilde{V}(\check{\tau}) + \tilde{p}(\check{\tau})$ are satisfied when solving the homogeneous system at step 2. In addition, we know that $\tilde{p}$ is a monotone decreasing function, and that $\tau = \tilde{p}^{-1}(w - v)$. Combining this with the bounds on v and w we obtain that $\tau \in [\check{\tau}, \hat{\tau}]$ and then the domain $\mathbf{E}$ is invariant for the homogeneous system.

Let us now focus on the evolution step 3. Skipping the index ν for simplicity, we remind that we have:

$$w^+ = w^- + \frac{\Delta t}{\delta}\left(\tilde{V}(\tau) - v^-\right) = w^-\left(1 - \frac{\Delta t}{\delta}\right) + \frac{\Delta t}{\delta}\left(\tilde{V}(\tau) + \tilde{p}(\tau)\right),$$
$$v^+ = w^+ - \tilde{p}(\tau) = v^-\left(1 - \frac{\Delta t}{\delta}\right) + \frac{\Delta t}{\delta}\tilde{V}(\tau).$$

Let $u^- = (\tau, w^-) \in \mathbf{E}$. The inequality $v^+ \leq w^+$ is straightforward. Assuming $\Delta t \leq \delta$, we distinguish the following situations:

- Case 1: The velocity is above the equilibrium speed

  $$v^- \geq \tilde{V}(\tau) \Leftrightarrow w^- \geq \tilde{V}(\tau) + \tilde{p}(\tau).$$

  Then

  $$\tilde{V}(\check{\tau}) \leq \tilde{V}(\tau)\left(1 - \frac{\Delta t}{\delta}\right) + \frac{\Delta t}{\delta}\tilde{V}(\tau) \leq v^+ \leq v^- \leq \tilde{V}(\hat{\tau}),$$
  $$\tilde{V}(\hat{\tau}) + \tilde{p}(\hat{\tau}) \leq \tilde{V}(\tau) + \tilde{p}(\tau) \leq w^+ \leq w^- \leq \tilde{V}(\check{\tau}) + \tilde{p}(\check{\tau}),$$

  therefore $u^+ = (\tau, w^+) \in \mathbf{E}$.

- Case 2: The initial velocity is below the equilibrium speed

  $$v^- \leq \tilde{V}(\tau) \quad \Leftrightarrow \quad w^- \leq \tilde{V}(\tau) + \tilde{p}(\tau).$$

  Then

  $$\tilde{V}(\check{\tau}) \leq v^- \leq v^+ \leq \tilde{V}(\tau)\left(1 - \frac{\Delta t}{\delta}\right) + \frac{\Delta t}{\delta}\tilde{V}(\tau) \leq \tilde{V}(\hat{\tau}),$$
  $$\tilde{V}(\hat{\tau}) + \tilde{p}(\hat{\tau}) \leq w^- \leq w^+ \leq \tilde{V}(\tau) + \tilde{p}(\tau) \leq \tilde{V}(\check{\tau}) + \tilde{p}(\check{\tau}),$$

  thus $u^+ \in \mathbf{E}$.

□

The uniform TV bound is provided by the following lemma.

Lemma 2.2.2. *Assume that the strict subcharacteristic condition* (2.1.10) *is satisfied. For $\Delta t \leq \delta$, the total variation of the Riemann invariants of the constructed approximation U^ν is non-increasing in time:*

$$TV(w^\nu(t,\cdot)) + TV(v(U^\nu(t,\cdot))) \leq TV(w_0^\nu) + TV(v(U_0^\nu)), \quad \textit{for a.e. } t > 0.$$

Proof. When solving the homogeneous system in step 2, the total variation of both Riemann invariants is non increasing in time since we are dealing with a Temple class system [11]. We thus focus on the evolution of the total variation at step 3. We recall that

$$\begin{aligned}\tau(t_n^+,x) &= \tau(t_n^-,x),\\ w(t_n^+,x) &= w(t_n^-,x) + \frac{\Delta t}{\delta}\Big(\tilde V(\tau) - w + \tilde p(\tau)\Big)(t_n^-,x).\end{aligned}$$

Therefore

$$\begin{aligned}\big|w_r^+ - w_l^+\big| &= \Big|(w_r^- - w_l^-) + \frac{\Delta t}{\delta}\Big((\tilde V(\tau_r) - \tilde V(\tau_l)) + (\tilde p(\tau_r) - \tilde p(\tau_l)) - (w_r^- - w_l^-)\Big)\Big|,\\ \big|v_r^+ - v_l^+\big| &= \big|(w_r^+ - w_l^+) - (\tilde p(\tau_r) - \tilde p(\tau_l))\big|\\ &= \Big|(w_r^- - w_l^-) + \frac{\Delta t}{\delta}\Big((\tilde V(\tau_r) - \tilde V(\tau_l)) + (\tilde p(\tau_r) - \tilde p(\tau_l)) - (w_r^- - w_l^-)\Big)\\ &\qquad - (\tilde p(\tau_r) - \tilde p(\tau_l))\Big|.\end{aligned}$$

We distinguish three cases, depending on the wave arriving at $t = t_n^-$.

1-rarefaction wave. We denote by U_l and U_r respectively the left and right states of the wave hitting the line $t = t_n$ at $t = t_n^-$. Let us consider first the case where U_l and U_r are connected through a rarefaction wave. This implies $w_l^- = w_r^-$ and $\tau_l < \tau_r$ (and $v_l^- < v_r^-$). In addition, $\tilde V$ is an increasing function of τ, ie $\tilde V(\tau_l) < \tilde V(\tau_r)$. The same way, $\tilde p$ is a decreasing function of τ. Thus $\tilde p(\tau_l) > \tilde p(\tau_r)$. We have:

$$\begin{aligned}\big|w_r^+ - w_l^+\big| &= \frac{\Delta t}{\delta}\big|\underbrace{\big(\tilde V(\tau_r) - \tilde V(\tau_l)\big)}_{\geq 0} + \underbrace{\big(\tilde p(\tau_r) - \tilde p(\tau_l)\big)}_{\leq 0}\big|,\\ \big|v_r^+ - v_l^+\big| &= \big|\frac{\Delta t}{\delta}\underbrace{\big(\tilde V(\tau_r) - \tilde V(\tau_l)\big)}_{\geq 0} + \big(1 - \frac{\Delta t}{\delta}\big)\underbrace{\big(\tilde p(\tau_l) - \tilde p(\tau_r)\big)}_{\geq 0}\big|.\end{aligned}$$

In addition:

$$\big|w_r^- - w_l^-\big| + \big|v_r^- - v_l^-\big| = \big|v_r^- - v_l^-\big| = \tilde p(\tau_l) - \tilde p(\tau_r).$$

By applying the subcharacteristic condition (2.1.10), we have:

$$\begin{aligned}\tilde p(\tau_r) - \tilde p(\tau_l) &= \int_{\tau_l}^{\tau_r} \underbrace{\tilde p'(\tau)}_{\leq 0}\, d\tau,\\ \tilde p(\tau_l) - \tilde p(\tau_r) &= \int_{\tau_l}^{\tau_r} |\tilde p'(\tau)|\, d\tau \geq \int_{\tau_l}^{\tau_r} |\underbrace{\tilde V'(\tau)}_{\geq 0}| d\tau = \tilde V(\tau_r) - \tilde V(\tau_l).\end{aligned}$$

Then:

$$\begin{aligned}\left|w_r^+ - w_l^+\right| &= \frac{\Delta t}{\delta}\big((\tilde{p}(\tau_l) - \tilde{p}(\tau_r)) - (\tilde{V}(\tau_r) - \tilde{V}(\tau_l))\big) \\ &= \frac{\Delta t}{\delta}\big((v_r^- - v_l^-) - (\tilde{V}(\tau_r) - \tilde{V}(\tau_l))\big).\end{aligned}$$

Since $\Delta t \leq \delta$, we get

$$\left|v_r^+ - v_l^+\right| = \frac{\Delta t}{\delta}\big(\tilde{V}(\tau_r) - \tilde{V}(\tau_l)\big) + \big(1 - \frac{\Delta t}{\delta}\big)\left|v_r^- - v_l^-\right|.$$

Finally,

$$\left|w_r^+ - w_l^+\right| + \left|v_r^+ - v_l^+\right| = \left|w_r^- - w_l^-\right| + \left|v_r^- - v_l^-\right|,$$

thus the total variation of the Riemann invariants is conserved through the splitting step.

1-shock wave. We now assume that U_l and U_r are connected by a shock. This means that $w_l^- = w_r^-$ and $\tau_l > \tau_r$. We also have, by monotonicity of $\tilde{V}$ and $\tilde{p}$, $\tilde{V}(\tau_l) > \tilde{V}(\tau_r)$ and $\tilde{p}(\tau_l) < \tilde{p}(\tau_r)$. We can apply the same computations as before:

$$\begin{aligned}\left|w_r^+ - w_l^+\right| &= \frac{\Delta t}{\delta}\big|\underbrace{\big(\tilde{V}(\tau_r) - \tilde{V}(\tau_l)\big)}_{\leq 0} + \underbrace{\big(\tilde{p}(\tau_r) - \tilde{p}(\tau_l)\big)}_{\geq 0}\big|, \\ \left|v_r^+ - v_l^+\right| &= \big|\frac{\Delta t}{\delta}\underbrace{\big(\tilde{V}(\tau_r) - \tilde{V}(\tau_l)\big)}_{\leq 0} + \big(1 - \frac{\Delta t}{\delta}\big)\underbrace{\big(\tilde{p}(\tau_l) - \tilde{p}(\tau_r)\big)}_{\leq 0}\big|.\end{aligned}$$

In addition,

$$\left|w_r^- - w_l^-\right| + \left|v_r^- - v_l^-\right| = \left|v_r^- - v_l^-\right| = \tilde{p}(\tau_r) - \tilde{p}(\tau_l).$$

The subcharacteristic condition still yields that

$$\tilde{p}(\tau_r) - \tilde{p}(\tau_l) \geq \tilde{V}(\tau_l) - \tilde{V}(\tau_r).$$

Thus we have

$$\begin{aligned}\left|w_r^+ - w_l^+\right| &= \frac{\Delta t}{\delta}\Big(\big(\tilde{V}(\tau_r) - \tilde{V}(\tau_l)\big) + \big(\tilde{p}(\tau_r) - \tilde{p}(\tau_l)\big)\Big), \\ \left|v_r^+ - v_l^+\right| &= -\Big(\frac{\Delta t}{\delta}\big(\tilde{V}(\tau_r) - \tilde{V}(\tau_l)\big) + \big(1 - \frac{\Delta t}{\delta}\big)\big(\tilde{p}(\tau_l) - \tilde{p}(\tau_r)\big)\Big).\end{aligned}$$

Finally,

$$\left|w_r^+ - w_l^+\right| + \left|v_r^+ - v_l^+\right| = \left|w_r^- - w_l^-\right| + \left|v_r^- - v_l^-\right|.$$

2-contact discontinuity. We now consider the case where U_l and U_r are connected through a 2-contact discontinuity, which means $v_l^- = v_r^-$. We compute

$$\begin{aligned}\left|w_r^+ - w_l^+\right| &= \Big| \left(\tilde{p}(\tau_r) - \tilde{p}(\tau_l)\right) + \frac{\Delta t}{\delta}\big(\tilde{V}(\tau_r) - \tilde{V}(\tau_l)\big)\Big|,\\ \left|v_r^+ - v_l^+\right| &= \Big|(w_r^- - w_l^-) + \frac{\Delta t}{\delta}\big(\tilde{V}(\tau_r) - \tilde{V}(\tau_l)\big) - \left(\tilde{p}(\tau_r) - \tilde{p}(\tau_l)\right)\Big|\\ &= \frac{\Delta t}{\delta}\Big|\tilde{V}(\tau_r) - \tilde{V}(\tau_l)\Big|.\end{aligned}$$

In addition

$$\left|w_r^- - w_l^-\right| + \left|v_r^- - v_l^-\right| = \left|w_r^- - w_l^-\right| = \left|\tilde{p}(\tau_r) - \tilde{p}(\tau_l)\right|.$$

We note that

$$\left(\tilde{p}(\tau_r) - \tilde{p}(\tau_l)\right) \cdot \big(\tilde{V}(\tau_r) - \tilde{V}(\tau_l)\big) \leq 0.$$

Since $\Delta t \leq \delta$, we have:

$$\begin{aligned}\left|w_r^+ - w_l^+\right| &= \operatorname{sgn}\left(\tilde{p}(\tau_r) - \tilde{p}(\tau_l)\right)\Big(\left(\tilde{p}(\tau_r) - \tilde{p}(\tau_l)\right) + \frac{\Delta t}{\delta}\big(\tilde{V}(\tau_r) - \tilde{V}(\tau_l)\big)\Big),\\ \left|v_r^+ - v_l^+\right| &= -\operatorname{sgn}\left(\tilde{p}(\tau_r) - \tilde{p}(\tau_l)\right)\frac{\Delta t}{\delta}\big(\tilde{V}(\tau_r) - \tilde{V}(\tau_l)\big),\end{aligned}$$

and thus

$$\left|w_r^+ - w_l^+\right| + \left|v_r^+ - v_l^+\right| = \left|w_r^- - w_l^-\right| + \left|v_r^- - v_l^-\right|.$$

□

Lemma 2.2.3. *Let $\nu \in \mathbb{N}$ and $U_0^\nu \in \mathcal{D}(M)$. Then there exist a constant C_M independent of δ, and a constant L_δ such that, $\forall\ a < b, \forall\ 0 \leq s < t$:*

$$\int_a^b |\tau^\nu(t,X) - \tau^\nu(s,X)|dX \leq C_M(t-s), \tag{2.2.6}$$

$$\int_a^b |w^\nu(t,X) - w^\nu(s,X)|dX \leq (C_M + L_\delta)(t - s + \Delta t). \tag{2.2.7}$$

Proof. Lemmas 2.2.1 and 2.2.2 imply that $U^\nu(t,\cdot) \in \mathcal{D}(M)$ for all $t > 0$. Let $s, t \in \mathbb{R}$ such that $0 \leq s < t$. If there are no time-steps between s and t, (2.2.6) and (2.2.7) are true for any $L_\delta \geq 0$, as a direct application of Temple class system properties, see [137, Theorem 13.3.1] and [11, Theorem 1].
Suppose now that there are $N+1$ time-steps between s and t:

$$s \leq k\Delta t \leq (k+1)\Delta t \leq \cdot\cdot \leq (k+N)\Delta t \leq t \quad \text{for } \geq 1,$$

so that $N\Delta t \leq t - s$.
Let $a < b$ given and $X \in]a, b[$. We can then write:

$$\begin{aligned}
|\tau^\nu(t,X) - \tau^\nu(s,X)| &= |\tau^\nu(t,X) - \tau^\nu((k+N)\Delta t, X) \\
&\quad + \sum_{i=k}^{k+N-1} (\tau^\nu((i+1)\Delta t, X) - \tau^\nu(i\Delta t, X)) \\
&\quad + \tau^\nu(k\Delta t, X) - \tau^\nu(s,X)| \\
&\leq |\tau^\nu(t,X) - \tau^\nu((k+N)\Delta t, X)| \\
&\quad + \sum_{i=k}^{k+N-1} |\tau^\nu((i+1)\Delta t, X) - \tau^\nu(i\Delta t, X)| \\
&\quad + |\tau^\nu(k\Delta t, X) - \tau^\nu(s,X)|.
\end{aligned}$$

Since τ^ν does not change through the splitting process, we can apply the previous property between two consecutive time-steps to obtain (2.2.6):

$$\begin{aligned}
\int_a^b |\tau^\nu(t,X) - \tau^\nu(s,X)| dX &\leq C_M \big[(t - (k+N)\Delta t) + \sum_{i=k}^{k+N-1} \Delta t + (k\Delta t - s)\big] \\
&\leq C_M(t-s).
\end{aligned}$$

For the second inequality, we have to consider an additional term, since w^ν is modified at each splitting-step. We can then write:

$$\begin{aligned}
&\sum_{i=k}^{k+N} \int_a^b |w^\nu(i\Delta t+, X) - w^\nu(i\Delta t-, X)| dX \\
&\qquad = \sum_{i=k}^{k+N} \frac{\Delta t}{\delta} \int_a^b |\tilde{V}(\tau^\nu(i\Delta t-, X)) - v(i\Delta t-, X)| dX \\
&\qquad \leq \frac{\Delta t}{\delta}(N+1)(b-a) \sup_{U^\nu \in \mathcal{D}(M)} |\tilde{V}(\tau^\nu) - (w^\nu - \tilde{p}(\tau^\nu))| \\
&\qquad \leq L_\delta(t - s + \Delta t),
\end{aligned}$$

where

$$L_\delta = \frac{(b-a)}{\delta} \sup_{U^\nu \in \mathcal{D}(M)} |\tilde{V}(\tau^\nu) - (w^\nu - \tilde{p}(\tau^\nu))|.$$

Summing this term with the estimates that remain valid between two consecutive time-steps, we obtain (2.2.7). □

2.3 Convergence of the WFT approximations to a solution of the relaxed ARZ system

The following theorem ensures the existence of weak entropy solutions of the Cauchy problem (2.1.8), (2.1.9).

Theorem 2.3.1. *Let $U_0 = (\tau_0, w_0) \in \mathcal{D}(M)$ for some $M > 0$ and, for any $\delta > 0$ fixed, denote by $U^\delta = (\tau^\delta, w^\delta)$ the limit of a subsequence $U^\nu = (\tau^\nu, w^\nu)$ of WFT approximate solutions as $\nu \to \infty$. Then U^δ is a weak entropic solution of* (2.1.8), (2.1.9).

Proof. The proof follows the guidelines of [52]. The existence of the limit U^δ and the convergence in $\mathbf{L}^1_{\text{loc}}([0,+\infty[\times\mathbb{R})$ is guaranteed by [20, Theorem 2.4]. Moreover, each component of U^δ satisfies (2.2.6) and (2.2.7). For simplicity of notations, we will drop the δ index in the proof and name U the limit of a subsequence of WFT approximate solutions.

System (2.1.8) can be rewritten as:

$$U_t + [F(U)]_X = G(U),$$

with

$$U = \begin{pmatrix} \tau \\ w \end{pmatrix}, \qquad F(U) = \begin{pmatrix} -(w - \tilde{p}(\tau)) \\ 0 \end{pmatrix}, \qquad G(U) = \begin{pmatrix} 0 \\ \frac{\tilde{V}(\tau) - (w - \tilde{p}(\tau))}{\delta} \end{pmatrix}.$$

Let $T > 0$ a given finite time-horizon. Let $\phi \in C^1_c([0,T[\times\mathbb{R})$. To be a weak solution of (2.1.8), U must satisfy:

$$\int_{-\infty}^{+\infty} \phi(0,X)U_0(X)dX + \int_0^T \int_{-\infty}^{+\infty} [\phi_t(t,X)U(t,X) + \phi_X(t,X)F(U(t,X))]dXdt + \int_0^T \int_{-\infty}^{+\infty} \phi(t,X)G(U(t,X))dXdt = 0. \quad (2.3.1)$$

We define $N^\nu \in \mathbb{N}$ such that $T = N^\nu \Delta t^\nu + \beta^\nu, \beta^\nu \in [0, \Delta t^\nu[$. We will proceed component by component. Let us begin with τ.
For each $k \in \{0, .., N_\nu - 1\}$, since τ^ν satisfies the first equation of (2.1.8) we have:

$$\begin{aligned} \int_{k\Delta t^\nu}^{(k+1)\Delta t^\nu} \int_{-\infty}^{+\infty} [\phi_t \tau^\nu - \phi_X(w^\nu - \tilde{p}(\tau^\nu))]dXdt \\ = \int_{-\infty}^{+\infty} \phi((k+1)\Delta t^\nu, X)\tau^\nu((k+1)\Delta t^\nu -, X)dX \\ - \int_{-\infty}^{+\infty} \phi(k\Delta t^\nu, X)\tau^\nu(k\Delta t^\nu +, X)dX. \end{aligned} \quad (2.3.2)$$

Then

$$\begin{aligned}\int_0^T \int_{-\infty}^{+\infty} [\phi_t \tau^\nu - \phi_X(w^\nu - \tilde{p}(\tau^\nu))] dX dt = \\ \sum_{k=0}^{N^\nu - 1} \int_{k\Delta t^\nu}^{(k+1)\Delta t^\nu} \int_{-\infty}^{+\infty} [\phi_t \tau^\nu - \phi_X(w^\nu - \tilde{p}(\tau^\nu))] dX dt \\ + \int_{N^\nu \Delta t^\nu}^{T} \int_{-\infty}^{+\infty} [\phi_t \tau^\nu - \phi_X(w^\nu - \tilde{p}(\tau^\nu))] dX dt \\ = \int_{-\infty}^{+\infty} \phi(N^\nu \Delta t^\nu, X) \tau^\nu(N^\nu \Delta t^\nu -, X) dX - \int_{-\infty}^{+\infty} \phi(0, X) \tau^\nu(0+, X) dX \\ + \int_{N^\nu \Delta t^\nu}^{T} \int_{-\infty}^{+\infty} [\phi_t \tau^\nu - \phi_X(w^\nu - \tilde{p}(\tau^\nu))] dX dt.\end{aligned}$$

Thus, by reordering,

$$\begin{aligned}\int_{-\infty}^{+\infty} \phi(0, X) \tau_0(X) dX + \int_0^T \int_{-\infty}^{+\infty} [\phi_t \tau^\nu - \phi_X(w^\nu - \tilde{p}(\tau^\nu))] dX dt = \\ \int_{-\infty}^{+\infty} \phi(N^\nu \Delta t^\nu, X) \tau^\nu(N^\nu \Delta t^\nu -, X) dX \\ + \int_{N^\nu \Delta t^\nu}^{T} \int_{-\infty}^{+\infty} [\phi_t \tau^\nu - \phi_X(w^\nu - \tilde{p}(\tau^\nu))](t, X) dX dt.\end{aligned}$$

Since $T - N^\nu \Delta t^\nu < \Delta t^\nu$, and since ϕ has compact support, there exist η such that:

$$\phi(t, X) = 0, \quad \forall \nu > \eta, \forall X \in \mathbb{R}, \forall t \geq N^\nu \Delta t^\nu.$$

Thus the right hand side converges to 0 when $\nu \to \infty$ and then τ satisfies (2.3.1).

Let us now consider w. The approximate function w^ν satisfies:

$$\begin{aligned}\int_{k\Delta t^\nu}^{(k+1)\Delta t^\nu} \int_{-\infty}^{+\infty} \phi_t w^\nu dX dt = \int_{-\infty}^{+\infty} \phi((k+1)\Delta t^\nu, X) w^\nu((k+1)\Delta t^\nu -, X) dX \\ - \int_{-\infty}^{+\infty} \phi(k\Delta t^\nu, X) w^\nu(k\Delta t^\nu +, X) dX \\ = \int_{-\infty}^{+\infty} \phi((k+1)\Delta t^\nu, X) w^\nu((k+1)\Delta t^\nu -, X) dX \\ - \int_{-\infty}^{+\infty} \phi(k\Delta t^\nu, X) \Big[w^\nu(k\Delta t^\nu -, X) + \Delta t^\nu \frac{\tilde{V}(\tau^\nu) - v^\nu}{\delta}(k\Delta t^\nu -, X) \Big] dX.\end{aligned}$$

Then we get

$$\begin{aligned}
&\int_0^T \int_{-\infty}^{+\infty} \phi_t w^\nu dX dt = \\
&\sum_{k=0}^{N^\nu-1} \int_{-\infty}^{+\infty} \Big[\phi((k+1)\Delta t^\nu, X) w^\nu((k+1)\Delta t^\nu -, X) - \phi(k\Delta t^\nu, X) w^\nu(k\Delta t^\nu -, X)\Big] dX \\
&\qquad - \sum_{k=0}^{N^\nu-1} \int_{-\infty}^{+\infty} \phi(k\Delta t^\nu, X)\Delta t^\nu \frac{\tilde{V}(\tau^\nu) - v^\nu}{\delta}(k\Delta t^\nu -, X) dX \\
&\qquad + \int_{N^\nu \Delta t^\nu}^{T} \int_{-\infty}^{+\infty} \phi_t w^\nu dX dt \\
&\qquad = \int_{-\infty}^{+\infty} \phi(N^\nu \Delta t^\nu, X) w^\nu(N^\nu \Delta t^\nu -, X) dX - \int_{-\infty}^{+\infty} \phi(0, X) w_0(X) dX \\
&\qquad - \sum_{k=0}^{N^\nu-1} \int_{-\infty}^{+\infty} \phi(k\Delta t^\nu, X)\Delta t^\nu \frac{\tilde{V}(\tau^\nu) - v^\nu}{\delta}(k\Delta t^\nu -, X) dX \\
&\qquad + \int_{N^\nu \Delta t^\nu}^{T} \int_{-\infty}^{+\infty} \phi_t w^\nu dX dt. \qquad (2.3.3)
\end{aligned}$$

By the same argument as before, picking Δt^ν small enough, we have:

$$\int_{-\infty}^{+\infty} \phi(N^\nu \Delta t^\nu, X) w^\nu(N^\nu \Delta t^\nu -, X) dX + \int_{N^\nu \Delta t^\nu}^{T} \int_{-\infty}^{+\infty} \phi_t w^\nu dX dt = 0.$$

Let us define the sequence of functions ψ^ν such that

$$\psi^\nu(t) = \sum_{k=0}^{N^\nu-1} \chi_{[k\Delta t^\nu,(k+1)\Delta t^\nu[}(t) \int_{-\infty}^{+\infty} \phi(k\Delta t^\nu, X) \frac{\tilde{V}(\tau^\nu) - v^\nu}{\delta}(k\Delta t^\nu -, X) dX. \qquad (2.3.4)$$

Setting for any $(\tau, v) \in \mathbb{R}_+^2$

$$g_\nu(t, X, \tau, v) = \sum_{k=0}^{N^\nu-1} \chi_{[k\Delta t^\nu,(k+1)\Delta t^\nu[}(t) \frac{\tilde{V}(\tau) - v}{\delta}(k\Delta t^\nu -, X), \qquad (2.3.5)$$

we observe that g_ν converges uniformly to $\frac{\tilde{V}(\tau)-v}{\delta}$ on compact subsets of $[0,T] \times \mathbb{R} \times \mathbb{R}_+^2$. In addition, $\tau^\nu \to \tau$ and $v^\nu \to v$ in $\mathbf{L}^1_{\text{loc}}$. Thus, for almost every $t \in [0,T]$:

$$\psi^\nu(t) \to \int_{-\infty}^{+\infty} \phi(t, X) \frac{\tilde{V}(\tau) - v}{\delta}(t, X) dX = \psi(t).$$

We notice that

$$\begin{aligned}\int_0^T \psi^\nu(t)dt &= \int_0^T \sum_{k=0}^{N^\nu-1} \chi_{[k\Delta t^\nu,(k+1)\Delta t^\nu[}(t) \int_{-\infty}^{+\infty} \phi(k\Delta t^\nu, X)\frac{\tilde{V}(\tau^\nu)-v^\nu}{\delta}(k\Delta t^\nu-, X)dXdt \\ &= \sum_{k=0}^{N^\nu-1} \int_0^T \chi_{[k\Delta t^\nu,(k+1)\Delta t^\nu[}(t)dt \int_{-\infty}^{+\infty} \phi(k\Delta t^\nu, X)\frac{\tilde{V}(\tau^\nu)-v^\nu}{\delta}(k\Delta t^\nu-, X)dX \\ &= \sum_{k=0}^{N^\nu-1} \Delta t^\nu \int_{-\infty}^{+\infty} \phi(k\Delta t^\nu, X)\frac{\tilde{V}(\tau^\nu)-v^\nu}{\delta}(k\Delta t^\nu-, X)dX.\end{aligned}$$

By the Lebesgue dominated convergence theorem,

$$\lim_{\Delta t^\nu\to 0}\int_0^T \psi^\nu(t)dt = \int_0^T \psi(t)dt.$$

Passing to the limit in (2.3.3) we recover

$$\begin{aligned}\int_{-\infty}^{+\infty} \phi(0,X)w_0(X)dX + \int_0^T\int_{-\infty}^{+\infty} \phi_t(t,X)w(t,X)dXdt \\ + \int_0^T\int_{-\infty}^{+\infty} \phi(t,X)\frac{\tilde{V}(\tau)-v}{\delta}dXdt = 0.\end{aligned}$$

Therefore the limit U of our sequence of approximate solutions is a weak solution of (2.1.8). Let us prove that U is an entropic solution as well. We fix a smooth convex entropy η with associated flux q. By definition, it satisfies:

$$\begin{aligned}&\nabla\eta^T(z)DF(z) = \nabla^T q(z),\\ &\nabla\eta^T(z)G(z) \le 0,\end{aligned} \qquad \text{for } z\in\mathbb{R}^2_+.$$

Existence of such an entropy, entropy-flux pair is guaranteed by [38, Theorem 3.2].

Let $\phi \in C^1_c([0,T[,\mathbb{R})$, $\phi\ge 0$. We need to show that

$$\begin{aligned}&\int_0^T\int_{-\infty}^{+\infty} \Big[\eta(U(t,X))\phi_t(t,X) + q(U(t,X))\phi_X(t,X) \\ &+ \nabla\eta^T(U(t,X))G(t,X,U(t,X))\phi(t,X)\Big]dXdt + \int_{-\infty}^{+\infty}\phi(0,X)\eta(U_0(X))dX \ge 0. \quad (2.3.6)\end{aligned}$$

As we did in (2.3.3), we can write:

$$\begin{aligned}&\int_0^T\int_{-\infty}^{+\infty} \Big[\eta(U^\nu(t,X))\phi_t(t,X) + q(U^\nu(t,X))\phi_X(t,X)\Big]dXdt \\ &\ge \sum_{k=0}^{N^\nu-1}\int_{-\infty}^{+\infty}\Big[\eta(U^\nu((k+1)\Delta t^\nu-,X))\phi((k+1)\Delta t^\nu-,X) - \eta(U^\nu(k\Delta t^\nu+,X))\phi(k\Delta t^\nu+,X)\Big]dX \\ &\quad + \int_{N^\nu\Delta t^\nu}^T\int_{-\infty}^{+\infty} \Big[\eta(U^\nu(t,X))\phi_t(t,X) + q(U^\nu(t,X))\phi_X(t,X)\Big]dXdt + \mathcal{O}(\epsilon_\nu).\end{aligned}$$

By the same compactness argument than before, we state that the last integral is identically zero for Δt^ν small enough.
The remaining terms give

$$\begin{aligned}
&\int_0^T \int_{-\infty}^{+\infty} \Big[\eta(U^\nu(t,X))\phi_t(t,X) + q(U^\nu(t,X))\phi_x(t,X)\Big] dX dt \\
\geq &\sum_{k=1}^{N^\nu} \int_{-\infty}^{+\infty} \Big[\eta(U^\nu(k\Delta t^\nu-,X))\phi(k\Delta t^\nu-,X) - \eta(U^\nu(k\Delta t^\nu+,X))\phi(k\Delta t^\nu+,X)\Big] dX \\
&+ \int_{-\infty}^{+\infty} \eta(U^\nu(N^\nu\Delta t^\nu+,X)) \underbrace{\phi(N^\nu\Delta t^\nu+,X)}_{=0} dX - \int_{-\infty}^{+\infty} \phi(0,X)\eta(U_0(X))dX + \mathcal{O}(\epsilon_\nu) \\
\geq &-\Delta t^\nu \sum_{k=1}^{N^\nu} \int_{-\infty}^{+\infty} \partial_w \eta(U^\nu(k\Delta t^\nu+,X)) \frac{\tilde{V}(\tau^\nu) - v^\nu}{\delta}(k\Delta t^\nu-,X)\phi(k\Delta t^\nu,X)dX \\
&- \int_{-\infty}^{+\infty} \phi(0,X)\eta(U_0(X))dX + \mathcal{O}(\epsilon_\nu).
\end{aligned}$$

With the same reasoning as before we pass to the limit using the dominated convergence theorem, obtaining the desired inequality (2.3.6). □

2.4 Estimates of positive waves

Oleĭnik type entropy estimates [122, 124] are known for scalar equations [93], genuinely non-linear systems [22, 24, 30], in particular of Temple class [4, 25], and also balance laws [40, 41, 77]. In this section, we provide a decay estimate for positive waves of the ARZ system with relaxation, accounting for the source term contribution.

Proposition 2.4.1. *Assume that* $\exists c_0 > 0$ *such that* $\forall u, u' \in \mathbf{E}$*:*

$$\begin{aligned}
&|\lambda_1(u) - \lambda_1(u')| = |\tilde{p}'(\tau) - \tilde{p}'(\tau')| \leq c_0, \\
&|\lambda_1(u) - \lambda_2(u')| = |\tilde{p}'(\tau)| \geq 2c_0.
\end{aligned} \tag{2.4.1}$$

Then, there exists a constant $C > 0$ *such that, for any interval* $]a,b[$*, for any time horizon* $T > 0$*, and every initial condition* (2.1.9)*, the measure* $\mu_T^{1+}(]a,b[)$ *of positive 1-waves contained in the solution of* (2.1.8) *obtained as limit of the proposed wave-front tracking approximations satisfies*

$$\mu_T^{1+}(]a,b[) \leq C\frac{b-a}{T} e^{C\frac{T}{\delta}(TV(w_0)+TV(v_0))} + C\frac{T}{\delta}\left(TV(w_0) + TV(v_0)\right). \tag{2.4.2}$$

Proof. Consider the sequence $U^\nu(t,x) = (\tau^\nu, w^\nu)(t,x)$ of piecewise constant approximate solutions constructed by the WFT algorithm proposed in Section 2.2.1. In Riemann-invariant coordinates, we denote this approximate solution by $W^\nu = (v^\nu, w^\nu)$, and then

$\tau^\nu = (\tilde{p})^{-1}(w^\nu - v^\nu)$.
We recall that a *backward 1-characteristic* is an absolutely continuous curve $x = x(t)$ such that $\dot{x}(t) \in [\lambda_1(W^\nu(t, x(t)+)), \lambda_1(W^\nu(t, x(t)-))]$, see[20, Section 10]. On each subinterval $[t_n, t_{n+1}]$, if $x(t)$ does not coincide with a wavefront $x_\alpha(t)$, then $\dot{x}(t) = \lambda_1(W^\nu(t, x(t)))$. Else we have $\dot{x}(t) = \dot{x}_\alpha(t)$. We call $y(t)$ a *minimal backward 1-characteristic* through a point $\bar{x}$ if

$$y(t) = \min\{x(t), x \text{ is a backward 1-characteristic}, x(T) = \bar{x}\}.$$

Let us fix $T > 0$ and an interval $]a, b]$, and call $t \mapsto a(t)$; $t \mapsto b(t)$ the minimal backward 1-characteristics passing through a, b at time T. Let $I(t) =]a(t), b(t)]$. We call $x_\alpha(t)$ the position of wavefronts at time t. Each wavefront belongs to a family $k_\alpha \in 1, 2$ with a size σ_α. The first family is genuinely non-linear, thus we set $\sigma_1 = \lambda_1(W^\nu(t, x_\alpha(t)+)) - \lambda_1(W^\nu(t, x_\alpha(t)-))$. The second is linearly degenerated, then we take $\sigma_2 = w^\nu(t, x_\alpha(t)+) - w^\nu(t, x_\alpha(t)-)$.

Let $z(t) := b(t) - a(t) \geq 0$.

$$\begin{aligned}
\dot{z}(t) &= \dot{b}(t) - \dot{a}(t) \\
&= \lambda_1(W^\nu(t, b(t)+)) - \lambda_1(W^\nu(t, a(t)+)) \\
&= \sum_{\substack{k_\alpha=1,2 \\ x_\alpha(t)\in I(t)}} [\lambda_1(W^\nu(t, x_\alpha(t)+)) - \lambda_1(W^\nu(t, x_\alpha(t)-))] \\
&= \sum_{\substack{k_\alpha=1 \\ x_\alpha(t)\in I(t)}} \Delta\lambda_1(W^\nu(t, x_\alpha(t))) + \sum_{\substack{k_\alpha=2 \\ x_\alpha(t)\in I(t)}} \Delta\lambda_1(W^\nu(t, x_\alpha(t))).
\end{aligned} \tag{2.4.3}$$

Note that $\forall\ k_\alpha = 2,\ x_\alpha(t) \in I(t)$,

$$\begin{aligned}
\exists(v_\alpha, w_\alpha) : \Delta\lambda_1(W^\nu(t, x_\alpha(t))) &= \nabla_{v,w}\lambda_1(v_\alpha, w_\alpha) \cdot (W^\nu(t, x_\alpha(t)+) - W^\nu(t, x_\alpha(t)-)) \\
&= \frac{\tilde{p}''(\tilde{p}^{-1}(w_\alpha^\nu - v_\alpha^\nu))}{\tilde{p}'(\tilde{p}^{-1}(w_\alpha^\nu - v_\alpha^\nu))} \left(w^\nu(t, x_\alpha(t)+) - w^\nu(t, x_\alpha(t)-)\right).
\end{aligned}$$

Since the domain $\mathbf{E}$ is compact, the mapping $W^\nu \mapsto \lambda_1(W^\nu)$ is Lipschitz continuous with Lipschitz constant $C_p = \max_{\tau\in(\check{\tau},\hat{\tau})} |\frac{\tilde{p}''(\tau)}{\tilde{p}'(\tau)}|$, see (2.1.2).
For almost every t (outside splitting moments), from (2.4.3) we obtain

$$\dot{z}(t) \geq M(t) - C_p K(t), \tag{2.4.4}$$

with

$$M^\nu(t) := \sum_{\substack{k_\alpha=1 \\ x_\alpha(t)\in I(t)}} \sigma_\alpha = \sum_{\substack{k_\alpha=1 \\ x_\alpha(t)\in I(t)}} \Delta\lambda_1(W^\nu(t, x_\alpha(t))), \tag{2.4.5}$$

$$K^\nu(t) := \sum_{\substack{k_\alpha=2 \\ x_\alpha(t)\in I(t)}} |\sigma_\alpha| = \sum_{\substack{k_\alpha=2 \\ x_\alpha(t)\in I(t)}} |w^\nu(t, x_\alpha(t)+) - w^\nu(t, x_\alpha(t)-)|. \tag{2.4.6}$$

To estimate $K^\nu(t)$, let

$$\Phi(t) := \sum_{\substack{k_\alpha=2 \\ x_\alpha(t)\in I(t)}} \phi(t, x_\alpha(t))|\sigma_\alpha|,$$

with

$$\phi(t,x) := \begin{cases} 1 & \text{if } x < a(t), \\ \frac{b(t)-x(t)}{z(t)} & \text{if } x \in [a(t), b(t)[, \\ 0 & \text{if } x \geq b(t). \end{cases}$$

Away from interaction points and splitting times the $|\sigma_\alpha|$ are constants and in $]a(t), b(t)]$ we have by (2.4.1)

$$\begin{aligned} \frac{d}{dt}\ \phi(t, x_\alpha(t)) &= \frac{\dot{b}(t) - \dot{x_\alpha}(t)}{z(t)} - \frac{\dot{z}(t)(b(t) - x_\alpha(t))}{z(t)^2} \\ &\leq \frac{\dot{b}(t) - \dot{x_\alpha}(t) + |\dot{b}(t) - \dot{a}(t)|}{z(t)} \\ &\leq -\frac{c_0}{z(t)}\,, \end{aligned}$$

therefore

$$\dot{\Phi}(t) \leq -\frac{c_0}{z(t)} K^\nu(t).$$

At interaction points (except splitting times), the quantity $\sum_{k_\alpha=2} \phi(t, x_\alpha(t))|\sigma_\alpha|$ is constant, since wave strength does not change when measured in Riemann coordinates (and for a linearly degenerate field). Thus

$$\dot{z}(t) - \frac{C_p}{c_0} z(t)\dot{\Phi}(t) - M^\nu(t) \geq 0. \tag{2.4.7}$$

We seek now for a uniform bound for $M^\nu(t)$:

$$M^\nu(t) = \sum_{\substack{k_\alpha=1 \\ x_\alpha(t)\in I(t)}} \left[\lambda_1(W^\nu(t, x_\alpha(t)+)) - \lambda_1(W^\nu(t, x_\alpha(t)-))\right].$$

Note that for any $k_\alpha = 1, x_\alpha(t) \in I(t)$,

$$\begin{aligned} \exists (v_\alpha, w_\alpha) : \Delta\lambda_1(W^\nu(t, x_\alpha(t))) &= \nabla_{v,w}\lambda_1(v_\alpha, w_\alpha) \cdot (W^\nu(t, x_\alpha(t)+) - W^\nu(t, x_\alpha(t)-)) \\ &= -\frac{\tilde{p}''(\tilde{\rho}^{-1}(w_\alpha^\nu - v_\alpha^\nu))}{\tilde{p}'(\tilde{\rho}^{-1}(w_\alpha^\nu - v_\alpha^\nu))} \left(v^\nu(t, x_\alpha(t)+) - v^\nu(t, x_\alpha(t)-)\right). \end{aligned}$$

Now observe that

$$\widetilde{M}^\nu(t) := \sum_{\substack{k_\alpha=1 \\ x_\alpha(t)\in I(t)}} \left[v^\nu(t, x_\alpha(t)+) - v^\nu(t, x_\alpha(t)-)\right]$$

is constant except at splitting times, since we are in the case of a Temple class system, and is equivalent to M^ν again due to the Lipschitzianeity of the mapping $W \mapsto \lambda_1(W)$, see (2.1.2).

Let us estimate the changes occuring when the source term is integrated at a given splitting time $t = t_n = n\Delta t^\nu$, for a given n. Setting $g^\nu_\delta(t,x) = \dfrac{\tilde V(\tilde p^{-1}(w^\nu - v^\nu))) - v^\nu}{\delta}(x,t)$, we have:

$$\begin{aligned}
\widetilde{M}^\nu(t_n+) &= \sum_{\substack{k_\alpha(t_n+)=1\\ x_\alpha(t_n+)\in I(t_n+)}} [v^\nu(t_n+, x_\alpha(t_n+)+) - v^\nu(t_n+, x_\alpha(t_n+)-)] \\
&= \sum_{x_\alpha(t_n)\in I(t_n)} [v^\nu(t_n-, x_\alpha(t_n)+) - v^\nu(t_n-, x_\alpha(t_n)-)] \\
&\qquad\qquad + \Delta t^\nu \left[g^\nu_\delta(t_n-, x_\alpha(t_n)+) - g^\nu_\delta(t_n-, x_\alpha(t_n)-)\right] \\
&= \widetilde{M}^\nu(t_n-) + \sum_{x_\alpha(t_n)\in I(t_n)} \Delta t^\nu \left[g^\nu_\delta(t_n-, x_\alpha(t_n)+) - g^\nu_\delta(t_n-, x_\alpha(t_n)-)\right],
\end{aligned}$$

where we used that if there is a 1-wave in $x_\alpha(t_n-)$, then there is at least one 1-wave in $x_\alpha(t_n+)$. For each ν, we define N^ν such that $T \in [N^\nu\Delta t^\nu, (N^\nu+1)\Delta t^\nu[$. Assume now $t \in [(N_0-1)\Delta t^\nu, N_0\Delta t^\nu[$. Since $\widetilde{M}^\nu$ is constant outside of splitting times, we have:

$$\begin{aligned}
\widetilde{M}^\nu(T) &= \widetilde{M}^\nu(t) + \sum_{n=N_0}^{N^\nu} \Delta\widetilde{M}(t_n) \\
&= \widetilde{M}^\nu(t) + \sum_{n=N_0}^{N^\nu} \sum_{x_\alpha(t_n)\in I(t_n)} \Delta t^\nu \left[g^\nu_\delta(t_n-, x_\alpha(t_n)+) - g^\nu_\delta(t_n-, x_\alpha(t_n)-)\right].
\end{aligned}$$

Therefore we have:

$$\begin{aligned}
M^\nu(t) \geq \frac{\widetilde{M}^\nu(t)}{c_M} &= \frac{1}{c_M}\left(\widetilde{M}^\nu(T) - \sum_{n=N_0}^{N^\nu} \sum_{x_\alpha(t_n)\in I(t_n)} \Delta t^\nu \left[g^\nu_\delta(t_n-, x_\alpha(t_n)+) - g^\nu_\delta(t_n-, x_\alpha(t_n)-)\right]\right) \\
&\geq \frac{M^\nu(T)}{c_M^2} - \frac{1}{c_M}\sum_{n=N_0}^{N^\nu} \sum_{x_\alpha(t_n)\in I(t_n)} \Delta t^\nu \left[g^\nu_\delta(t_n-, x_\alpha(t_n)+) - g^\nu_\delta(t_n-, x_\alpha(t_n)-)\right].
\end{aligned}$$

Then from (2.4.7) we recover

$$\begin{aligned}
\dot z(t) - \frac{C_p}{c_0} z(t)\dot\Phi(t) - \frac{M^\nu(T)}{c_M^2} \\
+ \frac{1}{c_M}\sum_{n=N_0}^{N^\nu} \sum_{x_\alpha(t_n)\in I(t_n)} \Delta t^\nu \left[g^\nu_\delta(t_n-, x_\alpha(t_n)+) - g^\nu_\delta(t_n-, x_\alpha(t_n)-)\right] \geq 0,
\end{aligned}$$

which can be rewritten as

$$\begin{aligned}\dot{z}(t)-\frac{C_p}{c_0}z(t)\dot{\Phi}(t)-\frac{M^\nu(T)}{c_M^2}&\geq -\frac{1}{c_M}\sum_{n=N_0}^{N^\nu}\sum_{x_\alpha(t_n)\in I(t_n)}\Delta t^\nu\left[g_\delta^\nu(t_n-,x_\alpha(t_n)+)-g_\delta^\nu(t_n-,x_\alpha(t_n)-)\right]\\&\geq -\frac{1}{c_M}\sum_{n=1}^{N^\nu}\sum_{x_\alpha(t_n)\in I(t_n)}\Delta t^\nu|g_\delta^\nu(t_n-,x_\alpha(t_n)+)-g_\delta^\nu(t_n-,x_\alpha(t_n)-)|\\&\geq -\frac{1}{c_M}\sum_{n=1}^{N^\nu}\Delta t^\nu TV\left(g_\delta^\nu(t_n-,\cdot);I(t_n)\right).\end{aligned}$$

Hence the solution of (2.4.7) satisfies:

$$\begin{aligned}z(T)&\geq e^{\int_0^T\frac{C_p}{c_0}\dot{\Phi}(t)dt}\left[z(0)+\left(\frac{M^\nu(T)}{c_M^2}-\frac{1}{c_M}\sum_{n=1}^{N^\nu}\Delta t^\nu TV\left(g_\delta^\nu(t_n-,\cdot);I(t_n)\right)\right)\int_0^T e^{-\int_0^t\frac{C_p}{c_0}\dot{\Phi}(s)ds}dt\right]\\&\geq e^{\int_0^T\frac{C_p}{c_0}\dot{\Phi}(t)dt}\left[\left(\frac{M^\nu(T)}{c_M^2}-\frac{1}{c_M}\sum_{n=1}^{N^\nu}\Delta t^\nu TV\left(g_\delta^\nu(t_n-,\cdot);I(t_n)\right)\right)\int_0^T e^{-\int_0^t\frac{C_p}{c_0}\dot{\Phi}(s)ds}dt\right],\end{aligned}$$

which gives

$$\begin{aligned}M^\nu(T)&\leq\frac{c_M^2z(T)e^{-\int_0^T\frac{C_p}{c_0}\dot{\Phi}(t)dt}}{\int_0^T e^{-\int_0^t\frac{C_p}{c_0}\dot{\Phi}(s)ds}dt}+c_M\sum_{n=1}^{N^\nu}\Delta t^\nu TV\left(g_\delta^\nu(t_n-,\cdot);I(t_n)\right)\\&\leq\frac{c_M^2z(T)}{T}e^{-\int_0^T\frac{C_p}{c_0}\dot{\Phi}(t)dt}dt+c_M\sum_{n=1}^{N^\nu}\Delta t^\nu TV\left(g_\delta^\nu(t_n-,\cdot);I(t_n)\right).\end{aligned}$$

By the same process as above, we can estimate the contribution given by Φ as follows:

$$\begin{aligned}\int_0^T\dot{\Phi}(t)dt&=\Phi(T)-\sum_{n=1}^{N^\nu}(\Phi(n\Delta t+)-\Phi(n\Delta t-))-\Phi(0)\\&\geq\Phi(T)-\Phi(0)-\sum_{n=1}^{N^\nu}|\Delta\Phi(n\Delta t)|\\&\geq\Phi(T)-\Phi(0)-\sum_{n=1}^{N^\nu}|\Delta K^\nu(n\Delta t)|\\&\geq\Phi(T)-\Phi(0)-\sum_{n=1}^{N^\nu}\Delta t^\nu TV\left(g_\delta^\nu(t_n-,\cdot);I(t_n)\right)\end{aligned}$$

since ϕ is time-continuous, and we obtain

$$M^\nu(T) \leq \frac{c_M^2 z(T)}{T} e^{-\int_0^T \frac{C_p}{c_0}\dot{\Phi}(t)dt} dt + c_M \sum_{n=1}^{N^\nu} \Delta t^\nu TV\left(g_\delta^\nu(t_n-,\cdot); I(t_n)\right)$$
$$\leq \frac{c_M^2 z(T)}{T} e^{\frac{C_p}{c_0}\left(\Phi(0)-\Phi(T)+\sum_{n=1}^{N^\nu}\Delta t^\nu TV\left(g_\delta^\nu(t_n-,\cdot);I(t_n)\right)\right)} + c_M \sum_{n=1}^{N^\nu} \Delta t^\nu TV\left(g_\delta^\nu(t_n-,\cdot); I(t_n)\right).$$

This estimate remains valid for any finite number l of disjoints intervals $I_i =]a_i, b_i]$. We call $M_i^\nu(T)$ the sum of strength of of 1-waves in $W^\nu(T,.)$ contained in $]a_i, b_i]$ and write $TV\left(g_\delta^\nu(t,\cdot); I_i(t)\right)$ the total variation associated to the interval $]a_i(t), b_i(t)]$:

$$M_i(T) = \sum_{k_\alpha=1, x_\alpha \in]a_i,b_i]} \sigma_\alpha.$$

We now consider a given open-interval $]a,b[$. We assume that the front tracking approximation U^ν initially contains N shocks emanating from the initial datum. We can now define half-open disjoint intervals $I_i =]a_i, b_i]$, $1 \leq i \leq N+1$, such that:

- every 1-rarefaction front in W^ν at T lying in $]a,b[$ is contained in an interval I_i.
- each interval I_i can only contain shocks originating from the integration of the splitting term at a time t_n, and cannot contain shocks originating from the initial datum.

The measure of positive 1-waves in $W^\nu(T,\cdot)$ is then

$$\mu_T^{1+}(]a,b[) = \sum_{i=1}^{l} M_i(T). \tag{2.4.8}$$

We have the following bound:

$$\sum_{i=1}^{l} TV_i\left(g_\delta^\nu(t_n-,\cdot); I_i(t_n)\right) \leq TV\left(g_\delta^\nu(t_n-,\cdot);]a,b[\right). \tag{2.4.9}$$

By definition of $g_\delta^\nu(t,\cdot)$, we have

$$TV\left(g_\delta^\nu(t,\cdot);]a,b[\right) \leq \frac{1}{\delta} TV\left(\tilde{V}\circ\tilde{p}^{-1}(w^\nu - v^\nu)(t,\cdot);]a,b[\right) + TV\left(v^\nu(t,\cdot);]a,b[\right)$$
$$\leq \frac{C_{Vp}}{\delta}\left(TV\left(w^\nu(t,\cdot);]a,b[\right) + TV\left(v^\nu(t,\cdot);]a,b[\right)\right)$$
$$\leq \frac{C_{Vp}}{\delta}\left(TV(w_0^\nu) + TV(v_0^\nu)\right)$$
$$\leq \frac{C_{Vp}}{\delta}\left(TV(w_0) + TV(v_0)\right),$$

where we used the Lipschitz-continuity of $\tilde{V} \circ \tilde{p}^{-1}$ on the domain $\mathbf{E}$ and the result of Lemma 2.2.2. Finally we get

$$\begin{aligned}
\mu_T^{1+}(]a,b[) &\leq \sum_{i=1}^{l} \frac{c_M^2(b_i-a_i)}{T} e^{\frac{C_p}{c_0}\left(\Phi_i(0)-\Phi_i(T)+T\frac{C_{Vp}}{\delta}(TV(w_0)+TV(v_0))\right)} \\
&\qquad + c_M T \frac{C_{Vp}}{\delta}\left(TV(w_0)+TV(v_0)\right) \\
&\leq c_M^2 \frac{b-a}{T} e^{\frac{C_p}{c_0}\left(\Phi(0)+T\frac{C_{Vp}}{\delta}(TV(w_0)+TV(v_0))\right)} + c_M T \frac{C_{Vp}}{\delta}\left(TV(w_0)+TV(v_0)\right) \\
&\leq c_M^2 \frac{b-a}{T} e^{\frac{C_p}{c_0}\left(TV(w_0)+T\frac{C_{Vp}}{\delta}(TV(w_0)+TV(v_0))\right)} + c_M C_{Vp} \frac{T}{\delta}\left(TV(w_0)+TV(v_0)\right),
\end{aligned}$$

proving (2.4.2) with $C = \max\left\{c_M^2 e^{\frac{C_p}{c_0}TV(w_0)}, c_M C_{Vp}, \frac{C_p}{c_0}, \frac{C_p C_{Vp}}{c_0}\right\}$. □

Remark. Unfortunately, the lower semicontinuity of the total variation does not allow to pass to the limit as $\nu \to \infty$ in the term $TV\left(g_\delta^\nu(t_n-,\cdot);]a,b[\right)$ to recover a sharper estimate depending on the time integral of the total variation of the relaxation term.

2.5 Convergence of the relaxed ARZ system towards the LWR model

In this section, we follow the methodology of [2] to prove that the solutions of the the relaxed ARZ system (2.1.8) converge towards a solution of the equilibrium LWR equation as $\delta \to 0$. For each $\delta > 0$, we constructed a sequence of approximate WFT solutions whose limit solves (2.1.8) in the weak sense. We recall that, under the assumptions of Lemma 2.2.3, for any $a < b$ and $0 \leq s \leq t$ they satisfy estimates (2.2.6) and (2.2.7):

$$\begin{aligned}
&\int_a^b |\tau^\nu(t,X) - \tau^\nu(s,X)|dX \leq C_M(t-s), \\
&\int_a^b |w^\nu(t,X) - w^\nu(s,X)|dX \leq (C_M + L_\delta)(t-s+\Delta t^\nu).
\end{aligned}$$

To pass to the limit as $\delta \to 0$, we need a stronger estimate on L_δ.

Lemma 2.5.1. *Assume that the subcharacteristic condition* (2.1.10) *is satisfied. Under the same assumptions of Lemma 2.2.3, we have the following estimate:*

$$L_\delta \leq \frac{2}{\delta} e^{-\frac{s}{\delta}} \int_a^b |\tilde{V}(\tau_0(X)) - v_0(X)|dX. \tag{2.5.1}$$

Proof. Let $\delta > 0$ and ν be given. For each $k \geq 1$, we define:

$$g_k^\pm = \int_a^b |\tilde{V}(\tau^\nu(k\Delta t^\nu \pm, X)) - v^\nu(k\Delta t^\nu \pm, X)|dX.$$

We develop

$$\begin{aligned} g_k^+ =& \int_a^b |\tilde{V}(\tau^\nu(k\Delta t^\nu+, X)) - v^\nu(k\Delta t^\nu+, X)|dX \\ =& \int_a^b |\tilde{V}(\tau^\nu(k\Delta t^\nu-, X)) - \big(v^\nu(k\Delta t^\nu-, X) + \frac{\Delta t^\nu}{\delta}(\tilde{V}(\tau^\nu(k\Delta t^\nu-, X)) - v^\nu(k\Delta t^\nu-, X))\big)|dX \\ =& \big(1 - \frac{\Delta t^\nu}{\delta}\big) g_k^-. \end{aligned} \tag{2.5.2}$$

Therefore we get

$$\begin{aligned} g_k^- - g_{k-1}^+ &= \int_a^b |\tilde{V}(\tau^\nu(k\Delta t^\nu-, X)) - v^\nu(k\Delta t^\nu-, X)| \\ &\qquad - |\tilde{V}(\tau^\nu((k-1)\Delta t^\nu+, X)) - v^\nu((k-1)\Delta t^\nu+, X)|dX \\ &\le \int_a^b \big|\big(\tilde{V}(\tau^\nu(k\Delta t^\nu-, X)) - v^\nu(k\Delta t^\nu-, X)\big) \\ &\qquad - \big(\tilde{V}(\tau^\nu((k-1)\Delta t^\nu+, X)) - v^\nu((k-1)\Delta t^\nu+, X)\big)\big|dX \\ &\le \int_a^b \big|\big(\tilde{V}(\tau^\nu(k\Delta t^\nu-, X)) - \tilde{V}(\tau^\nu((k-1)\Delta t^\nu+, X))\big) \\ &\qquad - \big(w^\nu(k\Delta t^\nu-, X) - w^\nu((k-1)\Delta t^\nu+, X)\big) \\ &\qquad + \big(\tilde{p}(\tau^\nu(k\Delta t^\nu-, X)) - \tilde{p}(\tau^\nu((k-1)\Delta t^\nu+, X))\big)\big|dX \\ &\le \sup_{U^\nu \in \mathcal{D}(M)} (|\tilde{V}'(\tau^\nu)| + |\tilde{p}'(\tau^\nu)|) C_M \Delta t^\nu \\ &\le K_1 \Delta t^\nu, \end{aligned} \tag{2.5.3}$$

where $K_1 := \sup_{U^\nu \in \mathcal{D}(M)} (|\tilde{V}'(\tau^\nu)| + |\tilde{p}'(\tau^\nu)|) C_M$. Combining (2.5.2) and (2.5.3) we obtain:

$$\begin{aligned} g_k^- &\le K_1 \Delta t^\nu \sum_{i=0}^{k-1} \left(1 - \frac{\Delta t^\nu}{\delta}\right)^i + \left(1 - \frac{\Delta t^\nu}{\delta}\right)^{k-1} g_0^+ \\ &\le K_1 \delta + \left(1 - \frac{\Delta t^\nu}{\delta}\right)^{k-1} g_0^+. \end{aligned}$$

As in the proof of Lemma 2.2.3, we write:

$$\begin{aligned}\sum_{i=k}^{k+N^\nu}\int_a^b |w^\nu(i\Delta t^\nu+,X)-w^\nu(i\Delta t^\nu-,X)|dX \\ &= \frac{\Delta t^\nu}{\delta}\sum_{i=k}^{k+N^\nu} g_i^- \\ &\le \frac{\Delta t^\nu}{\delta}\sum_{i=k}^{k+N^\nu}\left[K_1\delta+\left(1-\frac{\Delta t^\nu}{\delta}\right)^{i-1} g_0^+\right] \\ &\le K_1(t-s+\Delta t^\nu)+g_0^+\left(1-\frac{\Delta t^\nu}{\delta}\right)^{k-1}\left[1-\left(1-\frac{\Delta t^\nu}{\delta}\right)^{N^\nu+1}\right].\end{aligned}$$

Taking $\Delta t^\nu \le \frac{\delta}{2}$, we have $2\left(1-\frac{\Delta t^\nu}{\delta}\right)\ge 1$ and

$$\begin{aligned}\sum_{i=k}^{k+N^\nu}\int_a^b |w^\nu(i\Delta t^\nu+,X)-w^\nu(i\Delta t^\nu-,X)|dX &\le K_1(t-s+\Delta t^\nu) \\ &\quad + 2g_0^+\left(1-\frac{\Delta t^\nu}{\delta}\right)^{k}(N+1)\frac{\Delta t^\nu}{\delta} \\ &\le (t-s+\Delta t^\nu)\left[K_1+2\frac{g_0^+}{\delta}e^{-\frac{s}{\delta}}\right].\end{aligned}$$

Then the result holds with another constant C_M large enough. □

We can now present the main result of this chapter.

Theorem 2.5.2. *Let $U_0=(\tau_0,w_0)\in\mathcal{D}(M)$ for some $M>0$, and denote by $\bar U=(\bar\tau,\bar w)$ the limit as $\delta\to 0$ of a subsequence of weak entropy solutions $U^\delta=(\tau^\delta,w^\delta)$ of (2.1.8), (2.1.9), obtained as limit of the proposed wave-front tracking approximations. Then $\bar w=\tilde V(\bar\tau)+\tilde p(\bar\tau)$ and $\bar\tau$ is a weak solution of the scalar Cauchy problem:*

$$\begin{cases}\partial_t\tau-\partial_X\tilde V(\tau)=0,\\ \tau(0,\cdot)=\tau_0(\cdot),\end{cases}\qquad X\in\mathbb{R},\ t>0. \tag{2.5.4}$$

Proof. First we remind that the constant C_M in (2.2.6) and (2.2.7) does not depend on δ. In addition, thanks to (2.5.1), the constant L_δ can be bounded uniformly as $\delta\to 0$ on any set $[1/n,\infty[\times[-n,n]$ for $n\in\mathbb{N}$. If $\frac{1}{n}\le s\le t$ then, for a given constant C only depending on the initial datum, there holds

$$L_\delta\le\frac{C}{\delta}(b-a)e^{-\frac{1}{n\delta}}. \tag{2.5.5}$$

For n fixed, the right-hand side goes to zero with δ.

By Helly's theorem, there exists a subsequence $\delta_k \to 0$, such that the sequence (τ^{δ_k}) converges to a function $\bar{\tau}$ in $\mathbf{L}^1_{\text{loc}}([0,+\infty[\times\mathbb{R})$. In addition we have by construction $\bar{\tau}(0,\cdot) = \tau_0(\cdot)$ and the limit also satisfies the Lipschitz inequality.

For $\bar{w}$ we can reason on the set $[1,+\infty[\times[-1,1]$. We can extract a subsequence δ_k^1 from δ_k such that $w^{\delta_k^1}$ converges to a function $\bar{w}$ in $\mathbf{L}^1_{\text{loc}}([1,+\infty[\times[-1,1])$. Passing to the limit in (2.3.1) we obtain

$$\bar{w}(t,\cdot) = \tilde{V}(\bar{\tau}(t,\cdot)) + \tilde{p}(\bar{\tau}(t,\cdot))$$

on the set $[1,+\infty[\times[-1,1]$, and then $\bar{\tau}_t - \tilde{V}(\bar{\tau})_x = 0$.

Similarly, for any $n \in \mathbb{N}$, we can extract a subsequence δ_k^n of δ_k^{n-1} such that $w^{\delta_k^n}$ converges to $\bar{w}$ in $\mathbf{L}^1_{\text{loc}}([1/n,+\infty[\times[-n,n])$. For any $\frac{1}{n} \leq s \leq t$, (2.5.5) combined with (2.2.7) provides:

$$\int_{-n}^{n} |\bar{w}(t,X) - \bar{w}(s,X)|dX \leq C_M|t-s|. \tag{2.5.6}$$

We can then construct by a diagonal process a sequence $(\tau^{\delta_k^n}, w^{\delta_k^n})$ that converges to $(\bar{\tau},\bar{w})$ in $\mathbf{L}^1_{\text{loc}}(]0,+\infty[\times\mathbb{R})$. For any compact subset of $[0,+\infty[\times\mathbb{R}$, we know that $(\tau^{\delta_k^n}, w^{\delta_k^n})$ converges to $(\bar{\tau},\bar{w})$ in $\mathbf{L}^1_{\text{loc}}([1/n,+\infty[\times[-n,n])$, and it is bounded by construction. Therefore, we get convergence in $\mathbf{L}^1_{\text{loc}}([0,+\infty[\times\mathbb{R})$.

Inequality (2.5.6) holds for any $0 < s < t$ and any $n \in \mathbb{N}$, we can thus pass to the limit when $t \to 0$, and define:

$$\bar{w}(0,\cdot) = \lim_{t\to 0} \bar{w}(t,\cdot) = \lim_{t\to 0} \tilde{V}(\bar{\tau}(t,\cdot)) + \tilde{p}(\bar{\tau}(t,\cdot)) = \tilde{V}(\tau_0(\cdot)) + \tilde{p}(\tau_0(\cdot)). \tag{2.5.7}$$

Then $\bar{\tau}$ is a weak solution of (2.5.4), which corresponds to the usual LWR model. □

Remark. Proving that the solutions of the ARZ system with relaxation (2.1.8) converge to the (unique) entropy weak solution of (2.5.4) is still an open problem, see [99, Section 5] and [2, Section 4] for related discussions. In [38, Theorem 3.2], the authors prove that for any entropy/entropy-flux pair (ϕ,ψ) of the equilibrium equation (2.5.4), under the strict subcharacteristic condition, there exists a strictly convex entropy pair (η,q) for the system (2.1.8) over an open set Ω_ϕ containing the equilibrium curve. Unfortunately, we cannot provide the necessary L^∞ uniform estimates to ensure that, for δ small enough, $U^\delta \subset \Omega_\phi$. The mild decay estimate (2.4.2) does not give useful information for $\delta \to 0$. Recently, a deep investigation of the question was proposed in [55]. Following the idea of [55, Section 2], we may derive an explicit expression of an entropy function η for (2.1.8), which is not convex. Nevertheless, following the methodology of [55], one may be able to show that the negative entropy production vanishes in the limit.

Appendix

The present work was motivated by the lack of complete convergence results of the relaxed ARZ model (2.1.3) to the equilibrium LWR equation

$$\partial_t \rho + \partial_x V_e(\rho) = 0.$$

Following [8, 81], we made the choice of working in Lagrangian coordinates, which significantly simplifies computations. The same procedure could be carried out for the original problem in Eulerian coordinates. Besides, as mentioned in the introduction, the choice of the WFT scheme for constructing approximate solutions was motivated by the lack of TV bounds on classical Godunov approximations. This was already pointed out in [132] for system (2.1.3), but remains valid in Lagrangian coordinates. Indeed, Godunov scheme for the homogeneous step (2.2.3) reads (see [8, Eq. (4.8)]) as

$$\begin{aligned} \tau_i^{n+1} &= \tau_i^n + \frac{\Delta t}{\Delta X}\left(v_{i+1}^n - v_i^n\right), \\ w_i^{n+1} &= w_i^n, \end{aligned}$$

see also Figure 2.2. Note that, in general, the solution of the Riemann problem with initial data (U_i^n, U_{i+1}^n), accounts for a wave of the first family traveling with negative speed and a stationary contact discontinuity.

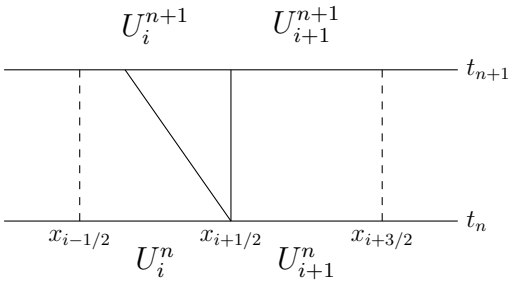

Figure 2.2 – Notations used for Godunov scheme, with $U_i^n = (\tau_i^n, w_i^n)$.

By construction, and relying on the fact that τ is a conserved variable, we have that $\tau_i^{n+1} \in I\left(\tau_i^n, \tau_{i+1}^n\right)$, with the notation $I(a,b) := [\min\{a,b\}, \max\{a,b\}]$. Therefore $\tilde{p}(\tau_i^{n+1}) \in I\left(\tilde{p}\left(\tau_i^n\right), \tilde{p}\left(\tau_{i+1}^n\right)\right)$, since $\tilde{p}$ is monotone. This gives

$$v_i^{n+1} \in I\Big(w_i^n - \tilde{p}\left(\tau_i^n\right), w_i^n - \tilde{p}\left(\tau_{i+1}^n\right)\Big) = I\Big(v_i^n, v_{i+1}^n + \left(w_i^n - w_{i+1}^n\right)\Big) \neq I\left(v_i^n, v_{i+1}^n\right),$$

since $w_i^n - w_{i+1}^n \neq 0$ in general. In particular, we may have $v_i^{n+1} \notin I\left(v_i^n, v_{i+1}^n\right)$. This may generate spurious oscillations around contact discontinuities, see for example [36].

Chapter 3

Well-posedness of a macroscopic traffic flow model with bounded acceleration

Abstract

In this chapter we propose a new macroscopic traffic flow model accounting for the boundedness of traffic acceleration, which is required for physical realism. Our model is built on the coupling between the scalar conservation law accounting for the conservation of vehicles and a number of ordinary differential equations describing the trajectories of accelerating vehicles, which we treat as moving constraints. We propose a wave-front tracking algorithm to construct approximate solutions of the model, with general flux functions. With wave-front tracking, we show existence of solutions to the Cauchy problem. Finally, we use the algorithm to numerically simulate several urban situations, from a single Riemann problem to sequences of traffic lights, and confront the results to numerical simulations of the LWR model.

The content of this chapter was published or submitted under the following references:

N. Laurent-Brouty, G. Costeseque, and P. Goatin. A coupled PDE-ODE model for bounded acceleration in macroscopic traffic flow models. *IFAC-PapersOnLine*, 51(9):37 – 42, 2018. 15th IFAC Symposium on Control in Transportation Systems CTS 2018;

N. Laurent-Brouty, G. Costeseque, and P. Goatin. A macroscopic traffic flow model accounting for bounded acceleration. preprint, June 2019.

3.1 Introduction

As detailed in Chapter 1, macroscopic traffic flow models can display discontinuous solutions in space and time, giving rise to infinite acceleration or deceleration rates. In this chapter, we focus on situations in which the solutions to the LWR model and second order models present an unbounded acceleration of traffic. This is the case when the traffic conditions display downward jumps in density, corresponding to upward jumps in velocity. These situations may occur at downward discontinuities of the initial density datum or can be generated by boundary conditions, for instance downstream a merge or a bottleneck whose positions are known. It happens for example when a traffic light turns green. At these locations, the weak entropy solution to the classical LWR model consists of a rarefaction wave, accounting for an instantaneous jump from a lower velocity to a higher velocity, which corresponds to an infinite acceleration of the leading vehicle and bounded but unrealistic acceleration values for the following ones. This prevents any coupling of the LWR model (and also second order models like [126, 143] and [9, 146]) with consumption and pollution models (see for example [140] and references therein), in which the acceleration component plays a crucial role. This coupling is crucial to implement in order to control traffic emissions, since urban areas are repeatedly faced with severe episodes of atmospheric pollution. Bounded acceleration of vehicles may also have an impact on management procedures, such as traffic signals optimization, which require a precise estimation of queue dissipation times (see [5] and references therein). Macroscopic models accounting for bounded acceleration of vehicles have been previously addressed in the engineering literature. In particular, [107, 108] propose a two phase model in which the bounded acceleration phase is described by a non-strictly hyperbolic system of balance laws, while [113] applies to rather restrictive cases limited to piecewise affine fundamental diagrams.

Following the ideas introduced in [108] and observing that situations with unbounded acceleration only appear for specific initial datum, we derive a model in which accelerating vehicles are treated as moving local constraints. We then propose to couple the LWR model with a number of Ordinary Differential Equations (ODEs), each accounting for the trajectory of a leading vehicle, initially located at a downward jump in density, and accelerating at a constant rate. We assume that all vehicles accelerate at the same constant rate, and that overtaking is not possible. Thus, the leading vehicles will accelerate and regulate upstream traffic. These vehicles will then act as moving constraints, enforcing a zero flux along their trajectory, until they catch the downstream traffic. We investigate the well-posedness of our new approach to account for the finite acceleration of vehicles from a macroscopic point of view. We provide a rigorous constructive algorithm to compute approximate solutions to our model, which can be applied to a large class of fundamental diagrams, and use it to illustrate the solutions behavior. Unlike [107, 108, 113, 114], our approach is general and can be applied to a large class of fundamental diagrams, or even to higher order models.

The idea of modeling the interaction of specific vehicles (like buses or trucks) with the

surrounding traffic through strongly coupled PDE-ODE systems was introduced in [110] and then studied analytically in [58, 100, 119], see also [15, 35, 62, 141] for a numerical treatment and an extension to second order models. Compared to the above literature, the *moving constraint* presents in our approach a non-linear trajectory imposed by the acceleration bound, which is independent of the downstream traffic conditions as long as the leading vehicle, *i.e.* the bottleneck, has not rejoined the preceding vehicles. The bottleneck dynamics, and its impact on traffic, are therefore different from the framework described in [58]. Yet, at this stage, we are only interested in constructing a fine approximation algorithm and in proving existence of solutions for piecewise constant initial data.

This chapter is organized as follows: in Section 3.2 we describe the mathematical formulation of the proposed PDE-ODE model, and define its solutions. We then analyse the associated Riemann problem, and propose a wave-front tracking algorithm to approximate the solutions to the Cauchy problem. In Section 3.3 we prove existence of a weak solution to our model. To do so, we first show convergence of approximate solutions to a limit, and then prove that this limit actually satisfies the definition of solutions. In Section 3.4 we present several numerical simulations, from the solution to the Riemann problem to illustrations of a sequence of traffic lights, and confront the results to the solution of the LWR model. After a brief conclusion of the chapter in Section 3.5, we detail the key aspects of the numerical implementation of wave-front tracking in Appendix.

3.2 A coupled PDE-ODE model accounting for bounded acceleration

3.2.1 Mathematical formulation and definition of solutions

We consider an initial value problem for which the initial datum ρ^0 is piecewise constant, and admits $I \in \mathbb{N}$ downward jumps in density. For this reason, we introduce I moving bottlenecks, and propose the following model, based on the moving constraint model of [58, 110]. In the following, we will use $\mathcal{I} := \{1 \leq i \leq I, i \in \mathbb{N}\}$.

$$\partial_t \rho + \partial_x f(\rho) = 0, \qquad x \in \mathbb{R},\ t > 0, \tag{3.2.1a}$$
$$\rho(0,x) = \rho^0(x), \qquad x \in \mathbb{R}, \tag{3.2.1b}$$
$$f\left(\rho(t, y_i(t))\right) - \rho(t, y_i(t))\dot{y}_i(t) \leq 0, \qquad t > 0,\ i \in \mathcal{I}, \tag{3.2.1c}$$
$$\dot{y}_i(t) = \omega_i\left(t, y_i(t)\right), \qquad t > 0,\ i \in \mathcal{I}, \tag{3.2.1d}$$
$$y_i(0) = y_i^0, \qquad i \in \mathcal{I}, \tag{3.2.1e}$$

In Equation (3.2.1d), we define

$$\omega_i(t, y_i(t)) := \min\left\{At + v_i^0, v(\rho(t, y_i(t)+)\right\},$$

where $v_i^0 = v(\rho^0(y_i^0-))$ stands for the initial speed of the moving bottleneck starting at position y_i^0 and $A > 0$ is the constant acceleration rate (assumed to be equal for all vehicles). The map $y_i : t \mapsto y_i(t)$ denotes the trajectory of the i-th moving bottleneck.

In our model, the traffic density evolution is described by the scalar conservation law (3.2.1a) and the corresponding initial condition (3.2.1b), corresponding to the classical LWR model. Equation (3.2.1c) accounts for the assumption that no overtaking is possible. It enforces that the flux directly upstream of the bottlenecks created by the leading vehicles is bounded by the flux along their trajectory. The ODE (3.2.1d) provides the trajectory of each accelerating leader starting from the position given by the initial condition (3.2.1e), i.e. any point of downward jump in the density.

Remark 3.1. In the specific case where the initial datum does not contain downward jumps ($I = 0$), there is no moving bottleneck and the model reduces to the LWR model with (3.2.1a), (3.2.1b).

In addition, we consider the following assumptions:

(A1) The map $v : \rho \mapsto v(\rho)$ is decreasing, Lipschitz continuous and satisfies $v(0) = V_{\max}$ and $v(\rho_{\max}) = 0$.

(A2) The map $f : \rho \mapsto f(\rho)$ is strictly concave, differentiable, satisfies $f(0) = f(\rho_{\max}) = 0$ and we denote by $\rho_{\text{crit}} \in]0, \rho_{\max}[$ the point of maximum of f.

(A3) The initial datum $\rho^0 \in BV(\mathbb{R}; [0, \rho_{\max}])$ is a piecewise constant function with a finite number of jumps. In addition, it admits I downward jumps. For every $i \in \mathcal{I}$, it satisfies $\rho^0(y_i^0-) > \rho^0(y_i^0+)$.

Remark 3.2. Concerning assumption **(A3)** above, we remark that any function in $BV(\mathbb{R}; [0, \rho_{\max}])$ can be approximated by a piecewise constant function with a finite number of jumps, see [20, Lemma 2.2], but we will not treat this general case here.

Following [58], we propose the following definition of weak solutions solutions to System (3.2.1).

Definition 3.2.1 (Weak solution of the PDE-ODE model)**.** Let $T > 0$ be a given finite time horizon. We call $(\rho, y) \in C^0([0,T]; \mathbf{L}^1 \cap BV(\mathbb{R}; [0, \rho_{max}])) \times \mathbf{W}^{1,1}([0,T]; \mathbb{R}^I)$ a solution to (3.2.1) if and only if

(i) ρ is a weak solution of (3.2.1a), (3.2.1b), i.e. $\forall \phi \in C_c^1(]-\infty, T[\times\mathbb{R}; \mathbb{R})$,

$$\int_0^T \int_{-\infty}^{\infty} (\rho\phi_t + f(\rho)\phi_x) \mathrm{d}x\mathrm{d}t + \int_{-\infty}^{\infty} \rho^0(x)\phi(0,x)\mathrm{d}x = 0 \tag{3.2.2}$$

and it satisfies the Kružkov entropy condition on $([0,T[\times\mathbb{R}) \backslash \bigcup_{i=1}^{I} \{(t, y_i(t)) : t \in [0,T]\}$, *i.e.* for any $k \in [0, \rho_{\max}]$ and $\forall \phi \in C_c^1([-\infty, T[\times\mathbb{R}; \mathbb{R}^+)$ such that $\phi(t, y_i(t)) = 0$, $t \in [0,T]$, $i \in \mathcal{I}$,

$$\int_0^T \int_{-\infty}^{\infty} (|\rho - k|\phi_t + \operatorname{sgn}(\rho - \kappa)\,(f(\rho) - f(k))\,\phi_x)\,\mathrm{d}x\mathrm{d}t + \int_{-\infty}^{\infty} |\rho^0(x) - k|\phi(0,x)\mathrm{d}x \geq 0; \tag{3.2.3}$$

(ii) for $i \in \mathcal{I}$, each component y_i of y is a Carathéodory solution of (3.2.1d), (3.2.1e), *i.e.*

$$y_i(t) = y_i^0 + \int_0^t \omega_i\left(s, y_i(s)\right) \mathrm{d}s \text{ for any } t \in [0,T]; \tag{3.2.4}$$

(iii) the constraint (3.2.1c) is satisfied for almost every $t \in [0,T]$ and any $i \in \mathcal{I}$.

We can now propose our main result.

Theorem 3.2.1 (Existence of a weak solution)**.** *Assume that assumptions **(A1)**, **(A2)** and **(A3)** are satisfied. Then the Cauchy problem* (3.2.1) *admits a solution in the sense of Definition 3.2.1.*

3.2.2 The Riemann problem

We first focus on the Riemann problem associated to System (3.2.1), *i.e.* when the initial datum is piecewise constant with a single discontinuity:

$$\begin{cases} \rho_L & \text{if} \quad x < y^0, \\ \rho_R & \text{if} \quad x \geq y^0. \end{cases} \tag{3.2.5}$$

For simplicity, we have droped the lower-index notation, since we will have at maximum one bottleneck. Solutions with unbounded acceleration only appear in the case $\rho_L > \rho_R$, when a platoon of vehicles has to accelerate from an initial velocity $v(\rho_L)$ to a higher one $v(\rho_R)$. The case $\rho_L \leq \rho_R$ provides the classical solution to the LWR model *i.e.* a shock wave. The definition of the classical Riemann solver $\mathcal{R}$ for scalar conservation laws is provided by Definition 1.1.6.

We now assume that $\rho_L > \rho_R$ such that the initial datum ρ^0 has a unique downward jump ($I = 1$). In this case, we use the constrained Riemann solver proposed in [58].

Definition 3.2.2 (The constrained Riemann solver)**.** For any $V \in [0, V_{\max}]$, let $\hat{\rho} \in]0, \rho_{\max}]$ such that $v(\hat{\rho}) = V$. Consider the constrained Riemann solver proposed in [58], where the scalar conservation law is coupled to a flux constraint with constant maximal velocity V:

$$\partial_t \rho + \partial_x f(\rho) = 0, \qquad x \in \mathbb{R},\ t > 0, \tag{3.2.6a}$$

$$\rho(0,x) = \begin{cases} \rho_L & \text{if} \quad x < y^0, \\ \rho_R & \text{if} \quad x \geq y^0, \end{cases} \tag{3.2.6b}$$

$$f\left(\rho(t,y(t)) - \rho(t,y(t))\dot{y}(t) \leq 0, \qquad t > 0, \right. \tag{3.2.6c}$$

$$\dot{y}(t) = \min\{V, v(\rho_R)\}, \tag{3.2.6d}$$

$$y(0) = y^0. \tag{3.2.6e}$$

Setting $\xi := (x - y^0)/t$, we define a solution $\rho(t,x) = \mathcal{R}_V(\rho_L, \rho_R)(\xi)$ to (3.2.6) as follows:

- if $f(\mathcal{R}(\rho_L,\rho_R)(V)) - V\,\mathcal{R}(\rho_L,\rho_R)(V) > 0$, then the bottleneck is active and

$$\mathcal{R}_V(\rho_L,\rho_R)(\xi) = \begin{cases} \mathcal{R}(\rho_L,\hat{\rho})(\xi), & \text{if } \xi < V, \\ \mathcal{R}(0,\rho_R)(\xi), & \text{if } \xi \geq V, \end{cases} \quad \text{and} \quad y(t) = y^0 + Vt,$$

- if $f(\mathcal{R}(\rho_L,\rho_R)(V)) - V\,\mathcal{R}(\rho_L,\rho_R)(V) \leq 0$, then the bottleneck is inactive and

$$\mathcal{R}_V(\rho_L,\rho_R)(\xi) = \mathcal{R}(\rho_L,\rho_R)(\xi) \quad \text{for all } \xi \quad \text{and} \quad y(t) = y^0 + \min\{V, v(\rho_R)\}t.$$

3.2.3 Construction of approximate solutions with Wave-Front Tracking

To construct a sequence of approximate solutions $\{\rho_N, y_{i,N}\}_{i\in\mathcal{I},N\in\mathbb{N}}$ to (3.2.1), we adopt the Wave-Front Tracking technique (Section 1.1.3). For any $N \in \mathbb{N}$, we set a grid of densities consisting of $2^N + 1$ points as follows

$$\mathcal{M}_N := 2^{-N}\rho_{\max}\mathbb{N} \cap [0, \rho_{\max}], \tag{3.2.7}$$

and we denote the mesh size by $\epsilon_N := 2^{-N}\rho_{\max}$. In particular, for any distinct $\rho_1, \rho_2 \in \mathcal{M}_N$, we have $|\rho_1 - \rho_2| \geq \epsilon_N$. Moreover, we denote by $v_{j,N}$ the speed corresponding to density $\rho_{j,N} \in \mathcal{M}_N$, that is $v_{j,N} := v(\rho_{j,N})$. We take an approximation ρ_N^0 of the initial datum ρ^0 taking values on the grid, with the same number and location of discontinuities as ρ^0, such that $\mathrm{TV}(\rho_N^0) \leq \mathrm{TV}(\rho^0)$ (existence is guaranteed by [20, Section 2]). In the remaining, we will elude the index N for sake of clarity, when it is not necessary for the computations. Since the moving bottleneck corresponds to a transitory phase describing acceleration of vehicles from a low velocity to a higher one, we expect moving bottlenecks to disappear, and that is why we propose the following definition.

Definition 3.2.3 (Interaction time between a moving bottleneck and downstream traffic)**.** Consider $\{\rho_N, y_{i,N}\}_{i\in\mathcal{I},N\in\mathbb{N}}$ a sequence of approximate solutions to (3.2.1) obtained via wave-front tracking. For any $i \in \mathcal{I}$, we define the interaction time $t_{i,N}^{\mathrm{int}}$ as

$$t_{i,N}^{\mathrm{int}} := \inf\left\{t > 0 \colon v\left(\rho_N(t, y_{i,N}(t)-)\right) \geq v\left(\rho_N(t, y_{i,N}(t)+)\right)\right\}.$$

Remark 3.3. The interaction time $t_{i,N}^{\mathrm{int}}$ corresponds to the instant at which the i-th moving bottleneck catches up with downstream traffic if existing, else it corresponds to the moment when the bottleneck reaches the maximal speed. By definition, we immediately have that $t_{i,N}^{\mathrm{int}} \leq \frac{V_{\max}}{A}, \forall i \in \mathcal{I}$. Since the sequence $\{t_{i,N}^{\mathrm{int}}\}_{N\in\mathbb{N}}$ is uniformly bounded, there exists a subsequence which converges towards some point $t_i^{\mathrm{int}} \leq \frac{V_{\max}}{A}$.

The acceleration phase of the leading vehicle of the i-th moving bottleneck lasts until it reaches its maximal speed $V_{\max}$ or until it catches up with preceding traffic, happening at $t = t_i^{\mathrm{int}}$ in a continuous setting. During this period, it accelerates at a constant rate A. Its trajectory, described by Equation (3.2.1d), is thus given by a parabola

$$y_i(t) = \frac{A}{2}t^2 + v(\rho^0(y_i^0-))t + y_i^0.$$

In the discrete setting, for $i \in \mathcal{I}, N \in \mathbb{N}$, the i-th moving bottleneck is considered active up to time $t = t^{\text{int}}_{i,N}$. To construct our wave-front tracking approximations, we will approximate each parabola by a piecewise linear trajectory, such that the initial slope is equal to $v(\rho^0_N(y^0_i-))$, and then it increases along the grid $\mathcal{M}_N$, taking values $v(\rho^0_N(y^0_i-) - \epsilon_N)$, $v(\rho^0_N(y^0_i-) - 2\epsilon_N)$ and so on, as long as the moving bottleneck is active. This construction is thus valid on a time horizon $[0, t^{\text{int}}_{i,N}[$, which we partition in sub-intervals $[t^n_{i,N}, t^{n+1}_{i,N}[$, where, for any n small enough, $t^n_{i,N}$ is defined for each grid-parameter N such that

$$\begin{cases} t^0_{i,N} = 0, \quad t^{n+1}_{i,N} = t^n_{i,N} + \Delta t^n_{i,N}, \\ \Delta t^n_{i,N} := \dfrac{1}{A}\left[v\left(\rho^0_N(y^0_i-) - (n+1)\epsilon_N\right) - v\left(\rho^0_N(y^0_i-) - n\epsilon_N\right)\right]. \end{cases} \tag{3.2.8}$$

The interval $\Delta t^n_{i,N}$ corresponds to the time necessary to accelerate between two consecutive velocities on the grid $v(\rho^0_N(y^0_i-) - n\epsilon_N)$ and $v(\rho^0_N(y^0_i-) - (n+1)\epsilon_N)$ at a constant acceleration rate A. The approximate trajectory of the active moving bottleneck $y_{i,N}$ is then defined for each grid-parameter N and $t \in [0, t^{\text{int}}_{i,N}[$ as

$$y_{i,N}(t) := y^0_i + \sum_{j=0}^{n-1} v(\rho^0_N(y^0_i-) - j\epsilon_N)\Delta t^j_{i,N} + v(\rho^0_N(y^0_i-) - n\epsilon_N)(t - t^n_{i,N}), \quad \forall\, t \in [t^n_{i,N}, t^{n+1}_{i,N}[.$$

For $t \geq t^{\text{int}}_{i,N}$, *i.e.* when the bottleneck is not active anymore, the trajectory is approximated by:

$$y_{i,N}(t) = y_{i,N}(t^{\text{int}}_{i,N}) + \int_{t^{\text{int}}_{i,N}}^{t} v(\rho_N(s, y_{i,N}(s)+))ds.$$

We now detail the algorithm to construct the wave-front tracking approximations denoted by $\{\rho_N\}_{N\in\mathbb{N}}$ (see Figure 3.1). Let $T > 0$ given.

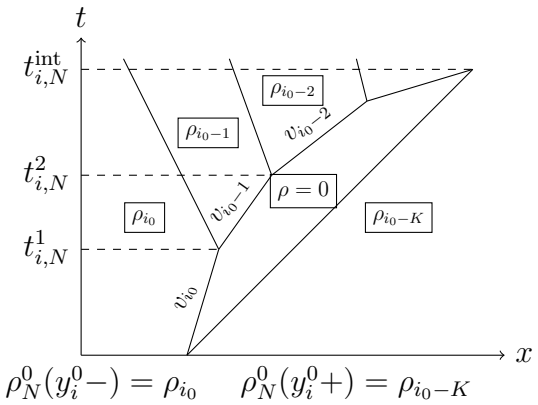

Figure 3.1 – Example of the WFT approximate solution and notation used in the algorithm, focused on the i-th bottleneck, where we have set $\rho^0_N(y^0_i-) =: \rho_{i_0} \in \mathcal{M}_N$ and $v_j = v(\rho_j)$.

Algorithm 1 (Wave-Front Tracking (WFT))**.** Consider a given $N \in \mathbb{N}$.

Step 0. Approximate the initial datum $x \mapsto \rho^0(x)$ by a piecewise constant function $x \mapsto \rho_N^0(x)$ taking values on the grid $\mathcal{M}_N$ defined in (3.2.7). Denote by $\left\{x_j^0\right\}_{j=1,\dots,J}$ the set of J jump locations of ρ_N^0.

Step 1. At $t = 0$, using the constrained Riemann solution $\mathcal{R}_V$ given by Definition 3.2.2, solve the constrained Riemann problem at every density jump location x_j^0 by setting $V = v\left(\rho_N^0(x_j^0-)\right)$.

(i) If $\rho^0(x_j^0-) > \rho^0(x_j^0+)$ and $x_j^0 = y_i^0$ for some $i \in \mathcal{I}$, the solution consists in a jump discontinuity (the moving bottleneck) between $\rho_N^0(y_i^0-)$ and 0, moving at speed $v(\rho_N^0(y_i^0-))$, eventually followed by a shock between 0 and $\rho_N^0(y_i^0+)$, moving at speed $v(\rho_N^0(y_i^0+))$.

(ii) Else, the solution consists in a classical shock between $\rho_N^0(x_j^0-)$ and $\rho_N^0(x_j^0+)$.

The solution can then be prolonged up to some time $\bar{t}$, the first time at which either an interaction between two waves occurs, or at least one of the moving bottlenecks changes its velocity, for instance bottleneck i at $t_{i,N}^1 = \dfrac{v\left(\rho_N^0(y_i^0-) - \epsilon_N\right) - v\left(\rho_N^0(y_i^0-)\right)}{A}$.

Step 2. (i) If $\bar{t}$ is an instant when a change of velocity for bottlenecks occurs, $\bar{t} = t_{i,N}^1$ for some $i \in \mathcal{I}$. Then the speed of the moving bottleneck $y_{i,N}$ is set equal to $v\left(\rho_N^0(y_i^0-) - \epsilon_N\right)$ and we solve the constrained Riemann problem with $\mathcal{R}_V$, where $V = v\left(\rho_N^0(y_i^0-) - \epsilon_N\right)$: the solution consists of an approximate rarefaction jump of size ϵ_N between $\rho_N^0(y_i^0-)$ and $\rho_N^0(y_i^0-) - \epsilon_N$, moving at speed

$$\lambda = \frac{f(\rho_N^0(y_i^0-)) - f(\rho_N^0(y_i^0-) - \epsilon_N)}{\epsilon_N},$$

followed by a (non-classical) jump discontinuity between $\rho_N^0(y_i^0-) - \epsilon_N$ and 0, moving at speed $v\left(\rho_N^0(y_i^0-) - \epsilon_N\right)$. In this case the number of waves increases by one.

(ii) Else, $\bar{t}$ is an interaction time between two waves (it is not restrictive to assume that an interaction between three or more waves cannot occur, by possibly changing slightly the velocities of waves). We denote respectively by ρ_L, ρ_M, ρ_R the traffic densities on the left, middle, and right of the interaction. Different cases may occur:

(a) Both waves are classical shocks. Then $\rho_L < \rho_M < \rho_R$, and the solution at $t = \bar{t}+$ is a classical shock between ρ_L and ρ_R. The number of waves diminishes.

(b) The first wave is a shock and the second wave is an approximate rarefaction. Then $\rho_L < \rho_M = \rho_R + \epsilon_N$, and thus $\rho_L < \rho_R$. The solution at $t = \bar{t}+$ is a classical shock between ρ_L and ρ_R. Again, the number of waves diminishes.

(c) The first wave is a rarefaction and the second wave is a shock. Then $\rho_L = \rho_M + \epsilon_N$, $\rho_M < \rho_R$ and $\rho_L \leq \rho_R$. The solution at $t = \bar{t}+$ is either a classical shock between ρ_L and ρ_R or no wave is produced if $\rho_L = \rho_R$. The number of waves is non-increasing.

(d) The first wave is a moving bottleneck and the second wave is a shock. The concavity of the flux function implies that an interaction occurs if and only if $\rho_L < \rho_R$. Then the solution at $t = \bar{t}+$ is a classical shock between ρ_L and ρ_R, and the number of waves diminishes.

Step 3. We repeat Step 2 until $t = T$.

Remark 3.4. Step 2 (ii) lists all interactions that can possibly occur. Due to the strict concavity of the flux function f (assumption **(A2)**), the following cases cannot happen:

- The first wave is a classical shock and the second wave is a moving bottleneck. Then $\rho_L < \rho_M$, $\rho_R = 0$. Hence the first wave moves at speed $\dfrac{f(\rho_M) - f(\rho_L)}{\rho_M - \rho_L}$ and the second at speed $\dfrac{f(\rho_M)}{\rho_M}$, but $\dfrac{f(\rho_M) - f(\rho_L)}{\rho_M - \rho_L} < \dfrac{f(\rho_M)}{\rho_M}$, by concavity of f.

- Both waves are rarefactions: $\rho_L > \rho_M > \rho_R$. By concavity of the flux function, this interaction is also not possible.

- The first wave is a rarefaction and the second wave is a moving bottleneck. Then we also have $\rho_L > \rho_M > \rho_R$ and the interaction is in fact not possible.

- The first wave is a moving bottleneck and the second wave is a rarefaction. This case cannot happen, since we have $\rho_M = 0$.

- Both waves are moving bottlenecks. This interaction cannot happen as well since the first wave would have a lower speed than the second, evolving at $V_{\max}$.

From the description of Algorithm 1, we deduce that the number of waves increases only when a rarefaction front is generated at a time where a bottleneck updates its speed. Nonetheless, for each grid parameter N, each bottleneck can only change its speed at most 2^N times. In addition, the number of bottlenecks is bounded by assumption **(A3)**. Therefore the number of waves remains finite and the construction can be carried on up to any positive time T.

Corollary 3.2.2. *As a direct consequence, the following holds:*

(i) A moving bottleneck (non-classical wave) can only be generated at time $t = 0$.

(ii) Two moving bottlenecks cannot interact.

(iii) A moving bottleneck can only interact with a classical shock. In this case, only a classical shock is generated.

3.3 Existence of weak solutions

The following section is devoted to the proof of Theorem 3.2.1. We provide first technical results.

3.3.1 Convergence of approximate solutions

For each solution $\{\rho_N\}_{N\in\mathbb{N}}$ constructed via wave-front tracking, we define the following Glimm-type functional:

$$\Upsilon(t) = \Upsilon\left(\rho_N(t,\cdot)\right) = \begin{cases} \mathrm{TV}(\rho_N^0(\cdot)) + 2\sum_{i=1}^{I} \rho_N^0(y_i^0+) & \text{if } t = 0, \\ \mathrm{TV}(\rho_N(t,\cdot)) & \text{if } t > 0. \end{cases}$$

Lemma 3.3.1. *The map $t \to \Upsilon(t)$ is non-increasing.*

Proof. It is easy to check that $\Upsilon(0) \geq \Upsilon(0+)$. Indeed, the total variation can increase only when a moving bottleneck originates between two states $\rho_N^0(y_i^0-) > \rho_N^0(y_i^0+)$, and an intermediate vacuum state is introduced, increasing the total variation by $2\rho_N^0(y_i^0+)$. We assume now that two wave fronts interact or a moving bottleneck changes speed at time $\bar{t} > 0$. As detailed in Step 2 of Algorithm 1, the total variation never increases in such situations, therefore $\Upsilon(\bar{t}+) \leq \Upsilon(\bar{t}-)$. □

Lemma 3.3.2. *There exists a subsequence of $\{\rho_N\}_{N\in\mathbb{N}}$ which converges to some function $\rho \in \mathbf{L}^1_{loc}([0,T]\times\mathbb{R};[0,\rho_{\max}])$.*

Proof. From Lemma 3.3.1 and assumption **(A3)**, we deduce that, for any $N \in \mathbb{N}$ and any $t > 0$, we have $TV(\rho_N(t,\cdot)) \leq TV(\rho_N^0(\cdot)) + 2\sum_{i=1}^{I} \rho_N^0(y_i^0+) \leq C$, for some constant $C > 0$ independent of N. Note that $|\rho_N(t,x)| \leq \rho_{\max}$ for any $(t,x) \in [0,T]\times\mathbb{R}$.

We must prove that for all $s, t \geq 0$, we have:

$$\int_{-\infty}^{\infty} |\rho_N(t,x) - \rho_N(s,x)| \mathrm{d}x \leq L|t-s|, \tag{3.3.1}$$

for some L independent of N. By construction of the WFT approximations, the speeds of wave fronts in $\rho_N(t,\cdot)$ are uniformly bounded by $\|f'\|_{\mathbf{L}^\infty([0,\rho_{\max}])}$, since the approximate solutions take values in $[0,\rho_{\max}]$. Inequality (3.3.1) thus holds with $L = C\,\|f'\|_{\mathbf{L}^\infty([0,\rho_{\max}])}$. We refer the reader to [20, Section 6] for additional details.

We can then apply Helly's Theorem (Theorem 1.1.5), which ensures that there exists a subsequence, that we still denote by $\{\rho_N\}_{N\in\mathbb{N}}$, converging to a limit ρ in $\mathbf{L}^1_{\mathrm{loc}}([0,\infty[\,\times\mathbb{R};\mathbb{R})$. The limit satisfies

$$\int_{-\infty}^{\infty} |\rho(t,x) - \rho(s,x)| dx \leq L|t-s| \text{ for all } t, s \geq 0.$$

□

We then show the convergence of each piecewise linear bottleneck trajectory $\{y_{i,N}\}_{N\in\mathbb{N}}$ towards the parabola described by the i-th accelerating vehicle.

Lemma 3.3.3. *For any $i \in \mathcal{I}$ and for any $T > 0$, there exists a subsequence of $\{y_{i,N}\}_{N\in\mathbb{N}}$ which converges uniformly to some function y_i on $[0, T]$.*

Proof. Since the sequence $\{y_{i,N}\}_{N\in\mathbb{N}}$ is uniformly bounded on any interval $[0, T]$ and equicontinuous, Ascoli-Arzela Theorem guarantees existence of a subsequence uniformly convergent. □

Lemma 3.3.4. *For any $i \in \mathcal{I}$ the limit function y_i satisfies:*

$$y_i(t) = \frac{A}{2}t^2 + v(\rho^0(y_i^0-))t + y_i^0 \quad \text{if } t < t_i^{int}.$$

Proof. Let $i \in \mathcal{I}$ and $n \in \mathbb{N}$. We define

$$\bar{y}_i(t) = \frac{A}{2}t^2 + v(\rho^0(y_i^0-))t + y_i^0 \quad \text{for } t < t_i^{\text{int}}.$$

For any $t \in [t_i^n, t_i^{n+1}[$, we have

$$\begin{aligned}
\dot{\bar{y}}_i(t) - \dot{y}_{i,N}(t) &= At + v(\rho^0(y_i^0-)) - v(\rho_N^0(y_i^0-) - n\epsilon_N) \\
&= v(\rho^0(y_i^0-)) - v(\rho_N^0(y_i^0-) - n\epsilon_N) + At_i^n + A(t - t_i^n) \\
&= v(\rho^0(y_i^0-)) - v(\rho_N^0(y_i^0-) - n\epsilon_N) + A(t - t_i^n) \\
&\qquad + A\sum_{l=0}^{n-1} \frac{1}{A}\left[v\left(\rho_N^0(y_i^0-) - (l+1)\epsilon_N\right) - v\left(\rho_N^0(y_i^0-) - l\epsilon_N\right)\right] \\
&= A(t - t_i^n).
\end{aligned}$$

For any $T \in [t_i^n, t_i^{n+1}[$, since $y_{i,N}$ is differentiable almost everywhere, we can write:

$$\begin{aligned}
\bar{y}_i(T) - y_{i,N}(T) &= \int_0^T (\dot{\bar{y}}_i(t) - \dot{y}_{i,N}(t))dt \\
&= \sum_{l=0}^{n-1} \int_{t_i^l}^{t_i^{l+1}} (\dot{\bar{y}}_i(t) - \dot{y}_{i,N}(t))dt + \int_{t_i^n}^{T} (\dot{\bar{y}}_i(t) - \dot{y}_{i,N}(t))dt \\
&= \frac{A}{2}\sum_{l=0}^{n-1} (\Delta t_{i,N}^l)^2 + \frac{A}{2}(T - t_i^n)^2 \geq 0.
\end{aligned}$$

We compute

$$\begin{aligned}\sum_{l=0}^{n-1}(\Delta t_{i,N}^{l})^2 &= \frac{1}{A^2}\sum_{l=0}^{n-1}\left[v\left(\rho_N^0(y_i^0-)-(l+1)\epsilon_N\right)-v\left(\rho_N^0(y_i^0-)-l\epsilon_N\right)\right]^2\\ &\leq \frac{||v'||_\infty^2}{A^2}\sum_{i=0}^{n-1}\epsilon_N^2\\ &= \frac{||v'||_\infty^2}{A^2}\sum_{i=0}^{n-1}2^{-2N}\underset{N\to+\infty}{\longrightarrow}0.\end{aligned}$$

Thus $\{y_{i,N}(t)\}_{N\in\mathbb{N}}$ converges to $\bar{y}_i(t)$ pointwise almost everywhere, and then $y_i(t)$ satisfies the required equality. □

3.3.2 Existence of weak solutions

We now prove that $\rho = \lim_{N\to+\infty}\rho_N$ is a weak solution of (3.2.1a)–(3.2.1b).

Lemma 3.3.5. *ρ is a weak solution of* (3.2.1a), (3.2.1b), *i.e.* $\forall\phi\in C_c^1([0,T]\times\mathbb{R};\mathbb{R})$,

$$\int_0^T\int_{-\infty}^{\infty}(\rho\phi_t+f(\rho)\phi_x)\mathrm{d}x\mathrm{d}t+\int_{-\infty}^{\infty}\rho^0(x)\phi(0,x)\mathrm{d}x=0 \tag{3.3.2}$$

Proof. All the waves, including the non-classical waves, generated by the Wave-Front Tracking Algorithm 1, satisfy the Rankine-Hugoniot condition. Hence, for any N, the function ρ_N is a weak solution of the approximated problem

$$\begin{cases}\partial_t\rho+\partial_x f_N(\rho)=0, & x\in\mathbb{R},\ t>0,\\ \rho(0,x)=\rho_N^0(x), & x\in\mathbb{R},\end{cases}$$

where f_N is the piecewise linear function coinciding with f on the grid $\mathcal{M}_N$, see [63, Section 3.4]. Therefore, $\forall N,\forall\phi\in C_c^1(]-\infty,T]\times\mathbb{R};\mathbb{R})$, we have

$$\int_0^T\int_{-\infty}^{\infty}(\rho_N\phi_t+f(\rho_N)\phi_x)\mathrm{d}x\mathrm{d}t+\int_{-\infty}^{\infty}\rho_N^0(x)\phi(0,x)\mathrm{d}x=0.$$

Since f is Lipschitz continuous, and since ρ_N converges towards ρ in the $\mathbf{L}^1$-norm, we can apply the dominated convergence theorem to conlude that ρ is a weak solution of (3.2.1a), (3.2.1b). □

Remark 3.5. The entropy inequality (3.2.3) can be proven analogously, see [20].

3.3.3 The trajectory is a Caratheodory solution

We now prove that $y_i := \lim_{N\to+\infty} y_{i,N}$ is a Carathéodory solution to (3.2.1d) and (3.2.1e), for any $i \in \mathcal{I}$. We first provide a technical result.

Lemma 3.3.6. *For any $i \in \mathcal{I}$ and any $N \in \mathbb{N}$, the approximate bottleneck trajectories satisfy*

$$\dot{y}_{i,N}(t) = \begin{cases} v\left(\rho_N^0(y_i^0-) - n\epsilon_N\right) & \text{if} \quad t \in [t_{i,N}^n, t_{i,N}^{n+1}[, \\ v\left(\rho_N(t, y_{i,N}(t)+)\right) & \text{if} \quad t > t_{i,N}^{int}, \end{cases} \leq At + v(\rho_N^0(y_i^0-)).$$

Proof. We first assume that $t \leq t_{i,N}^{\text{int}}$. Then there exists $n \in \mathbb{N}$ such that $t \in [t_{i,N}^n, t_{i,N}^{n+1}[$. By construction, we have that

$$\begin{aligned} \dot{y}_{i,N}(t) &= v\left(\rho_N^0(y_i^0-) - n\epsilon_N\right) \\ &= At_{i,N}^n + v(\rho_N^0(y_i^0-)) \\ &\leq At + v(\rho_N^0(y_i^0-)). \end{aligned}$$

Now let $t > t_{i,N}^{\text{int}}$. By construction, we have $\dot{y}_{i,N}(t) = v\left(\rho_N(t, y_{i,N}(t)+)\right)$. Let $n \in \mathbb{N}$ such that $t_{i,N}^{\text{int}} \in [t_{i,N}^n, t_{i,N}^{n+1}[$. Just before disappearing, the moving bottleneck has a velocity equal to $v\left(\rho_N^0(y_i^0-) - n\epsilon_N\right)$. The moving bottleneck catches downstream traffic only if its speed is higher that the velocity of downstream traffic. This implies

$$At + v(\rho_N^0(y_i^0-)) > At_{i,N}^n + v(\rho_N^0(y_i^0-)) = v(\rho_N^0(y_i^0-) - n\epsilon_N) > v(\rho_N(t_{i,N}^{\text{int}}, y_{i,N}(t_{i,N}^{\text{int}})+)). \tag{3.3.3}$$

The previous inequality yields $\rho_N(t_{i,N}^{\text{int}}, y_{i,N}(t_{i,N}^{\text{int}})+) > \rho_N^0(y_i^0-) - n\epsilon_N$. Since $\rho_N(t_{i,N}^{\text{int}}, y_{i,N}(t_{i,N}^{\text{int}})+) \in \mathcal{M}_N$, we have in fact $\rho_N(t_{i,N}^{\text{int}}, y_{i,N}(t_{i,N}^{\text{int}})+) - \rho_N^0(y_i^0-) \geq (-n+1)\epsilon_N$. We now need to compare the evolution of the velocity $v(\rho_N(t, y_{i,N}(t)+))$ and $At+v(\rho_N^0(y_i^0-))$. Starting from $t_{i,N}^{\text{int}}$, the velocity on the right of the trajectory only increases when it meets a rarefaction wave. We may assume that it will cross a succession of rarefaction waves coming from a given downstream moving bottleneck j. When it encounters a first rarefaction wave at time t, the density decreases by one grid point, and we then have $\rho_N(t, y_{i,N}(t)+) - \rho_N^0(y_i^0-) \geq -n\epsilon_N$. Let us now focus on the second rarefaction encountered, assuming it occurs at time $t' > t$. The speed increases of the difference between two consecutive speeds on the mesh, such that $v(\rho_N(t', y_{i,N}(t')+)) = v(\rho_N(t, y_{i,N}(t)+) - \epsilon_N)$. In addition, since these rarefactions are generated by a given bottleneck j, there exists a time index k such that $v(\rho_N(t, y_{i,N}(t)+) - \epsilon_N) - v(\rho_N(t, y_{i,N}(t)+)) = A\Delta t_{j,N}^k$. In the same time, by construction of the WFT approximations, the second rarefaction was emitted $A\Delta t_{j,N}^k$ after the first one, and then the right hand side $At + v(\rho_N^0(y_i^0-))$ will increase by at least $A\Delta t_{j,N}^k$ (the second rarefaction travels faster that the first one by concavity of the flux function). This reasoning can then be iterated and combined with (3.3.3) to ensure that $v(\rho_N(t, y_{i,N}(t)+)) \leq At + v(\rho_N^0(y_i^0-))$ for any $t > t_{i,N}^{\text{int}}$. □

The result can directly be extended to the limit of the WFT approximations.

Lemma 3.3.7. *For any $i \in \mathcal{I}$:*

$$\omega_i(t, y_i(t)) = \min\left\{At + v(\rho^0(y_i^0-)), v(\rho(t, y_i(t)+)\right\} = \begin{cases} At + v(\rho^0(y_i^0-)) & \text{if} \quad t \leq t_i^{int}, \\ v\left(\rho(t, y_i(t)+)\right) & \text{if} \quad t > t_i^{int}, \end{cases}$$

where t_i^{int} denotes the limit of a subsequence of $\{t_{i,N}^{int}\}_{N\in\mathbb{N}}$.

Proposition 3.3.8. *For any $i \in \mathcal{I}$, y_i is a Carathéodory solution of* (3.2.1d)–(3.2.1e)*,* i.e.

$$y_i(t) = y_i^0 + \int_0^t \omega_i\left(s, y_i(s)\right) \mathrm{d}s \qquad \text{for any } t \in [0, T]. \tag{3.3.4}$$

Proof. Let t_i^{int} be the limit of a subsequence of $\{t_{i,N}^{\text{int}}\}_{N\in\mathbb{N}}$ and fix $\delta > 0$ sufficiently small. Assume first that $t \leq t_i^{\text{int}} - \delta$. For N large enough, the i-th bottleneck is active on the interval $[0, t]$ and we have $\dot{y}_{i,N}(t) = v\left(\rho_N^0(y_i^0-) - n\epsilon_N\right)$ for all $t \in [t_{i,N}^n, t_{i,N}^{n+1}[$.
We can write

$$y_{i,N}(t) = y_i^0 + \int_0^t \dot{y}_{i,N}(s)\mathrm{d}s.$$

By construction of each approximated parabola $y_{i,N}$ we have for $s \in [0, t]$

$$\lim_{N\to+\infty} \dot{y}_{i,N}(s) = As + v\left(\rho^0(y_i^0-)\right) \leq v\left(\rho(y_i+)\right) = V_{\max}.$$

We can then apply the dominated convergence theorem to pass to the limit within the integral and conbine with Lemma 3.3.7 to obtain (3.3.4).
Now assume that $t > t_i^{\text{int}} + \delta$. In this case, the moving constraint is not active anymore, and ρ is a weak entropy solution of (3.2.1a) on the time interval $[t_i^{\text{int}} + \delta, t]$. The convergence of traces is therefore assured, see e.g. [49], and the result (3.3.4) is straightforward. □

3.3.4 Proof of the flux constraint

Lemma 3.3.9. *The limit ρ satisfies the flux constraint* (3.2.1c)*:*

$$f\left(\rho(t, y_i(t))\right) - \rho(t, y_i(t))\dot{y}_i(t) \leq 0, \qquad t > 0, \forall\ i \in \mathcal{I}.$$

Proof. By construction of the WFT approximations, we have that

$$f\left(\rho_N(t, y_{i,N}(t))\right) - \rho_N(t, y_{i,N}(t))\dot{y}_{i,N}(t) \leq 0, \qquad t > 0, \forall\ i \in \mathcal{I}, \forall\ N \in \mathbb{N}. \tag{3.3.5}$$

We know that for any N, the function ρ_N is a weak solution of the approximated problem

$$\begin{cases} \partial_t \rho + \partial_x f_N(\rho) = 0, & x \in \mathbb{R},\ t > 0, \\ \rho(0, x) = \rho_N^0(x), & x \in \mathbb{R}. \end{cases}$$

Thus we have $\forall N, \forall \phi \in C_c^1([0,T]\times\mathbb{R};\mathbb{R})$,

$$\int_0^T \int_{-\infty}^{\infty} (\rho_N \phi_t + f(\rho_N)\phi_x) \mathrm{d}x\mathrm{d}t + \int_{-\infty}^{\infty} \rho_N^0(x)\phi(0,x)\mathrm{d}x = 0,$$

since $f_N(\rho_N(t,x)) = f(\rho_N(t,x))$. Now, consider a time-space domain $]0,T[\times\Omega_i$, $\Omega_i = \{]y_i(t)-a, y_i(t)+b[, t\in]0,T[\}$, where $a,b>0$ are sufficiently small, so that Ω_i contains only the i-th moving bottleneck. By uniform convergence, Ω_i contains also all $y_{i,N}$, for N sufficiently large (up to a subsequence). The idea is to change space variables, center the solution around the moving bottleneck, and use the Green-Gauss theorem (see e.g. [6, section 5]). We define

$$\tilde{\rho}_{i,N}(t,x) := \rho_N(t, x+y_i(t)) \qquad \text{for } x\in]-a,b[,\ t\in]0,T[.$$

Then $\tilde{\rho}_{i,N}$ is a weak solution of

$$\partial_t \tilde{\rho}_{i,N}(t,x) + \partial_x[f(\tilde{\rho}_{i,N})(t,x) - \dot{y}_{i,N}(t)\tilde{\rho}_{i,N}(t,x)] = 0. \tag{3.3.6}$$

Let $\psi \in C_c^1([0,T])$ a compact test function of time, and $\xi \in C_c^1(]-a,b[)$ a compact test function of space such that $\xi(0)=1$. Applying the weak formulation of (3.3.6) and the Green Gauss theorem, we obtain

$$\begin{aligned}\int_0^T \int_{-a}^0 \tilde{\rho}_{i,N}(t,x)\dot{\psi}(t)\xi(x) + [f(\tilde{\rho}_{i,N})(t,x) - \dot{y}_{i,N}(t)\tilde{\rho}_{i,N}(t,x)]\psi(t)\xi'(x)\ \mathrm{d}x\mathrm{d}t \\ = \int_0^T \left(f(\tilde{\rho}_{i,N})(t,0-) - \dot{y}_{i,N}(t)\tilde{\rho}_{i,N}(t,0-)\right)\psi(t)\ \mathrm{d}t \le 0.\end{aligned} \tag{3.3.7}$$

Calling $\tilde{\rho}_i(t,x) = \lim_{N\to+\infty} \tilde{\rho}_{i,N}(t,x)$, we can pass to the limit in (3.3.7) and obtain

$$\begin{aligned}0 \ge & \lim_{N\to+\infty} \int_0^T \int_{-a}^0 \tilde{\rho}_{i,N}(t,x)\dot{\psi}(t)\xi(x) + [f(\tilde{\rho}_{i,N})(t,x) - \dot{y}_{i,N}(t)\tilde{\rho}_{i,N}(t,x)]\psi(t)\xi'(x)\ \mathrm{d}x\mathrm{d}t \\ = & \int_0^T \int_{-a}^0 \tilde{\rho}_i(t,x)\dot{\psi}(t)\xi(x) + [f(\tilde{\rho}_i)(t,x) - \dot{y}_i(t)\tilde{\rho}_i(t,x)]\psi(t)\xi'(x)\ \mathrm{d}x\mathrm{d}t \\ = & \int_0^T \left(f(\tilde{\rho}_i)(t,0-) - \dot{y}_i(t)\tilde{\rho}_i(t,0-)\right)\psi(t)\ \mathrm{d}t.\end{aligned}$$

This ensures convergence of the traces along the moving constraint. We can then revert back to the original coordinates in order to obtain (3.2.1c). □

3.4 Numerical simulations of the PDE-ODE model

In this section, we compare numerical simulations of the solutions to the LWR model (1.2.2) and to our coupled PDE-ODE model (3.2.1) obtained via the wave-front tracking method. Our numerical code is entirely based on Algorithm 1. The key implementation aspects are detailed in Appendix.

3.4.1 The Riemann problem

In this first example, we consider a simple Riemann problem (3.2.5). We adopt the following values

$$\rho(0,x) = \begin{cases} \rho_L = 180 \text{ veh/km} & \text{if} \quad x < y^0 = 400 \text{ m}, \\ \rho_R = 80 \text{ veh/km} & \text{if} \quad x \geq y^0 = 400 \text{ m}. \end{cases} \tag{3.4.1}$$

This situation corresponds to a near bumper-to-bumper situation on the left of the discontinuity and to a free-flow situation on the right. Since we mainly expect acceleration and deceleration effects in urban areas, we choose to represent a stretch of road by a segment $[0, L]$ measuring $L = 1000$m. The parameter for our density grid is set to $N = 10$.

In the following numerical illustrations, we consider the speed-density function

$$v(\rho) = V_{\max}\left(1 - \frac{\rho}{\rho_{\max}}\right), \qquad \rho \in [0, \rho_{\max}].$$

This leads to a quadratic flow-density fundamental diagram of Greenshields type, with $\rho_{\text{crit}} = \frac{\rho_{\max}}{2}$. The maximal density corresponds to a bumper-to-bumper situation, so we select $\rho_{\max} = 200$ veh/km. In addition, we set $V_{\max} = 110$ km/h. The acceleration rate is fixed to $A = 2$ m/sec^2, which is a standard value for average vehicles.

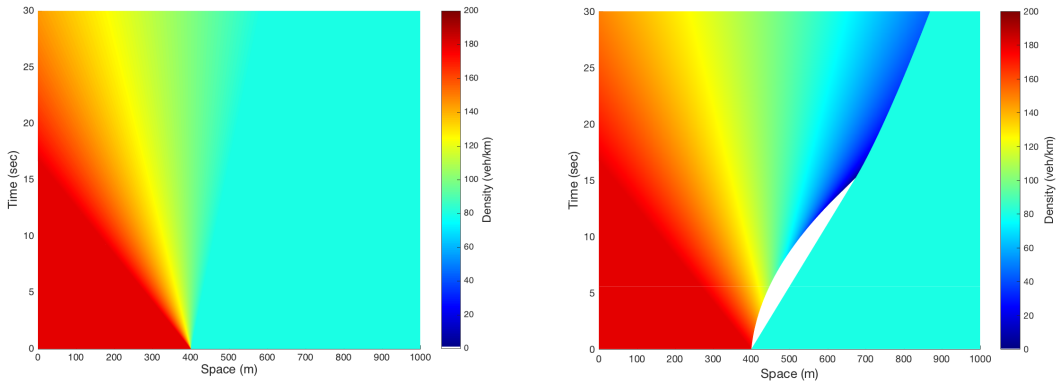

(a) Solution to the LWR model. (b) Solution to our PDE-ODE model.

Figure 3.2 – Comparison of solutions for a Riemann initial datum (3.4.1).

The classical solution to the LWR model with such an initial condition consists in a rarefaction wave (Figure 3.2a). The solution to the LWR model with bounded acceleration is displayed on Figure 3.2b, while the difference of densities between the classical LWR model and the bounded acceleration model is shown on Figure 3.3. We can observe on Figure 3.2b the creation of a vacuum state in front of the first accelerating vehicle during its acceleration. This vacuum lasts for approximately 15 seconds and covers around 300 meters, which is not negligible from an applicative point of view. Moreover, it is noteworthy that the differences in terms of density spread over a wider area (Figure 3.3). Indeed, the bounded acceleration of the first vehicle affects all the following vehicles. From this simple example, one can see that the bounded acceleration has not just a local effect. We observe that the traffic is first condensed (green and blue zones) and then it is relaxed (yellow to pink zones) in comparison to the classical solution with differences up to around 80 veh/km in some regions.

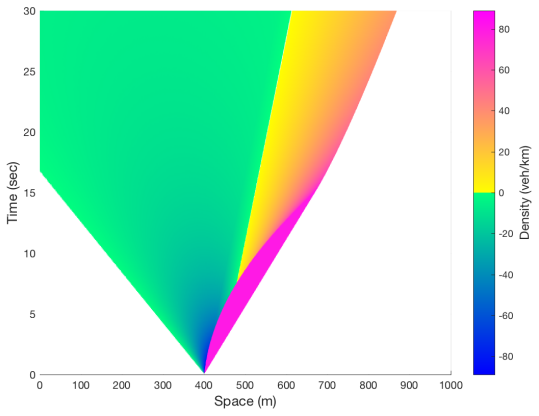

Figure 3.3 – Density difference between the solution to the LWR model and the solution to the PDE-ODE model for a Riemann initial datum (3.4.1).

We can also compare the solutions of both models by evaluating the queues generated by both models. We define a queue length as the distance between extremal points for which the density is higher or equal to $\frac{3}{4}\rho_{\max}$. With our choice of a linear speed-density function, we know that this density is above the critical density $\rho_{\text{crit}} = \frac{\rho_{\max}}{2}$. The result is given on Figure 3.4. While the queue length is also non-increasing during the considered time period for the LWR model, there is an increase for the PDE-ODE model that corresponds to the very beginning of the bounded acceleration phase. Interestingly, this gap of more or less 45 meters is conserved for the whole simulated period.

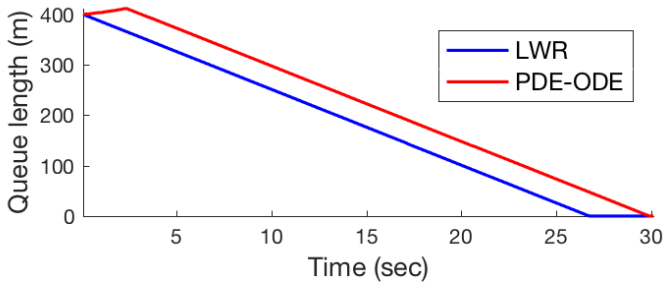

Figure 3.4 – Queue lengths obtained for the LWR model and the PDE-ODE model for a Riemann initial datum (3.4.1).

3.4.2 A Cauchy problem with several moving bottlenecks

Now that we have detailed the Riemann problem, we want to illustrate the behavior of our model when the initial density presents several downward jumps. In this section, we try to highlight the impact of bounded acceleration for a realistic situation of successive traffic lights turning simultaneously green at time $t = 0$. We select $V_{\max} = 50$ km/h to simulate an arterial road situation and we consider three traffic signals located respectively at positions $x = 300$, 700 and 1000 meters. We assume that initially, queues are present before each traffic signal with local Riemann problems such that $\rho_L = \rho_{\max}$ and $\rho_R = 0$. The initial datum contains additional Riemann problems upstream of each traffic light, accounting for the cars that did not reach the initial queues at time $t = 0$. The parameter for our density grid is set to $N = 10$.

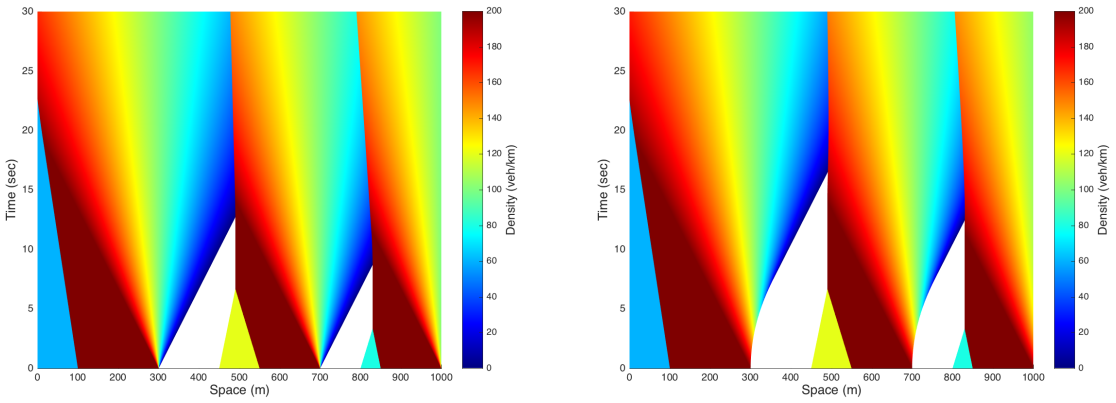

(a) Solution to the LWR model.

(b) Solution to our PDE-ODE model.

Figure 3.5 – Comparison of solutions for a series of traffic lights.

The solution to our coupled PDE-ODE model is displayed on Figure 3.5b while the solution to the classical LWR model appears on Figure 3.5a. The reader can note the

formation of rarefactions (dissipation of queues) and shockwaves as well as the interactions between all these waves when vehicles join downstream traffic. The difference of densities due to the bounded acceleration shown on Figure 3.6 reveals high discrepancies along interacting shockwaves and rarefaction fans (in pink). We recover the same phenomenon than in the previous example with condensed (in green) and relaxed (in yellow) traffic due to the bounded acceleration behavior.

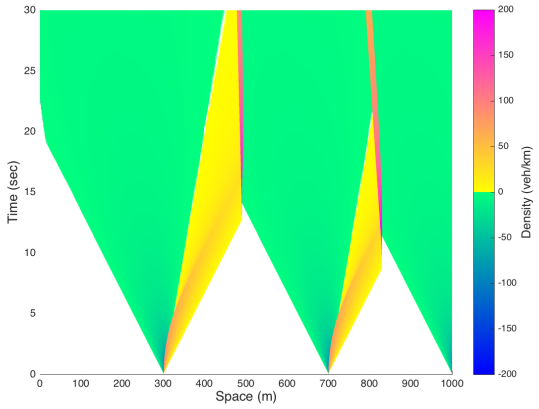

Figure 3.6 – Density difference between the solution to the LWR model and the solution to the PDE-ODE model for the series of traffic lights.

The study of the cumulative queues carried over on Figure 3.7 with the same threshold $\rho \geq \frac{3}{4}\rho_{\max}$ exhibits a significant difference with and without bounded acceleration. For instance, the model with bounded acceleration captures up to 50 additional meters of queues over a 1000 meters long road, which is significant if one thinks to responsive traffic signals based on an estimation of queue lengths.

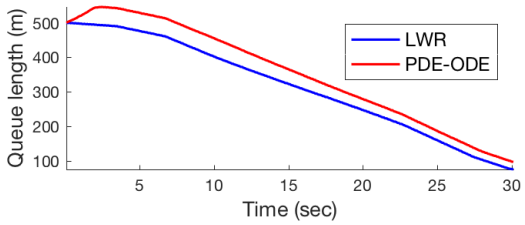

Figure 3.7 – Queue lengths obtained for the LWR model and the PDE-ODE model.

3.4.3 A dynamic sequence of traffic lights

In this last section, we investigate the behavior of our model when several traffic signals are present, which successively alternate colors. We model two traffic lights, respectively located at $x = 300$m and $x = 700$m. The first traffic light is initially red, and changes color every 15 seconds. When the traffic light is red, we enforce numerically a zero-flux constraint at its location [48], thus solving a Riemann problem with $\rho_L = \rho_{\max}$ and $\rho_R = 0$. The sequence of traffic lights is designed in order to obtain a "green-wave" with the LWR model: the second traffic light turns green as soon as the first vehicle, traveling at maximum speed, reaches it. It also changes color every 15 seconds. The maximal speed is again set to $V_{\max} = 50$km/h. Here, the parameter for our density grid is set to $N = 8$.

We observe the following results:

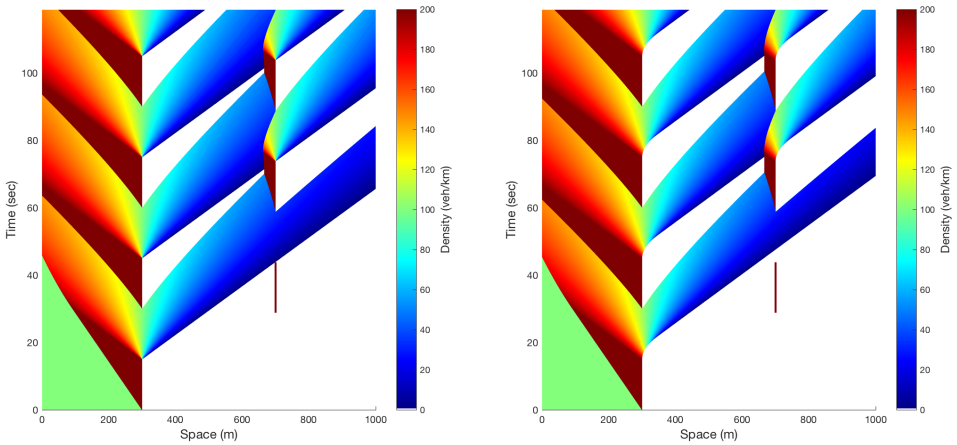

(a) Solution to the LWR model. (b) Solution to our PDE-ODE model.

Figure 3.8 – Comparison of solutions for the same sequence of traffic lights.

As illustrated in Figure 3.9, we observe that the flow moving downstream of both traffic lights is significantly more important with the LWR model than with our PDE-ODE model, with differences up to 15%. As a consequence, the queues upstream of each traffic light are longer when simulating solutions to our model. At this step, since we did not compare models on real traffic data, we cannot assert that our coupled PDE-ODE model is more realistic than the seminal LWR model. Nonetheless, the simulations reveal that optimizing traffic light sequences based on the LWR model may lead to a significant drop of capacity and an increase of congestion, because this model assumes that vehicles have unbounded acceleration from zero to the maximal speed. This lack of physical realism may have a significant impact in urban areas, in which traffic encounters multiple flux constraints like traffic lights and stop signs, thus passing through multiple acceleration phases.

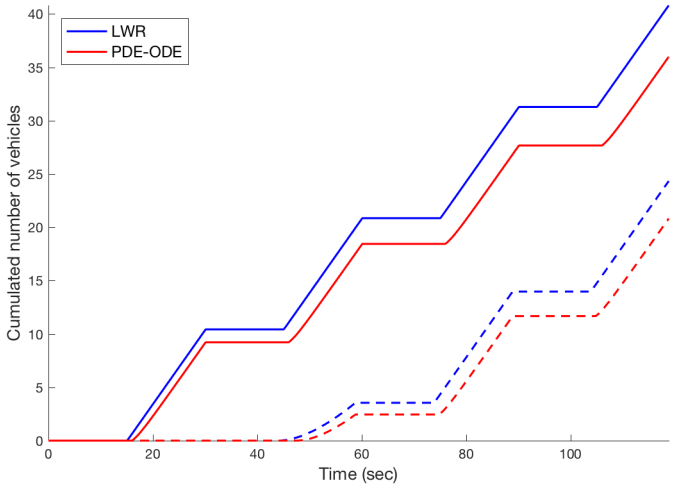

Figure 3.9 – Cumulated number of vehicles passing through the first (plain lines) and second (dashed lines) traffic light with respect to time.

3.5 Conclusion

In this chapter, we have proposed a strongly coupled PDE-ODE model accounting for the required boundedness of traffic acceleration. Physical representation of this traffic characteristic is essential for urban applications, like controlling fuel consumption and vehicle emissions. We have showed the existence of solutions to this PDE-ODE model for piecewise constant initial data and we have detailed how to construct them via the wave-front tracking technique. It would be interesting to extend the results to more general data, and check the stability of the corresponding solutions. We could also investigate the theoretical stability of the proposed algorithm. From an applicative point of view, we still need to confront our model to urban traffic data in order to compare our results to the LWR model. Finally, even though vehicles have lower acceleration abilities than deceleration ones, we may extend the model to also include bounded braking phases, which would impact the representation of the shock waves in the solution.

Appendix

In this appendix, we highlight the key aspects of the software implementation of wave front tracking. All our simulations were developed on *Matlab R2017a* and run on a computer containing a 2.9 Ghz processor intel i5 and 16 Go of Ram. The code was fully programmed in collaboration with Guillaume Costeseque. We will focus on the computation of approximate solutions to our coupled PDE-ODE model (3.2.1). The computation of the solutions to the LWR model can be derived with the same principles, and the implementation is actually easier since it does not involve any bottleneck or flux constraint.

While detaling Algorithm 1 is clear and simple with words, a few difficulties arise when programming the method. The main difficulty lies in solving accurately the wave-front tracking method, which is pretty different from the classical finite element and finite volume methods. In this case, we do not compute the solution on given meshes, but we keep track of the wave fronts, and combine them a posteriori with the initial datum to reconstruct the solution over the time-space domain. In addition, we underline that the method requires machine precision error, in order to exactly detect the intersection of waves and propagate them accurately.

At a given time t, the representation of the density $\rho(t,\cdot)$, which is piecewise constant, is numerically represented as two vectors. The first vector, of size $l \in \mathbb{N}$, will contain the successive values of density from the left to the right of the space domain, while the second vector y, of size $l-1$, will store the position of the discontinuities. Let us go through each step of Algorithm 1, and detail the non-trivial aspects.

[Step 0.] consists in approximating the initial datum ρ^0 by a function $\rho^0_{\text{on grid}}$ whose values lie on the grid $\mathcal{M}_N$. For each element of ρ_0, we choose to approximate it by its nearest neighbor on the grid.

[Step 1.] consists in solving several Riemann problems at time t (initially, $t=0$). For each discontinuity located at a given position y_i ($i \in \{0,\dots,l-1\}$), separating $\rho_L = \rho_i$ from $\rho_R = \rho_{i+1}$, we solve the associated Riemann problem. The input of the solver is a vector of density values ρ associated to the location of discontinuities y. The output of such a function must be a set of waves. Each wave is described by a column vector W of size 5, such that

$$W = [y_i;\ \lambda;\ t;\ \rho_L; \text{NonClassical}]^\intercal \tag{3.5.1}$$

where:

- y_i corresponds to the initial location of the wave front at time t,
- λ is the speed of the wave,
- t is the time of resolution of the Riemann problem,
- ρ_L represents the density on the left of the wave front,

- NonClassical is a boolean value, which is set equal to 1 if the wave corresponds to a non-classical moving bottleneck, and to 0 otherwise. This boolean value enables to keep track of every bottleneck during the simulation.

We describe the pseudo-code to solve a given Riemann problem in Algorithm 2. In order to manipulate the data, we decided to store the wave fronts in a matrix M of size $5 \times K$, where K is the number of waves, each column vector corresponding to one front. We insist on the crucial point that this matrix must remain ordered at all times, *i.e.* at time t the wave corresponding to column j is spatially located on the left of any following column $j+1, j+2, ...$ This aspect is a necessary condition in order to identify exactly the interaction points of wave fronts. In addition, it provides numerical efficiency. If the matrix of size K was not ordered, we would need to realize $\mathcal{O}(K^2)$ operations to determine intersection times between all waves, while in our case we only realize $\mathcal{O}(K)$ operations for the same result.

Algorithm 2 Riemann solver

Input: ρ_L, ρ_R, y_i, t
Output: M ▷ Matrix containing 5 elements column vectors
  $\lambda = \dfrac{(f(\rho_L) - f(\rho_R))}{(\rho_L - \rho_R)}$ ▷ compute Rankine Hugoniot speed
  if $\rho_l < \rho_r$ **then**
    $M \leftarrow [y_i;\ \lambda;\ t;\ \rho_L;\ 0]^\intercal$ ▷ shock wave
  else if $\rho_L - \rho_R = \epsilon_N$ **then**
    $M \leftarrow [y_i;\ \lambda;\ t;\ \rho_L;\ 0]^\intercal$ ▷ approximate rarefaction wave
  else
    $M \leftarrow [y_i,\ v(\rho_L),\ t, \rho_L,\ 1]^\intercal$ ▷ moving bottleneck
    if $\rho_R > 0$ **then**
      $M \leftarrow [M;\ [y_i;\ v(\rho_R);\ t;\ 0;\ 0]^\intercal]$ ▷ initial shockwave
    end if
  end if

Once the matrix M is generated, we need to identify the first time $t_{\text{collision}}$ at which two wave collides after time t. Since the matrix is ordered from left to right, it is sufficient to compute the collision time of each pair of consecutive waves, and select the minimum. The pseudo-code for this procedure is detailed in Algorithm 3. Once the collision time $t_{\text{collision}}$ is identified, we compare it to the next time instant at which at least one of the moving bottlenecks i changes its velocity, for instance at time $t_i^n, n \in \mathbb{N}$. These times of change can be computed a priori when a moving bottleneck is generated and stored once and for all in memory.

If $t_i^n < t_{\text{collision}}$, we proceed with [Step 2.(i)]. We modify the Matrix M, by changing the speed of the considered moving bottlenecks, and by inserting the associated approximate rarefaction waves. We then again compute the next collision time with Algorithm 3, and restart at the beginning of [Step 2.].

Algorithm 3 identification of the first collision time $t_{\text{collision}} > t$

Input: $M = [W_1;\ W_2;\ \ldots;\ W_K], t$
Output: $t_{\text{collision}}$ and index $j, j+1$
  for $i = 1 : K-1$ **do**
    $W_i = [y_i;\ \lambda_i;\ t_i;\ \rho_{L,i}; \text{NonClassical}_i]^\intercal$
    $W_{i+1} = [y_{i+1};\ \lambda_{i+1};\ t_{i+1};\ \rho_{L,i+1}; \text{NonClassical}_{i+1}]^\intercal$
    $t_{\text{vector}}[i] \leftarrow \dfrac{y_i - \lambda_i t_i - y_{i+1} + \lambda_{i+1} t_{i+1}}{\lambda_{i+1} - \lambda_i}$
  end for
  $t_{\text{collision}} \leftarrow t_{\text{vector}}[j] = \min\{t_{\text{vector}}[i] > t\}$ ▷ returns the smallest collision time and index $j, j+1$ of colliding waves

Else, we have $t_i^n \geq t_{\text{collision}}$. We then compute the solution ρ and the vector of discontinuities y at time $t = t_{\text{collision}}$ corresponding to matrix M with Algorithm 4. We then solve a new series of Riemann problem at each discontinuity according to [Step 2.(ii)] with Algorithm 2 and generate a new Matrix M.

Algorithm 4 computing the density vector ρ from M at time t

Input: $M = [W_1;\ W_2;\ \ldots;\ W_K], t, \rho^0$
Output: ρ, y
  for $i = 1 : K$ **do**
    $W_i = [y_{i,0};\ \lambda_i;\ t_{i,0};\ \rho_{L,i}; \text{NonClassical}_i]^\intercal$
    $\rho_i \leftarrow \rho_{L,i}$
    $y_i \leftarrow y_{i,0} + (t - t_{i,0})\lambda_i$
    $\rho_{K+1} = \rho^0[\text{end}]$
  end for

With this procedure, we can iterate [Step 2.] until $t = T$. Numerical convergence is guaranteed since the number of waves remains finite in finite time. In order to represent the approximate solution $\rho_N(t,x), \forall\ t \in [0,T], x \in \mathbb{R}$ a posteriori, we note that it is necessary to store in an appropriate manner the different arrays ρ and M computed iteratively. The option we chose was to store the solution as polygonal objects, each polygon being associated to a compact subset of $[0,T] \times \mathbb{R}$ and a given constant value of density $\rho_j \in \mathcal{M}_N$. These polygons can then be easily used to provide representations of the solution, like the ones in Section 3.4.

Chapter 4

A macroscopic traffic flow model with finite buffers on networks: Well-posedness by means of Hamilton-Jacobi equations

Abstract

In this chapter we introduce a model dealing with conservation laws on networks and coupled boundary conditions at the junctions. In particular, we introduce buffers of fixed arbitrary size and time-dependent split ratios at the junctions, which represent how traffic is routed through the network, while guaranteeing spill-back phenomena at nodes. The dynamics are first defined on the level of conservation laws, and then transformed in an Hamilton-Jacobi formulation. We write boundary datum of incoming and outgoing junctions as functions of the queue sizes and vice-versa. The Hamilton-Jacobi formulation provides the necessary regularity estimates to derive a fixed-point problem in a proper Banach space setting, which is used to prove well-posedness of the model. Finally, we detail how to apply our framework to a non-trivial road network, with several intersections and finite-length links.

The content of this chapter was submitted under the following references:
N. Laurent-Brouty, A. Keimer, P. Goatin, and A. M. Bayen. A macroscopic traffic flow model with finite buffers on networks: Well-posedness by means of Hamilton-Jacobi equations. preprint, May 2019.

4.1 Introduction

In this chapter, we investigate the modeling of the behavior of traffic at junctions, which is not mathematically trivial, due to phenomena like traveling congestion on incoming and outgoing roads and allocation of traffic on outgoing roads. We will consider the LWR model (1.2.2), whose mathematical properties are now totally detailed in the literature [20]. Modeling traffic on road networks is essential in order to address the *Dynamic Traffic Assignment* (DTA) problem, which consists in optimizing trajectories of vehicles on networks in order to reduce travel times and congestion. Mathematically, the difficulty lies in defining the appropriate boundary conditions at intersections, in order to provide existence and uniqueness of solutions. To treat this difficulty, different solutions have been proposed in the literature. Two main approaches can be identified. The first consists in defining Riemann solvers at the junctions (see Section 1.2.3.a), which are mappings that provide solutions to Cauchy problems with constant initial data on each link. Once these mappings are defined, wave-front tracking or finite volume schemes enable one to build solutions to more general Cauchy problems. The main limitation of this approach is that the solution does not necessarily depend in a Lipschitz continuous way on the initial datum, as pointed out in [69, Section 5] and [31]. The other approach is to couple incoming and outgoing links by a buffer located at the junction (see Section 1.2.3.b). The state of this buffer is then governed by an ordinary differential equation, taking into account the boundary conditions at the junction so that conservation of vehicles is guaranteed. This modeling framework was first introduced for supply-chain networks in [80, 84, 88] and then adapted to traffic flow on networks in [27, 28, 29, 66, 71, 89]. This approach provides stability estimates which are crucial from a control point of view, but may lead to a potential loss of information at the junctions, depending on how the buffer is modeled and whether one aggregates commodities at the junction level or not. The mentioned drawbacks of existing models (missing regularity or loss of information) prevent from implementing control strategies at the intersection level, mandatory to address the DTA problem. We develop a control framework by implementing time-varying routing functions at junctions, which assign a ratio of the incoming flow to the outgoing edges. Depending on the capacity of outgoing links and the values of these ratios, incoming flows might not be fully assignable to outgoing roads at specific times. We then implement a buffer at the entrance of any outgoing road, with arbitrary chosen limited capacity, which takes into account the possible exceed on demand. Once the buffer has reached its limited capacity, the unsatisfied demand impacts the incoming roads, so that back-travelling phenomena are intrinsically treated. To address well-posedness of the model, we transform the described problem into a fixed-point problem at the level of Hamilton-Jacobi partial differential equations (H-J PDEs), relying on the higher regularity of solutions. For the general theory of Hamilton-Jacobi equations we refer the reader to [1, 51, 94] and to [7, 42, 43, 65] for applications to traffic flow modeling. Our analysis strongly relies on previous contributions in [27, 28, 29], where a similar fixed-point problem was posed. In these articles, the authors assume that the routing of each population is predetermined initially, and use transport equations to propagate this

information and to keep track of different populations having different routes. On the other hand, we propose an approach which enables real-time routing modifications, by enforcing time-varying routing functions at junctions. For other approaches to traffic routing in a macroscopic non-stationary setting, we refer the reader to [53, 68, 136].

In this chapter, we provide a rigorous well-posedness result for every finite buffer size, when changing involved input data in the proper topology. This enables us to study optimal control problems in which we control the routing parameters at junctions in an optimal way assuming a uniform BV bound on the routing, a reasonable assumption as the change of traffic flow should not be too irregular. We also detail how the prototype junction model, defined on semi-infinite incoming and outgoing links, can be generalized to realistic networks. The main idea here is to use the finite propagation speed of information, so that one can decouple the fixed-point problems at the different junctions for sufficiently small times.

The chapter is organized as follows. In Section 4.2, we introduce the model, detail the dynamics governing links and buffers and explain how to derive the Hamilton-Jacobi formulation of the problem, starting from the conservation law formulation. In Section 4.3, we propose a rigorous definition of solutions, based on the literature and on the modeling assumptions. After recalling some fundamental results about Hamilton-Jacobi equations in Section 4.4.1, we define the Banach fixed-point problem in Section 4.4.2 and study its properties in Section 4.4.3. In Section 4.4.4, we show the existence and uniqueness of a fixed-point, and thus the well-posedness of the Hamilton-Jacobi formulation of the problem. Section 4.5 provides some stability results of solutions with respect to the routing ratios, initial datum of incoming and outgoing roads and the initial state of the buffers. In Section 4.6 we show that our framework enables us to write an optimal control problem with respect to routing, and to prove the existence of a minimizer. In Section 4.7 we detail how to use the framework on a physical road network, containing several intersections and finite-length links, providing explicit solutions to the Hamilton-Jacobi formulation. Finally, Section 4.8 presents the conclusions and suggests additional and future topics for research.

4.2 The model

In this section, we present the dynamical model on the network. We first introduce an archetype network and then define the link dynamics and the node dynamics. On each link, we model the traffic dynamics with the LWR model, and at each intersection, we model the dynamics based on the boundary conditions of the scalar conservation law and on the state of the buffer. Note that the topology of the considered archetype network is sufficient to generalize to arbitrary connected and directed graphs.

4.2.1 Network representation

We consider as archetype network a single node v with incoming $\mathcal{I}$ and outgoing $\mathcal{O}$ links as illustrated in Figure 4.1. For simplicity, we first assume that each entering link

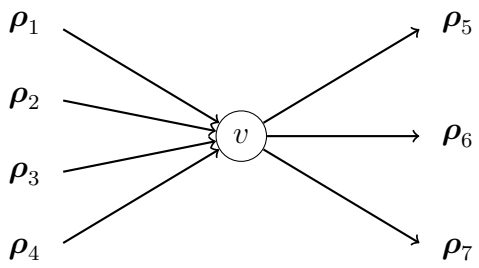

Figure 4.1 – Illustration of the archetype network, a node with incoming $\mathcal{I} \coloneqq \{1,2,3,4\}$ and outgoing $\mathcal{O} \coloneqq \{5,6,7\}$ links.

$i \in \mathcal{I}$ is characterized by the spatial segment $(-\infty, 0]$. Similarly, each exiting link $j \in \mathcal{O}$ is characterized by the open segment $[0, \infty)$ so that we assume semi-infinite roads. In Section 4.7 we will discuss how we can generalize the proposed dynamics to general networks in a straightforward manner.

4.2.2 Link dynamics

We denote by $\boldsymbol{\rho}_i(t,x)$, $i \in \mathcal{I}$, the density of vehicles on the incoming links at space-time coordinate $(t,x) \in (0,T) \times \mathbb{R}_{<0}$ and by $\boldsymbol{\rho}_j(t,x)$ the density on the outgoing links $j \in \mathcal{O}$ at space-time coordinate $(t,x) \in (0,T) \times \mathbb{R}_{>0}$ for a given and fixed time horizon $T \in \mathbb{R}_{>0}$.

Remark 4.1. In the following, bold notations will be used to denote vectors and matrices. For instance, $\boldsymbol{\rho}_i$, $i \in \mathcal{I}$ denotes the i-th component of $\boldsymbol{\rho} \in \mathbb{R}^{|\mathcal{I}|}$.

On each link of the network, we assume that the density of vehicles satisfies the LWR model for given specific flux functions so that the dynamics read for $i \in \mathcal{I}$ and $j \in \mathcal{O}$

$$\begin{cases} \partial_t \boldsymbol{\rho}_i(t,x) + \partial_x \mathbf{f}_i(\boldsymbol{\rho}_i(t,x)) = 0, & (t,x) \in (0,T) \times \mathbb{R}_{<0}, \\ \boldsymbol{\rho}_i(0,x) = \boldsymbol{\rho}_{0,i}^{\text{in}}(x), & x \in \mathbb{R}_{<0}, \end{cases} \tag{4.2.1}$$

$$\begin{cases} \partial_t \boldsymbol{\rho}_j(t,x) + \partial_x \mathbf{f}_j(\boldsymbol{\rho}_j(t,x)) = 0, & (t,x) \in (0,T) \times \mathbb{R}_{>0}, \\ \boldsymbol{\rho}_j(0,x) = \boldsymbol{\rho}_{0,j}^{\text{out}}(x), & x \in \mathbb{R}_{>0}. \end{cases} \tag{4.2.2}$$

Assumption 4.2.1 (Assumptions on the flux function)**.** *We assume that the initial densities are bounded, i.e.*

$$\boldsymbol{\rho}_{0,i}^{in} \in [0, \boldsymbol{\rho}_i^{\max}], \qquad \boldsymbol{\rho}_{0,j}^{out} \in [0, \boldsymbol{\rho}_j^{\max}]$$

for some $\boldsymbol{\rho}_i^{\max} \in \mathbb{R}_{>0}$, $i \in \mathcal{I}$, $\boldsymbol{\rho}_j^{\max} \in \mathbb{R}_{>0}$, $j \in \mathcal{O}$. *Moreover, we assume that the flux functions* $\mathbf{f}_i$, $\mathbf{f}_j$ *are smooth and strictly concave:*

$$\begin{aligned} \forall i \in \mathcal{I}: \ \mathbf{f}_i \in C^2([0, \boldsymbol{\rho}_i^{\max}]), \quad \mathbf{f}_i''(z) < 0 \ \forall z \in [0, \boldsymbol{\rho}_i^{\max}], \quad \mathbf{f}_i(0) = \mathbf{f}_i(\boldsymbol{\rho}_i^{\max}) = 0, \\ \forall j \in \mathcal{O}: \ \mathbf{f}_j \in C^2([0, \boldsymbol{\rho}_j^{\max}]), \quad \mathbf{f}_j''(z) < 0 \ \forall z \in [0, \boldsymbol{\rho}_j^{\max}], \quad \mathbf{f}_j(0) = \mathbf{f}_j(\boldsymbol{\rho}_j^{\max}) = 0. \end{aligned}$$

We define the critical densities $\boldsymbol{\rho}_i^{\text{crit}}, \boldsymbol{\rho}_j^{\text{crit}}$ *such that:*

$$\boldsymbol{\rho}_i^{\text{crit}} \in [0, \boldsymbol{\rho}_i^{\max}] : \ \mathbf{f}_i'(\boldsymbol{\rho}_i^{\text{crit}}) = 0, \qquad \boldsymbol{\rho}_j^{\text{crit}} \in [0, \boldsymbol{\rho}_j^{\max}] : \ \mathbf{f}_j'(\boldsymbol{\rho}_j^{\text{crit}}) = 0.$$

4.2.3 Node dynamics

The node dynamics are realized by a buffer and the boundary flux of incoming and outgoing roads. We present three different models for the buffer:

- the **Single-Buffer/Multi-Queues** in Section 4.2.3.a,
- the **Single-Buffer/Single-Queue** in Section 4.2.3.b,
- the **Independent-Buffers** in Section 4.2.3.c.

4.2.3.a Single-Buffer/Multi-Queues

In the Single-Buffer/Multi-Queues scenario, for each $j \in \mathcal{O}$ and any $t \in [0, T]$ we define a queue state $\mathbf{q}_j(t) \geq 0$ which describes the number of vehicles queued before entering link j serving all incoming links $i \in \mathcal{I}$. In addition, we assume that the intersection can store a maximum quantity of vehicles $M \in \mathbb{R}_{>0}$, which corresponds to a buffer size. The space left in the buffer at any time t is then $M - \sum_{j \in \mathcal{O}} \mathbf{q}_j(t)$.
For each incoming link $i \in \mathcal{I}$, we define a time-dependent priority coefficient $\mathbf{c}_i \in \mathbf{L}^\infty((0,T); \mathbb{R}_{\geq 0})$ which denotes the order of priority given to the entry in the junction. We then set the boundary incoming flux on any link $i \in \mathcal{I}$ such that it minimizes the demand from traffic and the supply of space in the buffer for $t \in (0, T)$:

$$\boldsymbol{\Gamma}_i(t) = \min \left\{ \begin{cases} \mathbf{f}_i(\boldsymbol{\rho}_i(t, 0-)) & \text{if } \boldsymbol{\rho}_i(t,0) \leq \boldsymbol{\rho}_i^{\text{crit}} \\ \mathbf{f}_i^{\max} & \text{if } \boldsymbol{\rho}_i(t,0) > \boldsymbol{\rho}_i^{\text{crit}} \end{cases}, \mathbf{c}_i(t) \left(M - \sum_{j \in \mathcal{O}} \mathbf{q}_j(t) \right) \right\}.$$

This formulation takes into account the fact that the available space in the buffer might be limited and not sufficient to support the demand function. The minimum selects the inflow as the corresponding demand to the density on the entering link, except if it exceeds the capacity of the buffer, in which case it allocates for the boundary condition the space left inside. We will prove later that the buffer never reaches capacity, *i.e.* the right hand side of the minimum remains strictly positive over time.
In the same way as we have defined the maximum possible flux entering, we now define the maximum possible flux exiting , which corresponds to the supply function. Denoting by

$$0 \leq \boldsymbol{\theta}_{i,j}(t) \leq 1, \quad t \in [0, T]$$

the time-dependent fraction of vehicles traveling from road $i \in \mathcal{I}$ into $j \in \mathcal{O}$ with $\sum_{j \in \mathcal{O}} \boldsymbol{\theta}_{i,j}(t) = 1$, we set the exiting boundary condition as the minimum between the demand of traffic and the supply of space on the exit:

$$\boldsymbol{\Gamma}_j(t) = \begin{cases} \begin{cases} \mathbf{f}_j^{\max} & \text{if } \boldsymbol{\rho}_j(t,0) \leq \boldsymbol{\rho}_j^{\text{crit}} \\ \mathbf{f}_j(\boldsymbol{\rho}_j(t,0+)) & \text{if } \boldsymbol{\rho}_j(t,0) > \boldsymbol{\rho}_j^{\text{crit}} \end{cases} & \text{if } \mathbf{q}_j(t) > 0, \\ \min\left\{ \begin{cases} \mathbf{f}_j^{\max} & \text{if } \boldsymbol{\rho}_j(t,0) \leq \boldsymbol{\rho}_j^{\text{crit}} \\ \mathbf{f}_j(\boldsymbol{\rho}_j(t,0+)) & \text{if } \boldsymbol{\rho}_j(t,0) > \boldsymbol{\rho}_j^{\text{crit}} \end{cases}, \sum_{i\in\mathcal{I}} \boldsymbol{\theta}_{i,j}(t)\boldsymbol{\Gamma}_i(t) \right\} & \text{if } \mathbf{q}_j(t) = 0. \end{cases}$$

For $t \in [0,T]$, if $\mathbf{q}_j(t) > 0$ for $j \in \mathcal{O}$, vehicles are stored in the buffer and wait to access the outgoing road. Thus, the boundary condition is determined by the supply on the exit road. Either the traffic is in free flow, and we can allocate $\mathbf{f}_j^{\max}$, or it is congested, and we can assign the flux corresponding to the traffic state on the specific road. If $\mathbf{q}_j(t) = 0$, the incoming flow at the intersection can directly exit onto the outgoing road. Thus, the minimum assigns as a boundary condition the minimum between the supply and the demand.

Finally, we need to define the dynamics governing the buffer states with an additional equation ensuring the conservation of vehicles at the junction, taking into account the flow which enters and leaves the buffer at time $t \in [0,T]$:

$$\mathbf{q}_j'(t) = \sum_{i\in\mathcal{I}} \boldsymbol{\theta}_{i,j}(t)\boldsymbol{\Gamma}_i(t) - \boldsymbol{\Gamma}_j(t), \quad t \in [0,T],\ j \in \mathcal{O}. \tag{4.2.3}$$

4.2.3.b Single-Buffer/Single-Queue

In the Single-Buffer/Single-Queue scenario (see [66]), we do not assign one buffer per exiting link, but only define one scalar buffer state at the level of the intersection, $q_{\text{s}}(t)$ for $t \in [0,T]$, serving all incoming and outgoing roads. The remaining space in the buffer at time t is $M - q_{\text{s}}(t)$ for $M \in \mathbb{R}_{>0}$ and we set

$$\boldsymbol{\Gamma}_i(t) = \min\left\{ \begin{cases} \mathbf{f}_i(\boldsymbol{\rho}_i(t,0-)) & \text{if } \boldsymbol{\rho}_i(t,0) \leq \boldsymbol{\rho}_i^{\text{crit}} \\ \mathbf{f}_i^{\max} & \text{if } \boldsymbol{\rho}_i(t,0) > \boldsymbol{\rho}_i^{\text{crit}} \end{cases}, \mathbf{c}_i(t)\big(M - q_{\text{s}}(t)\big) \right\}.$$

Denoting by $0 \leq \boldsymbol{\theta}_j(t) \leq 1$ the time-dependent fraction of vehicles traveling to the road $j \in \mathcal{O}$ with $\sum_{j\in\mathcal{O}} \boldsymbol{\theta}_j(t) = 1$ (which is here independent of the incoming links), we set

$$\boldsymbol{\Gamma}_j(t) = \begin{cases} \begin{cases} \mathbf{f}_j^{\max} & \text{if } \boldsymbol{\rho}_j(t,0) \leq \boldsymbol{\rho}_j^{\text{crit}} \\ \mathbf{f}_j(\boldsymbol{\rho}_j(t,0+)) & \text{if } \boldsymbol{\rho}_j(t,0) > \boldsymbol{\rho}_j^{\text{crit}} \end{cases} & \text{if } q_{\text{s}}(t) > 0, \\ \min\left\{ \begin{cases} \mathbf{f}_j^{\max} & \text{if } \boldsymbol{\rho}_j(t,0) \leq \boldsymbol{\rho}_j^{\text{crit}} \\ \mathbf{f}_j(\boldsymbol{\rho}_j(t,0+)) & \text{if } \boldsymbol{\rho}_j(t,0) > \boldsymbol{\rho}_j^{\text{crit}} \end{cases}, \boldsymbol{\theta}_j(t) \sum_{i\in\mathcal{I}} \boldsymbol{\Gamma}_i(t) \right\} & \text{if } q_{\text{s}}(t) = 0. \end{cases}$$

The dynamics for the queue are then

$$q_{\text{s}}'(t) = \sum_{i\in\mathcal{I}} \boldsymbol{\Gamma}_i(t) - \sum_{j\in\mathcal{O}} \boldsymbol{\Gamma}_j(t). \tag{4.2.4}$$

4.2.3.c Independent-Buffers

In this case, we allocate one buffer $\mathbf{M}_j \in \mathbb{R}_{>0}$ and one queue $\mathbf{q}_j(t)$ to each exit link $j \in \mathcal{O}$. The remaining space in each buffer is then $\mathbf{M}_j - \mathbf{q}_j(t)$, $t \in [0,T]$, and $\boldsymbol{\theta}_{i,j}$ is the ratio of flow which is assigned from road $i \in \mathcal{I}$ to road $j \in \mathcal{O}$ satisfying conservation of flow, i.e. $\sum_{j\in\mathcal{O}} \boldsymbol{\theta}_{i,j}(t) = 1, 0 \leq \boldsymbol{\theta}_{i,j} \leq 1 \ \forall (i,j) \in \mathcal{I} \times \mathcal{O}$. We then obtain for the incoming roads the dynamics

$$\boldsymbol{\Gamma}_i(t) = \min\left\{ \begin{cases} \mathbf{f}_i(\boldsymbol{\rho}_i(t,0-)) & \text{if } \boldsymbol{\rho}_i(t,0) \leq \boldsymbol{\rho}_i^{\text{crit}} \\ \mathbf{f}_i^{\max} & \text{if } \boldsymbol{\rho}_i(t,0) > \boldsymbol{\rho}_i^{\text{crit}} \end{cases}, \min_{j\in\mathcal{O}} \frac{\mathbf{M}_j - \mathbf{q}_j(t)}{\boldsymbol{\theta}_{i,j}(t)} \right\}, \ i \in \mathcal{I},$$

and for the outgoing links the boundary terms read for $j \in \mathcal{O}$ as

$$\boldsymbol{\Gamma}_j(t) = \begin{cases} \begin{cases} \mathbf{f}_j^{\max} & \text{if } \boldsymbol{\rho}_j(t,0) \leq \boldsymbol{\rho}_j^{\text{crit}} \\ \mathbf{f}_j(\boldsymbol{\rho}_j(t,0+)) & \text{if } \boldsymbol{\rho}_j(t,0) > \boldsymbol{\rho}_j^{\text{crit}} \end{cases} & \text{if } \mathbf{q}_j(t) > 0, \\ \min\left\{ \begin{cases} \mathbf{f}_j^{\max} & \text{if } \boldsymbol{\rho}_j(t,0) \leq \boldsymbol{\rho}_j^{\text{crit}} \\ \mathbf{f}_j(\boldsymbol{\rho}_j(t,0+)) & \text{if } \boldsymbol{\rho}_j(t,0) > \boldsymbol{\rho}_j^{\text{crit}} \end{cases}, \sum_{i\in\mathcal{I}} \boldsymbol{\theta}_{i,j}(t)\boldsymbol{\Gamma}_i(t) \right\} & \text{if } \mathbf{q}_j(t) = 0. \end{cases}$$

In the case $\boldsymbol{\theta}_{i,j}(t) = 0$, we set $\frac{\mathbf{M}_j - \mathbf{q}_j(t)}{\boldsymbol{\theta}_{i,j}(t)} = +\infty$. The dynamics for the queues are stated as

$$\mathbf{q}_j'(t) = \sum_{i\in\mathcal{I}} \boldsymbol{\theta}_{i,j}(t)\boldsymbol{\Gamma}_i(t) - \boldsymbol{\Gamma}_j(t), \quad t \in [0,T], \ j \in \mathcal{O} \tag{4.2.5}$$

with the bounds on the queues

$$\mathbf{0} \leq \mathbf{q}_j(t) \leq \mathbf{M}_j, \quad \forall\, t \in [0,T], \ j \in \mathcal{O}.$$

4.2.4 Derivation of the corresponding Hamilton-Jacobi framework

In this section, we will show formally how to derive the proper Hamilton-Jacobi framework for the considered problem class, assuming smooth solutions of the conservation laws. We will only consider the **Single-Buffer/Multi-Queues** case, the other two cases can be derived the same way.

4.2.4.a Number of vehicles exiting an entry link

On any incoming link $i \in \mathcal{I}$ the initial condition $\boldsymbol{\rho}_{0,i}^{\text{in}}$ on the level of conservation laws can be used to define the initial datum of the Hamilton-Jacobi formulation for $x \in \mathbb{R}_{<0}$:

$$\mathbf{V}_0^{\text{in}}(x) = \int_{-\infty}^{x} \boldsymbol{\rho}_0^{\text{in}}(y)\,\mathrm{d}y.$$

$\mathbf{V}_i^{\text{in}}$ is the integrated variable of the density for $t \in [0,T]$:

$$\begin{aligned} \partial_x \mathbf{V}_i^{\text{in}}(t,x) &= \boldsymbol{\rho}_i(t,x), \\ \mathbf{V}_i^{\text{in}}(t,x) &= \int_{-\infty}^{x} \boldsymbol{\rho}_i(t,y)\,\mathrm{d}y. \end{aligned}$$

The function $\mathbf{V}^{\text{in}}$ is in traffic simulation often called *Moskowitz* function (compare for instance [34, 85]). We can then write the conservation of vehicles on $\mathbb{R}_{<0}$, with $\boldsymbol{N}_i(t) = \int_0^t \mathbf{f}_i(\boldsymbol{\rho}_i(s,0))\,\mathrm{d}s$ the total number of vehicles that have left the link $i \in \mathcal{I}$ at time $t \in (0,T)$:

$$\begin{aligned}\tfrac{\mathrm{d}}{\mathrm{d}s}\int_{-\infty}^{0} \boldsymbol{\rho}_i(s,y)\,\mathrm{d}y &= -\mathbf{f}_i(\boldsymbol{\rho}_i(s,0)),\\ \int_0^t \tfrac{\mathrm{d}}{\mathrm{d}s}\int_{-\infty}^{0} \boldsymbol{\rho}_i(s,y)\,\mathrm{d}y\,\mathrm{d}s &= -\int_0^t \mathbf{f}_i(\boldsymbol{\rho}_i(s,0))\,\mathrm{d}s.\end{aligned}$$

Thus, we obtain for $t \in (0,T)$

$$\boldsymbol{N}_i(t) = \mathbf{V}^{\text{in}}_{0,i}(0) - \mathbf{V}^{\text{in}}_i(t,0).$$

4.2.4.b Number of vehicles reaching the intersection

$\boldsymbol{N}_i(t)$ represents the number of vehicles that reached the intersection during the time interval $[0,t]$. Among these vehicles, some want to access a given road $j \in \mathcal{O}$. We name $\mathbf{F}_j(t)$ the number of vehicles that have reached the intersection before time t and wish to turn into a given road $j \in \mathcal{O}$. We can then integrate and state for $t \in [0,T]$:

$$\begin{aligned}\mathbf{F}_j(t) &= \mathbf{q}_j(0) + \sum_{i\in\mathcal{I}} \int_0^t \boldsymbol{\theta}_{i,j}(s)\boldsymbol{N}_i'(s)ds\\ &= \mathbf{q}_j(0) + \sum_{i\in\mathcal{I}} \Big[\boldsymbol{\theta}_{i,j}(s)\boldsymbol{N}_i(s)\Big]_0^t - \sum_{i\in I}\int_0^t \boldsymbol{\theta}'_{i,j}(s)\boldsymbol{N}_i(s)\,\mathrm{d}s\\ &= \mathbf{q}_j(0) + \sum_{i\in\mathcal{I}} \boldsymbol{\theta}_{i,j}(t)\boldsymbol{N}_i(t) - \sum_{i\in\mathcal{I}}\int_0^t \boldsymbol{\theta}'_{i,j}(s)\boldsymbol{N}_i(s)\,\mathrm{d}s\\ &= \mathbf{q}_j(0) + \sum_{i\in\mathcal{I}} \boldsymbol{\theta}_{i,j}(t)(\mathbf{V}^{\text{in}}_{0,i}(0) - \mathbf{V}^{\text{in}}_i(t,0)) - \sum_{i\in\mathcal{I}}\int_0^t \boldsymbol{\theta}'_{i,j}(s)(\mathbf{V}^{\text{in}}_{0,i}(0) - \mathbf{V}^{\text{in}}_i(s,0))\,\mathrm{d}s.\end{aligned}$$

This formulation of $\mathbf{F}$ will be used later to define the proper fixed-point mapping in Section 4.4.2.

4.2.4.c Number of vehicles reaching a given exit $j \in \mathcal{O}$

Let us now apply the same reasoning for a given exit $j \in \mathcal{O}$. The initial condition reads as follows:

$$\mathbf{V}^{\text{out}}_0(x) = \int_0^x \boldsymbol{\rho}^{\text{out}}_0(y)\,\mathrm{d}y, \quad x \in (0,\infty).$$

$\mathbf{V}^{\text{out}}$ is the cumulative number of vehicles so that we obtain for $(t,x) \in (0,T)\times\mathbb{R}_{>0}$, $j \in \mathcal{O}$

$$\begin{aligned}\partial_x \mathbf{V}_j^{\text{out}}(t,x) &= \boldsymbol{\rho}_j(t,x),\\ \mathbf{V}_j^{\text{out}}(t,x) &= \int_0^x \boldsymbol{\rho}_j(t,y)\,\mathrm{d}y + \boldsymbol{\beta}(t),\end{aligned}$$

with $\boldsymbol{\beta}$ a function yet to be determined. $\mathbf{V}_j^{\text{out}}$ satisfies the following Hamilton-Jacobi equation:

$$\begin{aligned}\partial_t \mathbf{V}_j^{\text{out}}(t,x) + \mathbf{f}_j(\partial_x \mathbf{V}_j^{\text{out}}(t,x)) &= 0\\ \int_0^x \partial_t \boldsymbol{\rho}_j(t,y)\,\mathrm{d}y + \boldsymbol{\beta}'(t) + \mathbf{f}_j(\boldsymbol{\rho}_j(t,x)) &= 0.\end{aligned}$$

Plugging in $x = 0$

$$\boldsymbol{\beta}(t) + \int_0^t \mathbf{f}_j(\boldsymbol{\rho}_j(s,0))\,\mathrm{d}s = 0,$$

we then obtain

$$\mathbf{V}_j^{\text{out}}(t,x) = \int_0^x \boldsymbol{\rho}_j(t,y)\,\mathrm{d}y - \int_0^t \mathbf{f}_j(\boldsymbol{\rho}_j(s,0))\,\mathrm{d}s.$$

We can then write the conservation of vehicles on any segment $[0,x]$:

$$\begin{aligned}\tfrac{\mathrm{d}}{\mathrm{d}s}\int_0^x \boldsymbol{\rho}_j(s,y)\,\mathrm{d}y &= \mathbf{f}_j(\boldsymbol{\rho}_j(s,0)) - \mathbf{f}_j(\boldsymbol{\rho}_j(s,x))\\ \int_0^t \tfrac{\mathrm{d}}{\mathrm{d}s}\int_0^x \boldsymbol{\rho}_j(s,y)\,\mathrm{d}y\,\mathrm{d}s &= \int_0^t \Big[\mathbf{f}_j(\boldsymbol{\rho}_j(s,0)) - \mathbf{f}_j(\boldsymbol{\rho}_j(s,x))\Big]\,\mathrm{d}s\\ \int_0^x \boldsymbol{\rho}_j(t,y)\,\mathrm{d}y - \int_0^x \boldsymbol{\rho}_j(0,y)\,\mathrm{d}y &= \int_0^t \Big[\mathbf{f}_j(\boldsymbol{\rho}_j(s,0)) - \mathbf{f}_j(\boldsymbol{\rho}_j(s,x))\Big]\,\mathrm{d}s\\ \mathbf{V}_j^{\text{out}}(t,x) + \int_0^t \mathbf{f}_j(\boldsymbol{\rho}_j(s,0))\,\mathrm{d}s - \mathbf{V}_{0,j}^{\text{out}}(x) &= \int_0^t \mathbf{f}_j(\boldsymbol{\rho}_j(s,0))\,\mathrm{d}s - \int_0^t \mathbf{f}_j(\boldsymbol{\rho}_j(s,x))\,\mathrm{d}s\\ \mathbf{V}_{0,j}^{\text{out}}(x) - \mathbf{V}_j^{\text{out}}(t,x) &= \int_0^t \mathbf{f}_j(\boldsymbol{\rho}_j(s,x))\,\mathrm{d}s.\end{aligned}$$

Thus the number $\mathbf{V}_{0,j}^{\text{out}}(x) - \mathbf{V}_j^{\text{out}}(t,x)$ represents the number of vehicles that have crossed the location $x \in \mathbb{R}_{>0}$ during the interval $[0,t]$. In particular, if we call $\boldsymbol{S}_j$ the total number of vehicles that have entered the link $j \in \mathcal{O}$ at time $t \in [0,T]$,

$$\boldsymbol{S}_j(t) = -\mathbf{V}_j^{\text{out}}(t,0).$$

4.2.4.d Queue length

As a direct consequence of the conservation of mass, the buffer will store the difference between the number of vehicles that wanted to access $j \in \mathcal{O}$ and the number of vehicles that actually entered $j \in \mathcal{O}$. Thus, the length of the queue at the entrance of j is given by:

$$\mathbf{q}_j(t) = \mathbf{F}_j(t) - \boldsymbol{S}_j(t),\ t \in [0,T].$$

Remark. We will prove later in Lemma 4.4.12 that the buffer can never exceed the prescribed capacity $\mathbf{M}$, making the model reasonable. This is due to the dynamics which cause a natural spill-back when the buffer gets close to capacity so that less vehicles can actually enter in the buffer, and the associated flow decreases.

4.3 Definition of solutions

As a solution on a given junction in the conservation law framework we define:

Definition 4.3.1 (Solutions of the system of conservation laws and buffers)**.** We consider a junction with $i \in \mathcal{I}$ incoming links and $j \in \mathcal{O}$ outgoing links. We assume in addition that Assumption 4.2.1 is satisfied and initial data $\boldsymbol{\rho}_{0,i} \in \mathbf{L}^1(\mathbb{R}_{<0}) \cap \mathbf{L}^\infty(\mathbb{R}_{<0})$ with $0 \leq \boldsymbol{\rho}_{0,i} \leq \boldsymbol{\rho}_i^{\max}$ and $\boldsymbol{\rho}_{0,j} \in \mathbf{L}^1(\mathbb{R}_{>0}) \cap \mathbf{L}^\infty(\mathbb{R}_{>0})$ with $0 \leq \boldsymbol{\rho}_{0,j} \leq \boldsymbol{\rho}_j^{\max}$ be given. A solution to the initial boundary value problem with buffers as in Section 4.2 is given iff:

1. $\boldsymbol{\rho}^{\text{in}}, \boldsymbol{\rho}^{\text{out}}$ are weak entropy solutions of the conservation laws at the entering and exiting links and satisfy

$$\boldsymbol{\rho}_i^{\text{in}} \in C\left([0,T]; \mathbf{L}^1(\mathbb{R}_{\leq 0})\right),\ i \in \mathcal{I}, \qquad \boldsymbol{\rho}_j^{\text{out}} \in C\left([0,T]; \mathbf{L}^1(\mathbb{R}_{\geq 0})\right),\ j \in \mathcal{O}.$$

2. For the three different types of queues with buffer as stated in Section 4.2.3 we have
   - **Single-Buffer/Multi-Queues:** For a given $M \in \mathbb{R}_{>0}$ the queues $\mathbf{q}$ are determined by Equation (4.2.3) for a given split ratio $\boldsymbol{\theta}_{i,j} \in BV((0,T))$ satisfying

$$0 \leq \boldsymbol{\theta}_{i,j}(t) \leq 1, \qquad \sum_{j \in \mathcal{O}} \boldsymbol{\theta}_{i,j}(t) = 1,\ \forall t \in [0,T] \text{ a.e.},\ \forall (i,j) \in \mathcal{I} \times \mathcal{O}. \tag{4.3.1}$$

   - **Single-Buffer/Single-Queue:** For a given $M \in \mathbb{R}_{>0}$, the queue q_{s} is determined by Equation (4.2.4) for a given split ratio $\boldsymbol{\theta}_j \in BV((0,T))$ satisfying

$$0 \leq \boldsymbol{\theta}_j(t) \leq 1, \qquad \sum_{j \in \mathcal{O}} \boldsymbol{\theta}_j(t) = 1,\ \forall t \in [0,T] \text{ a.e.},\ j \in \mathcal{O}.$$

   - **Independent-Buffers:** For given $\mathbf{M} \in \mathbb{R}_{>0}^{|\mathcal{O}|}$ the queues $\mathbf{q}$ are determined by Equation (4.2.5) for a given split ratio $\boldsymbol{\theta}_{i,j} \in BV((0,T))$ satisfying

$$0 \leq \boldsymbol{\theta}_{i,j}(t) \leq 1, \qquad \sum_{j \in \mathcal{O}} \boldsymbol{\theta}_{i,j}(t) = 1,\ \forall t \in [0,T] \text{ a.e.},\ \forall (i,j) \in \mathcal{I} \times \mathcal{O}.$$

3. For the three different types of queues with buffer, the boundary conditions on any incoming link $i \in \mathcal{I}$ and any outgoing link $j \in \mathcal{O}$ are respectively given by
   - **Single-Buffer/Multi-Queues:** Section 4.2.3.a,
   - **Single-Buffer/Single-Queue:** Section 4.2.3.b,
   - **Independent-Buffers:** Section 4.2.3.c.

   In the stated initial boundary values problems in $\boldsymbol{\rho}$, the boundary datum is prescribed in the sense of Bardos-Leroux-Nédélec [13], see [48].

4.4 Existence and uniqueness of solutions to the Hamilton-Jacobi formulation

In the following, we will provide mathematical results for the Single-Buffer/Multi-Queues case, the results for the Single-Buffer/Single-Queue and the Independent-Buffers cases can be derived the same way.

4.4.1 Basic results and properties of Hamilton-Jacobi equations

Definition 4.4.1 (The Legendre-Fenchel transform)**.** Suppose we have a flux function $f \in C^2([0, \rho^{\max}]; \mathbb{R}_{\geq 0})$, strictly concave with $\rho^{\max} \in \mathbb{R}_{>0}$ given. Then, we define the Legendre-Fenchel transform f^* of f as

$$f^*(x) \coloneqq \inf_{u \in [0, \rho^{\max}]} \{ux - f(u)\}, \ x \in \mathrm{Dom}(f^*).$$

Thereby, the domain for the Legendre transform f^* is defined as

$$\mathrm{Dom}(f^*) \coloneqq \left\{ x^* \in \mathbb{R} : \inf_{x \in [0, \rho^{\max}]} \{xx^* - f(x)\} < \infty \right\} = \mathbb{R}.$$

Lemma 4.4.1 (Properties of the Legendre-Fenchel transform)**.** *Let the Legendre-Fenchel transform f^* as defined in Definition 4.4.1 be given. Then, the following properties hold:*

1. *f^* is Lipschitz-continuous, i.e. $|f^*(x) - f^*(y)| \leq \rho^{\max}|x - y| \ \forall x, y \in \mathrm{Dom}(f^*)$.*
2. *f^* is concave with $\mathrm{Dom}(f^*) = \mathbb{R}$.*
3. *The infimum in the definition of f^* is attained, i.e.*

$$\inf_{u \in [0, \rho^{\max}]} \{ux - f(u)\} = \min_{u \in [0, \rho^{\max}]} \{ux - f(u)\}.$$

4. *f^* is bounded from above, i.e. $\max_{x \in \mathbb{R}} f^*(x) \leq -f(0) = 0$.*
5. *The dual of f^* is f in the following meaning: for any $x \in [0, \rho^{\max}]$ the following equality holds $f(x) = \inf_{u \in \mathbb{R}} \{ux - f^*(u)\}$.*

Proof. 1. Let $x, y \in \mathrm{Dom}(f^*)$ and let $v^* \in [0,1]$ denote the point where the infimum is reached for the expression $f^*(y)$. Then, we obtain

$$\begin{aligned} f^*(x) - f^*(y) &= \inf_{u\in[0,\rho^{\max}]} \{ux - f(u)\} - \inf_{v\in[0,\rho^{\max}]} \{vy - f(v)\} \\ &\leq v^*x - f(v^*) - v^*y + f(v^*) \leq v^*(x-y) \leq v^*|x-y| \leq \rho^{\max}|x-y|. \end{aligned}$$

By reverting the role of x and y, we conclude that f^* is Lipschitz-continuous with Lipschitz-constant $\rho^{\max}$.

5. See [16].

□

For the following results it becomes mandatory to present a theorem for one-sided boundary datum and initial value of Hamilton-Jacobi equations. The following theorem provides an explicit solution formula in terms of a minimization problem and precise the relation of the solution formula to the corresponding conservation law with one-sided boundary datum.

Theorem 4.4.2 (Explicit solutions of Hamilton-Jacobi equations)**.** *Consider the following Hamilton-Jacobi equation:*

$$\begin{cases} \partial_t \tilde{v}(t,x) + g(\partial_x \tilde{v}(t,x)) = 0, & (t,x) \in (0,T) \times \mathbb{R}_{>0}, \\ \tilde{v}(0,x) = \tilde{v}_0(x), & x \in \mathbb{R}_{>0}, \\ \partial_x \tilde{v}(t, x=0) = \bar{\rho}_b(t), & t \in (0,T), \end{cases}$$

with $g \in C^2(\mathbb{R};\mathbb{R})$ being strictly convex, satisfying $\lim_{y\to\pm\infty} \frac{g(y)}{|y|} = \infty$ and $\rho_b \in \mathbf{L}^\infty((0,T))$ given with $\bar{\rho}_b(t) = \max\{\rho_b(t), \lambda\}$. λ is implicitly defined as $g(\lambda) = \min_{u\in\mathbb{R}} g(u)$ and the initial datum satisfies $\rho_0 \in \mathbf{L}^\infty(\mathbb{R}_{>0}) \cap \mathbf{L}^1(\mathbb{R}_{>0})$ with $v_0(x) \equiv \int_0^x \rho_0(y)\,\mathrm{d}y$, $x \in \mathbb{R}_{>0}$. Then, the solution of the Hamilton-Jacobi equation can be stated in terms of a minimization problem involving boundary and initial terms and reads for $(t,x) \in [0,T] \times \mathbb{R}_{>0}$ as

$$\begin{aligned} \tilde{v}(t,x) = \min \Bigg\{ & \min_{y\in\mathbb{R}_{\geq 0}} \Big\{ t g^*\big(\tfrac{x-y}{t}\big) + \tilde{v}_0(y) \Big\}, \\ & \min_{\substack{0\leq t_2\leq t_1\leq t \\ y\in\mathbb{R}_{\geq 0}}} \left\{ \tilde{v}_0(y) + g^*\big(\tfrac{-y}{t_2}\big) t_2 + \big(t-t_1\big) g^*\Big(\tfrac{x}{t-t_1}\Big) - \int_{t_2}^{t_1} g(\bar{\rho}_b(\theta))\,\mathrm{d}\theta \right\} \Bigg\}, \end{aligned}$$

where

$$g^*(x) \coloneqq \sup_{u\in\mathbb{R}} \{ux - g(u)\}.$$

In addition, $\tilde{v} \in \mathrm{Lip}([0,T] \times \mathbb{R}_{\geq 0})$ and the partial derivative of v with respect to the spatial variable is the weak entropy solution of the corresponding conservation law satisfying the boundary condition in the sense of Bardos-Leroux-Nédélec [13] :

$$\begin{cases} \partial_t \rho(t,x) + \partial_x g(\rho(t,x)) = 0, & (t,x) \in (0,T) \times \mathbb{R}_{\geq 0}, \\ \rho(0,x) = \rho_0(x), & x \in \mathbb{R}_{\geq 0}, \\ \rho(t,0) = \bar{\rho}_b(t), & t \in (0,T). \end{cases}$$

Proof. The proof can be found in [94]. □

Lemma 4.4.3 (Solution formula related to (4.2.1),(4.2.2))**.** *Let $\rho_0 \in \mathbf{L}^1(\mathbb{R}_{<0}) \cap \mathbf{L}^\infty(\mathbb{R}_{<0})$ with $0 \leq \rho_0(x) \leq \rho^{\max}$, $x \in \mathbb{R}_{<0}$ a.e. be given. Assume the flux function $f \in C^2(\mathbb{R};\mathbb{R})$ being strictly concave, satisfying $\lim_{y \to \pm\infty} \frac{f(y)}{|y|} = -\infty$. Consider the following conservation law on the half plane:*

$$\begin{cases} \partial_t \rho(t,x) + \partial_x f(\rho(t,x)) = 0, & (t,x) \in (0,T) \times \mathbb{R}_{<0}, \\ \rho(0,x) = \rho_0(x), & x \in \mathbb{R}_{<0}, \\ f(\rho(t,0)) = h(t), & t \in (0,T), \end{cases}$$

with $h \in \mathbf{L}^\infty((0,T))$ and $0 \leq h(t) \leq f^{\max}$, $t \in (0,T)$ a.e. be given. Then, the solution of the associated Hamilton-Jacobi equation can be stated in terms of a maximization problem involving boundary and initial term and reads for $(t,x) \in [0,T] \times \mathbb{R}_{\geq 0}$ as

$$v(t,x) = \max \left\{ \max_{y \in \mathbb{R}_{\leq 0}} \left\{ t f^*\left(\tfrac{x-y}{t}\right) + v_0(y) \right\}, \right.$$
$$\left. \max_{\substack{0 \leq t_2 \leq t_1 \leq t \\ y \in \mathbb{R}_{\leq 0}}} \left\{ v_0(y) + f^*\left(\tfrac{-y}{t_2}\right) t_2 + \left(t - t_1\right) f^*\left(\tfrac{x}{t-t_1}\right) - \int_{t_2}^{t_1} h(\theta)\, \mathrm{d}\theta \right\} \right\}.$$

Proof. We define $\bar{\rho}_{\mathrm{b}}(t)$ as the solution of $f(\bar{\rho}_{\mathrm{b}}(t)) = h(t)$ such that $\bar{\rho}_{\mathrm{b}}(t) \in [\rho^{\mathrm{crit}}, \rho^{\max}]$. Consider the strictly convex function g such that $g \equiv -f$. given $x \in \mathbb{R}$, the following identity holds

$$f^*(x) = \inf_{y \in \mathbb{R}} \{yx - f(y)\} = -\sup_{y \in \mathbb{R}} \{-yx + f(y)\} = -\sup_{y \in \mathbb{R}} \{-yx - g(y)\} = -g^*(-x).$$

Then we can apply Theorem 4.4.2 to obtain the solution to the following IBVP problem

$$\begin{cases} \partial_t\, \tilde{v}(t,x) + g(\partial_x \tilde{v}(t,x)) = 0, & (t,x) \in (0,T) \times \mathbb{R}_{\geq 0}, \\ \tilde{v}(0,x) = \tilde{v}_0(x), & x \in \mathbb{R}_{\geq 0}, \\ \partial_x \tilde{v}(t, x=0), = \bar{\rho}_{\mathrm{b}}(t), & t \in (0,T), \end{cases}$$

for $(t,x) \in [0,T] \times \mathbb{R}_{\geq 0}$. We have

$$\tilde{v}(t,x) = \min \left\{ \min_{y \in \mathbb{R}_{\geq 0}} \left\{ t g^*\left(\tfrac{x-y}{t}\right) + \tilde{v}_0(y) \right\}, \right.$$
$$\left. \min_{\substack{0 \leq t_2 \leq t_1 \leq t \\ y \in \mathbb{R}_{\geq 0}}} \left\{ \tilde{v}_0(y) + g^*\left(\tfrac{-y}{t_2}\right) t_2 + \left(t - t_1\right) g^*\left(\tfrac{x}{t-t_1}\right) - \int_{t_2}^{t_1} g(\bar{\rho}_{\mathrm{b}}(\theta))\, \mathrm{d}\theta \right\} \right\}.$$

For $x \in \mathbb{R}_{\leq 0}$ define $v(t,x) = -\tilde{v}(t,-x)$. Then v is a solution of

$$\begin{cases} -\partial_t v(t,x) + g(\partial_x v(t,x)) = 0, & (t,x) \in (0,T) \times \mathbb{R}_{\leq 0}, \\ v(0,x) = -\tilde{v}_0(-x), & x \in \mathbb{R}_{\leq 0}, \\ \partial_x v(t,x=0) = \bar{\rho}_{\mathrm{b}}(t), & t \in (0,T), \end{cases}$$

which is, by construction, the solution of

$$\begin{cases} \partial_t v(t,x) + f(\partial_x v(t,x)) = 0, & (t,x) \in (0,T) \times \mathbb{R}_{\leq 0}, \\ v(0,x) = -\tilde{v}_0(-x) = v_0(x), & x \in \mathbb{R}_{\leq 0}, \\ \partial_x v(t,x=0) = \bar{\rho}_{\mathrm{b}}(t), & t \in (0,T). \end{cases}$$

This is detailed in the following manipulations. Let $(t,x) \in [0,T] \times \mathbb{R}_{\geq 0}$ be given, we have

$$\begin{aligned} v(t,x) &= -\tilde{v}(t,-x) \\ &= -\min\Bigg\{ \min_{y \in \mathbb{R}_{\geq 0}} \Big\{ t g^*\big(\tfrac{-x-y}{t}\big) + \tilde{v}_0(y) \Big\}, \\ &\qquad \min_{\substack{0 \leq t_2 \leq t_1 \leq t \\ y \in \mathbb{R}_{\geq 0}}} \Bigg\{ \tilde{v}_0(y) + g^*\big(\tfrac{-y}{t_2}\big) t_2 + \big(t - t_1\big) g^*\Big(\tfrac{-x}{t-t_1}\Big) - \int_{t_2}^{t_1} g(\bar{\rho}_{\mathrm{b}}(\theta))\,\mathrm{d}\theta \Bigg\} \Bigg\} \\ &= \max\Bigg\{ \max_{y \in \mathbb{R}_{\geq 0}} \Big\{ -t g^*\big(\tfrac{-x-y}{t}\big) - \tilde{v}_0(y) \Big\}, \\ &\qquad \max_{\substack{0 \leq t_2 \leq t_1 \leq t \\ y \in \mathbb{R}_{\geq 0}}} \Bigg\{ -\tilde{v}_0(y) - g^*\big(\tfrac{-y}{t_2}\big) t_2 - \big(t - t_1\big) g^*\Big(\tfrac{-x}{t-t_1}\Big) + \int_{t_2}^{t_1} g(\bar{\rho}_{\mathrm{b}}(\theta))\,\mathrm{d}\theta \Bigg\} \Bigg\} \\ &= \max\Bigg\{ \max_{y \in \mathbb{R}_{\geq 0}} \Big\{ t f^*\big(\tfrac{x+y}{t}\big) - \tilde{v}_0(y) \Big\}, \\ &\qquad \max_{\substack{0 \leq t_2 \leq t_1 \leq t \\ y \in \mathbb{R}_{\geq 0}}} \Bigg\{ -\tilde{v}_0(y) + f^*\big(\tfrac{y}{t_2}\big) t_2 + \big(t - t_1\big) f^*\Big(\tfrac{x}{t-t_1}\Big) + \int_{t_2}^{t_1} g(\bar{\rho}_{\mathrm{b}}(\theta))\,\mathrm{d}\theta \Bigg\} \Bigg\} \\ &= \max\Bigg\{ \max_{y \in \mathbb{R}_{\leq 0}} \Big\{ t f^*\big(\tfrac{x-y}{t}\big) + v_0(y) \Big\}, \\ &\qquad \max_{\substack{0 \leq t_2 \leq t_1 \leq t \\ y \in \mathbb{R}_{\leq 0}}} \Bigg\{ v_0(y) + f^*\big(\tfrac{-y}{t_2}\big) t_2 + \big(t - t_1\big) f^*\Big(\tfrac{x}{t-t_1}\Big) - \int_{t_2}^{t_1} f(\bar{\rho}_{\mathrm{b}}(\theta))\,\mathrm{d}\theta \Bigg\} \Bigg\} \end{aligned}$$

which is indeed the claimed formula. □

Remark 4.2. We note that in [94] the supremum in the Legendre-Fenchel transform is selected on all $\mathbb{R}$ and not on a compact subset. In the present case, we restrict ourselves to $[0, \rho^{\max}]$ since the initial density is chosen in $[0, \rho^{\max}]$ and then the characteristics in the conservation law setting can only travel with speeds contained in $[f'(\rho^{\max}), f'(0)]$.

Lemma 4.4.4 (Semi-group property of the formula presented in Theorem 4.4.2)**.** *Given the formula for v in Theorem 4.4.2, it satisfies the semi-group property, i.e. $\forall x \in \mathbb{R}_{\geq 0}$, $\forall t, \tilde{t} \in [0,T], t > \tilde{t}$*

$$v(t,x) = \min\left\{ \min_{y\in\mathbb{R}_{\geq 0}} \left\{ (t-\tilde{t}) f^*\left(\tfrac{x-y}{t-\tilde{t}}\right) + v(\tilde{t},y) \right\}, \right.$$
$$\left. \min_{\substack{\tilde{t}\leq t_2\leq t_1\leq t \\ y\in\mathbb{R}_{\geq 0}}} \left\{ v(\tilde{t},y) + f^*\left(\tfrac{-y}{t_2}\right) t_2 + \left(t-t_1\right) f^*\left(\tfrac{x}{t-t_1}\right) - \int_{t_2}^{t_1} f(\bar{\rho}_b(\theta))\,\mathrm{d}\theta \right\} \right\}.$$

Proof. We refer the reader to [63] for the proof for the Cauchy problem. The extension with boundary datum can be derived similarly. □

Theorem 4.4.5 (Relation between H-J equations and conservation laws)**.** *Let $F \in \mathrm{Lip}([0,T];\mathbb{R}_{\geq 0})$ be given and consider for $T \in \mathbb{R}_{>0}$ and $\rho_0 \in BV(\mathbb{R}_{\geq 0})$ the initial boundary value problem*

$$\begin{cases} \partial_t \rho(t,x) + \partial_x f(\rho(t,x)) = 0, & (t,x) \in (0,T)\times\mathbb{R}_{\geq 0}, \\ \rho(0,x) = \rho_0(x), & x \in \mathbb{R}_{\geq 0}, \end{cases}$$

supplemented by the boundary datum at $x = 0$ for $t \in (0,T)$ as

$$f(\rho(t,0)) = b(t),$$

where $b(t)$ is defined as

$$b(t) \coloneqq \begin{cases} \begin{cases} f^{\max} & \text{if } \rho(t,0) \leq \rho^{\mathrm{crit}} \\ f(\rho(t,0)) & \text{if } \rho(t,0) > \rho^{\mathrm{crit}} \end{cases} & \text{if } q(t) > 0, \\ \min\left\{ \begin{cases} f^{\max} & \text{if } \rho(t,0) \leq \rho^{\mathrm{crit}} \\ f(\rho(t,0)) & \text{if } \rho(t,0) > \rho^{\mathrm{crit}} \end{cases}, F'(t) \right\} & \text{if } q(t) = 0, \end{cases}$$

and $q \in \mathbf{W}^{1,\infty}((0,T);\mathbb{R}_{\geq 0})$ be given. Then, the correspondent Hamilton-Jacobi equation in v reads as

$$\begin{cases} \partial_t v(t,x) + f(\partial_x v(t,x)) = 0, & (t,x) \in (0,T)\times\mathbb{R}_{\geq 0}, \\ v(0,x) = \displaystyle\int_0^x \rho_0(y)\,\mathrm{d}y = v_0(x), & x \in \mathbb{R}_{\geq 0}, \\ f(\partial_x v(t,0)) = b(t), & t \in (0,T), \end{cases}$$

and admits the explicit solution formula in terms of a minimization for $(t,x) \in (0,T)\times\mathbb{R}_{\geq 0}$

$$v(t,x) = \max\left\{ \max_{y\in\mathbb{R}_{\geq 0}} \left\{ v_0(y) + t f^*\left(\tfrac{x-y}{t}\right) \right\}, \max_{0\leq t_1\leq t} \left\{ -F(t_1) + (t-t_1) f^*\left(\tfrac{x}{t-t_1}\right) \right\} \right\}.$$

Moreover, the solution v is Lipschitz-continuous and its spatial derivative provides the weak entropy solution of the conservation law with boundary data in the sense of Bardos-Leroux-Nédélec [13].

Proof. The proof can be found in [27, Section 8]. □

Remark 4.3 (Relation between the mapping F and $\mathbf{F}_j$). The function $F(t),\ t \in [0,T]$, will correspond in our framework to $\mathbf{F}_j,\ j \in \mathcal{O}$, the number of vehicles that reached the intersection at time t and want to access exit j.

Definition 4.4.2 (Definition of initial data for the Hamilton-Jacobi equations)**.** Given the initial datum for the conservation laws in Definition 4.3.1, we define the initial datum for the Hamilton-Jacobi equations as

$$\mathbf{V}^{\text{in}}_{0,i}(x) \coloneqq \int_{-\infty}^{x} \boldsymbol{\rho}_{0,i}(z)\,\mathrm{d}z,\ x \in \mathbb{R}_{\leq 0},\ i \in \mathcal{I}, \qquad \mathbf{V}^{\text{out}}_{0,j}(x) \coloneqq \int_{0}^{x} \boldsymbol{\rho}_{0,j}(z)\,\mathrm{d}z,\ x \in \mathbb{R}_{\geq 0}\ j \in \mathcal{O}.$$

4.4.2 The fixed-point problem

As formally shown in Section 4.2 we can pose the considered problem as a fixed-point problem on the level of Hamilton-Jacobi PDEs. Thereby, the buffer and queues defined in Section 4.2.3 are coupled to the boundary datum of the incoming and outgoing fluxes. In addition, these fluxes are also dependent on the state of the buffer and queues. This all will be made rigorous in the following section.

Definition 4.4.3 (The decomposition of the fixed-point mapping)**.** We define the following mappings:

- Let the priority function $\mathbf{c}_i \in \mathbf{L}^\infty\left((0,T);\mathbb{R}_{\geq 0}\right)$ and $\mathbf{f}_i^{\max} \in \mathbb{R}_{>0}$ for $i \in \mathcal{I}$ be given. Then, we define the mapping

$$\mathbf{h} : \begin{cases} \mathrm{Lip}\left([0,T];\mathbb{R}^{|\mathcal{O}|}\right) & \to \mathrm{Lip}\left([0,T];\mathbb{R}^{|\mathcal{I}|}\right) \\ \mathbf{q} & \mapsto \left(t \mapsto \min\left\{\mathbf{f}^{\max}, \mathbf{c}(t)\cdot\left(M - \textstyle\sum_{j\in\mathcal{O}} \mathbf{q}_j(t)\right)\right\}\right). \end{cases} \tag{4.4.1}$$

  Thereby, the min is meant component-wise.

- For $i \in \mathcal{I}$ given initial datum $\mathbf{V}_0^{\text{in}}$ as defined in Definition 4.4.2 and $\mathbf{f}_i^{\max} \in \mathbb{R}_{>0}$ with $X \coloneqq \mathrm{Lip}([0,T])$ we define

$$\bar{\mathbf{V}}_i^{\text{in}} : \begin{cases} X & \to \mathrm{Lip}([0,T]\times\mathbb{R}_{\leq 0}) \\ \mathbf{h}_i & \mapsto (t,x) \mapsto \max\left\{ \begin{array}{c} \max\limits_{y\in\mathbb{R}_{\leq 0}} \left\{\mathbf{V}^{\text{in}}_{0,i}(y) + t\mathbf{f}_i^*\left(\frac{x-y}{t}\right)\right\}, \\ \max\limits_{\substack{y\in\mathbb{R}_{\leq 0}\\ 0\leq t_2\leq t_1\leq t}} \left\{\mathbf{V}^{\text{in}}_{0,i}(y) + t_2\mathbf{f}_i^*\left(\frac{-y}{t_2}\right) + (t-t_1)\mathbf{f}_i^*\left(\frac{x}{t-t_1}\right) - \int_{t_2}^{t_1}\mathbf{h}_i(s)\,\mathrm{d}s\right\} \end{array} \right\}. \end{cases} \tag{4.4.2}$$

In addition, we define the solution evaluated at $x = 0$, $\mathbf{V}^{\text{in}} \equiv \bar{\mathbf{V}}^{\text{in}}(\cdot, 0)$ on $[0, T]$ and $X \coloneqq \text{Lip}([0, T])$

$$\mathbf{V}_i^{\text{in}} : \begin{cases} X & \to X \\ \mathbf{h}_i & \mapsto (t) \mapsto \max \left\{ \begin{array}{c} \max\limits_{y \in \mathbb{R}_{\leq 0}} \left\{ \mathbf{V}_{0,i}^{\text{in}}(y) + t\mathbf{f}_i^*\left(\frac{-y}{t}\right) \right\}, \\ \max\limits_{\substack{y \in \mathbb{R}_{\leq 0} \\ 0 \leq t_2 \leq t_1 \leq t}} \left\{ \mathbf{V}_{0,i}^{\text{in}}(y) + t_2\mathbf{f}_i^*\left(\frac{-y}{t_2}\right) - (t - t_1)\mathbf{f}_i^{\max} - \int_{t_2}^{t_1} \mathbf{h}_i(s)\, \mathrm{d}s \right\} \end{array} \right\}. \end{cases} \tag{4.4.3}$$

- Let $\mathbf{q}^0 \in \mathbb{R}_{\geq 0}^{|\mathcal{O}|}$ with $\|\mathbf{q}^0\|_1 \leq M$ and $\boldsymbol{\theta}$ as in Section 4.3 and Item 2, we define

$$\mathbf{F} : \begin{cases} \text{Lip}\left([0, T]; \mathbb{R}^{|\mathcal{I}|}\right) & \mapsto \text{Lip}\left([0, T]; \mathbb{R}^{|\mathcal{O}|}\right) \\ \mathbf{V}^{\text{in}} & \mapsto \left(t \mapsto \mathbf{q}^0 - \sum\limits_{i \in I} \int_0^t \frac{\mathrm{d}}{\mathrm{d}s} \mathbf{V}_i^{\text{in}}(s) \boldsymbol{\theta}_i(s)\, \mathrm{d}s \right). \end{cases} \tag{4.4.4}$$

- Let $\mathbf{V}_0^{\text{out}}$ as defined in Definition 4.4.2 be given and $j \in \mathcal{O}$ we define for $X \coloneqq \text{Lip}([0, T])$

$$\bar{\mathbf{V}}_j^{\text{out}} : \begin{cases} X & \to \text{Lip}([0, T] \times \mathbb{R}_{\geq 0}) \\ \mathbf{F}_j & \mapsto (t, x) \mapsto \max \left\{ \max\limits_{y \in \mathbb{R}_{\geq 0}} \left\{ \mathbf{V}_{0,j}^{\text{out}}(y) + t\mathbf{f}_j^*\left(\frac{x-y}{t}\right) \right\}, \max\limits_{0 \leq t_1 \leq t} \left\{ -\mathbf{F}_j(t_1) + (t - t_1)\mathbf{f}_j^*\left(\frac{x}{t-t_1}\right) \right\} \right\}. \end{cases} \tag{4.4.5}$$

In addition, we define the solution evaluated at $x = 0$, $\mathbf{V}^{\text{out}} \equiv \bar{\mathbf{V}}^{\text{out}}(\cdot, 0)$ on $[0, T]$

$$\mathbf{V}_j^{\text{out}} : \begin{cases} X & \to X \\ \mathbf{F}_j & \mapsto (t) \mapsto \max \left\{ \max\limits_{y \in \mathbb{R}_{\geq 0}} \left\{ \mathbf{V}_{0,j}^{\text{out}}(y) + t\mathbf{f}_j^*\left(\frac{-y}{t}\right) \right\}, \max\limits_{0 \leq t_1 \leq t} \left\{ -\mathbf{F}_j(t_1) - (t - t_1)\mathbf{f}_j^{\max} \right\} \right\}. \end{cases} \tag{4.4.6}$$

- Finally, we define

$$\boldsymbol{\Lambda} : \begin{cases} \text{Lip}\left([0, T]; \mathbb{R}^{|\mathcal{O}|}\right) \times \text{Lip}\left([0, T]; \mathbb{R}^{|\mathcal{O}|}\right) & \to \text{Lip}\left([0, T]; \mathbb{R}^{|\mathcal{O}|}\right) \\ (\mathbf{F}, \mathbf{V}^{\text{out}}) & \mapsto \Big(t \mapsto \mathbf{F}(t) + \mathbf{V}^{\text{out}}(t) \Big). \end{cases} \tag{4.4.7}$$

Remark 4.4 (Mappings defined in Definition 4.4.3). The above mappings are in fact the rigorous generalization of the physical process described in Section 4.2. To each value of the queue $\mathbf{q}$ we associate $\mathbf{h}$, the corresponding boundary flux at the entry of the intersection. From this condition, we can obtain $\bar{\mathbf{V}}_i^{\text{in}}$, the accumulated number of vehicles on each entry link $i \in \mathcal{I}$ and its evaluation $\mathbf{V}_i^{\text{in}}$ at $x = 0$. Then, for each $j \in \mathcal{O}$, we can compute $\mathbf{F}_j$ which corresponds to the number of vehicles that reached the intersection and wish to access exit j. The function $\bar{\mathbf{V}}_j^{\text{out}}$ corresponds to the accumulated number that actually entered exit j and $\mathbf{V}_j^{\text{out}}$ is its evaluation at $x = 0$. Finally, $\boldsymbol{\Lambda}$ is the mapping that updates the queue length, by adding to the initial queue value the difference between the number of vehicles that have reached the intersection and the number of vehicles that left the junction.

Given the introduced mappings we are now in a position to formulate the proposed dynamics in Definition 4.3.1 in terms of a fixed-point problem.

Lemma 4.4.6 (solution to the Fixed-point problem)**.** *There exists a solution of the dynamics as proposed in Definition 4.3.1 if the following fixed-point problem admits a unique solution on* $[0,T]$*:*

$$\mathbf{q} \equiv \mathbf{\Lambda} \circ (\mathbf{F} \circ \mathbf{V}^{\text{in}} \circ \mathbf{h} \circ \mathbf{q}, \mathbf{V}^{\text{out}} \circ \mathbf{F} \circ \mathbf{V}^{\text{in}} \circ \mathbf{h} \circ \mathbf{q}),\ \mathbf{q} \in C\left([0,T]; \mathbb{R}^{|\mathcal{O}|}\right)$$

with the involved operators satisfying Definition 4.4.3.

So far, we have claimed in Definition 4.4.3 that these mappings actually map into the proper spaces. This will be justified in the next lemmas. The following trivial result on the maximum and minimum of Lipschitz functions is required to provide the necessary estimates.

Lemma 4.4.7 (Lipschitz-continuous functions and $\max, \min$)**.** *Let* $I \subseteq \mathbb{R}$ *be given and assume* $a, b \in \text{Lip}(I; \mathbb{R})$*. Then, the mappings*

$$c : \begin{cases} I & \to \mathbb{R} \\ x & \mapsto \max\{a(x), b(x)\} \end{cases} \qquad d : \begin{cases} I & \to \mathbb{R} \\ x & \mapsto \min\{a(x), b(x)\} \end{cases} \tag{4.4.8}$$

are also Lipschitz-continuous with Lipschitz-constant $\max\{L_a, L_b\}$*, where* $L_a, L_b \in \mathbb{R}_{\geq 0}$ *denote the Lipschitz constants of the function* a*,* b *respectively.*

Proof. Following the definition of Lipschitz-continuity we show that for any $x, y \in I$

$$|c(x) - c(y)| \leq \max\{L_a, L_b\}|x - y|.$$

We need to distinguish the four cases, depending on which sides the maximum gets picked. Let $x, y \in I$ given. First assume $|c(x) - c(y)| = |a(x) - a(y)|$. Then the inequality follows directly from the Lipschitz-continuity of a. The same reasoning can be applied if $|c(x) - c(y)| = |b(x) - b(y)|$.
Now assume $c(x) - c(y) = a(x) - b(y)$. Then we get

$$\begin{aligned} c(x) - c(y) = a(x) - b(y) \leq a(x) - a(y) \leq L_a|x - y| \\ c(x) - c(y) = a(x) - b(y) \geq b(x) - b(y) \geq L_b|x - y|. \end{aligned}$$

The last case can be obtained in the same way. □

4.4.3 Estimates for the involved mappings

In order to obtain the required regularity for the fixed-point theory, the previously introduced mappings in Definition 4.4.3 have to be Lipschitz-continuous and satisfy additional properties. Thus, we will present the named properties in Lemma 4.4.8, Proposition 4.4.9:

Lemma 4.4.8 (Space-dependent $\bar{\mathbf{V}}^{\mathrm{out}}$ and $\bar{\mathbf{V}}^{\mathrm{in}}$)**.** *Let* $\mathbf{F}, \tilde{\mathbf{F}} \in \mathrm{Lip}\left([0,T];\mathbb{R}^{|\mathcal{O}|}\right)$ *and* $\mathbf{h}, \tilde{\mathbf{h}} \in \mathrm{Lip}\left([0,T];\mathbb{R}^{|\mathcal{I}|}\right)$.

1. *For the spatial dependent* $\bar{\mathbf{V}}^{\mathrm{out}}$ *as in Definition 4.4.3 we obtain for* $j \in \mathcal{O}$*:*

$$\begin{aligned}&|\bar{\mathbf{V}}_j^{\mathrm{out}}[\mathbf{F}_j](t,x) - \bar{\mathbf{V}}_j^{\mathrm{out}}[\mathbf{F}_j](\tilde{t},\tilde{x})| \\ &\quad \le \boldsymbol{\rho}_j^{\max}|x-\tilde{x}| + \max\left\{\mathbf{f}_j^{\max}, \|\mathbf{F}'_j\|_{\mathbf{L}^\infty((0,T))}\right\}|t-\tilde{t}| \end{aligned} \qquad \forall (t,x),(\tilde{t},\tilde{x}) \in (0,T)\times\mathbb{R}_{\ge 0},$$

$$\|\bar{\mathbf{V}}_j^{\mathrm{out}}[\mathbf{F}_j](\cdot,0) - \bar{\mathbf{V}}_j^{\mathrm{out}}[\tilde{\mathbf{F}}_j](\cdot,0)\|_{C([0,t])} \le \|\mathbf{F}_j - \tilde{\mathbf{F}}_j\|_{C([0,t])}, \qquad \forall t \in (0,T].$$

2. *For the spatial dependent* $\bar{\mathbf{V}}^{\mathrm{in}}$ *as in Definition 4.4.3 we obtain for* $i \in \mathcal{I}$*:*

$$\left\|\bar{\mathbf{V}}_i^{\mathrm{in}}[\mathbf{h}_i](\cdot,0) - \mathbf{V}_i^{\mathrm{in}}[\tilde{\mathbf{h}_i}](\cdot,0)\right\|_{C([0,t])} \le \|\mathbf{h}_i - \tilde{\mathbf{h}}_i\|_{\mathbf{L}^1((0,t))}, \qquad \forall t \in (0,T].$$

In addition, $\forall (t,x),(\tilde{t},\tilde{x}) \in [0,T]\times\mathbb{R}_{<0}$ *we have*

$$\left|\bar{\mathbf{V}}_i^{\mathrm{in}}[\mathbf{h}_i](t,x) - \bar{\mathbf{V}}_i^{\mathrm{in}}[\mathbf{h}_i](\tilde{t},\tilde{x})\right| \le \boldsymbol{\rho}_i^{\max}|x-\tilde{x}| + \max\left\{\mathbf{f}_i^{\max}, \|\mathbf{h}_i\|_{C([0,t])}\right\}|t-\tilde{t}|,$$

$$\tfrac{\mathrm{d}}{\mathrm{dt}}\bar{\mathbf{V}}_i^{\mathrm{in}}[\mathbf{h}_i](t,0) \le 0, \qquad \forall t \in (0,T) \text{ a.e., } \mathbf{h}_i \ge 0. \tag{4.4.9}$$

Proof. 1. Let $\mathbf{F} \in \mathrm{Lip}([0,T];\mathbb{R}^{|\mathcal{O}|})$ and $j \in \mathcal{O}$ be given, the first term in the outer maximum of the solution formula presented for $\bar{\mathbf{V}}^{\mathrm{out}}$ in Definition 4.4.3 is again Lipschitz continuous by [63, Section 3.3, Lemma 2] and for the second term we assume that for $(t,x) \in [0,T]\times(0,L)$ the maximum is attained for $t_1 \in [0,T]$. Then, we have for $(\tilde{t},\tilde{x}) \in [0,T]\times[0,L]$

$$\begin{aligned}&\bar{\mathbf{V}}_j^{\mathrm{out}}[\mathbf{F}_j](t,x) - \bar{\mathbf{V}}_j^{\mathrm{out}}[\mathbf{F}_j](t,\tilde{x}) \\ &= -\mathbf{F}_j(t_1) + (t-t_1)\mathbf{f}_j^*\left(\tfrac{x}{t-t_1}\right) - \max_{0\le t_1\le t}\left\{-\mathbf{F}_j(t_1) + (t-t_1)\mathbf{f}_j^*\left(\tfrac{\tilde{x}}{t-t_1}\right)\right\} \\ &\le (t-t_1)\left(\mathbf{f}_j^*\left(\tfrac{x}{t-t_1}\right) - \mathbf{f}_j^*\left(\tfrac{\tilde{x}}{t-t_1}\right)\right) \le \boldsymbol{\rho}_i^{\max}|x-\tilde{x}|\end{aligned}$$

by the Lipschitz-continuity of $\mathbf{f}_j^*$ as stated in Lemma 4.4.1. The lower bound follows analogously by exchanging x and $\tilde{x}$. For the Lipschitz-continuity w.r.t. time, we recall that for the left part of the solution formula which only consists of initial datum the proof can also be found in [63, Section 3.3, Lemma 2] and one obtains in that case

$$\left|\bar{\mathbf{V}}_j^{\mathrm{out}}[\mathbf{F}_j](t,x) - \bar{\mathbf{V}}_j^{\mathrm{out}}[\mathbf{F}_j](\tilde{t},x)\right| \le \mathbf{f}_j^{\max}|t-\tilde{t}|.$$

For the right part involving also the boundary datum assume for now that $\tilde{t} \ge t$. Then we obtain in the case that the maximum is attained at $t_1 \in [0,t]$

$$\begin{aligned}&\bar{\mathbf{V}}_j^{\mathrm{out}}[\mathbf{F}_j](t,x) - \bar{\mathbf{V}}_j^{\mathrm{out}}[\mathbf{F}_j](\tilde{t},x) \\ &\qquad = -\mathbf{F}_j(t_1) + (t-t_1)\mathbf{f}_j^*\left(\tfrac{x}{t-t_1}\right) - \max_{0\le\tilde{t}_1\le\tilde{t}}\left\{-\mathbf{F}_j(\tilde{t}_1) + (\tilde{t}-\tilde{t}_1)\mathbf{f}_j^*\left(\tfrac{x}{\tilde{t}-\tilde{t}_1}\right)\right\} \\ &\qquad \overset{\tilde{t}_1=\tilde{t}-t+t_1}{\le} -\mathbf{F}_j(t_1) + (t-t_1)\mathbf{f}_j^*\left(\tfrac{x}{t-t_1}\right) + \mathbf{F}_j(\tilde{t}-t+t_1) - (t-t_1)\mathbf{f}_j^*\left(\tfrac{x}{t-t_1}\right) \\ &\qquad \le \|\mathbf{F}'_j\|_{\mathbf{L}^\infty((0,T))}|t-\tilde{t}|.\end{aligned}$$

By interchanging the terms where the maximum is attained we can show the same estimate in case of $\tilde{t} \leq t$. The same argumentation can also be used to obtain a lower bound and will be omitted. Applying Lemma 4.4.7, we obtain the claimed estimate.

For the Lipschitz-continuity w.r.t. $\mathbf{F}_j, \tilde{\mathbf{F}}_j$ we recall again that the solution formula for $\bar{\mathbf{V}}^{\text{out}}$ in Definition 4.4.3 only depends on $\mathbf{F}_j, \tilde{\mathbf{F}}_j$ in the second part of the maximum, so that we can only consider that part invoking Lemma 4.4.7. It yields then assuming that the first term takes its maximum at $t_1 \in [0,t]$

$$\begin{aligned}
&\bar{\mathbf{V}}_j^{\text{out}}[\mathbf{F}_j](t,0) - \bar{\mathbf{V}}_j^{\text{out}}[\tilde{\mathbf{F}}_j](t,0) \\
&\leq -\mathbf{F}_j(t_1) - (t-t_1)\mathbf{f}_j^{\max} - \max_{0\leq t_1\leq t}\left\{-\tilde{\mathbf{F}}_j(t_1) - (t-t_1)\mathbf{f}_j^{\max}\right\} \\
&\leq \tilde{\mathbf{F}}_j(t_1) - \mathbf{F}_j(t_1) \leq \|\tilde{\mathbf{F}}_j - \mathbf{F}_j\|_{C([0,t])}.
\end{aligned}$$

The lower bound can be obtained by exchanging roles and considering the point $\bar{t}_1 \in [0,t]$ where the second term takes its maximum.

2. The Lipschitz-estimate w.r.t. $\mathbf{h}, \tilde{\mathbf{h}}$ follows by standard arguments.

For the Lipschitz-continuity in space and time, first note that the first part of the maximum is Lipschitz-continuous on $(t,x) \in (0,T)\times\mathbb{R}_{\leq 0}$ as a direct consequence of [63], since it involves only the initial datum.

For the second part of the maximum, we detail the computations, following [94].

Suppose $x, \tilde{x} \in \mathbb{R}_{\leq 0}$ are given. Assuming that for $(t,x) \in [0,T]\times\mathbb{R}_{\leq 0}$ the maximum in $\mathbf{V}_i^{\text{in}}[\mathbf{h}_i](t,x)$ is attained for $(y,t_2,t_1) \in \mathbb{R}_{\leq 0}\times[0,t]^2$ with $t_1 \geq t_2$, we obtain

$$\begin{aligned}
&\bar{\mathbf{V}}_i^{\text{in}}[\mathbf{h}_i](t,x) - \bar{\mathbf{V}}_i^{\text{in}}[\mathbf{h}_i](t,\tilde{x}) \\
&= \bar{\mathbf{V}}_{0,i}^{\text{in}}(y) + t_2\mathbf{f}_i^*\left(\tfrac{-y}{t_2}\right) + (t-t_1)\mathbf{f}_i^*\left(\tfrac{x}{t-t_1}\right) - \int_{t_2}^{t_1}\mathbf{h}_i(s)\,\mathrm{d}s \\
&\quad - \max_{\substack{y\in\mathbb{R}_{\leq 0}\\ 0\leq t_2\leq t_1\leq \tilde{t}}}\left\{\mathbf{V}_{0,i}^{\text{in}}(y) + t_2\mathbf{f}_i^*\left(\tfrac{-y}{t_2}\right) + (t-t_1)\mathbf{f}_i^*\left(\tfrac{\tilde{x}}{t-t_1}\right) - \int_{t_2}^{t_1}\mathbf{h}_i(s)\,\mathrm{d}s\right\} \\
&\leq (t-t_1)\left(\mathbf{f}_i^*\left(\tfrac{x}{t-t_1}\right) - \mathbf{f}_i^*\left(\tfrac{\tilde{x}}{t-t_1}\right)\right) \\
&\leq (t-t_1)\boldsymbol{\rho}_i^{\max}\tfrac{1}{t-t_1}|x-\tilde{x}| = \boldsymbol{\rho}_i^{\max}|x-\tilde{x}|
\end{aligned}$$

by Lemma 4.4.1. The analogue argumentation can be used to obtain a lower bound with the same Lipschitz-constant by assuming that the second part actually takes its maximum at a given point (y,t_2,t_1) and estimating the first term from below.

For Lipschitz-continuity of the second part of the maximum w.r.t. the time variable suppose $t, \tilde{t} \in [0,T]$ be given. Then, we obtain for $t \geq \tilde{t}$ and $i \in \mathcal{I}$ by applying Lemma 4.4.4 with a concave flux function

$$\begin{aligned}
&\bar{\mathbf{V}}_i^{\text{in}}[\mathbf{h}_i](t,x) - \bar{\mathbf{V}}_i^{\text{in}}[\mathbf{h}_i](\tilde{t},x) \\
&\quad = \max_{\substack{y\in\mathbb{R}_{\leq 0}\\ \tilde{t}\leq t_2\leq t_1\leq t}}\left\{\mathbf{V}_i^{\text{in}}(\tilde{t},y) + t_2\mathbf{f}_i^*\left(\tfrac{-y}{t_2}\right) + (t-t_1)\mathbf{f}_i^*\left(\tfrac{x}{t-t_1}\right) - \int_{t_2}^{t_1}\mathbf{h}_i(s)\,\mathrm{d}s - \mathbf{V}_i^{\text{in}}(\tilde{t},x)\right\},
\end{aligned}$$

using the previous estimate for the spatial Lipschitz-continuity

$$\begin{aligned}
&\leq \max_{\substack{y\in\mathbb{R}_{\leq 0}\\ \tilde{t}\leq t_2\leq t_1\leq t}} \left\{ \boldsymbol{\rho}_i^{\max}|y-x| + t_2\mathbf{f}_i^*\left(\tfrac{-y}{t_2}\right) + (t-t_1)\mathbf{f}_i^*\left(\tfrac{x}{t-t_1}\right) - \int_{t_2}^{t_1}\mathbf{h}_i(s)\,\mathrm{d}s \right\} \\
&= \max_{\substack{y\in\mathbb{R}_{\leq 0}\\ \tilde{t}\leq t_2\leq t_1\leq t}} \left\{ \boldsymbol{\rho}_i^{\max}|y-x| + (t+t_2-t_1)\left(\tfrac{t_2}{t+t_2-t_1}\mathbf{f}_i^*\left(\tfrac{-y}{t_2}\right) + \tfrac{t-t_1}{t+t_2-t_1}\mathbf{f}_i^*\left(\tfrac{x}{t-t_1}\right)\right) \right. \\
&\qquad\qquad \left. - \int_{t_2}^{t_1}\mathbf{h}_i(s)\,\mathrm{d}s \right\},
\end{aligned} \tag{4.4.10}$$

using the concavity of $\mathbf{f}_i^*$ as stated in Lemma 4.4.1

$$\leq \max_{\substack{y\in\mathbb{R}_{\leq 0}\\ \tilde{t}\leq t_2\leq t_1\leq t}} \left\{ \boldsymbol{\rho}_i^{\max}|y-x| + (t+t_2-t_1)\mathbf{f}_i^*\left(\tfrac{x-y}{t+t_2-t_1}\right) - \int_{t_2}^{t_1}\mathbf{h}_i(s)\,\mathrm{d}s \right\},$$

substituting $z = \frac{x-y}{t+t_2-t_1}$

$$\leq \max_{\tilde{t}\leq t_2\leq t_1\leq t} \left\{ \max_{z\in\left[\frac{x}{t+t_2-t_1},\infty\right)} \left\{ (t+t_2-t_1)\left(\boldsymbol{\rho}_i^{\max}|z| + \mathbf{f}_i^*(z)\right) - \int_{t_2}^{t_1}\mathbf{h}_i(s)\,\mathrm{d}s \right\} \right\},$$

setting $\tilde{z} = -z$ and using the monotonicity of $\mathbf{f}_i^*$

$$\begin{aligned}
&\leq \max_{\tilde{t}\leq t_2\leq t_1\leq t} \left\{ \max_{\tilde{z}\in\left(-\infty,-\frac{x}{t+t_2-t_1}\right]} \left\{ (t+t_2-t_1)\left(\mathbf{f}_i^*(\tilde{z}) - \boldsymbol{\rho}_i^{\max}\tilde{z}\right) - \int_{t_2}^{t_1}\mathbf{h}_i(s)\,\mathrm{d}s \right\} \right\} \\
&\leq \max_{w\in[0,\boldsymbol{\rho}_i^{\max}]} \left\{ \max_{\substack{z\in\mathbb{R}\\ \tilde{t}\leq t_2\leq t_1\leq t}} \left\{ (t+t_2-t_1)\left(\mathbf{f}_i^*(z) - wz\right) - \int_{t_2}^{t_1}\mathbf{h}_i(s)\,\mathrm{d}s \right\} \right\} \\
&= \max_{w\in[0,\boldsymbol{\rho}_i^{\max}]} \left\{ -\min_{\substack{z\in\mathbb{R}\\ \tilde{t}\leq t_2\leq t_1\leq t}} \left\{ (t+t_2-t_1)\left(wz - \mathbf{f}_i^*(z)\right) + \int_{t_2}^{t_1}\mathbf{h}_i(s)\,\mathrm{d}s \right\} \right\},
\end{aligned} \tag{4.4.11}$$

using Lemma 4.4.1, stating that $\mathbf{f}^{**} \equiv \mathbf{f}$

$$\leq \|\mathbf{h}_i\|_{C([0,T])}|t-\tilde{t}|.$$

For the lower bound, we recall that $x \in \mathbb{R}_{\leq 0}$ and estimate assuming that for $(\tilde{t}, x) \in$

$(0,t)\times\mathbb{R}_{\leq 0}$ the minimum is attained at $(\tilde{y},\tilde{t}_1,\tilde{t}_2)$

$$\begin{aligned}
&\bar{\mathbf{V}}_i^{\text{in}}[\mathbf{h}_i](\tilde{t},x)-\bar{\mathbf{V}}_i^{\text{in}}[\mathbf{h}_i](t,x)\\
&=\mathbf{V}_{0,i}^{\text{in}}(\tilde{y})+\tilde{t}_2\mathbf{f}_i^*\left(\tfrac{-\tilde{y}}{\tilde{t}_2}\right)+(\tilde{t}-\tilde{t}_1)\mathbf{f}_i^*\left(\tfrac{x}{\tilde{t}-\tilde{t}_1}\right)-\int_{\tilde{t}_2}^{\tilde{t}_1}\mathbf{h}_i(s)\,\mathrm{d}s\\
&\quad-\max_{\substack{y\in\mathbb{R}_{\leq 0}\\0\leq t_2\leq t_1\leq t}}\left\{\mathbf{V}_{0,i}^{\text{in}}(y)+t_2\mathbf{f}_i^*\left(\tfrac{-y}{t_2}\right)+(t-t_1)\mathbf{f}_i^*\left(\tfrac{x}{t-t_1}\right)-\int_{t_2}^{t_1}\mathbf{h}_i(s)\,\mathrm{d}s\right\},
\end{aligned}$$

setting $y=\tilde{y},\ t_2=\tilde{t_2},\ t_1=t-\tilde{t}+\tilde{t}_1$

$$\leq\int_{\tilde{t}_1}^{t-\tilde{t}+\tilde{t}_1}\mathbf{h}_i(s)\,\mathrm{d}s\leq\|\mathbf{h}_i\|_{C([0,t])}|t-\tilde{t}|.$$

Due to the previously deduced Lipschitz-estimate which guarantees the differentiability of $\bar{\mathbf{V}}^{\text{in}}$ w.r.t. space and time, it suffices to show Inequality (4.4.9) to prove that $t\mapsto\bar{\mathbf{V}}^{\text{in}}(t,0)$ is monotonically decreasing. However, this has already been carried out in Equation (4.4.11) as long as $\mathbf{h}_i$ is nonnegative (which is always the case for the considered fixed-point equation). This concludes the proof.

□

Proposition 4.4.9 (Lipschitz-continuity of the mappings)**.** *For the mappings in Definition 4.4.3 we obtain the following Lipschitz-bounds when measuring in the uniform topology and also when considering them as operators.*

1. *For* $\mathbf{h}$ *as in Equation* (4.4.1) *with* $\mathbf{q},\tilde{\mathbf{q}}\in\mathrm{Lip}\left([0,T];\mathbb{R}^{|\mathcal{O}|}\right)$ *we obtain for every* $i\in\mathcal{I}$

$$\left|\mathbf{h}_i[\mathbf{q}](t)-\mathbf{h}_i[\mathbf{q}](\tilde{t})\right|\leq\|\mathbf{c}_i\|_{\mathbf{L}^\infty((0,T))}\sum_{j\in\mathcal{O}}\|\mathbf{q}_j'\|_{\mathbf{L}^\infty((0,T))}|t-\tilde{t}|\qquad\forall t,\tilde{t}\in[0,T],\tag{4.4.12}$$

$$|\mathbf{h}_i[\mathbf{q}](t)-\mathbf{h}_i[\tilde{\mathbf{q}}](t)|\leq\|\mathbf{c}_i\|_{\mathbf{L}^\infty((0,t))}\sum_{j\in\mathcal{O}}|\mathbf{q}_j(t)-\tilde{\mathbf{q}}_j(t)|\qquad\forall t\in(0,T].\tag{4.4.13}$$

2. *For* $\mathbf{F}$ *as in Equation* (4.4.4) *with* $\mathbf{V},\tilde{\mathbf{V}}\in\mathrm{Lip}\left([0,T];\mathbb{R}^{|\mathcal{I}|}\right)$ *we obtain for* $j\in\mathcal{O}$

$$\left|\mathbf{F}_j[\mathbf{V}](t)-\mathbf{F}_j[\mathbf{V}](\tilde{t})\right|\leq\sum_{i\in\mathcal{I}}\left\|\tfrac{\mathrm{d}}{\mathrm{d}t}\mathbf{V}_i\right\|_{\mathbf{L}^\infty((0,T))}|t-\tilde{t}|\qquad\forall t,\tilde{t}\in[0,T],\tag{4.4.14}$$

$$\|\mathbf{F}_j[\mathbf{V}]-\mathbf{F}_j[\tilde{\mathbf{V}}]\|_{C([0,t])}\leq\sum_{i\in\mathcal{I}}(\|\boldsymbol{\theta}_{i,j}\|_{TV((0,t))}+1)\|\mathbf{V}_i-\tilde{\mathbf{V}}_i\|_{C([0,t])}\quad\forall t\in(0,T].\tag{4.4.15}$$

3. *For* $\mathbf{V}^{\text{out}}$ *as in Equation* (4.4.6) *let* $\mathbf{F},\tilde{\mathbf{F}}\in\mathrm{Lip}\left([0,T];\mathbb{R}^{|\mathcal{O}|}\right)$*. Then, we obtain for* $j\in\mathcal{O}$

$$\left|\mathbf{V}_j^{\text{out}}[\mathbf{F}_j](t)-\mathbf{V}_j^{\text{out}}[\mathbf{F}_j](\tilde{t})\right|\leq\left\{\|\mathbf{F}_j'\|_{\mathbf{L}^\infty((0,T))},\mathbf{f}_j^{\max}\right\}|t-\tilde{t}|\qquad\forall t,\tilde{t}\in[0,T],\tag{4.4.16}$$

$$\left\|\mathbf{V}_j^{\text{out}}[\mathbf{F}_j]-\mathbf{V}_j^{\text{out}}[\tilde{\mathbf{F}}_j]\right\|_{C([0,t])}\leq\left\|\mathbf{F}_j-\tilde{\mathbf{F}}_j\right\|_{C([0,t])}\qquad\forall t\in(0,T].\tag{4.4.17}$$

4. For $\mathbf{\Lambda}$ *as in Equation* (4.4.7) *let* $(\mathbf{F}, \mathbf{V}^{\text{out}}), (\tilde{\mathbf{F}}, \tilde{\mathbf{V}^{\text{out}}}) \in \text{Lip}\left([0,T];\mathbb{R}^{|\mathcal{O}|}\right) \times \text{Lip}\left([0,T];\mathbb{R}^{|\mathcal{O}|}\right)$ *be given. Then, we have for* $j \in \mathcal{O}$ *and* $\forall t, \tilde{t} \in [0,T]$

$$\left|\mathbf{\Lambda}_j[\mathbf{F}, \mathbf{V}^{\text{out}}](t) - \mathbf{\Lambda}_j[\mathbf{F}, \mathbf{V}^{\text{out}}](\tilde{t})\right| \leq \left(\|\mathbf{F}_j'\|_{\mathbf{L}^\infty((0,T))} + \left\|\tfrac{\mathrm{d}}{\mathrm{d}t}\mathbf{V}_j^{\text{out}}\right\|_{\mathbf{L}^\infty((0,T))}\right)|t-\tilde{t}|, \tag{4.4.18}$$

$$\left\|\mathbf{\Lambda}_j[\mathbf{F}, \mathbf{V}^{\text{out}}] - \mathbf{\Lambda}_j[\tilde{\mathbf{F}}, \tilde{\mathbf{V}}^{\text{out}}]\right\|_{C([0,t])} \leq \left\|\mathbf{F}_j - \tilde{\mathbf{F}}_j\right\|_{C([0,t])} + \|\mathbf{V}_j^{\text{out}} - \tilde{\mathbf{V}}_j^{\text{out}}\|_{C([0,t])}. \tag{4.4.19}$$

5. For $\mathbf{V}^{\text{in}}$ *as in Equation* (4.4.3) *and* $\mathbf{h}, \tilde{\mathbf{h}} \in \text{Lip}\left([0,T];\mathbb{R}^{\mathcal{I}}\right)$ *we obtain*

$$\left|\mathbf{V}_i^{\text{in}}[\mathbf{h}_i](t) - \mathbf{V}_i^{\text{in}}[\mathbf{h}_i](\tilde{t})\right| \leq \max\left\{\|\mathbf{h}_i\|_{C([0,T])}, \mathbf{f}_i^{\max}\right\}|t-\tilde{t}| \quad \forall t, \tilde{t} \in [0,T], \tag{4.4.20}$$

$$\left\|\mathbf{V}_i^{\text{in}}[\mathbf{h}_i] - \mathbf{V}_i^{\text{in}}[\tilde{\mathbf{h}_i}]\right\|_{C([0,t])} \leq \|\mathbf{h}_i - \tilde{\mathbf{h}}_i\|_{\mathbf{L}^1((0,t))} \quad \forall t \in (0,T]. \tag{4.4.21}$$

Proof. 1. We apply Lemma 4.4.7 and have, since $\mathbf{f}_i^{\max}$ is a constant function,

$$\left|\mathbf{h}_i[\mathbf{q}](t) - \mathbf{h}_i[\mathbf{q}](\tilde{t})\right| \leq \|\mathbf{c}_i\|_{\mathbf{L}^\infty((0,T))} \sum_{j\in\mathcal{O}} \|\mathbf{q}_j'\|_{\mathbf{L}^\infty((0,T))}|t-\tilde{t}|.$$

For the second inequality, we first assume that $\mathbf{f}_i^{\max} \geq \mathbf{c}_i(t)\Big(M - \sum_{j\in\mathcal{O}} \tilde{\mathbf{q}}_j(t)\Big)$ for $t \in [0,T]$ given. Then, we obtain

$$\begin{aligned}\mathbf{h}_i[\mathbf{q}](t) - \mathbf{h}_i[\tilde{\mathbf{q}}](t) &= \min\left\{\mathbf{f}_i^{\max}, \mathbf{c}_i(t)\Big(M - \sum_{j\in\mathcal{O}} \mathbf{q}_j(t)\Big)\right\} - \mathbf{c}_i(t)\Big(M - \sum_{j\in\mathcal{O}} \tilde{\mathbf{q}}_j(t)\Big) \\ &\leq |\mathbf{c}_i(t)| \sum_{j\in\mathcal{O}} |\mathbf{q}_j(t) - \tilde{\mathbf{q}}_j(t)|.\end{aligned}$$

For $\mathbf{f}_i^{\max} \leq \mathbf{c}_i(t)\Big(M - \sum_{j\in\mathcal{O}} \tilde{\mathbf{q}}_j(t)\Big)$ we obtain

$$\begin{aligned}&\mathbf{h}_i[\mathbf{q}](t) - \mathbf{h}_i[\tilde{\mathbf{q}}](t) \\ &= \min\left\{\mathbf{f}_i^{\max}, \mathbf{c}_i(t)\Big(M - \sum_{j\in\mathcal{O}} \mathbf{q}_j(t)\Big)\right\} - \mathbf{f}_i^{\max} \leq 0 \leq |\mathbf{c}_i(t)| \sum_{j\in\mathcal{O}} |\mathbf{q}_j(t) - \tilde{\mathbf{q}}_j(t)|.\end{aligned}$$

The lower bound can be obtained by exchanging $\mathbf{h}_i[\mathbf{q}]$ with $\mathbf{h}_i[\tilde{\mathbf{q}}]$ and applying the same reasoning.

2. We estimate directly the formula for $\mathbf{F}$ and recall the uniform bound on $\boldsymbol{\theta}$ in Equation (4.3.1)

$$\begin{aligned}\left|\mathbf{F}_j[\mathbf{V}](t) - \mathbf{F}_j[\mathbf{V}](\tilde{t})\right| &= \left|\sum_{i\in\mathcal{I}} \int_0^t \tfrac{\mathrm{d}}{\mathrm{d}s}\mathbf{V}_i(s)\boldsymbol{\theta}_{i,j}(s)\,\mathrm{d}s - \int_0^{\tilde{t}} \tfrac{\mathrm{d}}{\mathrm{d}s}\mathbf{V}_i(s)\boldsymbol{\theta}_{i,j}(s)\,\mathrm{d}s\right| \\ &\leq \sum_{i\in\mathcal{I}} \left|\int_t^{\tilde{t}} \tfrac{\mathrm{d}}{\mathrm{d}s}\mathbf{V}_i(s)\boldsymbol{\theta}_{i,j}(s)\,\mathrm{d}s\right| \leq \sum_{i\in\mathcal{I}} |t-\tilde{t}|\left\|\tfrac{\mathrm{d}}{\mathrm{d}s}\mathbf{V}_i\right\|_{C([0,\max t,\tilde{t}])}.\end{aligned}$$

For the second estimate we require an integration by parts formula for functions of BV functions so that we have

$$\begin{aligned}
&\left|\mathbf{F}_j[\mathbf{V}](t) - \mathbf{F}_j[\tilde{\mathbf{V}}](t)\right| \\
&= \left|\sum_{i\in\mathcal{I}} \int_0^t \tfrac{\mathrm{d}}{\mathrm{d}s}\left(\mathbf{V}_i(s) - \tilde{\mathbf{V}}_i(s)\right)\boldsymbol{\theta}_{i,j}(s)\,\mathrm{d}s\right| \\
&= \sum_{i\in\mathcal{I}}\left|-\int_0^t \left(\mathbf{V}_i(s) - \tilde{\mathbf{V}}_i(s)\right)\mathrm{d}\boldsymbol{\theta}'_{i,j}(s) + \boldsymbol{\theta}_{i,j}(t)\Big(\mathbf{V}_i(t) - \tilde{\mathbf{V}}_i(t)\Big) - \boldsymbol{\theta}_{i,j}(0)\Big(\mathbf{V}_i(0) - \tilde{\mathbf{V}}_i(0)\Big)\right| \\
&\leq \sum_{i\in\mathcal{I}}\left(\|\mathbf{V}_i - \tilde{\mathbf{V}}_i\|_{C([0,t])}\|\boldsymbol{\theta}_{i,j}\|_{TV((0,t))} + \|\mathbf{V}_i - \tilde{\mathbf{V}}_i\|_{C([0,t])}\right).
\end{aligned}$$

3. See Lemma 4.4.8 as this directly follows when reconsidering $\bar{\mathbf{V}}^{\mathrm{out}}(\cdot,0) \equiv \mathbf{V}^{\mathrm{out}}$ as stated in Definition 4.4.3.
4. This follows directly by the linearity of the operator $\boldsymbol{\Lambda}$.
5. See Lemma 4.4.8 as this directly follows when reconsidering $\bar{\mathbf{V}}^{\mathrm{in}}(\cdot,0) \equiv \mathbf{V}^{\mathrm{in}}$ as stated in Definition 4.4.3.

□

Corollary 4.4.10 (Well-posedness of the fixed-point mapping Lemma 4.4.6)**.** *The mapping*

$$\boldsymbol{\mathfrak{G}} \coloneqq \boldsymbol{\Lambda} \circ (\mathbf{F} \circ \mathbf{V}^{\mathrm{in}} \circ \mathbf{h} \circ \cdot, \mathbf{V}^{\mathrm{out}} \circ \mathbf{F} \circ \mathbf{V}^{\mathrm{in}} \circ \mathbf{h} \circ \cdot) : \mathrm{Lip}\left([0,T];\mathbb{R}^{|\mathcal{O}|}\right) \to \mathrm{Lip}\left([0,T];\mathbb{R}^{|\mathcal{O}|}\right)$$

explicitly given in Definition 4.4.3 is well-defined.

Proof. This is a direct consequence of Proposition 4.4.9, particularly Inequalities (4.4.12), (4.4.14), (4.4.16), (4.4.18) and (4.4.20). □

4.4.4 Existence and uniqueness of solutions

Now that we have detailed the necessary estimates on the mappings in Section 4.4.3, we now detail the fixed-point problem describing the dynamics at the intersections and prove existence and uniqueness of solutions in the proper topological setup.

Theorem 4.4.11 (Existence and uniqueness of a fixed-point)**.** *Let $T \in \mathbb{R}_{>0}$ be given, the fixed-point problem*

$$\boldsymbol{\mathfrak{G}}[\mathbf{q}] = \mathbf{q} \qquad \text{in } \boldsymbol{\Omega}_T$$

as defined in Lemma 4.4.6 has a unique solution with

$$\boldsymbol{\Omega}_T \coloneqq \left\{\mathbf{q} \in \mathrm{Lip}\left([0,T];\mathbb{R}^{|\mathcal{O}|}_{\geq 0}\right) : \ \left\|\mathbf{q}'_j\right\|_{\mathbf{L}^\infty((0,T))} \leq 2\max\left\{\sum_{i\in\mathcal{I}} \mathbf{f}_i^{\max}, \mathbf{f}_j^{\max}\right\} \forall j \in \mathcal{O}\right\}. \tag{4.4.22}$$

Proof. As mentioned before, we only prove the **Single-Buffer/Multi-Queues** case in Definition 4.3.1. Pick $T^* \in [0,T]$ and $\mathbf{q} \in \mathbf{\Omega}_{T^*}$. We first show that $\mathfrak{G}[\mathbf{\Omega}_{T^*}] \subseteq \mathbf{\Omega}_{T^*}$, *i.e.* $\mathfrak{G}[\mathbf{q}]$ is a self-mapping. By the previous well-posedness of the fixed-point mapping in Corollary 4.4.10 it is sufficient to show that the weak derivative of $\mathfrak{G}$ satisfies the postulated bounds. Recalling the definition of $\mathfrak{G}$ in Lemma 4.4.6 we thus obtain for $j \in \mathcal{O}$ and $t \in [0,T^*]$ a.e.

$$\left|\tfrac{\mathrm{d}}{\mathrm{d}t}\mathfrak{G}_j[\mathbf{q}](t)\right| = \left|\tfrac{\mathrm{d}}{\mathrm{d}t}\mathbf{\Lambda}_j\left[\mathbf{F}\circ\mathbf{V}^{\mathrm{in}}\circ\mathbf{h}\circ\mathbf{q}, \mathbf{V}^{\mathrm{out}}\circ\mathbf{F}\circ\mathbf{V}^{\mathrm{in}}\circ\mathbf{h}\circ\mathbf{q}\right](t)\right|,$$

applying Inequality (4.4.18)

$$\leq \left(\left\|\tfrac{\mathrm{d}}{\mathrm{d}t}\mathbf{F}_j\left[\mathbf{V}^{\mathrm{in}}\circ\mathbf{h}\circ\mathbf{q}\right]\right\|_{\mathbf{L}^\infty((0,T))} + \left\|\tfrac{\mathrm{d}}{\mathrm{d}t}\mathbf{V}_j^{\mathrm{out}}\left[\mathbf{F}\circ\mathbf{V}^{\mathrm{in}}\circ\mathbf{h}\circ\mathbf{q}\right]\right\|_{\mathbf{L}^\infty((0,T))}\right),$$

applying Inequality (4.4.16)

$$\leq 2\max\left\{\left\|\tfrac{\mathrm{d}}{\mathrm{d}t}\mathbf{F}_j\left[\mathbf{V}^{\mathrm{in}}\circ\mathbf{h}\circ\mathbf{q}\right]\right\|_{\mathbf{L}^\infty((0,T))}, \mathbf{f}_j^{\max}\right\},$$

applying Inequality (4.4.14)

$$\leq 2\max\left\{\sum_{i\in\mathcal{I}}\left\|\tfrac{\mathrm{d}}{\mathrm{d}t}\mathbf{V}_i^{\mathrm{in}}\left[\mathbf{h}\circ\mathbf{q}\right]\right\|_{\mathbf{L}^\infty((0,T))}, \mathbf{f}_j^{\max}\right\},$$

applying Inequality (4.4.20) and the uniform bound on $\boldsymbol{\theta}$ as in Equation (4.3.1)

$$\leq 2\max\left\{\sum_{i\in\mathcal{I}}\max\left\{\left\|\mathbf{h}_i\left[\mathbf{q}\right]\right\|_{\mathbf{L}^\infty((0,T))}, \mathbf{f}_i^{\max}\right\}, \mathbf{f}_j^{\max}\right\},$$

applying the definition of $\mathbf{h}$ in Definition 4.4.3

$$\begin{aligned}
&\leq 2\max\left\{\sum_{i\in\mathcal{I}}\max\left\{\mathbf{f}_i^{\max}, \min\left\{\mathbf{f}_i^{\max},\right.\right.\right.\\
&\qquad\qquad\left.\left.\left.\|\mathbf{c}_i\|_{\mathbf{L}^\infty((0,T))}\left\|M-\textstyle\sum_{j\in J}\mathbf{q}_j\right\|_{C([0,T])}\right\}\right\}, \mathbf{f}_j^{\max}\right\}\\
&\leq 2\max\left\{\sum_{i\in\mathcal{I}}\mathbf{f}_i^{\max}, \mathbf{f}_j^{\max}\right\}.
\end{aligned}$$

For the positivity, we pick again $j \in \mathcal{O}$ and $t \in [0,T]$ and estimate for $\mathbf{q} \in \mathbf{\Omega}_{T^*}$ applying Definition 4.4.3

$$\begin{aligned}
\mathfrak{G}_j[\mathbf{q}](t) &= \mathbf{\Lambda}_j\left[\mathbf{F}\circ\mathbf{V}^{\mathrm{in}}\circ\mathbf{h}\circ\mathbf{q}, \mathbf{V}^{\mathrm{out}}\circ\mathbf{F}\circ\mathbf{V}^{\mathrm{in}}\circ\mathbf{h}\circ\mathbf{q}\right](t)\\
&= \mathbf{F}_j\left[\mathbf{V}^{\mathrm{in}}\circ\mathbf{h}\circ\mathbf{q}\right](t) + \mathbf{V}_j^{\mathrm{out}}\left[\mathbf{F}\circ\mathbf{V}^{\mathrm{in}}\circ\mathbf{h}\circ\mathbf{q}\right](t),
\end{aligned}$$

applying Definition 4.4.3

$$\geq \mathbf{F}_j\big[\mathbf{V}^{\text{in}} \circ \mathbf{h} \circ \mathbf{q}\big](t) + \max_{0\leq t_1\leq t} \big\{-\mathbf{F}_j\big[\mathbf{V}^{\text{in}} \circ \mathbf{h} \circ \mathbf{q}\big](t_1) - (t-t_1)\mathbf{f}_j^{\max}\big\} \geq 0$$

by choosing $t_1 = t$. This is true for any time $t \in [0,T]$ and every $j \in \mathcal{O}$ so that we obtain the lower bound.

As a next step we will show that the fixed-point mapping $\mathfrak{G}$ is a contraction in $\mathbf{\Omega}_t$ as defined in Equation (4.4.22) for sufficiently small time horizon in the uniform topology. Thus, let $\mathbf{q}, \tilde{\mathbf{q}} \in \mathbf{\Omega}_{T^*}$ be given as well as $t \in [0,T]$. Then, we obtain by applying the fixed-point equation in Lemma 4.4.6 for $j \in \mathcal{O}$

$$\begin{aligned}
&|\mathfrak{G}_j[\mathbf{q}](t) - \mathfrak{G}_j[\tilde{\mathbf{q}}](t)| \\
&\leq \Big|\mathbf{\Lambda}_j\big[\mathbf{F} \circ \mathbf{V}^{\text{in}} \circ \mathbf{h} \circ \mathbf{q}, \mathbf{V}^{\text{out}} \circ \mathbf{F} \circ \mathbf{V}^{\text{in}} \circ \mathbf{h} \circ \mathbf{q}\big](t) \\
&\qquad - \mathbf{\Lambda}_j\big[\mathbf{F} \circ \mathbf{V}^{\text{in}} \circ \mathbf{h} \circ \tilde{\mathbf{q}}, \mathbf{V}^{\text{out}} \circ \mathbf{F}_j \circ \mathbf{V}^{\text{in}} \circ \mathbf{h} \circ \tilde{\mathbf{q}}\big](t)\Big|,
\end{aligned}$$

applying Definition 4.4.3 and Inequality (4.4.19)

$$\begin{aligned}
&\leq \big|\mathbf{F}_j\big[\mathbf{V}^{\text{in}} \circ \mathbf{h} \circ \mathbf{q}\big](t) - \mathbf{F}_j\big[\mathbf{V}^{\text{in}} \circ \mathbf{h} \circ \tilde{\mathbf{q}}\big](t)\big| \\
&\qquad + \big|\mathbf{V}_j^{\text{out}}\big[\mathbf{F} \circ \mathbf{V}^{\text{in}} \circ \mathbf{h} \circ \mathbf{q}\big](t) - \mathbf{V}_j^{\text{out}}\big[\mathbf{F} \circ \mathbf{V}^{\text{in}} \circ \mathbf{h} \circ \tilde{\mathbf{q}}\big](t)\big|,
\end{aligned}$$

applying Definition 4.4.3 and Inequality (4.4.17)

$$\begin{aligned}
&\leq \big|\mathbf{F}_j\big[\mathbf{V}^{\text{in}} \circ \mathbf{h} \circ \mathbf{q}\big](t) - \mathbf{F}_j\big[\mathbf{V}^{\text{in}} \circ \mathbf{h} \circ \tilde{\mathbf{q}}\big](t)\big| + \big\|\mathbf{F}_j\big[\mathbf{V}^{\text{in}} \circ \mathbf{h} \circ \mathbf{q}\big] - \mathbf{F}_j\big[\mathbf{V}^{\text{in}} \circ \mathbf{h} \circ \tilde{\mathbf{q}}\big]\big\|_{C([0,t])} \\
&\leq 2\big\|\mathbf{F}_j\big[\mathbf{V}^{\text{in}} \circ \mathbf{h} \circ \mathbf{q}\big] - \mathbf{F}_j\big[\mathbf{V}^{\text{in}} \circ \mathbf{h} \circ \tilde{\mathbf{q}}\big]\big\|_{C([0,t])},
\end{aligned}$$

applying Definition 4.4.3 and Inequality (4.4.15)

$$\leq 2\sum_{i\in\mathcal{I}} \big(|\boldsymbol{\theta}_{i,j}|_{TV((0,t))} + 1\big)\big\|\mathbf{V}_i^{\text{in}}\big[\mathbf{h} \circ \mathbf{q}\big] - \mathbf{V}_i^{\text{in}}\big[\mathbf{h} \circ \tilde{\mathbf{q}}\big]\big\|_{C([0,t])},$$

applying Definition 4.4.3 and Inequality (4.4.21)

$$\leq 2\sum_{i\in\mathcal{I}} \big(|\boldsymbol{\theta}_{i,j}|_{TV((0,t))} + 1\big)\big\|\mathbf{h}_i\big[\mathbf{q}\big] - \mathbf{h}_i\big[\tilde{\mathbf{q}}\big]\big\|_{\mathbf{L}^1((0,t))},$$

applying Definition 4.4.3 and Inequality (4.4.13) as well as Hölder's inequality to estimate the $\mathbf{L}^1$ norm

$$\leq 2t\sum_{i\in\mathcal{I}} \big(|\boldsymbol{\theta}_{i,j}|_{TV((0,t))} + 1\big)\|\mathbf{c}_i\|_{\mathbf{L}^\infty((0,T))}\sum_{j\in\mathcal{O}}\|\mathbf{q}_j - \tilde{\mathbf{q}}_j\|_{C([0,t])}.$$

Since the presented estimate is uniform in t, we can sum over $j \in \mathcal{O}$ and obtain

$$\begin{aligned}
&\sum_{j\in\mathcal{O}} \|\mathfrak{G}_j[\mathbf{q}] - \mathfrak{G}_j[\tilde{\mathbf{q}}]\|_{C([0,t])} \\
&\leq 2t\|\mathbf{c}\|_{\mathbf{L}^\infty((0,T);\mathbb{R}^{|\mathcal{I}|})}\left(\sum_{(i,j)\in\mathcal{I}\times\mathcal{O}} \big(|\boldsymbol{\theta}_{i,j}|_{TV((0,T))} + 1\big)\right)\sum_{j\in\mathcal{O}}\|\mathbf{q}_j - \tilde{\mathbf{q}}_j\|_{C([0,t])}.
\end{aligned}$$

Thus, picking $T^* \in (0, T]$ such that

$$T^* := \frac{1}{4\|\mathbf{c}\|_{\mathbf{L}^\infty((0,T);\mathbb{R}^{|\mathcal{I}|})}\left(\sum_{(i,j)\in\mathcal{I}\times\mathcal{O}}\left(|\boldsymbol{\theta}_{i,j}|_{TV((0,T))}+1\right)\right)} > 0$$

it yields

$$\sum_{j\in\mathcal{O}} \|\mathfrak{G}_j[\mathbf{q}] - \mathfrak{G}_j[\tilde{\mathbf{q}}]\|_{C([0,T^*])} \leq \tfrac{1}{2}\sum_{j\in\mathcal{O}} \|\mathbf{q}_j - \tilde{\mathbf{q}}_j\|_{C([0,T^*])},$$

so that $\mathfrak{G}$ is a self-mapping and a contraction on $\boldsymbol{\Omega}_{T^*}$. Since $\boldsymbol{\Omega}_{T^*}$ is closed in the uniform topology, we can apply Banach's fixed-point theorem [145, Theorem 1.A] and obtain a unique solution of the fixed-point problem stated in Lemma 4.4.6.

The assumption in T^* being sufficiently small is not restrictive. Due to the semigroup property of the dynamical system we can restart the fixed-point problem at time $t = T^*$ with new initial queues, and initial and boundary datum on incoming and outgoing edges. However, as neither the self-mapping property nor the contraction depend on those data, we can apply the same reasoning as above to extend the solution to the time horizon $[0, 2T^*]$. This can be iterated up to the final time T. □

Lemma 4.4.12 ($\mathbf{q}$ respecting the size M of the buffer)**.** *The unique fixed-point $\mathbf{q}^* \in \boldsymbol{\Omega}_T$ of the fixed-point mappings stated in Lemma 4.4.6 and Theorem 4.4.11 satisfies for every $t \in [0, T]$*

$$0 \leq \sum_{j\in\mathcal{O}} \mathbf{q}_j^*(t) \leq M.$$

Proof. The lower bound has already been shown in the proof of Theorem 4.4.11. Next, we will provide the upper bound. For that, we use an argument based on Gronwall's Lemma and perform it for $j \in \mathcal{O}$ and $t \in [0, T]$ by recalling that $\mathbf{q}^*$ is the unique solution of the fixed-point equation in Lemma 4.4.6, guaranteed by Theorem 4.4.11

$$\mathbf{q}_j^*(t) = \mathfrak{G}_j[\mathbf{q}^*](t),$$

applying Lemma 4.4.6

$$= \mathbf{F}_j\left[\mathbf{V}^{\text{in}} \circ \mathbf{h} \circ \mathbf{q}^*\right](t) + \mathbf{V}_j^{\text{out}}\left[\mathbf{F}_j \circ \mathbf{V}^{\text{in}} \circ \mathbf{h} \circ \mathbf{q}^*\right](t),$$

applying Definition 4.4.3

$$= \mathbf{F}_j\left[\mathbf{V}^{\text{in}} \circ \mathbf{h} \circ \mathbf{q}^*\right](t) + \max_{t_1\in[0,t]}\left\{-\mathbf{F}_j\left[\mathbf{V}^{\text{in}} \circ \mathbf{h} \circ \mathbf{q}^*\right](t_1) - (t-t_1)\mathbf{f}_j^{\max}\right\},$$

applying that $\mathbf{F}_j \geq 0$ due to Definition 4.4.3 and Inequality (4.4.9)

$$\leq \mathbf{F}_j\left[\mathbf{V}^{\text{in}} \circ \mathbf{h} \circ \mathbf{q}^*\right](t),$$

applying Definition 4.4.3

$$\leq \mathbf{q}_{0,j} - \sum_{i\in\mathcal{I}} \int_0^t \tfrac{\mathrm{d}}{\mathrm{d}s}\mathbf{V}_i^{\text{in}}[\mathbf{h} \circ \mathbf{q}^*](s)\boldsymbol{\theta}_{i,j}(s)\,\mathrm{d}s.$$

Summarizing w.r.t. $j \in \mathcal{O}$ we obtain then

$$\sum_{j\in\mathcal{O}} \mathbf{q}_j^*(t) \leq \sum_{j\in\mathcal{O}} \mathbf{q}_{0,j} - \sum_{i\in\mathcal{I}} \int_0^t \tfrac{\mathrm{d}}{\mathrm{d}s} \mathbf{V}_i^{\mathrm{in}}[\mathbf{h}\circ\mathbf{q}^*](s)\,\mathrm{d}s \sum_{j\in\mathcal{O}} \boldsymbol{\theta}_{i,j}(s)\,\mathrm{d}s,$$

using Equation (4.3.1)

$$\begin{aligned}
&= \sum_{j\in\mathcal{O}} \mathbf{q}_{0,j} - \sum_{i\in\mathcal{I}} \int_0^t \tfrac{\mathrm{d}}{\mathrm{d}s} \mathbf{V}_i^{\mathrm{in}}[\mathbf{h}\circ\mathbf{q}^*](s)\,\mathrm{d}s \\
&= \sum_{j\in\mathcal{O}} \mathbf{q}_{0,j} - \sum_{i\in\mathcal{I}} \mathbf{V}_i^{\mathrm{in}}[\mathbf{h}\circ\mathbf{q}^*](t) + \sum_{i\in\mathcal{I}} \mathbf{V}_i^{\mathrm{in}}[\mathbf{h}\circ\mathbf{q}^*](0),
\end{aligned}$$

using Definition 4.4.2 and Definition 4.4.3

$$\begin{aligned}
&= \sum_{j\in\mathcal{O}} \mathbf{q}_{0,j} + \sum_{i\in\mathcal{I}} \mathbf{V}_i^{\mathrm{in}}(0) \\
&\quad - \sum_{i\in\mathcal{I}} \max_{\substack{y\in\mathbb{R}_{\leq 0}\\ 0\leq t_2\leq t_1\leq t}} \left\{ \mathbf{V}_i^{\mathrm{in}}(y) + t_2 \mathbf{f}_i^*(\tfrac{y}{t_2}) - (t-t_1)\mathbf{f}_i^{\max} - \int_{t_2}^{t_1} (\mathbf{h}\circ\mathbf{q})_i(s)\,\mathrm{d}s \right\} \\
&\leq \sum_{j\in\mathcal{O}} \mathbf{q}_{0,j} + \sum_{i\in\mathcal{I}} \mathbf{V}_i^{\mathrm{in}}(0) \\
&\quad - \sum_{i\in\mathcal{I}} \max_{0\leq t_2\leq t_1\leq t} \left\{ \mathbf{V}_i^{\mathrm{in}}(0) - (t+t_2-t_1)\mathbf{f}_i^{\max} - \int_{t_2}^{t_1} (\mathbf{h}\circ\mathbf{q})_i(s)\,\mathrm{d}s \right\},
\end{aligned}$$

choosing $t_2 = 0$ and $t_1 = t$

$$\leq \sum_{j\in\mathcal{O}} \mathbf{q}_{0,j} + \sum_{i\in\mathcal{I}} \int_0^t \mathbf{h}_i[\mathbf{q}^*](s)\,\mathrm{d}s,$$

using Definition 4.4.3

$$\begin{aligned}
&\leq \sum_{j\in\mathcal{O}} \mathbf{q}_{0,j} + \sum_{i\in\mathcal{I}} \int_0^t \min\left\{ \mathbf{f}_i^{\max}, \mathbf{c}_i(s)\Big(M - \sum_{j\in\mathcal{O}} \mathbf{q}_j^*(s)\Big) \right\} \mathrm{d}s \\
&\leq \sum_{j\in\mathcal{O}} \mathbf{q}_{0,j} + \sum_{i\in\mathcal{I}} \|\mathbf{c}_i\|_{\mathbf{L}^\infty((0,t))} \left(Mt - \int_0^t \sum_{j\in\mathcal{O}} \mathbf{q}_j^*(s)\,\mathrm{d}s \right).
\end{aligned}$$

We assume that there exists t_0 such that $\sum_{j\in\mathcal{O}} \mathbf{q}_j^*(t_0) > M$. Then, due to the continuity of $\mathbf{q}_j^*$ there exists a $t_* \in [0, t_0)$ such that $\sum_{j\in\mathcal{O}} \mathbf{q}_j^*(t_*) = M$ and $\sum_{j\in\mathcal{O}} \mathbf{q}_j^*(t) > M$ for any $t \in (t_*, t_0)$. Integrating $\sum_{j\in\mathcal{O}} \mathbf{q}_j^*(\cdot)$ between t_* and t_0 yields

$$\int_{t_*}^t \sum_{j\in\mathcal{O}} \mathbf{q}_j^*(s)\,\mathrm{d}s > M(t-t_*) \quad \forall t \in (t_*, t_0).$$

Using the previously deduced integral inequality, we obtain for $t \in [t_*, t_0]$

$$\begin{aligned}\sum_{j\in\mathcal{O}} \mathbf{q}_j^*(t) &\leq \sum_{j\in\mathcal{O}} \mathbf{q}_j^*(t_*) + \sum_{i\in\mathcal{I}} \|\mathbf{c}_i\|_{\mathbf{L}^\infty((0,T))} \int_{t_*}^t M - \sum_{j\in\mathcal{O}} \mathbf{q}_j^*(s)\,\mathrm{d}s \\ &\leq M + \sum_{i\in\mathcal{I}} \|\mathbf{c}_i\|_{\mathbf{L}^\infty((0,T))} \int_{t_*}^t \sum_{j\in\mathcal{O}} \mathbf{q}_j^*(s) - M\,\mathrm{d}s\end{aligned}$$

which is equivalent to

$$\sum_{j\in\mathcal{O}} \mathbf{q}_j^*(t) - M \leq \sum_{i\in\mathcal{I}} \|\mathbf{c}_i\|_{\mathbf{L}^\infty((0,T))} \int_{t_*}^t \sum_{j\in\mathcal{O}} \mathbf{q}_j^*(s) - M\,\mathrm{d}s, \quad t \in [t_*, t_0].$$

Then by Gronwall inequality, we obtain

$$\sum_{j\in\mathcal{O}} \mathbf{q}_j^*(t) - M \leq 0 \implies \sum_{j\in\mathcal{O}} \mathbf{q}_j^*(t) \leq M \quad t \in [t_*, t_0]. \tag{4.4.23}$$

This contradicts the assumption that there exists $t_0 \in [0, T]$ such that $\sum_{j\in\mathcal{O}} \mathbf{q}_j^*(t_0) > M$ so that we can conclude that $\sum_{j\in\mathcal{O}} \mathbf{q}_j^*(t) \leq M \ \forall t \in [0, T]$. □

4.5 Stability of the solution

In this section we investigate the stability of the solution when we introduce pertubations on the initial datum, the initial queues and the routing functions. Obviously, the stability results depend on the choice of topology. We aim for the most sharp stability result while still obtaining a uniform convergence of the solution. Since we model traffic, the queue length is a key criterion. We thus show its uniform convergence when measuring the input datum in $\mathbf{L}^1$-norm. This enables us to obtain also the stability of the solutions of the PDEs on the incoming and outgoing links.

We provide the following stability estimates for the mappings defined in Definition 4.4.3 with respect to initial datum, initial queue size, and routing ratios.

Lemma 4.5.1 (Lipschitz-continuity w.r.t. initial datum and routing)**.**

1. *Let* $\mathbf{h} \in \mathrm{Lip}\left([0,T]; \mathbb{R}^{|\mathcal{I}|}\right)$*. Recall Definition 4.4.3 and let* $\mathbf{V}^{\mathrm{in}}[\mathbf{h}]$ *and* $\tilde{\mathbf{V}}^{\mathrm{in}}[\mathbf{h}]$ *the functions computed with the mapping* $\mathbf{V}^{\mathrm{in}}$ *respectively applied to the initial datum of the conservation law* $\boldsymbol{\rho}_{0,i} \in \mathbf{L}^1((-\infty, 0))$ *and* $\tilde{\boldsymbol{\rho}}_{0,i} \in \mathbf{L}^1((-\infty, 0))$ *for any* $i \in \mathcal{I}$ *and the corresponding initial datum of the Hamilton-Jacobi equation as in Definition 4.4.2. Then, we have the following estimate:*

$$\|\mathbf{V}_i^{\mathrm{in}}\left[\mathbf{h}\right] - \tilde{\mathbf{V}}_i^{\mathrm{in}}\left[\mathbf{h}\right]\|_{C([0,T])} \leq \|\boldsymbol{\rho}_{0,i} - \tilde{\boldsymbol{\rho}}_{0,i}\|_{\mathbf{L}^1((-\infty,0))}.$$

2. *Let* $\mathbf{V} \in \mathrm{Lip}\left([0,T];\mathbb{R}^{|\mathcal{I}|}\right)$ *with* $\|\mathbf{V}_i'\|_{\mathbf{L}^\infty((0,T))} \leq \mathbf{f}_i^{\max}$ *for* $i \in \mathcal{I}$ *and* $\mathbf{F}[\mathbf{V}]$ *and* $\tilde{\mathbf{F}}[\mathbf{V}]$ *respectively correspond to the value obtained when computing* $\mathbf{F}$ *from* $\mathbf{q}_0, \boldsymbol{\theta}$ *and* $\tilde{\mathbf{q}}_0, \tilde{\boldsymbol{\theta}}$ *with* $\boldsymbol{\theta}, \tilde{\boldsymbol{\theta}} \in \mathbf{L}^1\left((0,T);\mathbb{R}^{|\mathcal{O}||\mathcal{I}|}\right)$*. Then, we have the following estimate:*

$$\forall j \in \mathcal{O} : \left\|\mathbf{F}_j[\mathbf{V}] - \tilde{\mathbf{F}}_j[\mathbf{V}]\right\|_{C([0,T])} \leq |\mathbf{q}_{0,j} - \tilde{\mathbf{q}}_{0,j}| + \sum_{i\in\mathcal{I}} \mathbf{f}_{\max}^i \|\boldsymbol{\theta}_{i,j} - \tilde{\boldsymbol{\theta}}_{i,j}\|_{\mathbf{L}^1((0,T))}.$$

3. *Let* $\mathbf{F} \in \mathrm{Lip}\left([0,T];\mathbb{R}^{|\mathcal{O}|}\right)$ *and* $\mathbf{V}^{\mathrm{out}}[\mathbf{F}]$ *and* $\tilde{\mathbf{V}}^{\mathrm{out}}[\mathbf{F}]$ *respectively correspond to the value obtained when computing* $\mathbf{V}^{\mathrm{out}}[\mathbf{F}]$ *from initial datum of the conservation law* $\boldsymbol{\rho}_{0,j} \in \mathbf{L}^1((0,\infty))$ *and* $\tilde{\boldsymbol{\rho}}_{0,j} \in \mathbf{L}^1((0,\infty))$ *for any* $j \in \mathcal{O}$ *with initial datum for the Hamilton-Jacobi equations as in Definition 4.4.2. Then, we have the following estimate:*

$$\left\|\mathbf{V}_j^{\mathrm{out}}\big[\mathbf{F}\big] - \tilde{\mathbf{V}}_j^{\mathrm{out}}\big[\mathbf{F}\big]_j\right\|_{C([0,T])} \leq \|\boldsymbol{\rho}_{0,j} - \tilde{\boldsymbol{\rho}}_{0,j}\|_{\mathbf{L}^1((0,\infty))}.$$

Proof. 1. Let $t \in [0,T]$ and $i \in \mathcal{I}$ and let us first assume that the dominating terms in the solution formula are in both cases stemming from the initial datum. Let us assume that the maximum of the first term is attained at $y^1 \in \mathbb{R}_{\leq 0}$ and for the second term at $y^2 \in \mathbb{R}_{\leq 0}$. Then, we obtain the two-sided estimate

$$\begin{aligned}
&\max_{y\in\mathbb{R}_{\leq 0}} \left\{\mathbf{V}_{0,i}^{\mathrm{in}}(y) + t\mathbf{f}_i^*\left(\tfrac{-y}{t}\right)\right\} - \max_{\tilde{y}\in\mathbb{R}_{\leq 0}} \left\{\tilde{\mathbf{V}}_{0,i}^{\mathrm{in}}(\tilde{y}) + t\mathbf{f}_i^*\left(\tfrac{-\tilde{y}}{t}\right)\right\} \\
&\qquad \leq \left\{\mathbf{V}_{0,i}^{\mathrm{in}}(y^1) + t\mathbf{f}_i^*\left(\frac{-y^1}{t}\right)\right\} - \max_{\tilde{y}\in\mathbb{R}_{\leq 0}} \left\{\tilde{\mathbf{V}}_{0,i}^{\mathrm{in}}(\tilde{y}) + t\mathbf{f}_i^*\left(\tfrac{-\tilde{y}}{t}\right)\right\} \\
&\qquad \leq |\mathbf{V}_{0,i}^{\mathrm{in}}(y^1) - \tilde{\mathbf{V}}_{0,i}^{\mathrm{in}}(y^1)| \leq \int_{-\infty}^{y^1} |\boldsymbol{\rho}_{0,i}(s) - \tilde{\boldsymbol{\rho}}_{0,i}(s)|\,\mathrm{d}s \leq \|\boldsymbol{\rho}_{0,i} - \tilde{\boldsymbol{\rho}}_{0,i}\|_{\mathbf{L}^1((-\infty,0))}
\end{aligned}$$

and

$$\begin{aligned}
&\max_{y\in\mathbb{R}_{\leq 0}} \left\{\mathbf{V}_{0,i}^{\mathrm{in}}(y) + t\mathbf{f}_i^*\left(\tfrac{-y}{t}\right)\right\} - \max_{\tilde{y}\in\mathbb{R}_{\leq 0}} \left\{\tilde{\mathbf{V}}_{0,i}^{\mathrm{in}}(\tilde{y}) + t\mathbf{f}_i^*\left(\tfrac{-\tilde{y}}{t}\right)\right\} \\
&\qquad \geq \max_{y\in\mathbb{R}_{\leq 0}} \left\{\mathbf{V}_{0,i}^{\mathrm{in}}(y) + t\mathbf{f}_i^*\left(\tfrac{-y}{t}\right)\right\} - \left\{\tilde{\mathbf{V}}_{0,i}^{\mathrm{in}}(y^2) + t\mathbf{f}_i^*\left(\frac{-y^2}{t}\right)\right\} \\
&\qquad \geq -\|\boldsymbol{\rho}_{0,i} - \tilde{\boldsymbol{\rho}}_{0,i}\|_{\mathbf{L}^1((-\infty,0))}.
\end{aligned}$$

Since the estimates are uniform in t, the claim follows. Concentrating on the case where the solution is a function of the boundary datum we obtain similarly by picking specific $t_1, t_2, y \in [0,T]^2 \times \mathbb{R}_{\leq 0}$ and by a similar argumentation as above

$$\begin{aligned}
&\Bigg| \max_{\substack{y\in\mathbb{R}_{\leq 0}\\ 0\leq t_2\leq t_1\leq t}} \left\{\mathbf{V}_{0,i}^{\mathrm{in}}(y) + t_2\mathbf{f}_i^*\left(\tfrac{-y}{t_2}\right) - (t-t_1)\mathbf{f}_i^{\max} - \int_{t_2}^{t_1} \mathbf{h}_i(s)\,\mathrm{d}s\right\} \\
&\qquad - \max_{\substack{y\in\mathbb{R}_{\leq 0}\\ 0\leq t_2\leq t_1\leq t}} \left\{\tilde{\mathbf{V}}_{0,i}^{\mathrm{in}}(y) + t_2\mathbf{f}_i^*\left(\tfrac{-y}{t_2}\right) - (t-t_1)\mathbf{f}_i^{\max} - \int_{t_2}^{t_1} \mathbf{h}_i(s)\,\mathrm{d}s\right\}\Bigg| \\
&\qquad\qquad \leq \|\boldsymbol{\rho}_{0,i} - \tilde{\boldsymbol{\rho}}_{0,i}\|_{\mathbf{L}^1((-\infty,0))}.
\end{aligned}$$

The other two mixed cases can be derived from those two recalling Lemma 4.4.7.

2. Let $t > 0$ and $j \in \mathcal{O}$, we obtain

$$\begin{aligned}\mathbf{F}_j[\mathbf{V}](t) - \tilde{\mathbf{F}}_j[\mathbf{V}](t) &= \mathbf{q}_{0,j} - \tilde{\mathbf{q}}_{0,j} - \sum_{i\in\mathcal{I}} \int_0^t \mathbf{V}_{i,s}(s)\boldsymbol{\theta}_{i,j}(s)\,\mathrm{d}s + \sum_{i\in\mathcal{I}} \int_0^t \mathbf{V}_{i,s}(s)\tilde{\boldsymbol{\theta}}_{i,j}(s)\,\mathrm{d}s \\ &= \mathbf{q}_{0,j} - \tilde{\mathbf{q}}_{0,j} + \sum_{i\in\mathcal{I}} \int_0^t \mathbf{V}_{i,s}(s)\left(\tilde{\boldsymbol{\theta}}_{i,j}(s) - \boldsymbol{\theta}_{i,j}(s)\right)\,\mathrm{d}s, \\ \left\|\mathbf{F}_j[\mathbf{V}] - \tilde{\mathbf{F}}_j[\mathbf{V}]\right\|_{C([0,T])} &\leq |\mathbf{q}_{0,j} - \tilde{\mathbf{q}}_{0,j}| + \sum_{i\in\mathcal{I}} \mathbf{f}^i_{\max}\|\boldsymbol{\theta}_{i,j} - \tilde{\boldsymbol{\theta}}_{i,j}\|_{\mathbf{L}^1((0,T))},\end{aligned}$$

   where the last inequality follows by the uniform Lipschitz-bound on $\mathbf{V}$.
3. The proof follows analogously to the argument in Item 1.

□

The previously stated Lemma 4.5.1 together with Proposition 4.4.9 enables us to obtain the following stability result in Theorem 4.5.2, which guarantees that, under small changes of the involved input datum, the solution, here the queue, can only have small limited variations.

Theorem 4.5.2 (Stability of the queue)**.** *Let the framework in Section 4.4 and $T > 0$ be given. Assume that $\mathbf{q}_0, \tilde{\mathbf{q}}_0 \in \mathbb{R}^{|\mathcal{O}|}_{\geq 0}$ with $\|\mathbf{q}_0\|_1 \leq M$ and $\|\tilde{\mathbf{q}}_0\|_1 \leq M$. Assume that in addition $\boldsymbol{\rho}_{0,i}, \tilde{\boldsymbol{\rho}}_{0,i} \in \mathbf{L}^\infty((-\infty,0)) \cap \mathbf{L}^1((-\infty,0))$ with $0 \leq \boldsymbol{\rho}_{0,i} \leq \boldsymbol{\rho}_i^{\max}$, $0 \leq \tilde{\boldsymbol{\rho}}_{0,i} \leq \boldsymbol{\rho}_i^{\max}$, $i \in \mathcal{I}$ and $\boldsymbol{\rho}_{0,j}, \tilde{\boldsymbol{\rho}}_{0,j} \in \mathbf{L}^\infty((0,\infty)) \cap \mathbf{L}^1((0,\infty))$ with $0 \leq \boldsymbol{\rho}_{0,j} \leq \boldsymbol{\rho}_j^{\max}$, $0 \leq \tilde{\boldsymbol{\rho}}_{0,j} \leq \boldsymbol{\rho}_j^{\max}$, $j \in \mathcal{O}$ be given as well as two routings $\boldsymbol{\theta}, \tilde{\boldsymbol{\theta}} \in BV\left((0,T); \mathbb{R}^{|\mathcal{O}|\times|\mathcal{I}|}_{\geq 0}\right)$ with $\sum_{j\in\mathcal{O}} \boldsymbol{\theta}_{i,j}(t) = 1 = \sum_{j\in\mathcal{O}} \tilde{\boldsymbol{\theta}}_{i,j}(t)$ for almost every $t \in [0,T]$. We denote by $\mathbf{q}, \tilde{\mathbf{q}}$ the corresponding solutions. The following stability estimate holds:*

$$\begin{aligned}&\|\mathbf{q} - \tilde{\mathbf{q}}\|_{C\left([0,T];\mathbb{R}^{|\mathcal{O}|}\right)} \\ &\qquad \leq \Big(2|\mathbf{q}_0 - \tilde{\mathbf{q}}_0|_1 + 2\sum_{(i,j)\in\mathcal{I}\times\mathcal{O}} \mathbf{f}^i_{\max}\|\boldsymbol{\theta}_{i,j} - \tilde{\boldsymbol{\theta}}_{i,j}\|_{\mathbf{L}^1((0,t))} + \|\boldsymbol{\rho}_0 - \tilde{\boldsymbol{\rho}}_0\|_{\mathbf{L}^1((0,\infty);\mathbb{R}^{|\mathcal{O}|}))} \\ &\qquad\qquad + 2\sum_{i,j\in\mathcal{I}\times\mathcal{O}} (\|\boldsymbol{\theta}_{i,j}\|_{TV((0,T))} + 1)\big(\|\boldsymbol{\rho}_{0,i} - \tilde{\boldsymbol{\rho}}_{0,i}\|_{\mathbf{L}^1((-\infty,0))}\big)\Big) \\ &\qquad\qquad\qquad \cdot \exp\Big(2\sum_{(i,j)\in\mathcal{I}\times\mathcal{O}} (\|\boldsymbol{\theta}_{i,j}\|_{TV((0,T))} + 1)\|\mathbf{c}_i\|_{\mathbf{L}^\infty((0,T))}T\Big)\end{aligned}$$

Proof. Let us first mention that $\mathbf{q}, \tilde{\mathbf{q}}$ exist and are unique due to Theorem 4.4.11. Thus, we can directly concentrate on the fixed-point mapping Lemma 4.4.6 which is satisfied by $\mathbf{q}, \tilde{\mathbf{q}}$, and indicate the involved functions dependent on the ˜datum by the corresponding ˜. Then, we obtain for $t \in [0,T]$ and $j \in \mathcal{O}$

$$\begin{aligned}|\mathbf{q}_j(t) - \tilde{\mathbf{q}}_j(t)| = \Big|&\boldsymbol{\Lambda}_j\big[\mathbf{F}\circ\mathbf{V}^{\mathrm{in}}\circ\mathbf{h}\circ\mathbf{q}, \mathbf{V}^{\mathrm{out}}\circ\mathbf{F}\circ\mathbf{V}^{\mathrm{in}}\circ\mathbf{h}\circ\mathbf{q}\big](t) \\ &- \boldsymbol{\Lambda}_j\big[\tilde{\mathbf{F}}\circ\tilde{\mathbf{V}}^{\mathrm{in}}\circ\mathbf{h}\circ\tilde{\mathbf{q}}, \tilde{\mathbf{V}}^{\mathrm{out}}\circ\tilde{\mathbf{F}}\circ\tilde{\mathbf{V}}^{\mathrm{in}}\circ\mathbf{h}\circ\tilde{\mathbf{q}}\big](t)\Big|,\end{aligned}$$

plugging in the definition of $\mathbf{\Lambda}$ in Definition 4.4.3

$$\begin{aligned}
&= \big|\mathbf{F}_j\big[\mathbf{V}^{\text{in}} \circ \mathbf{h} \circ \mathbf{q}\big](t) - \tilde{\mathbf{F}}_j\big[\tilde{\mathbf{V}}^{\text{in}} \circ \mathbf{h} \circ \tilde{\mathbf{q}}\big](t) \\
&\qquad + \mathbf{V}_j^{\text{out}}\big[\mathbf{F} \circ \mathbf{V}^{\text{in}} \circ \mathbf{h} \circ \mathbf{q}\big](t) - \tilde{\mathbf{V}}_j^{\text{out}}\big[\tilde{\mathbf{F}} \circ \tilde{\mathbf{V}}^{\text{in}} \circ \mathbf{h} \circ \tilde{\mathbf{q}}\big](t)\big| \\
&\leq \Big|\mathbf{F}_j\big[\mathbf{V}^{\text{in}} \circ \mathbf{h} \circ \mathbf{q}\big](t) - \tilde{\mathbf{F}}_j\big[\tilde{\mathbf{V}}^{\text{in}} \circ \mathbf{h} \circ \tilde{\mathbf{q}}\big](t)\Big| \\
&\qquad + \Big|\mathbf{V}_j^{\text{out}}\big[\mathbf{F} \circ \mathbf{V}^{\text{in}} \circ \mathbf{h} \circ \mathbf{q}\big](t) - \mathbf{V}_j^{\text{out}}\big[\tilde{\mathbf{F}} \circ \tilde{\mathbf{V}}^{\text{in}} \circ \mathbf{h} \circ \tilde{\mathbf{q}}\big](t)\Big| \\
&\qquad + \Big|\mathbf{V}_j^{\text{out}}\big[\tilde{\mathbf{F}} \circ \tilde{\mathbf{V}}^{\text{in}} \circ \mathbf{h} \circ \tilde{\mathbf{q}}\big](t) - \tilde{\mathbf{V}}_j^{\text{out}}\big[\tilde{\mathbf{F}} \circ \tilde{\mathbf{V}}^{\text{in}} \circ \mathbf{h} \circ \tilde{\mathbf{q}}\big](t)\Big|,
\end{aligned}$$

applying on the last terms Lemma 4.5.1 and Proposition 4.4.9

$$\leq 2\left\|\mathbf{F}_j\big[\mathbf{V}^{\text{in}} \circ \mathbf{h} \circ \mathbf{q}\big] - \tilde{\mathbf{F}}_j\big[\tilde{\mathbf{V}^{\text{in}}} \circ \mathbf{h} \circ \tilde{\mathbf{q}}\big]\right\|_{C([0,t])} + \|\boldsymbol{\rho}_{0,j} - \tilde{\boldsymbol{\rho}}_{0,j}\|_{\mathbf{L}^1((0,\infty))}.$$

Concentrating on the first term, we have

$$\begin{aligned}
&\left\|\mathbf{F}_j\big[\mathbf{V}^{\text{in}} \circ \mathbf{h} \circ \mathbf{q}\big] - \tilde{\mathbf{F}}_j\big[\tilde{\mathbf{V}^{\text{in}}} \circ \mathbf{h} \circ \tilde{\mathbf{q}}\big]\right\|_{C([0,t])} \\
&\leq \left\|\mathbf{F}_j\big[\mathbf{V}^{\text{in}} \circ \mathbf{h} \circ \mathbf{q}\big] - \tilde{\mathbf{F}}_j\big[\mathbf{V}^{\text{in}} \circ \mathbf{h} \circ \mathbf{q}\big]\right\|_{C([0,t])} + \left\|\tilde{\mathbf{F}}_j\big[\mathbf{V}^{\text{in}} \circ \mathbf{h} \circ \mathbf{q}\big] - \tilde{\mathbf{F}}_j\big[\tilde{\mathbf{V}^{\text{in}}} \circ \mathbf{h} \circ \tilde{\mathbf{q}}\big]\right\|_{C([0,t])},
\end{aligned}$$

using again Lemma 4.5.1 and Proposition 4.4.9 we obtain

$$\begin{aligned}
&\leq |\mathbf{q}_{0,j} - \tilde{\mathbf{q}}_{0,j}| + \sum_{i\in\mathcal{I}} \mathbf{f}^i_{\max}\|\boldsymbol{\theta}_{i,j} - \tilde{\boldsymbol{\theta}}_{i,j}\|_{\mathbf{L}^1((0,t))} \\
&\qquad + \sum_{i\in\mathcal{I}}(\|\boldsymbol{\theta}_{i,j}\|_{TV((0,T))} + 1)\left\|\mathbf{V}_i^{\text{in}}\big[\mathbf{h} \circ \mathbf{q}\big] - \tilde{\mathbf{V}}_i^{\text{in}}\big[\mathbf{h} \circ \tilde{\mathbf{q}}\big]\right\|_{C([0,t])}.
\end{aligned}$$

Finally, it remains to estimate the last term. We obtain for this term again using Lemma 4.5.1 and Proposition 4.4.9

$$\begin{aligned}
&\left\|\mathbf{V}_i^{\text{in}}\big[\mathbf{h} \circ \mathbf{q}\big] - \tilde{\mathbf{V}}_i^{\text{in}}\big[\mathbf{h} \circ \tilde{\mathbf{q}}\big]\right\|_{C([0,t])} \\
&\qquad \leq \left\|\mathbf{V}_i^{\text{in}}\big[\mathbf{h} \circ \mathbf{q}\big] - \tilde{\mathbf{V}}_i^{\text{in}}\big[\mathbf{h} \circ \mathbf{q}\big]\right\|_{C([0,t])} + \left\|\tilde{\mathbf{V}}_i^{\text{in}}\big[\mathbf{h} \circ \mathbf{q}\big] - \tilde{\mathbf{V}}^{\text{in}}\big[\mathbf{h} \circ \tilde{\mathbf{q}}\big]\right\|_{C([0,t])} \\
&\qquad \leq \|\boldsymbol{\rho}_{0,i} - \tilde{\boldsymbol{\rho}}_{0,i}\|_{\mathbf{L}^1((-\infty,0))} + \left\|\mathbf{h}_i\big[\mathbf{q}\big] - \mathbf{h}_i\big[\tilde{\mathbf{q}}\big]\right\|_{\mathbf{L}^1((0,t))} \\
&\qquad \leq \|\boldsymbol{\rho}_{0,i} - \tilde{\boldsymbol{\rho}}_{0,i}\|_{\mathbf{L}^1((-\infty,0))} + \|\mathbf{c}_i\|_{\mathbf{L}^\infty((0,t))} \sum_{j\in\mathcal{O}} \|\mathbf{q}_j - \tilde{\mathbf{q}}_j\|_{\mathbf{L}^1((0,t))}.
\end{aligned}$$

Combining all the upper estimates and summarizing, we then have for $t \in [0,T]$

$$\begin{aligned}
&|\mathbf{q}_j(t) - \tilde{\mathbf{q}}_j(t)| \leq 2|\mathbf{q}_{0,j} - \tilde{\mathbf{q}}_{0,j}| + 2\sum_{i\in\mathcal{I}} \mathbf{f}^i_{\max}\|\boldsymbol{\theta}_{i,j} - \tilde{\boldsymbol{\theta}}_{i,j}\|_{\mathbf{L}^1((0,t))} + \|\boldsymbol{\rho}_{0,j} - \tilde{\boldsymbol{\rho}}_{0,j}\|_{\mathbf{L}^1((0,\infty))} \\
&+ 2\sum_{i\in\mathcal{I}} \Big(\|\boldsymbol{\theta}_{i,j}\|_{TV((0,T))} + 1\Big)\Big(\|\boldsymbol{\rho}_{0,i} - \tilde{\boldsymbol{\rho}}_{0,i}\|_{\mathbf{L}^1((-\infty,0))} + \|\mathbf{c}_i\|_{\mathbf{L}^\infty((0,t))} \sum_{j\in\mathcal{O}} \|\mathbf{q}_j - \tilde{\mathbf{q}}_j\|_{\mathbf{L}^1((0,t))}\Big).
\end{aligned}$$

Summing over all j we obtain

$$\begin{aligned}\sum_{j\in\mathcal{O}}|\mathbf{q}_j(t)-\tilde{\mathbf{q}}_j(t)| \leq 2|\mathbf{q}_0-\tilde{\mathbf{q}}_0|_1 + 2\sum_{i,j\in\mathcal{I}\times\mathcal{O}}\mathbf{f}^i_{\max}\|\boldsymbol{\theta}_{i,j}-\tilde{\boldsymbol{\theta}}_{i,j}\|_{\mathbf{L}^1((0,t))}\\ + \|\boldsymbol{\rho}_0-\tilde{\boldsymbol{\rho}}_0\|_{\mathbf{L}^1((0,\infty);\mathbb{R}^{|\mathcal{O}|}))} + 2\sum_{(i,j)\in\mathcal{I}\times\mathcal{O}}\Big(\|\boldsymbol{\theta}_{i,j}\|_{TV((0,T))}+1\Big)\\ \cdot\Big(\|\boldsymbol{\rho}_{0,i}-\tilde{\boldsymbol{\rho}}_{0,i}\|_{\mathbf{L}^1((-\infty,0))} + \|\mathbf{c}_i\|_{\mathbf{L}^\infty((0,t))}\sum_{j\in\mathcal{O}}\|\mathbf{q}_j-\tilde{\mathbf{q}}_j\|_{\mathbf{L}^1((0,t))}\Big).\end{aligned}$$

We can now apply Gronwall's inequality in [125, Theorem 1.3.1] to obtain for any $t\in[0,T]$:

$$\begin{aligned}&\sum_{j\in\mathcal{O}}|\mathbf{q}_j(t)-\tilde{\mathbf{q}}_j(t)|\\ &\quad\leq\Bigg(2|\mathbf{q}_0-\tilde{\mathbf{q}}_0|_1 + 2\sum_{i,j\in\mathcal{I}\times\mathcal{O}}\mathbf{f}^i_{\max}\|\boldsymbol{\theta}_{i,j}-\tilde{\boldsymbol{\theta}}_{i,j}\|_{\mathbf{L}^1((0,t))}\\ &\qquad + \|\boldsymbol{\rho}_0-\tilde{\boldsymbol{\rho}}_0\|_{\mathbf{L}^1((0,\infty);\mathbb{R}^{|\mathcal{O}|}))} + 2\sum_{i,j\in\mathcal{I}\times\mathcal{O}}\Big(\|\boldsymbol{\theta}_{i,j}\|_{TV((0,T))}+1\Big)\\ &\qquad\cdot\Big(\|\boldsymbol{\rho}_{0,i}-\tilde{\boldsymbol{\rho}}_{0,i}\|_{\mathbf{L}^1((-\infty,0))}\Big)\Bigg)\cdot\exp\left(2\sum_{i,j\in\mathcal{I}\times\mathcal{O}}(\|\boldsymbol{\theta}_{i,j}\|_{TV((0,T))}+1)\|\mathbf{c}_i\|_{\mathbf{L}^\infty((0,t))}t\right).\end{aligned}$$

Taking the supremum over all $t\in[0,T]$, we obtain Lipschitz-continuity of the queues w.r.t. initial datum, initial buffer load and routing ratios. □

4.6 Optimal routing

In this section we investigate how to determine the optimal routing $\boldsymbol{\theta}$ *i.e.* the optimal trajectory of vehicles with respect to a given objective, for instance minimizing congestion. One way to approach this is to consider a minimization problem in which we minimize the queue size at a specific node, assuming that the smaller the queue size is the less the congestion becomes. We can also imagine a case in which we aim to minimize the congestion under limited variation of the routing ratios to prevent oscillations of the routing control. For the single destination case we consider in this article we can use the previously stated Theorem 4.5.2 to obtain existence of a minimizer. This is detailed in

Theorem 4.6.1 (Optimal Routing – multi queue buffer)**.** *Let a junction with $|\mathcal{I}|\in\mathbb{N}_{\geq 1}$ incoming and $|\mathcal{O}|\in\mathbb{N}_{\geq 1}$ outgoing links be given and assume the dynamics hold in the sense of Definition 4.3.1. Then, for any $p\in[1,\infty]$ and $K\in\mathbb{R}_{\geq 0}$ the two minimization problems*

$$\bullet\ \min_{\boldsymbol{\theta}\in\boldsymbol{\Theta}_K}\sum_{j\in\mathcal{O}}\|\mathbf{q}_j[\boldsymbol{\theta}]\|_{\mathbf{L}^p((0,T))} \qquad \bullet\ \min_{\boldsymbol{\theta}\in\boldsymbol{\Theta}}\sum_{j\in\mathcal{O}}\|\mathbf{q}_j[\boldsymbol{\theta}]\|_{\mathbf{L}^p((0,T))} + \sum_{(i,j)\in\mathcal{I}\times\mathcal{O}}\|\boldsymbol{\theta}_{i,j}\|_{TV((0,T))}$$

subject to the dynamics in Definition 4.3.1 with

$$\boldsymbol{\Theta} := \left\{ \boldsymbol{\theta} \in BV((0,T);\mathbb{R}^{|\mathcal{I}|\times|\mathcal{O}|}) : 0 \leq \boldsymbol{\theta}_{i,j}(t) \leq 1 \wedge \sum_{j\in\mathcal{O}} \boldsymbol{\theta}_{i,j}(t) = 1 \forall t \in [0,T] \text{ a.e. } \forall (i,j) \in \mathcal{I}\times\mathcal{O} \right\}$$

$$\boldsymbol{\Theta}_K := \left\{ \boldsymbol{\theta} \in \boldsymbol{\Theta} : \ \|\boldsymbol{\theta}\|_{TV((0,T);\mathbb{R}^{|\mathcal{I}|\times|\mathcal{O}|})} \leq K \right\}$$

admit a solution. We denote the dependency of $\mathbf{q}$ *w.r.t. assumed routing* $\boldsymbol{\theta}$ *by* $\mathbf{q}[\boldsymbol{\theta}]$.

Proof. We start with proving the claim for the first objective function. Due to the fact that the objective functions are both bounded from below, there exists a sequence $(\boldsymbol{\theta}_l)_{l\in\mathbb{N}} \subseteq \boldsymbol{\Theta}_K$ so that

$$\lim_{l\to\infty} \sum_{j\in\mathcal{O}} \|\mathbf{q}_j[\boldsymbol{\theta}_l]\|_{\mathbf{L}^p((0,T))} = \inf_{\boldsymbol{\theta}\in\boldsymbol{\Theta}} \sum_{j\in\mathcal{O}} \|\mathbf{q}_j[\boldsymbol{\theta}]\|_{\mathbf{L}^p((0,T))} \geq 0.$$

Since $BV((0,T)) \overset{c}{\hookrightarrow} \mathbf{L}^p((0,T))$, i.e. BV is for space dimension 1 compactly embedded into $\mathbf{L}^p((0,T))$ $\forall p \in [1,\infty)$ (see [115, Theorem 13.32 (Rellich Kondrachov), Theorem 13.35 (Compactness)] we can pick a subsequence $(\boldsymbol{\theta}_{l_m})_{m\in\mathbb{N}} \subset \boldsymbol{\Theta}_K$ such that

$$\exists \boldsymbol{\theta}^* \in \boldsymbol{\Theta}_K : \lim_{m\to\infty} \|\boldsymbol{\theta}^* - \boldsymbol{\theta}_{l_m}\|_{\mathbf{L}^1((0,T);\mathbb{R}^{|\mathcal{I}|\times|\mathcal{O}|})} = 0 \tag{4.6.1}$$

(see also [3, Proposition 3.13, Theorem 3.23]). Due to Theorem 4.5.2 we then know that

$$\lim_{m\to\infty} \|\mathbf{q}[\boldsymbol{\theta}^*] - \mathbf{q}[\boldsymbol{\theta}_{l_m}]\|_{C([0,T];\mathbb{R}^{|\mathcal{O}|})} = 0$$

so that in particular due to $C([0,T]) \hookrightarrow \mathbf{L}^p((0,T))$ the objective function also strongly converges. This proves the claim for the first minimization problem.

The same argumentation can be made for the second objective noticing that due to the BV norm in the objective function we have, for any minimizing sequence $(\boldsymbol{\theta}_k)_{k\in\mathbb{N}} \subset \boldsymbol{\Theta}$, that there exists $C \in \mathbb{R}_{>0}$ so that $\sup_{k\in\mathbb{N}} \sum_{(i,j)\in\mathcal{I}\times\mathcal{O}} \| \{\boldsymbol{\theta}_{i,j}\}_k \|_{BV((0,T))} \leq C$ so that we can follow the same reasoning as for the first objective function. □

Remark 4.5 (No uniqueness of the Optimal Control problem and different objective functions). It is not surprising that one does not obtain a uniqueness result for the previously mentioned optimal control problem for the first objective function. For instance consider zero initial datum for the incoming and outgoing edges, and assume that $\boldsymbol{q}_0 = \mathbf{0}$. Then, obviously every routing results in a queuing size of zero as long as the routing respects the bound $K \in \mathbb{R}_{\geq 0}$. The result also holds if there is significantly small initial datum of the incoming and outgoing links, so that there is never a buffer needed. A similar argument holds for the second objective. Even though any change in routing over time is penalized by the TV semi-norm for sufficiently small initial datum, any constant routing would produce a queueing size of zero.

One can replace the used objective functions in Theorem 4.6.1 with more general ones. The only requirement is the boundedness from below and the lower semicontinuity of the used norm.

4.7 Practical implementation of the model on road networks

This section implements our framework on a realistic road network, which contains several intersections and finite-length links. The classical argument used in the literature on conservation laws is that the information has finite propagation speed on road networks. We explore how this argument is detailed mathematically. The general idea is the following: consider a link of length $L \in \mathbb{R}_{>0}$, connecting intersections v_1 and v_2. We need to prove that for sufficiently small time, only a neighborhood of the link around v_1 can be affected by the information exiting this intersection, and the same for v_2. After this, we will know that outside these neighborhoods, the solution of Hamilton-Jacobi equations on this link can be solved only considering initial datum. This is a classical argument for conservation laws and we now detail this argument for the considered class of Hamilton-Jacobi equations. We then need to prove that, for a given finite-time horizon, there exists a distance d, such that if $|x| \geq d$, the solution formula always select information emanating from the initial datum, thus reducing the IBVP problem to a Cauchy problem. We prove the following lemma for an incoming link.

Lemma 4.7.1 (Finite propagation speed of information in Hamilton-Jacobi solutions)**.** *For $t \in [0,T]$ let $x \leq 0$ such that $x \leq \mathbf{f}_i'(\boldsymbol{\rho}_i^{\max})t$. Then*

$$\begin{aligned}\bar{\mathbf{V}}_i^{\text{in}}(t,x) &= \max\left\{\begin{array}{c}\max\limits_{y\in\mathbb{R}_{\leq 0}}\left\{\mathbf{V}_{0,i}^{\text{in}}(y)+t\mathbf{f}_i^*\left(\frac{x-y}{t}\right)\right\},\\ \max\limits_{\substack{y\in\mathbb{R}_{\leq 0}\\ 0\leq t_2\leq t_1\leq t}}\left\{\mathbf{V}_{0,i}^{\text{in}}(y)+t_2\mathbf{f}_i^*\left(\frac{-y}{t_2}\right)+(t-t_1)\mathbf{f}_i^*\left(\frac{x}{t-t_1}\right)-\int_{t_2}^{t_1}\mathbf{h}_i(s)\,\mathrm{d}s\right\}\end{array}\right\}\\ &= \max_{y\in\mathbb{R}_{\leq 0}}\left\{\mathbf{V}_{0,i}^{\text{in}}(y)+t\mathbf{f}_i^*\left(\tfrac{x-y}{t}\right)\right\}.\end{aligned}$$

Proof. We know that for any $x \in \mathbb{R}, f^*(x) \coloneqq \inf\limits_{u\in[0,\rho^{\max}]}\{ux - f(u)\}$, $x \in \mathrm{Dom}(f^*)$. Let $i \in \mathcal{I}$. Assume that $x < \mathbf{f}_i'(\boldsymbol{\rho}_i^{\max})$. Then for any $u \in [0, \boldsymbol{\rho}_i^{\max}[$ we have

$$\begin{aligned}x &< \frac{\mathbf{f}_i(u)-\mathbf{f}_i(\boldsymbol{\rho}_i^{\max})}{u-\boldsymbol{\rho}_i^{\max}}\\ ux-\mathbf{f}_i(u) &> \boldsymbol{\rho}_i^{\max}x.\end{aligned}$$

In addition we know that by picking as argument $u = \boldsymbol{\rho}_i^{\max}$ in the infimum we get $\mathbf{f}_i^*(x) \leq \boldsymbol{\rho}_i^{\max}x$. Now let us fix $t \in [0,T]$, $\mathbf{h}_i \in \mathrm{Lip}([0,T])$ and look at

$$\bar{\mathbf{V}}_i^{\text{in}}[\mathbf{h}_i](t,x) = \max\left\{\begin{array}{c}\max\limits_{y\in\mathbb{R}_{\leq 0}}\left\{\mathbf{V}_{0,i}^{\text{in}}(y)+t\mathbf{f}_i^*\left(\frac{x-y}{t}\right)\right\},\\ \max\limits_{\substack{y\in\mathbb{R}_{\leq 0}\\ 0\leq t_2\leq t_1\leq t}}\left\{\mathbf{V}_{0,i}^{\text{in}}(y)+t_2\mathbf{f}_i^*\left(\frac{-y}{t_2}\right)+(t-t_1)\mathbf{f}_i^*\left(\frac{x}{t-t_1}\right)-\int_{t_2}^{t_1}\mathbf{h}_i(s)\,\mathrm{d}s\right\}\end{array}\right\}.$$

For $t \in [0,T]$, let $x \le 0$ such that $\frac{x}{t} \le \mathbf{f}_i'(\boldsymbol{\rho}_i^{\max})$. Then for any $0 < t_1 < t$, we have $\frac{x}{t-t_1} \le \frac{x}{t} \le \mathbf{f}_i'(\boldsymbol{\rho}_i^{\max})$. In addition, for any $t_1 \le t$ we have $(t-t_1)\mathbf{f}_i^*\big(\frac{x}{t-t_1}\big) \le x\boldsymbol{\rho}_i^{\max}$. Thus

$$\max_{\substack{y\in\mathbb{R}_{\le 0}\\ 0\le t_2\le t_1\le t}} \Big\{\mathbf{V}_{0,i}^{\mathrm{in}}(y) + t_2\mathbf{f}_i^*\big(\tfrac{-y}{t_2}\big) + (t-t_1)\mathbf{f}_i^*\big(\tfrac{x}{t-t_1}\big) - \int_{t_2}^{t_1}\mathbf{h}_i(s)\,\mathrm{d}s\Big\}$$
$$\le x\boldsymbol{\rho}_i^{\max} + \max_{\substack{y\in\mathbb{R}_{\le 0}\\ 0\le t_2\le t}} \Big\{\mathbf{V}_{0,i}^{\mathrm{in}}(y) + t_2\mathbf{f}_i^*\big(\tfrac{-y}{t_2}\big)\Big\},$$

assuming that $\mathbf{h}_i \ge 0$. We need to prove now that

$$x\boldsymbol{\rho}_i^{\max} + \max_{\substack{y\in\mathbb{R}_{\le 0}\\ 0\le t_2\le t}} \Big\{\mathbf{V}_{0,i}^{\mathrm{in}}(y) + t_2\mathbf{f}_i^*\big(\tfrac{-y}{t_2}\big)\Big\} \le \max_{y\in\mathbb{R}_{\le 0}} \Big\{\mathbf{V}_{0,i}^{\mathrm{in}}(y) + t\mathbf{f}_i^*\big(\tfrac{x-y}{t}\big)\Big\}.$$

Picking $\bar{y}$ and $\bar{t}_2$ optimal in the left maximum, we need to look at $\bar{t}_2\mathbf{f}_i^*\big(\frac{-\bar{y}}{\bar{t}_2}\big) - t\mathbf{f}_i^*\big(\frac{x-y}{t}\big)$ and show ≤ 0:

$$x\boldsymbol{\rho}_i^{\max} + \max_{\substack{y\in\mathbb{R}_{\le 0}\\ 0\le t_2\le t}} \Big\{\mathbf{V}_{0,i}^{\mathrm{in}}(y) + t_2\mathbf{f}_i^*\big(\tfrac{-y}{t_2}\big)\Big\} - \max_{y\in\mathbb{R}_{\le 0}} \Big\{\mathbf{V}_{0,i}^{\mathrm{in}}(y) + t\mathbf{f}_i^*\big(\tfrac{x-y}{t}\big)\Big\}$$
$$\le \underbrace{x\boldsymbol{\rho}_i^{\max}}_{\le 0} + \underbrace{\bar{t}_2\mathbf{f}_i^*\big(\tfrac{-\bar{y}}{\bar{t}_2}\big)}_{\le 0}\underbrace{-t\mathbf{f}_i^*\big(\tfrac{x-\bar{y}}{t}\big)}_{\ge 0}.$$

- First, assume $\mathbf{f}_i'(\boldsymbol{\rho}_i^{\max}) \le \frac{x-\bar{y}}{t} \le \mathbf{f}_i'(0)$. Then $\mathbf{f}_i^*\big(\frac{x-\bar{y}}{t}\big) = u^*\frac{x-\bar{y}}{t} - \mathbf{f}_i(u^*)$ where $\mathbf{f}_i'(u^*) = \frac{x-\bar{y}}{t}$. By concavity of $\mathbf{f}_i$, the function $g : [0, \boldsymbol{\rho}_i^{\max}],\ u \mapsto u\mathbf{f}_i'(u) - u$ is decreasing, and can thus be lower bounded by $g(\boldsymbol{\rho}_i^{\max})$. Then $\mathbf{f}_i^*\big(\frac{x-\bar{y}}{t}\big) \ge \boldsymbol{\rho}_i^{\max}\mathbf{f}_i'(\boldsymbol{\rho}_i^{\max})$ and

$$x\boldsymbol{\rho}_i^{\max} + \bar{t}_2\mathbf{f}_i^*\big(\tfrac{-\bar{y}}{\bar{t}_2}\big) - t\mathbf{f}_i^*\big(\tfrac{x-\bar{y}}{t}\big) \le (x - t\mathbf{f}_i'(\boldsymbol{\rho}_i^{\max}))\boldsymbol{\rho}_i^{\max} \le 0.$$

- Now assume $\frac{x-\bar{y}}{t} > \mathbf{f}_i'(0)$ or $\frac{x-\bar{y}}{t} < f'(\boldsymbol{\rho}_i^{\max})$. Then, if $\frac{x-\bar{y}}{t} - 1 \ge 0$, the function $u \mapsto u\frac{x-\bar{y}}{t} - u$ is increasing on $[0, \boldsymbol{\rho}_i^{\max}]$, and thus $\mathbf{f}_i^*\big(\frac{x-\bar{y}}{t}\big) = 0$ which provides the requested bound. Else, if $\frac{x-\bar{y}}{t} - 1 < 0$, then the function $u \mapsto u\frac{x-\bar{y}}{t} - u$ is decreasing, and $\mathbf{f}_i^*\big(\frac{x-\bar{y}}{t}\big) = \boldsymbol{\rho}_i^{\max}\frac{x-\bar{y}}{t}$. Then

$$\begin{aligned} x\boldsymbol{\rho}_i^{\max} + \bar{t}_2\mathbf{f}_i^*\big(\tfrac{-\bar{y}}{\bar{t}_2}\big) - t\mathbf{f}_i^*\big(\tfrac{x-\bar{y}}{t}\big) &= x\boldsymbol{\rho}_i^{\max} + \bar{t}_2\mathbf{f}_i^*\big(\tfrac{-\bar{y}}{\bar{t}_2}\big) - t\boldsymbol{\rho}_i^{\max}\tfrac{x-\bar{y}}{t} \\ &= \bar{y}\boldsymbol{\rho}_i^{\max} + \bar{t}_2\mathbf{f}_i^*\big(\tfrac{-\bar{y}}{\bar{t}_2}\big) \le 0. \end{aligned}$$

In all cases, we thus have that if $x - \mathbf{f}_i'(\boldsymbol{\rho}_i^{\max})t \le 0$,

$$x\boldsymbol{\rho}_i^{\max} + \max_{\substack{y\in\mathbb{R}_{\le 0}\\ 0\le t_2\le t}} \Big\{\mathbf{V}_{0,i}^{\mathrm{in}}(y) + t_2\mathbf{f}_i^*\big(\tfrac{-y}{t_2}\big)\Big\} \le \max_{y\in\mathbb{R}_{\le 0}} \Big\{\mathbf{V}_{0,i}^{\mathrm{in}}(y) + t\mathbf{f}_i^*\big(\tfrac{x-y}{t}\big)\Big\}.$$

□

This proves the "finite propagation speed argument", which claims that, if we are far enough from an intersection, the solution to the initial boundary-value problem is in fact the solution of the initial-value problem, because the information could not travel the distance and reach the location. This key argument allows the implementation of our framework to any physical road network. The same argument can be proved if one considers an outgoing link. In this case, the initial-boundary value problem can be reduced to an initial-value problem if $x - \mathbf{f}_j'(0)t \geq 0,\ j \in \mathcal{O}$.
We consider a road network represented by a directed graph $G = (\mathcal{N}, \mathcal{L})$ containing n nodes and l finite-length links. For each link $l \in \mathcal{L}$, we denote its length by $L_l > 0$. We then want to solve the following Cauchy problem on each link $l \in \mathcal{L}$.

$$\begin{cases} \boldsymbol{\rho}_{l,t}(t,x) + \mathbf{f}_l(\boldsymbol{\rho}_l(t,x))_x = 0, & (t,x) \in (0,T) \times (0,L_l), \\ \boldsymbol{\rho}_l(0,x) = \boldsymbol{\rho}_{0,l}(x), & x \in (0,L_l). \end{cases} \tag{4.7.1}$$

The main idea of resolution is the following: For a small-enough time horizon, we can solve a fixed-point problem locally around each intersection, determining the solution locally on the incoming and outgoing links. The finite propagation speed of information ensures that the intersection will not be attained in this time-interval by information emanating from another junction. Outside of those neighborhood, *i.e.* far away from intersection, we solve on the same-time interval an initial value problem. Finally we treat the solution as an initial datum, restart the process and iterate. For each node $n \in \mathcal{N}$ Theorem 4.4.11 guarantees for each intersection existence of a finite time-horizon T_n on which the fixed point problem is well defined. We can then define $T_{\mathcal{N}} \coloneqq \min_{n \in \mathcal{N}} T_n$. In addition, we need to precise how we extend the initial value on semi-infinite links. Let us consider a given intersection v and two links $(i,j) \in \mathcal{I}_v \times \mathcal{O}_v$. For the exiting link j we can simply extend the initial datum $\boldsymbol{\rho}_{0,j}(x),\ x \in (0,L_j)$ by $\bar{\boldsymbol{\rho}}_{0,j}(x),\ x \geq 0$ such that

$$\begin{aligned} \bar{\boldsymbol{\rho}}_{0,j}(x) &= \begin{cases} \boldsymbol{\rho}_{0,j}(x) & \text{if } x \in (0,L_j), \\ 0 & \text{else,} \end{cases} \\ \mathbf{V}_{0,j}^{\text{out}}(x) &= \int_0^x \bar{\boldsymbol{\rho}}_{0,j}(y)\,\mathrm{d}y, \quad x \in (0,\infty). \end{aligned}$$

For the incoming link i we need to define a space variable $\bar{x} \in (-\infty, 0)$. For $x \in (0, L_i)$ consider the change of variable $\bar{x}$ defined by $\bar{x} = x - L_i$. We then define

$$\begin{aligned} \bar{\boldsymbol{\rho}}_{0,i}(\bar{x}) &= \begin{cases} \boldsymbol{\rho}_{0,i}(\bar{x} + L_i) & \text{if } \bar{x} \in (-L_i, 0), \\ 0 & \text{else,} \end{cases} \\ \mathbf{V}_{0,i}^{\text{in}}(\bar{x}) &= \int_{-\infty}^{\bar{x}} \bar{\boldsymbol{\rho}}_{0,i}(y)\,\mathrm{d}y \quad \bar{x} \in (-\infty, 0). \end{aligned}$$

For each intersection we can then solve the fixed point problem on $[0, T_{\mathcal{N}}]$ and obtain for all $n \in \mathcal{N},\ j \in \mathcal{O}_v,\ t \in [0, T_{\mathcal{N}}]$ the solution $t \mapsto \mathbf{q}_j^n(t)$.

Now that we have this solution, we explain how to obtain the solution to the inital Cauchy problem (4.7.1) on each link $l \in \mathcal{L}$. Let us focus on one link l connecting v_1 to v_2 whose space-coordinates can be indexed on $[0, L_l]$. By definition of $T_{\mathcal{N}}$ and application of Theorem 4.4.11, the fixed-point problem is well posed for each intersection v on $[0, T_{\mathcal{N}}]$. We now consider a new time-horizon T, defined as $T = \min\left\{T_{\mathcal{N}}, \frac{L_l}{\mathbf{f}_l'(0)-\mathbf{f}_l'(\boldsymbol{\rho}_l^{\max})}\right\}$, where $\frac{L_l}{\mathbf{f}_l'(0)-\mathbf{f}_l'(\boldsymbol{\rho}_l^{\max})}$ represents the first instant at which information emanating from both intersections may interact. Then, for any $x \in [0, L_l]$, where x denotes the distance from intersection v_1 and $-x+L_l$ denotes the distance to intersection v_2, we can define the solution in the following way:

- if $x < \mathbf{f}_i'(0)T$, the point is in the neighborhood of the first intersection v_1 and the solution depends on the initial datum and the boundary condition imposed by v_1. The Hamilton Jacobi solution to the problem is $\bar{\mathbf{V}}_l^{\text{out}}(t, x)$ obtained from solving the fixed-point problem around v_1. This corresponds to zone A in Figure 4.2.

- if $|x-L_l| < -\mathbf{f}_i'(\boldsymbol{\rho}_i^{\max})T,\ i \in \mathcal{I}$, the point is in the neighborhood of the second intersection v_2. Then the Hamilton Jacobi solution to the problem is $\bar{\mathbf{V}}_l^{\text{in}}(t, x - L_l)$ obtained from solving the fixed-point problem around v_2. This corresponds to zone C in Figure 4.2.

- else, the point is outside both neighborhoods, and can only be reached by information originating from the initial datum. This corresponds to zone B in Figure 4.2. The solution $\bar{\mathbf{V}}_l(t, x)$ is defined as the solution of the initial value problem

$$\begin{cases} \mathbf{v}_{l,t}(t,x) + \mathbf{f}_l(\mathbf{v}_x(t,x)) = 0 & (t,x) \in (0,T) \times \mathbb{R}_{\geq 0}, \\ \mathbf{v}(0,x) = \mathbf{v}_{0,l}(x) = \displaystyle\int_0^x \boldsymbol{\rho}_{0,l}(y)dy & x \in \mathbb{R}_{\geq 0}, \end{cases}$$

  i.e. $\bar{\mathbf{V}}_l(t, x) = \max\limits_{y \in \mathbb{R}_{\geq 0}} \left\{\mathbf{v}_{0,l}(y) + t\mathbf{f}_i^*\left(\frac{x-y}{t}\right)\right\}$. In any case, the formulation of $\bar{\mathbf{V}}_l^{\text{in}}(t, x)$ and $\bar{\mathbf{V}}_l^{\text{out}}(t, x)$ includes information emanating from the initial datum.

Since the solution $\bar{\mathbf{V}}_l(t, x)$ is Lipschitz-continuous, its spatial derivative can be be computed thanks to Rademacher's theorem (see for instance [115, Theorem 11.49]) or directly recalling the results in Theorems 4.4.2 and 4.4.5, thus obtaining the weak entropy solution to Cauchy problems (4.2.1), (4.2.2).

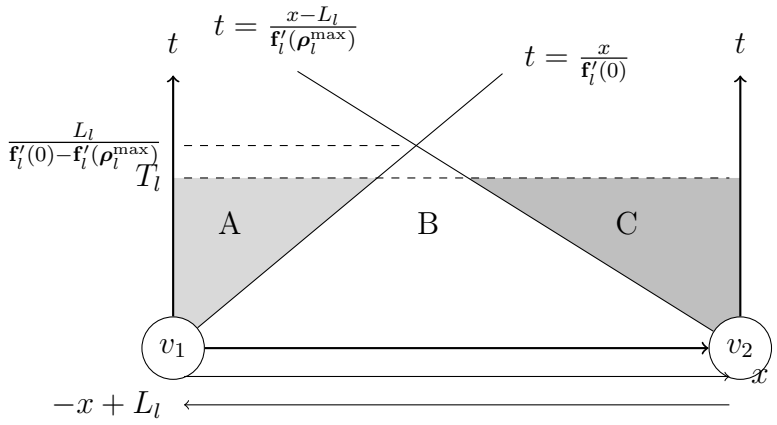

Figure 4.2 – Illustration of the finite speed propagation argument on one link.

4.8 Further work and conclusion

In this chapter we have rigorously built a framework able to provide weak solutions to the scalar conservation law on a network, obtaining regularity estimates on the Hamilton-Jacobi solutions. Nonetheless, from a traffic modeling point of view, this framework allows multiple origins but only a single destination. Adding multiple destinations for vehicles requires to add dynamics, keeping track of the different flows w.r.t. the different destinations, so called multi-commodity models. In addition to this extension, simulating the problem numerically seems appropriate to visualize the impact of the dynamics of buffers and routing functions on the solution. The developed Hamilton-Jacobi framework can thereby be used to implement a numerical scheme based on the considered fixed-point problem. Finally, the work detailed in Section 4.6 opens the door for *Dynamic Traffic Assignment*, *i.e.* optimizing the routing function with respect to the solution in real time or based on past information.

Conclusion and perspectives

In this thesis, we have explored the application of hyperbolic partial differential equations to urban traffic flow modeling. As discussed in the introduction, the existing models in the literature present several limitations in order to be implemented on urban road networks, and to be used to reduce the negative externalities of traffic.

In Chapter 2 we proved existence and uniqueness of weak entropy solutions for the Aw–Rascle–Zhang model with relaxation. To this end, we constructed wave-front tracking approximations of the solutions with a splitting technique in a Lagrangian setting. We showed theoretically than the relaxation term forces the solution to converge towards a weak solution of the LWR model, when the relaxation parameter is sent to zero. Nonetheless, uniqueness of this weak solution remains an open problem. Exploring this question, potentially following the recent methodology described in [55], may be pursued in the future.

Following the drawbacks of existing models presented in the introduction, we have proposed a new mathematical model accounting for the boundedness of traffic acceleration at a macroscopic scale in Chapter 3. Representing accurately traffic acceleration is essential for urban applications, such as estimation and control of vehicle emissions. We proposed a wave-front tracking algorithm to construct approximate solutions of the model, with general flux functions. We showed existence of solutions to the Cauchy problem. In addition, we proposed numerical illustrations simulating the model in urban situations, including sequences of traffic lights, and confronted the results to numerical simulations of the LWR model. Nonetheless, we cannot assert at this stage that our model is more realistic than the LWR model. In order to do so, we need to confront our model to real traffic data. The used dataset should be detailed enough to capture precisely the acceleration of traffic in real time. This cannot be achieved using loop detectors, but dense Floating Car Data represent an opportunity to investigate the question. In addition, our model does not extend yet to general initial data, since the existence result is restricted at the moment to a finite number of moving bottlenecks, and then a finite number of downward jumps in the initial density. Finally, this model could be adapted to model bounded deceleration phases, for the sake of realism.

In Chapter 4, we introduced a macroscopic traffic flow model on networks taking into account coupled boundary conditions at the junctions. Our model features buffers of finite size, time-dependent routing functions at the junctions and enables spill-back of congestion at the intersections. We proved the well-posedness of the model using a fixed-point argument and obtained stability of the solution with respect to the routing ratios, initial datum on incoming and outgoing roads and the initial state of the buffers. This stability is then used to write an optimal control problem with respect to the routing functions, and we showed existence of a global optimum. This control problem represents a formulation of the Dynamic Traffic Assignment problem. Finally, we detailed how to apply

our framework to a realistic road network, with several intersections and finite-length links, taking advantage of the finite propagation speed of information in the model. At this stage, our model allows multiple origins but only a single destination for the vehicles, which is a limitation to the implementation in traffic management systems. Further work might investigate the insertion of this multi-commodity aspect in the framework. In addition, we are currently investigating the numerical resolution of the model, in order to generate simulations and illustrate the behavior of the solution with respect to the buffers.

Bibliography

[1] Adimurthi, S. Mishra, and G. D. Veerappa Gowda. Explicit Hopf-Lax type formulas for Hamilton-Jacobi equations and conservation laws with discontinuous coefficients. *J. Differential Equations*, 241(1):1–31, 2007.

[2] D. Amadori and G. Guerra. Global BV solutions and relaxation limit for a system of conservation laws. *Proc. Roy. Soc. Edinburgh Sect. A*, 131(1):1–26, 2001.

[3] L. Ambrosio, N. Fusco, and D. Pallara. *Functions of bounded variation and free discontinuity problems*. Oxford Mathematical Monographs. The Clarendon Press, Oxford University Press, New York, 2000.

[4] F. Ancona and P. Goatin. Uniqueness and stability of L^∞ solutions for Temple class systems with boundary and properties of the attainable sets. *SIAM J. Math. Anal.*, 34(1):28–63, 2002.

[5] L. A. Anderson. *Data-Driven Methods for Improved Estimation and Control of an Urban Arterial Traffic Network*. University of California, Berkeley, 2015.

[6] B. Andreianov, C. Donadello, and M. D. Rosini. A second-order model for vehicular traffics with local point constraints on the flow. *Math. Models Methods Appl. Sci.*, 26(4):751–802, 2016.

[7] J.-P. Aubin, A. M. Bayen, and P. Saint-Pierre. Dirichlet problems for some Hamilton-Jacobi equations with inequality constraints. *SIAM J. Control Optim.*, 47(5):2348–2380, 2008.

[8] A. Aw, A. Klar, T. Materne, and M. Rascle. Derivation of continuum traffic flow models from microscopic follow-the-leader models. *SIAM J. Appl. Math.*, 63(1):259–278, 2002.

[9] A. Aw and M. Rascle. Resurrection of "second order" models of traffic flow. *SIAM J. Appl. Math.*, 60(3):916–938, 2000.

[10] P. Bagnerini and M. Rascle. A multiclass homogenized hyperbolic model of traffic flow. *SIAM J. Math. Anal.*, 35(4):949–973, 2003.

[11] P. Baiti and A. Bressan. The semigroup generated by a Temple class system with large data. *Differential Integral Equations*, 10(3):401–418, 1997.

[12] M. Bando, K. Hasebe, A. Nakayama, A. Shibata, and Y. Sugiyama. Dynamical model of traffic congestion and numerical simulation. *Phys. Rev. E*, 51:1035–1042, 1995.

[13] C. Bardos, A. Y. le Roux, and J.-C. Nédélec. First order quasilinear equations with boundary conditions. *Comm. Partial Differential Equations*, 4(9):1017–1034, 1979.

[14] S. Benzoni-Gavage and R. M. Colombo. An n-populations model for traffic flow. *European J. Appl. Math.*, 14(5):587–612, 2003.

[15] R. Borsche, R. M. Colombo, and M. Garavello. Mixed systems: ODEs - balance laws. *J. Differential Equations*, 252(3):2311–2338, 2012.

[16] S. Boyd and L. Vandenberghe. *Convex optimization*. Cambridge University Press, Cambridge, 2004.

[17] M. Brackstone and M. McDonald. Car-following: a historical review. *Transportation Research Part F: Traffic Psychology and Behaviour*, 2(4):181 – 196, 1999.

[18] A. Bressan. Global solutions of systems of conservation laws by wave-front tracking. *J. Math. Anal. Appl.*, 170(2):414–432, 1992.

[19] A. Bressan. The unique limit of the Glimm scheme. *Arch. Rational Mech. Anal.*, 130(3):205–230, 1995.

[20] A. Bressan. *Hyperbolic systems of conservation laws*, volume 20 of *Oxford Lecture Series in Mathematics and its Applications*. Oxford University Press, Oxford, 2000.

[21] A. Bressan and R. M. Colombo. The semigroup generated by 2×2 conservation laws. *Arch. Rational Mech. Anal.*, 133(1):1–75, 1995.

[22] A. Bressan and R. M. Colombo. Decay of positive waves in nonlinear systems of conservation laws. *Ann. Scuola Norm. Sup. Pisa Cl. Sci. (4)*, 26(1):133–160, 1998.

[23] A. Bressan, G. Crasta, and B. Piccoli. Well-posedness of the Cauchy problem for $n \times n$ systems of conservation laws. *Mem. Amer. Math. Soc.*, 146(694):viii+134, 2000.

[24] A. Bressan and P. Goatin. Oleinik type estimates and uniqueness for $n \times n$ conservation laws. *J. Differential Equations*, 156(1):26–49, 1999.

[25] A. Bressan and P. Goatin. Stability of L^∞ solutions of Temple class systems. *Differential Integral Equations*, 13(10-12):1503–1528, 2000.

[26] A. Bressan and P. LeFloch. Uniqueness of weak solutions to systems of conservation laws. *Arch. Rational Mech. Anal.*, 140(4):301–317, 1997.

[27] A. Bressan and K. T. Nguyen. Conservation law models for traffic flow on a network of roads. *Netw. Heterog. Media*, 10(2):255–293, 2015.

[28] A. Bressan and K. T. Nguyen. Optima and equilibria for traffic flow on networks with backward propagating queues. *Netw. Heterog. Media*, 10(4):717–748, 2015.

[29] A. Bressan and A. Nordli. The Riemann solver for traffic flow at an intersection with buffer of vanishing size. *Netw. Heterog. Media*, 12(2):173–189, 2017.

[30] A. Bressan and T. Yang. A sharp decay estimate for positive nonlinear waves. *SIAM J. Math. Anal.*, 36(2):659–677, 2004.

[31] A. Bressan and F. Yu. Continuous Riemann solvers for traffic flow at a junction. *Discrete Contin. Dyn. Syst.*, 35(9):4149–4171, 2015.

[32] G. Bretti, R. Natalini, and B. Piccoli. A fluid-dynamic traffic model on road networks. *Arch. Comput. Methods Eng.*, 14(2):139–172, 2007.

[33] S. Calvert, M. Minderhoud, H. Taale, I. Wilmink, and V. Knoop. Traffic assignment and simulation models. Technical report, 2016.

[34] E. S. Canepa and C. G. Claudel. Exact solutions to traffic density estimation problems involving the lighthill-whitham-richards traffic flow model using mixed integer programming. In *2012 15th International IEEE Conference on Intelligent Transportation Systems*, pages 832–839. IEEE, 2012.

[35] C. Chalons, M. L. Delle Monache, and P. Goatin. A conservative scheme for non-classical solutions to a strongly coupled PDE-ODE problem. *Interfaces and Free Boundaries*, 19(4):553–570, 2018.

[36] C. Chalons and P. Goatin. Godunov scheme and sampling technique for computing phase transitions in traffic flow modeling. *Interfaces Free Bound.*, 10(2):197–221, 2008.

[37] R. E. Chandler, R. Herman, and E. W. Montroll. Traffic dynamics: Studies in car following. *Operations Research*, 6(2):165–184, 1958.

[38] G. Q. Chen, C. D. Levermore, and T.-P. Liu. Hyperbolic conservation laws with stiff relaxation terms and entropy. *Comm. Pure Appl. Math.*, 47(6):787–830, 1994.

[39] G. Q. Chen and T.-P. Liu. Zero relaxation and dissipation limits for hyperbolic conservation laws. *Comm. Pure Appl. Math.*, 46(5):755–781, 1993.

[40] C. Christoforou and K. Trivisa. Sharp decay estimates for hyperbolic balance laws. *J. Differential Equations*, 247(2):401–423, 2009.

[41] C. Christoforou and K. Trivisa. Decay of positive waves of hyperbolic balance laws. *Acta Math. Sci. Ser. B Engl. Ed.*, 32(1):352–366, 2012.

[42] C. G. Claudel and A. M. Bayen. Lax-Hopf based incorporation of internal boundary conditions into Hamilton-Jacobi equation. Part I: Theory. *IEEE Trans. Automat. Control*, 55(5):1142–1157, 2010.

[43] C. G. Claudel and A. M. Bayen. Lax-Hopf based incorporation of internal boundary conditions into Hamilton-Jacobi equation. Part II: Computational methods. *IEEE Trans. Automat. Control*, 55(5):1158–1174, 2010.

[44] G. M. Coclite, M. Garavello, and B. Piccoli. Traffic flow on a road network. *SIAM J. Math. Anal.*, 36(6):1862–1886, 2005.

[45] R. M. Colombo. Hyperbolic phase transitions in traffic flow. *SIAM J. Appl. Math.*, 63(2):708–721, 2002.

[46] R. M. Colombo and A. Corli. Well posedness for multilane traffic models. *Ann. Univ. Ferrara Sez. VII Sci. Mat.*, 52(2):291–301, 2006.

[47] R. M. Colombo, P. Goatin, and F. S. Priuli. Global well posedness of traffic flow models with phase transitions. *Nonlinear Anal.*, 66(11):2413–2426, 2007.

[48] R. M. Colombo, P. Goatin, and M. D. Rosini. On the modelling and management of traffic. *ESAIM Math. Model. Numer. Anal.*, 45(5):853–872, 2011.

[49] R. M. Colombo and A. Marson. A Hölder continuous ode related to traffic flow. *Proceedings of the Royal Society of Edinburgh Section A: Mathematics*, 133(4):759–772, 2003.

[50] R. Courant and K. O. Friedrichs. *Supersonic Flow and Shock Waves*. Interscience Publishers, Inc., New York, N. Y., 1948.

[51] M. G. Crandall and P.-L. Lions. Viscosity solutions of Hamilton-Jacobi equations. *Trans. Amer. Math. Soc.*, 277(1):1–42, 1983.

[52] G. Crasta and B. Piccoli. Viscosity solutions and uniqueness for systems of inhomogeneous balance laws. *Discrete Contin. Dynam. Systems*, 3(4):477–502, 1997.

[53] E. Cristiani and F. S. Priuli. A destination-preserving model for simulating Wardrop equilibria in traffic flow on networks. *Netw. Heterog. Media*, 10(4):857–876, 2015.

[54] C. M. Dafermos. Polygonal approximations of solutions of the initial value problem for a conservation law. *J. Math. Anal. Appl.*, 38:33–41, 1972.

[55] C. M. Dafermos. Uniqueness of Zero Relaxation Limit. *SIAM J. Math. Anal.*, 51(3):1999–2018, 2019.

[56] C. F. Daganzo. Requiem for second-order fluid approximations of traffic flow. *Transportation Research Part B: Methodological*, 29(4):277–286, 1995.

[57] C. D'Apice and B. Piccoli. Vertex flow models for vehicular traffic on networks. *Math. Models Methods Appl. Sci.*, 18(suppl.):1299–1315, 2008.

[58] M. L. Delle Monache and P. Goatin. Scalar conservation laws with moving constraints arising in traffic flow modeling: an existence result. *J. Differential Equations*, 257(11):4015–4029, 2014.

[59] R. J. DiPerna. Global existence of solutions to nonlinear hyperbolic systems of conservation laws. *J. Differential Equations*, 20(1):187–212, 1976.

[60] Directorate-General for Mobility and Transport (European Commission). European urban mobility: Policy context. *Publications Office of the European Union*, 2017.

[61] Directorate-General for Mobility and Transport (European Commission). Sustainable urban mobility: European policy, practice and solutions. *Publications Office of the European Union*, 2017.

[62] N. S. Dymski, P. Goatin, and M. D. Rosini. Existence of BV solutions for a non-conservative constrained Aw-Rascle-Zhang model for vehicular traffic. *J. Math. Anal. Appl.*, 467(1):45–66, 2018.

[63] L. C. Evans. *Partial differential equations*, volume 19 of *Graduate Studies in Mathematics*. American Mathematical Society, Providence, RI, second edition, 2010.

[64] S. Fan, M. Herty, and B. Seibold. Comparative model accuracy of a data-fitted generalized Aw-Rascle-Zhang model. *Netw. Heterog. Media*, 9(2):239–268, 2014.

[65] H. Frankowska. On LeFloch's solutions to the initial-boundary value problem for scalar conservation laws. *J. Hyperbolic Differ. Equ.*, 7(3):503–543, 2010.

[66] M. Garavello and P. Goatin. The Cauchy problem at a node with buffer. *Discrete Contin. Dyn. Syst.*, 32(6):1915–1938, 2012.

[67] M. Garavello, K. Han, and B. Piccoli. *Models for vehicular traffic on networks*, volume 9 of *AIMS Series on Applied Mathematics*. American Institute of Mathematical Sciences (AIMS), Springfield, MO, 2016.

[68] M. Garavello and B. Piccoli. Source-destination flow on a road network. *Commun. Math. Sci.*, 3(3):261–283, 2005.

[69] M. Garavello and B. Piccoli. *Traffic flow on networks*, volume 1 of *AIMS Series on Applied Mathematics*. American Institute of Mathematical Sciences (AIMS), Springfield, MO, 2006. Conservation laws models.

[70] M. Garavello and B. Piccoli. Conservation laws on complex networks. *Ann. Inst. H. Poincaré Anal. Non Linéaire*, 26(5):1925–1951, 2009.

[71] M. Garavello and B. Piccoli. A multibuffer model for LWR road networks. In *Advances in dynamic network modeling in complex transportation systems*, volume 2 of *Complex Netw. Dyn. Syst.*, pages 143–161. Springer, New York, 2013.

[72] D. C. Gazis. *Traffic science*. New York : Wiley, 1974. "A Wiley-Interscience publication.".

[73] D. C. Gazis, R. Herman, and R. W. Rothery. Nonlinear follow-the-leader models of traffic flow. *Operations Research*, 9(4):545–567, 1961.

[74] F. Giorgi, L. Leclercq, and J.-B. Lesort. A traffic flow model for urban traffic analysis: extensions of the LWR model for urban and environmental applications. In *Transportation and Traffic Theory in the 21st Century: Proceedings of the 15th International Symposium on Transportation and Traffic Theory, Adelaide, Australia, 16-18 July 2002*, pages 393–415. Emerald Group Publishing Limited, 2002.

[75] J. Glimm. Solutions in the large for nonlinear hyperbolic systems of equations. *Comm. Pure Appl. Math.*, 18:697–715, 1965.

[76] P. Goatin. The Aw-Rascle vehicular traffic flow model with phase transitions. *Math. Comput. Modelling*, 44(3-4):287–303, 2006.

[77] P. Goatin and L. Gosse. Decay of positive waves for $n \times n$ hyperbolic systems of balance laws. *Proc. Amer. Math. Soc.*, 132(6):1627–1637, 2004.

[78] P. Goatin and N. Laurent-Brouty. The zero relaxation limit for the Aw-Rascle-Zhang traffic flow model. *Z. Angew. Math. Phys.*, 70(1):Art. 31, 24, 2019.

[79] E. Godlewski and P.-A. Raviart. *Numerical approximation of hyperbolic systems of conservation laws*, volume 118 of *Applied Mathematical Sciences*. Springer-Verlag, New York, 1996.

[80] S. Göttlich, M. Herty, and A. Klar. Network models for supply chains. *Commun. Math. Sci.*, 3(4):545–559, 2005.

[81] J. M. Greenberg. Extensions and amplifications of a traffic model of Aw and Rascle. *SIAM J. Appl. Math.*, 62(3):729–745, 2001/02.

[82] J. M. Greenberg, A. Klar, and M. Rascle. Congestion on multilane highways. *SIAM J. Appl. Math.*, 63(3):818–833, 2003.

[83] B. Greenshields, J. Bibbins, W. Channing, and H. Miller. A study of traffic capacity. *Highway Research Board proceedings*, 1935.

[84] M. Gugat, A. Keimer, G. Leugering, and Z. Wang. Analysis of a system of nonlocal conservation laws for multi-commodity flow on networks. *Netw. Heterog. Media*, 10(4):749–785, 2015.

[85] K. Han, B. Piccoli, and W. Szeto. Continuous-time link-based kinematic wave model: formulation, solution existence, and well-posedness. *Transportmetrica B: Transport Dynamics*, 4(3):187–222, 2016.

[86] D. Helbing. Improved fluid-dynamic model for vehicular traffic. *Phys. Rev. E*, 51:3164–3169, Apr 1995.

[87] M. Herty and A. Klar. Modeling, simulation, and optimization of traffic flow networks. *SIAM J. Sci. Comput.*, 25(3):1066–1087, 2003.

[88] M. Herty, A. Klar, and B. Piccoli. Existence of solutions for supply chain models based on partial differential equations. *SIAM J. Math. Anal.*, 39(1):160–173, 2007.

[89] M. Herty, J.-P. Lebacque, and S. Moutari. A novel model for intersections of vehicular traffic flow. *Netw. Heterog. Media*, 4(4):813–826, 2009.

[90] D. Hoff. Invariant regions for systems of conservation laws. *Trans. Amer. Math. Soc.*, 289(2):591–610, 1985.

[91] H. Holden and N. H. Risebro. A mathematical model of traffic flow on a network of unidirectional roads. *SIAM J. Math. Anal.*, 26(4):999–1017, 1995.

[92] H. Holden and N. H. Risebro. Models for dense multilane vehicular traffic. *arXiv preprint arXiv:1812.01361*, 2018.

[93] H. K. Jenssen and C. Sinestrari. On the spreading of characteristics for non-convex conservation laws. *Proc. Roy. Soc. Edinburgh Sect. A*, 131(4):909–925, 2001.

[94] K. T. Joseph and G. D. V. Gowda. Explicit formula for the solution of convex conservation laws with boundary condition. *Duke Math. J.*, 62(2):401–416, 03 1991.

[95] A. Keimer, N. Laurent-Brouty, F. Farokhi, H. Signargout, V. Cvetkovic, A. M. Bayen, and K. H. Johansson. Information patterns in the modeling and design of mobility management services. *Proceedings of the IEEE*, 106(4):554–576, 2018.

[96] B. S. Kerner. Phase transitions in traffic flow. In D. Helbing, H. J. Herrmann, M. Schreckenberg, and D. E. Wolf, editors, *Traffic and Granular Flow '99*, pages 253–283, Berlin, Heidelberg, 2000. Springer Berlin Heidelberg.

[97] A. Klar and R. Wegener. *Kinetic Traffic Flow Models*, pages 263–316. Birkhäuser Boston, Boston, MA, 2000.

[98] S. N. Kružkov. First order quasilinear equations with several independent variables. *Mat. Sb. (N.S.)*, 81 (123):228–255, 1970.

[99] C. Lattanzio and P. Marcati. The zero relaxation limit for the hydrodynamic Whitham traffic flow model. *J. Differential Equations*, 141(1):150–178, 1997.

[100] C. Lattanzio, A. Maurizi, and B. Piccoli. Moving bottlenecks in car traffic flow: a PDE-ODE coupled model. *SIAM J. Math. Anal.*, 43(1):50–67, 2011.

[101] N. Laurent-Brouty, G. Costeseque, and P. Goatin. A coupled PDE-ODE model for bounded acceleration in macroscopic traffic flow models. *IFAC-PapersOnLine*, 51(9):37 – 42, 2018. 15th IFAC Symposium on Control in Transportation Systems CTS 2018.

[102] N. Laurent-Brouty, G. Costeseque, and P. Goatin. A macroscopic traffic flow model accounting for bounded acceleration. preprint, June 2019.

[103] N. Laurent-Brouty, A. Keimer, P. Goatin, and A. M. Bayen. A macroscopic traffic flow model with finite buffers on networks: Well-posedness by means of Hamilton-Jacobi equations. preprint, May 2019.

[104] P. Lax. Shock waves and entropy. pages 603–634, 1971.

[105] P. D. Lax. Hyperbolic systems of conservation laws. II. *Comm. Pure Appl. Math.*, 10:537–566, 1957.

[106] J. Lebacque. A finite acceleration scheme for first order macroscopic traffic flow models. *IFAC Proceedings Volumes*, 30(8):787–792, 1997.

[107] J. Lebacque. A two phase extension of the LWR Model based on the boundedness of traffic acceleration. In *Transportation and Traffic Theory in the 21st Century*, pages 697–718. Emerald Group Publishing Limited, 2002.

[108] J.-P. Lebacque. Two-phase bounded-acceleration traffic flow model: analytical solutions and applications. *Transportation Research Record: Journal of the Transportation Research Board*, (1852):220–230, 2003.

[109] J.-P. Lebacque, H. Haj-Salem, and S. Mammar. Second order traffic flow modeling: supply-demand analysis of the inhomogeneous riemann problem and of boundary conditions. *Proceedings of the 10th Euro Working Group on Transportation (EWGT)*, 3(3), 2005.

[110] J.-P. Lebacque, J.-B. Lesort, and F. Giorgi. Introducing buses into first-order macroscopic traffic flow models. *Transportation Research Record: Journal of the Transportation Research Board*, 1644(1):70–79, 1998.

[111] J.-P. Lebacque, S. Mammar, and H. H. Salem. Generic second order traffic flow modelling. In *Transportation and Traffic Theory 2007*, 2007.

[112] L. Leclercq. *Modélisation dynamique du trafic et applications à l'estimation du bruit routier*. PhD thesis, Villeurbanne, INSA, 2002.

[113] L. Leclercq. Bounded acceleration close to fixed and moving bottlenecks. *Transportation Research Part B: Methodological*, 41(3):309–319, 2007.

[114] L. Leclercq. A new numerical scheme for bounding acceleration in the LWR model. In *4th IMA International Conference on Mathematics in Transport*, 2007.

[115] G. Leoni. *A first course in Sobolev spaces*, volume 105 of *Graduate Studies in Mathematics*. American Mathematical Society, Providence, RI, 2009.

[116] R. J. LeVeque. *Finite volume methods for hyperbolic problems*. Cambridge Texts in Applied Mathematics. Cambridge University Press, Cambridge, 2002.

[117] R. J. LeVeque and B. Temple. Stability of Godunov's method for a class of 2×2 systems of conservation laws. *Trans. Amer. Math. Soc.*, 288(1):115–123, 1985.

[118] T. Li. Global solutions of nonconcave hyperbolic conservation laws with relaxation arising from traffic flow. *J. Differential Equations*, 190(1):131–149, 2003.

[119] T. Liard and B. Piccoli. Well-Posedness for Scalar Conservation Laws with Moving Flux Constraints. *SIAM J. Appl. Math.*, 79(2):641–667, 2019.

[120] M. J. Lighthill and G. B. Whitham. On kinematic waves. II. A theory of traffic flow on long crowded roads. *Proc. Roy. Soc. London. Ser. A.*, 229:317–345, 1955.

[121] A. D. May. *Traffic flow fundamentals*. 1990.

[122] O. A. Oleĭnik. Discontinuous solutions of non-linear differential equations. *Uspehi Mat. Nauk (N.S.)*, 12(3(75)):3–73, 1957.

[123] O. A. Oleĭnik. On the uniqueness of the generalized solution of the Cauchy problem for a non-linear system of equations occurring in mechanics. *Uspehi Mat. Nauk (N.S.)*, 12(6(78)):169–176, 1957.

[124] O. A. Oleĭnik. Discontinuous solutions of non-linear differential equations. *Amer. Math. Soc. Transl. (2)*, 26:95–172, 1963.

[125] B. G. Pachpatte. *Inequalities for differential and integral equations*, volume 197 of *Mathematics in Science and Engineering*. Academic Press, Inc., San Diego, CA, 1998.

[126] H. J. Payne. Models of freeway traffic and control. *Mathematical models of public systems*, 1971.

[127] S. Peeta and A. K. Ziliaskopoulos. Foundations of dynamic traffic assignment: The past, the present and the future. *Networks and Spatial Economics*, 1(3):233–265, Sep 2001.

[128] L. A. Pipes. An operational analysis of traffic dynamics. *Journal of Applied Physics*, 24(3):274–281, 1953.

[129] I. Prigogine. A Boltzmann-like approach to the statistical theory of traffic flow. In *Theory of traffic flow*, pages 158–164. Elsevier, Amsterdam, 1961.

[130] I. Prigogine and F. C. Andrews. A Boltzmann-like approach for traffic flow. *Operations Res.*, 8:789–797, 1960.

[131] I. Prigogine and R. Herman. Kinetic theory of vehicular traffic. Technical report, 1971.

[132] M. Rascle. An improved macroscopic model of traffic flow: derivation and links with the Lighthill-Whitham model. *Math. Comput. Modelling*, 35(5-6):581–590, 2002.

[133] A. Reuschel. Fahrzeugbewegungen in der kolonne. *Osterreichisches Ingenieur Archiv*, 4:193–215, 1950.

[134] P. I. Richards. Shock waves on the highway. *Operations Res.*, 4:42–51, 1956.

[135] N. H. Risebro. A front-tracking alternative to the random choice method. *Proc. Amer. Math. Soc.*, 117(4):1125–1139, 1993.

[136] S. Samaranayake, W. Krichene, J. Reilly, M. L. D. Monache, P. Goatin, and A. Bayen. Discrete-time system optimal dynamic traffic assignment (SO-DTA) with partial control for physical queuing networks. *Transportation Science*, 52(4):982–1001, 2018.

[137] D. Serre. Systèmes de lois de conservation II. structures géométriques, oscillation et problèmes mixtes. 1996.

[138] B. Temple. Systems of conservation laws with invariant submanifolds. *Trans. Amer. Math. Soc.*, 280(2):781–795, 1983.

[139] J. Thai, N. Laurent-Brouty, and A. M. Bayen. Negative externalities of gps-enabled routing applications: A game theoretical approach. In *2016 IEEE 19th International Conference on Intelligent Transportation Systems (ITSC)*, pages 595–601, Nov 2016.

[140] M. Treiber and A. Kesting. *Traffic flow dynamics*. Springer-Verlag Berlin Heidelberg, 2013.

[141] S. Villa, P. Goatin, and C. Chalons. Moving bottlenecks for the Aw-Rascle-Zhang traffic flow model. *Discrete Contin. Dyn. Syst. Ser. B*, 22(10):3921–3952, 2017.

[142] D. H. Wagner. Equivalence of the Euler and Lagrangian equations of gas dynamics for weak solutions. *J. Differential Equations*, 68(1):118–136, 1987.

[143] G. B. Whitham. Linear and nonlinear waves. pages xvi+636, 1974. Pure and Applied Mathematics.

[144] G. C. K. Wong and S. C. Wong. A multi-class traffic flow model - an extension of lwr model with heterogeneous drivers. *Transportation Research Part A: Policy and Practice*, 36(9):827–841, 2002.

[145] E. Zeidler. *Applied functional analysis*, volume 108 of *Applied Mathematical Sciences*. Springer-Verlag, New York, 1995. Applications to mathematical physics.

[146] H. M. Zhang. A non-equilibrium traffic model devoid of gas-like behavior. *Transportation Research Part B: Methodological*, 36(3):275–290, 2002.